Passive Acoustic Monitoring of Harbour Porpoise Behaviour, Distribution and Density in Tidal Rapid Habitats

Jamie Donald John Macaulay

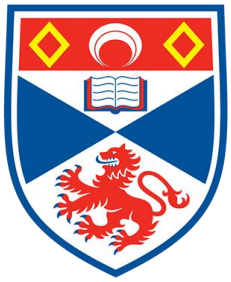

University of
St Andrews

This thesis is submitted in partial fulfilment for the degree of

Doctor of Philosophy (PhD)

at the University of St Andrews

February 2020

Candidate's declaration

I, Jamie Donald John Macaulay, do hereby certify that this thesis, submitted for the degree of PhD, which is approximately 60,000 words in length, has been written by me, and that it is the record of work carried out by me, or principally by myself in collaboration with others as acknowledged, and that it has not been submitted in any previous application for any degree.

I was admitted as a research student at the University of St Andrews in September 2013.

I received funding from an organisation or institution and have acknowledged the funder(s) in the full text of my thesis.

Date Signature of candidate

Supervisor's declaration

I hereby certify that the candidate has fulfilled the conditions of the Resolution and Regulations appropriate for the degree of PhD in the University of St Andrews and that the candidate is qualified to submit this thesis in application for that degree.

Date Signature of supervisor

Permission for publication

In submitting this thesis to the University of St Andrews we understand that we are giving permission for it to be made available for use in accordance with the regulations of the University Library for the time being in force, subject to any copyright vested in the work not being affected thereby. We also understand, unless exempt by an award of an embargo as requested below, that the title and the abstract will be published, and that a copy of the work may be made and supplied to any bona fide library or research worker, that this thesis will be electronically accessible for personal or research use and that the library has the right to migrate this thesis into new electronic forms as required to ensure continued access to the thesis.

I, Jamie Donald John Macaulay, confirm that my thesis does not contain any third-party material that requires copyright clearance.

The following is an agreed request by candidate and supervisor regarding the publication of this thesis:

Printed copy

No embargo on print copy.

Electronic copy

No embargo on electronic copy.

Date Signature of candidate

Date Signature of supervisor

Underpinning Research Data or Digital Outputs

Candidate's declaration

I, Jamie Donald John Macaulay, hereby certify that no requirements to deposit original research data or digital outputs apply to this thesis and that, where appropriate, secondary data used have been referenced in the full text of my thesis.

Date Signature of candidate

Dedicated to my father Iain Macaulay

and my Grandparents Donald and Ella MacAulay

Table of Contents

Abstract

Toothed whales produce regular echolocation clicks to sense their surroundings and hunt. These clicks can be detected on hydrophones allowing researchers to study and monitor animals, a methodology known as passive acoustic monitoring (PAM). PAM methods can be used to detect patterns of behaviour such as foraging, calculate absolute abundance and determine the 3D positions of soniferous animals. However, this requires robust detection, species classification and localisation algorithms alongside a statistical framework to estimate animal density. Detection, classification and localisation methods were developed to obtain fine scale behavioural information of toothed whales which was then integrated with a distance sampling-based framework to estimate density. These methods were applied to calculate the behaviour, 3D distribution and density of harbour porpoises in a tidal stream habitat.

Toothed whales produce clicks in sequences (clicks trains) which can provide information on behavioural state and aid in species identification. A click train detection algorithm was developed to extract these sequences and performance then tested on PAM data of sperm whales, delphinids and harbour porpoises.

Localisation in tidal rapids is difficult due to fast moving currents and high densities of toothed whales producing a complex soundscape. A drifting free-hanging vertical hydrophone array with movement sensors, click aliasing and track association algorithms was developed to collect geo-referenced 3D tracks of toothed whales in tidal streams.

The full 4π beam profile of a free-swimming captive harbour porpoise was measured. This showed that harbour porpoises have significant acoustic energy at extreme off-axis angles (>30°) which has implications for detectability on PAM devices.

Drifting sound recorders and vertical hydrophones arrays were used to survey a tidal rapid site. Detected click trains, dive data and the measured beam profile were used to inform simulations of detection probability of harbour porpoise clicks and calculate animal density and foraging rates.

Acknowledgements

SUPERVISORS AND COLLEGUES

I have been remarkably lucky to end up with three fantastic supervisors, Doug Gillespie, Jonathan Gordon and Simon Northridge. They collectively introduced me to marine mammal science over the last decade and involved me in some amazing projects around the globe. The guidance provided by all three has provided me with a comprehensive overview of the field, from designing equipment and working at sea to writing decent code and even the occasional manuscript in the office. Also, thanks to Simon Northridge's lab, especially Alex Coram who has put up with my inferior cups of tea for over a decade now. It has been a privilege to have had the opportunity to work with so many bright and interesting people in the Sea Mammal Research Unit.

Professor Peter Madsen not only welcomed me to his lab at Aarhus University when my partner started a PhD with him but also provided the equipment and expertise to allow me to carry out the harbour porpoise beam profile experiment in Chapter 4. Working with him and within his fantastic lab has been a privilege. A special shout out to Mark Johnson, Michael Ladegaard, Kristian Beedholm, Jakob Tougaard and Magnus Wahlberg for interesting discussions and getting me to up to speed on harbour porpoise sensory ecology. Peter Madsens's bioacoustics lab also has an amazing workshop which has been invaluable in much of the beam profile work so thanks to John Svane Jensen and Niels Kristiansen for all the technical help.

Density estimation methods can be difficult to get your head around and Danielle Harris, Tiago Marques and Len Thomas have all set aside their time help me out and talk me through ideas. They are a great asset for marine mammal science and have been an invaluable help over the last few years

This PhD was funded by the University of St Andrews Biology department. A special thanks to them for giving me the opportunity to do the work and write this thesis.

DATA COLLECTION

There were a lot of people involved in the projects that supplied the data for different chapters of this PhD.

Thanks to the field team who collected sperm whale data in Sitka, Alaska. It was great to work with Jan Starely and her team at the University of Alaska SE and to meet all the fishermen who took us out on their boats to study whales that regularly depredate their long lines. It was amazing to see a community with such a well-managed fishery and who are actively working to keep it that way. A special thanks to Dan Falvey and the Alaskan Long Line Fishermen's Association for hosting us, sorting out logistics and making us generally feel welcome in Sitka. Thanks to NOAA Fisheries for funding the project.

On the subject of fishing boats, thanks to Mikey Taylor-Firth for taking us out on his boat, Julie Girl, to collect data on harbour porpoises around gill nets. Thanks to Al Kingston for collecting SoundTrap data on gill nets all these years and Rene Swift who has been invaluable in making hydrophones, potting stuff and allowing me to use his lab for this project. None of this work could have been done without Graham Weatherup and Michael Oswald who were invaluable in designing the PAM system. Thanks to DEFRA for funding the gill net work.

Thanks to the porpoise trainers at Fjord & Bælt, notably Jakob Højer Kristensen, Josefin Larsson, Fredrik Johansson and also Chloe Malinka for setting up and collecting data with me in the freezing cold Danish winter. And of course, none of the beam profile work could have been done without the most studied porpoise in the world, Freja. Thanks to her for being so cooperative.

Thanks to the field team in Kylerhea and especially Arthur Lee, who stayed late into the night fixing hydrophones after I blew up a bunch of preamplifiers. Thanks to Gordon Hastie who has been doing amazing work in tidal rapids and been a great source of advice and ideas. There's a lot of background, proposal writing and admin to do on these projects and Carol Sparling has not only taken a lot of that work on but been great to work with. It can be a bit dangerous to give Jonathan, Doug and I free reign of a research vessel so thanks to the Hebridean Whale and Dolphin Trust for entrusting us with Silurian and putting up with all our gadgets and crazy ideas. Thanks to the Scottish Government for funding the tidal project field work.

Steven Benjamins, Denise Risch and Ben Wilson at the Scottish Association for Marine Science have been great to collaborate with over the years and have always been open to sharing ideas and data. They were kind enough to supply some of their passive acoustic drifter data for chapter 5 which was invaluable in completing the story of how harbour porpoises utilise the tidal stream in Kylerhea.

OTHER SPECIAL MENTIONS

This PhD has taken just under 5 and a half years (part time) and so as well as the folk directly involved there are a few honourable mentions along the way.

The PAMGuard team, Doug Gillespie and Michael Oswald, have always helped me to solve many bugs (many of which I introduced) in the program that was used to analyse data in every chapter of this PhD.

Gill Braulik has been an inspiration in her conservation work in developing countries, utilising PAM for rapid species assessment and monitoring blast fishing. It's been a privilege to work with her these past years.

The folks at NOAA South West, especially Shannon Rankin, Tiaki Sakai and Anne Simonis have been great to collaborate with over the years. They have been doing some amazing stuff with PAM, PAMGuard, open source software and citizen science.

Susannah Calderan has been a fantastic colleague to teach PAMGuard courses with and also a special shout out to Russel Leaper who is always one to talk to about complicated science.

Last but absolutely not least, thanks to my family for all the support and especially my partner Chloe Malinka and wee boy Maxwell Malinka Macaulay. Could not have done it without you.

Funding

This PhD was supported by the University of St Andrews (School of Biology); the Scottish Government [Marine Mammal Scientific Support Research Programme MMSS/002/15 and Marine Mammal Scientific Support Research Programme MMSS/001/11]; Department of Environment and Rural Affairs [MB5203/RMP5862 Cetacean Bycatch Observer Monitoring Scheme and MB5203/RMP5862 Cetacean Bycatch Observer Monitoring Scheme] and NOAA Fisheries [Bycatch Reduction Engineering Program]

Author Contributions

CHAPTER 2

Chapter 2 was prepared as a manuscript for publication in JASA and converted into a thesis chapter with some alterations. I formed the concepts, did the analysis and wrote the manuscript. Jonathan Gordon and Doug Gillespie commented on the manuscript before it was converted into a thesis chapter. Peter Madsen (Aarhus University) also provided comments.

CHAPTER 3

Chapter 3 is published in JASA and has been broadly into the thesis as a chapter with some alterations to the introduction and methods. The data analysis was solely performed by me. I initially wrote the manuscript and then the co-authors contributed ideas and text.

Citation:

Macaulay, J., Gordon, J., Gillespie, D., Malinka, C. & Northridge, S., 2017. Passive acoustic methods for fine-scale tracking of harbour porpoises in tidal rapids. *The Journal of the Acoustical Society of America*, 141(2), pp.1120–1132.

CHAPTER 4

Chapter 3 is a manuscript in JASA. It has been copied into this thesis as a chapter with some alterations to the introduction. The data analysis was almost solely performed by me with Chloe Malinka providing analysis of DTAG data. I wrote the manuscript and then co-authors Peter Madsen, Chloe Malinka and Doug Gillespie commented on and made changes to the text.

Citation:

Macaulay, J. D. J., C. E. Malinka, D. Gillespie, and P. T. Madsen. 2020. High resolution three-dimensional beam radiation pattern of harbour porpoise clicks with implications for passive acoustic monitoring. *The Journal of the Acoustical Society of America* 147, pp. 4175–4188.

CHAPTER 5

Chapter 5 was in the early stages of being prepared as a manuscript and was subsequently converted to a PhD chapter. I performed all the data analysis and wrote the manuscript. Comments and some changes to the text of the manuscript have been made by co-authors Danielle Harris (CREEM,

University of St Andrews), Gordon Hastie (SMRU, University of St Andrews), Chloe Malinka, Doug Gillespie and Jonathan Gordon.

Chloe Malinka proofread chapters.

Glossary of Notation and Terms

Term	Description
$\hat{p}_d(SNR)$	The probability of correctly classifying a received transient with respect to it's SNR.
$\hat{p}_f(SNR)$	The probability of falsely classifying a received transient with respect to it's SNR.
χ^2	In the context of this thesis refers to how well observed PAM data matches a model, specifically; *Chapter 2*: Describes the rate of change of descriptors (e.g. bearing, ICI, amplitude) in a click train. If the rate of change of descriptors is slow then χ^2 for the click train will be low. The χ^2 value is used to classify click trains from biological sources. *Chapter 3:* How well observed time delays fit simulated time delays for an animal located at *(x,y,z)*. If the delays are similar, then χ^2 will be low.
-3dB beamwidth	The angle from on-axis at which beam loss drops the click amplitude by 3dB multiplied by two.
4π beam profile	The measurement of all horizontal and vertical angles of a beam profile. i.e. measuring beam loss at all points on a sphere around an animal.
c	The speed of sound in water (~1500ms^{-1}).
$\hat{c}$	Cue rate. The rate at which detected cues are produced. In the context of this thesis this is the average click production rate, not including buzzes.
dB re 1µPa 0p	Zero to peak amplitude measurement in decibels.
dB re 1µPa pp	Peak to peak amplitude measurement in decibels.
dB re 1µPa rms	Root mean square amplitude measurement in decibels.
dB re 1µPa pp at 1m	The peak to peak level measured at 1m range from a source. Used to describe source levels.
Detection Probability/ Probability of Detection ($\hat{P}$)	The probability of detecting a click accounting for animal depth distribution.
Dive tracks, Dive Track Fragments.	Interpolated dive tracks calculated from localised clicks. These are usually fragmented because harbour porpoises have a narrow beam profile and thus during a dive will turn away from or move out of range of the array.
F	Number of buzzes per second.

ICI	Inter click interval. The intervals between clicks; usually refers to the intervals in successive clicks within a click train.
IMU	Inertial Measurement Unit. Measured heading, pitch and roll using a 3-axis magnetometer, accelerometer and gyroscope.
NL	Noise level measurement in dB.
Probability of Localisation ($\widehat{Pl}$)	The probability of detecting a click on a minimum number of hydrophones on a hydrophone array.
R	Range (usually the range from an animal to a hydrophone or prey target)
SD	Standard Deviation
SL	The source level. On-axis amplitude of an animal at 1m.
SNR	The signal to noise ratio. The ratio in amplitude between a click and the background noise in dB.
SNR_{min}	The minimum SNR for a detection to be registered by an automated algorithm
TL	The transmission loss due to propagation in the water column.
Transient	A short sound. Echolocation clicks are an example of transients.
Transient Noise	Unwanted transients. Not necessarily a physical phenomenon as may be a by-product of automated click detection algorithms.

Chapter 1: Introduction

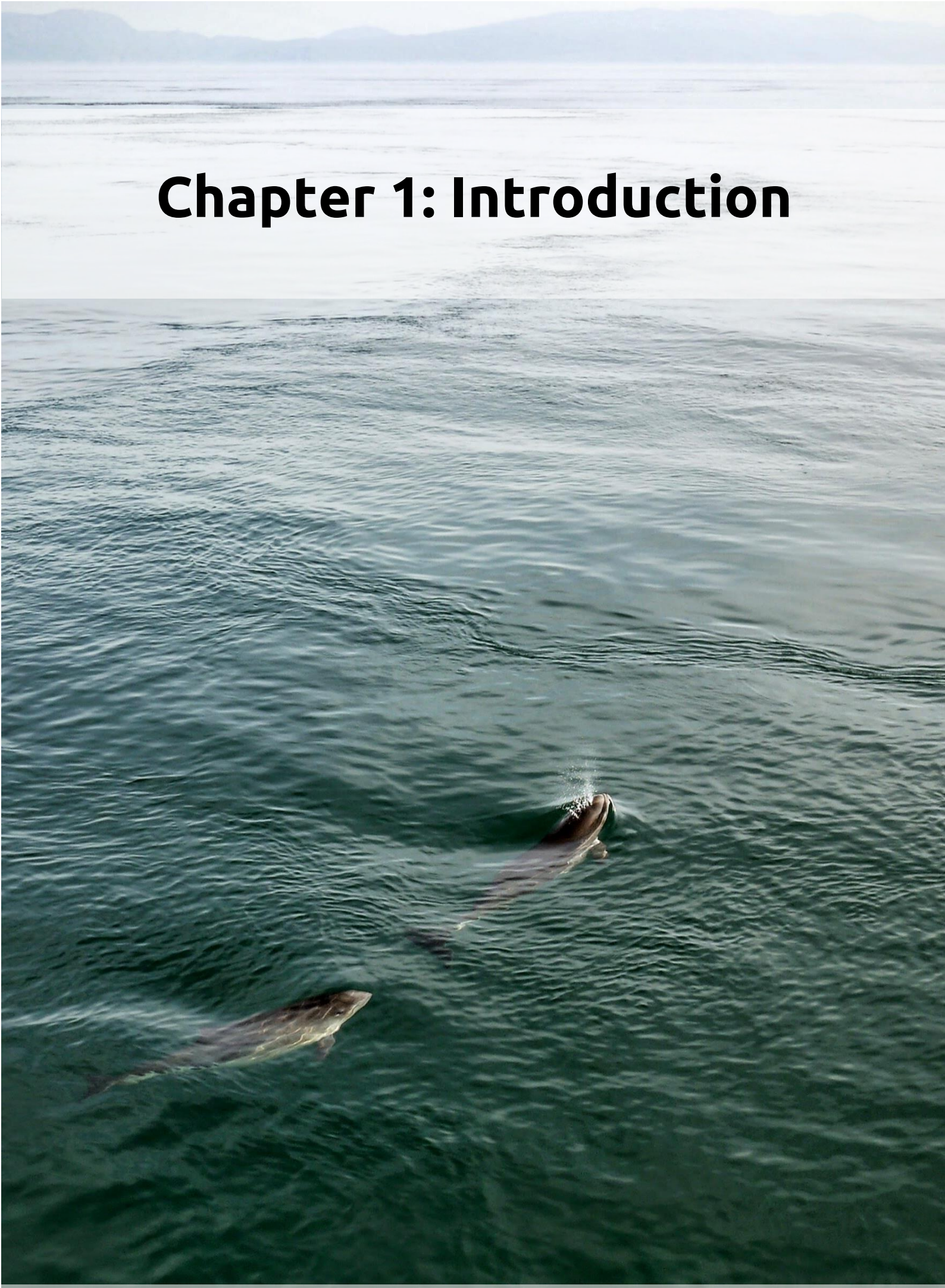

Two harbour porpoises in a tidal stream in the Great Race, Scotland.

Chapter 1: Introduction

Toothed whales (for example sperm whales, dolphins, beaked whales and porpoises) are top predators which enjoy enormous public interest and play a vital regulatory role within their ecosystem e.g. (Lavery et al. 2010) . The ecological diversity of toothed whales, the broad range of marine habitats in which they are found and the fact they feed at high trophic levels, means the status and health of toothed whale populations provides researchers with insights into changes in the broader environment; thus they act as important metrics for conservation and in assessing ecosystem health (Moore, 2008; Bossart, 2011).

Toothed whales are also surrounded by legislation, national laws and intergovernmental agreements. For example, in the United States toothed whales are protected under the Marine Mammal Protection Act and the Species At Risk Act (*U.S. Marine Mammal Protection Act of 1972. 16 U.S. Code Sections 1362 and 1372 (2000).* 1972), in the European Union by the Habitats Directive (European Commission 1992), ACCOBAMS[1] and ASCOBANS[2] and globally, the International Whaling Commission regulates whaling and addresses conservation issues under the International Convention for the Regulation of Whaling (1946). Thus, the monitoring of toothed whale populations is important from a scientific, conservation and often regulatory perspective.

Obtaining information on the distributions, abundance and health of toothed whales is difficult because they spend a large proportion of their time underwater. However, all species of toothed whales studied so far produce powerful transient sounds (clicks) to ensonify their surroundings, and then listen for the weak returning echoes to form an actively generated auditory scene. They use this sophisticated 'biosonar' to hunt, sense their surroundings and, in some cases communicate (Au 1993; Surlykke et al. 2014). Underwater acoustic recordings of these clicks and other vocalisation types provide researchers with a powerful means of acquiring data on the behaviour, biosonar capabilities, ecology and population levels of these often difficult to study animals.

[1] The Agreement on the Conservation of Cetaceans of the Black Sea, Mediterranean Sea and contiguous Atlantic area
[2] Agreement on the Conservation of Small Cetaceans of the Baltic, North East Atlantic, Irish and North Seas

The process of surveying animals using acoustic recorders is termed passive acoustic monitoring (PAM). In a marine context, drifting (e.g. Barlow et al. 2018), towed hydrophone arrays (e.g. Gillespie et al. 2005), hull mounted (e.g. Jiang et al., 2019), glider integrated (e.g. Bittencourt et al., 2018) and static (moored) (e.g. Gassmann et al. 2015) PAM systems have been used to monitor a range of species over extensive spatial and temporal ranges, often requiring very modest resources. At its most basic, PAM studies can determine the presence or absence of a soniferous species within an area (e.g. Wilson et al. 2013). However, more sophisticated PAM hardware, survey strategies (e.g. combining visual and acoustic monitoring) and/or analysis methodologies can be used to calculate fine scale behaviour (e.g. Miller & Dawson 2009) and the absolute density of animals over large spatial and temporal scales (e.g. Thomas et al. 2017; Carlén et al. 2018). The absolute density of a species is a key conservation metric and the ability to accurately and cost effectively obtain such information provides a powerful tool for conservation, management, and regulatory frameworks. However, the statistical framework for density estimation using acoustics is an active area of research (Marques et al. 2013). As such surveys expand, generating larger volumes of data, the need for highly automated and robust analysis methodologies to extract the relevant data from PAM recordings is becoming more urgent

Raw acoustic recordings collected on PAM devices contain an entire soundscape consisting of environmental noise, anthropogenic activity (e.g. boat noise, echosounders, sonar), and vocalisations of any soniferous species present. A key requirement of PAM is the ability to disentangle this complex acoustic scene, extract the vocalisations of the target species or taxa, and then reliably report on behaviour, animal presence, and/or density. Due to the large quantities of data recorded by PAM devices, this process must be semi or fully automated to be efficient, and thus sophisticated computer algorithms are required to initially extract the relevant data from acoustic recordings. This is then followed by additional analysis, such as localisation, and/or statistical modelling to convert the detected vocalisations to relative or absolute animal abundance estimates.

The development of effective PAM algorithms and accurate density estimation models requires some prior information on the expected acoustic properties of and variation in recorded vocalisations. Thus, a typical PAM workflow, from the automated detection and classification of

sounds to localisation and/or abundance estimation, often benefits from or requires a detailed understanding of aspects of the acoustic behaviour of the target species.

This PhD focuses on improving and creating new PAM methods to detect, classify, localise and calculate the density of toothed whale echolocation clicks. Aspects of the acoustic ecology of toothed whales are used to inform the development of these PAM methods which are then applied to calculate the fine-scale diving behaviour, distribution and density of harbour porpoises (*Phocoena phocoena*), in a challenging tidal rapid habitat in Scotland.

1.1 THE BIOSONAR OF A TOOTHED WHALE

Broadly, echolocation clicks can be split into four categories: sperm whales (*Physeter macrocephalus*) produce multi-pulsed 15 kHz (peak frequency) clicks (Møhl et al. 2003), most delphinids and river dolphins, use short broadband clicks (Au 1993, Ladegaard et al. 2015), beaked whales produce longer frequency-modulated pulses (Johnson et al. 2004, 2006) and porpoises (Li et al. 2007, Villadsgaard et al. 2007, Bassett et al. 2009), *Kogia* (Madsen et al. 2005), six species of delphinids (Shapiro et al. 2009, Götz et al. 2010) and one species of river dolphin (Melcón, et al. 2012) have (probably) convergently evolved to produce narrow band high frequency (NBHF) clicks (~130 kHz peak frequency) (Galatius et al. 2019). Despite this variation in the source properties of echolocation clicks, all toothed whales investigated thus far emit clicks in highly directional biosonar beams with similar directivity indices (Jensen et al. 2018).

Toothed whales produce clicks by forcing pressurised air through their right pair of phonic lips (lip like structures just underneath the blowhole) in their nasal complex (Madsen et al. 2013) which then is collimated using the skull and air sacs (Aroyan et al. 1992) to form a directional sound beam that is radiated into the water via an impedance-matching fatty melon on the animal's rostrum (Cranford et al. 1996, Cranford 2000). The directionality of the click is seemingly defined by the size and conformation of phonic lips, skull anatomy, air sac configuration, melon structure and composition, as well as the frequency of the echolocation click. Thus, as smaller species are physiologically constrained by having smaller sound producing structures, they must use higher frequency signals to maintain the same narrow acoustic field of view as larger toothed whales (Jensen et al. 2018). The high directionality of acoustic energy directed out from the melon generates higher source levels along the acoustic axis for the same power, which increases the range at which prey can be detected

in a noise-limited environment whilst also limiting clutter (Madsen and Surlykke 2013). A directional biosonar beam may also serve as a spatial filter of information (Madsen et al. 2013), aid localization of prey targets via a steep intensity gradient (Yovel et al. 2010) and direct sound energy away from their acute auditory system that must detect and process weak echoes milliseconds after the emission of a powerful click (Schrøder et al. 2017). However, whilst a narrow acoustic field of view seems to have been a significant driver in the co-evolution of nasal structures and in the scaling of spectral composition of echolocation clicks across three orders of magnitude of size in toothed whales, other factors, such as acoustic crypsis from killer whales (*Orcinus orca*), have likely also played a role. For example, poor killer whale hearing above 100 kHz may have led to the convergent evolution of NBHF clicks across several small toothed whales (Morisaka and Connor 2007, Kyhn et al. 2013, Galatius et al. 2019). For NBHF species (such as harbour porpoises), the consequence of using NBHF clicks for both echolocation and communication is that their active acoustic space is small and directional ahead of the communicating animal (Clausen et al. 2010, Sørensen et al. 2018), or that they must employ lower frequency clicks for communication (Martin et al. 2018). Thus, the source parameters and beam pattern of clicks used for both echolocation and communication are inextricably linked and valuable for understanding toothed whale sensory and evolutionary biology in the context of social behaviour, predator-prey interactions, foraging ecology and niche segregation (Madsen and Wahlberg 2007, Madsen and Surlykke 2013).

Echolocation clicks are not produced in isolation; toothed whales (and bats) produce clicks in specific sequences in which the interval between subsequent clicks and source level is dependent on the behavioural state of the animal. During foraging, echolocators generally emit a series of clicks at a relatively slow rate and then, once a prey target has been identified, begin an approach phase maintaining a decreasing inter click interval (ICI) which is slightly longer than the two way travel time (TWTT), i.e. the time for a click to reach the target and the echo to return to the animal plus a lag time in which processing occurs (Surlykke et al. 2014). The lag time has been reported as typically between 20 and 50 ms (Morozov et al. 1972, Au et al. 1974, Penner 1988) and is proposed to be the time it takes for the central nervous system of an animal to process a received echo (Au 1980, Au and Scheifele 1994). Maintaining an ICI above the TWTT is presumed to prevent range ambiguity, i.e. it prevents an animal confusing the range at which returning echoes are originating from between. However, deep diving animals such as sperm whales, Risso's dolphins (*Grampus griseus*) and

Blainville's beaked whales (*Mesoplodon densirostris*) often do not couple ICI with TWTT whilst approaching prey, instead maintaining a near constant ICI. It is theorised that in deep ocean environments this strategy may help maintain a longer range acoustic scene without the reverberation and acoustic clutter that would be expected in more shallow environments, potentially increasing foraging efficiency if multiple prey species are present (Madsen 2005, Fais et al. 2016, Jensen et al. 2020). Once the target is at short range, all toothed whales studies so far complete the approach click sequence with a terminal buzz, a series of very rapid clicks but with an ICI still greater than the TWTT (e.g. Johnson et al. 2004; Madsen et al. 2010; Wisniewska et al. 2016)

During this approach phase of echolocation, both bats and toothed whales also lower their source levels sustaining a roughly consistent ensonification of the target as decreasing range results in a decrease in transmission loss (Rasmussen et al. 2002, Au and Benoit-Bird 2003, Surlykke et al. 2014). It has been theorised that toothed whales may be physiologically constrained by a constant nasal pressurisation which effectively results in an automatic gain mechanism by which source level is reduced as ICI decreases (Au and Benoit-Bird 2003). This automatic gain control (AGC) is predicted to follow a "20log(*R*)" relationship (where *R* is range), and thus as an animal approaches a target, source levels significantly reduce. However, this is contradicted by several studies. Firstly, bottlenose dolphins (*Tursiops truncatus*) have been shown to only exhibit AGC near the terminal buzz phase as ICI drops below 30-40 ms (Jensen et al. 2009), harbour porpoises appear to change source level depending on how reverberant the surrounding environment is (Ladegaard and Madsen 2019), humpback dolphins (*Sousa sahulensis*) deviate substantially from this relationship (de Freitas et al. 2015), Ganges river dolphins (*Platanista gangetica*) show no relationship between source level and range (Jensen et al. 2013), and sperm whales, beaked whales and Risso's dolphins in deep water environments appear to exhibit little gain control until just before the terminal buzz phase (Madsen 2005, Fais et al. 2016, Jensen et al. 2020). Reduction in source level therefore appears to be both species-dependent and at least somewhat under cognitive control and thus a generalised rule for source level in relation to ICI is difficult to construct.

Whilst different species of echolocators share a context-dependent but somewhat generalised relationships between range, ICI, source level and beamwidth during foraging, the absolute values of ICI and source level are highly species specific, usually scaling with size (Jensen et al. 2018). For example, sperm whales - the largest toothed whale - produce clicks every ~0.5-2 s on average

(Whitehead and Weilgart 1990, Goold and Jones 1995, Douglas et al. 2005) whilst harbour porpoise, amongst the smallest species, click every 20 to 300 ms whilst searching for prey (Akamatsu et al. 2007, Verfuß et al. 2009) with average clicks rates (excluding buzzes) as low ~3600 clicks per hour also reported in tag studies (Linnenschmidt et al. 2013). Outside of using echolocation for tracking prey targets, different species can also exhibit unique clicking behaviour. For example, sperm whales produce codas, click sequences which are unique to specific groups and form the basis of sympatric cultural variation (Rendell and Whitehead 2003). Harbour porpoises, which, like sperm whales have a vocal repertoires entirely consisting of clicks, produce rapid buzz-like vocalisations with specific ICI patterns for communication (Clausen et al. 2010, Sørensen et al. 2018). Additionally, multiple delphinid species have been recorded generating brief bursts of ultra-high click rates (<20 µs) termed "burst pulses", likely used in social interaction (Dawson 2010). Longer range echolocation can also vary, with bottlenose dolphins observed producing short bursts of clicks, termed "click packets", which are theorised to be beneficial for long range target detection (Ladegaard et al. 2019).

A final layer of complexity in click train sequences results from the ability of animals to adjust the shape of their biosonar beam, often at low ICI or during the terminal buzz phase of prey capture. Significant widening of the half-power beamwidth has been observed in a captive bottlenose dolphin (Moore et al. 2008), wild Atlantic spotted dolphins (*Stenella frontalis*) (Jensen et al. 2015), amazon river dolphins (*Inia geoffrensis*) (Ladegaard et al. 2017), and harbour porpoises (Wisniewska et al. 2015), and is likely an adaptation to prevent prey escaping from the acoustic field of view of the animal in the final phase of prey capture.

1.2 PAM DETECTION/CLASSIFICATION AND DENSITY ESTIMATION

Any visually cryptic species which regularly produces detectible sounds is particularly suited for PAM. The independent evolution of echolocation in several different taxa (for example toothed whales, bats (e.g. Surlykke et al. 2009, 2013, Jakobsen et al. 2015), shrews (Forsman and Malmquist 1988), and at least 16 bird species (Price et al. 2004, Brinkløv et al. 2013)) has been driven by animals exploiting an environment where there is limited light to hunt and/or navigate surroundings. Echolocating species are then necessarily often difficult to visually study in their natural environments and, if their echolocation calls are readily detectible, PAM can be an especially useful monitoring methodology. The majority of toothed whales and bats fall into this category because

they regularly produce relatively high amplitude sounds. For example, bats, which are generally nocturnal, and share a remarkable functional convergence with toothed whales in the operation of their biosonar (Madsen and Surlykke 2013), are regularly monitored using PAM (e.g. Barlow et al. 2015, Newson et al. 2015, Mac Aodha et al. 2018). In underwater environments, sounds travels much further and faster than in air and thus it is perhaps not surprising that PAM has been widely used for decades to study cetaceans (for review see Booth et al. (2017)). However, whilst the acoustic recordings from PAM devices contain a wealth of ecological and behavioural information, there are significant analysis hurdles which must be overcome to make best use of data.

The goal in analysing PAM data is to extract vocalisations from raw data and then translate those data into inference about behaviour and/or presence/abundance of a certain species or taxa. PAM analysis is generally split into a series of concurrent processes – detection and classification which may then be followed by localisation and then density estimation - all of which must consider multiple aspects of the acoustic behaviour of the target species.

1.2.1 Detection and Classification

The analysis of PAM data can be achieved via automated computer algorithms and/or by manual analysis. Computer algorithms have the great advantage of being fast, however, they are complex to create, in general do not cope well with unexpected noise sources, and often require unique set-ups or customised training prior to application to different datasets. The process of manual analysis is slow and often inconsistent between analysts, but it can deal with unexpected discrepancies in data and is particularly adept at pattern recognition. For example, a security measure often used on the internet, CAPTCHA, or "Completely Automated Public Turing test to tell Computers and Humans Apart", requires the recognition of twisted letters with lines through them. This is something most humans have little problem in solving, but has been a significant challenge for computer algorithms (Von Ahn et al. 2008). Despite some of the advantages of manual analysts, automated or semi-automated algorithms (where there is minimal amount of manual input) are now increasingly a requirement of PAM, mainly due to the ever-increasing quantities of data collected by less expensive and more accessible hardware.

The key requirement of an automated analysis algorithm is to be able to identify and correctly classify as many relevant sounds as possible (true positives) whilst also minimising vocalisations which are

incorrectly classified (false positives). These two metrics, true positives and false positives, are inextricably linked – increasing one often increases the other, and both are generally highly dependent on the signal to noise ratio (SNR) of a received signal (Urick 1983).

Thus, no automated detector or classifier will (or can ever) be perfect, but assuming performance is somewhat reasonable, many applications simply require that a detector or classifier's performance according to differing SNR levels is quantified (e.g. Küsel et al. 2011). However, in some situations knowledge of detector performance is insufficient and optimising detection efficiency and minimising false positives is absolutely crucial. Caillat et al. (2013) showed that, in the situation of a mixed species group, where one species is much rarer than the other, then large errors in density estimation can occur for the rare species, even if the misclassification rate of an algorithm is well known. This is because the misclassification of sounds is inherently a random and independent event. Thus, for a given set of detected clicks, even if the average misclassification rate of a classifier is known, the actual number of sounds misclassified may vary somewhat. If one species is much more acoustically common than another, then that uncertainty in the exact number of misclassifications leads to large errors in the rare species density estimates. This is a fundamental challenge in PAM which requires the development of adequate classifiers with low misclassification rates, especially in situations where rare species are studied.

In the context of toothed whales, there are two primary target vocalisations to detect: whistles and echolocation clicks. Some species of toothed whales produce tonal narrowband, frequency modulated vocalisations termed whistles (amongst other vocalisations). These are less directional (Branstetter et al. 2012) and significantly longer and lower in frequency (2-30kHz) than most echolocation clicks. However, whistles are not produced continually (e.g. Jensen et al. 2011), production rate is dependent on social context (Quick and Janik 2008) and they are often highly complex and variable. Extracting whistles automatically from PAM data thus represents a significant analysis challenge. All toothed whales so far studied produce echolocation clicks. The fact that most species regularly produce clicks (with the exception of some taxa such as beaked whales which do not click or whistle at the sea surface (Zimmer et al. 2005, Aguilar de Soto et al. 2012)) is a significant advantage in PAM studies as an animal within range of a recorder is likely be detected. However, clicks of many species are relatively high frequency and thus specialised recording equipment is required to record them. The complex and context-dependent interplay between ICI, source level

and beam width within click sequences, as discussed in the previous section, also has significant implications for the analysis of received echolocation clicks.

1.2.1.1 Whistles and PAM

The automated detection and classification of toothed whale whistles has been a focus of methodologic development in passive acoustic monitoring for many years. Information on species type and behaviour is encoded in the spectral contour of a whistle (e.g. Steiner, 1981) , however, invariably in social interactions there will be many animals present and so received data on a PAM device often consists of many overlapping whistles. This is then further confounded by overlapping echolocation clicks and, due to amplitude modulation (e.g. Lammers et al., 2003) and frequency dependent attenuation, a frequency and time dependent variable SNR within contours.

Thus, the detection and classification of whistle contours can represent a particularly difficult pattern recognition problem for automated PAM algorithms. Tracing individual time x frequency contours is often the preliminary goal in whistle detection and classification primarily because near complete contours likely contain the best set of information for species classification (Oswald et al. 2007) and are often vital if used in behavioural studies, for example in detection of signature whistles (e.g. Quick and Janik 2012). There have been numerous attempts to automate the whistle contour extraction, usually based on the frequency time representation of acoustic data on a spectrogram. Most methods initially involve the detection of peaks or pixels on the spectrogram followed by an attempt to join the detected peaks together using a variety of algorithms, for example Kalman filters (Mallawaarachchi et al. 2008, Kershenbaum and Roch 2013), particle filters (White and Hadley 2008, Roch et al. 2011b) and phase tracking (Johansson and White 2011).

Interestingly, there are a subset of papers which have used a similar evaluation dataset (from the 5th International Workshop on Detection Classification, Localisation and Density Estimation (DCLDE) of marine mammals held in Oregon in August 2011) that contains annotated whistle contours from 6 different species of delphinid. Gillespie et al. (2013) used a series of click and noise removal algorithms followed by a connected region search to extract whistle contours. These were usually fragmented and so a species classification methodology which further split fragments to a uniform size and analysed their statistical distribution was utilized, providing correct classification rates of up to 58 - 94% which was the highest classification performance at the conference. The integration of the algorithm into open source software has subsequently facilitated it's use in other studies (e.g.

Erbs et al., 2017). Roch et al. (2011) used an alternative methodology, testing both a particle filter and graph based approach to attempt more complete whistle contour extraction and achieved an overall precision of 86%, recall of 76% and average of 1.2 detected fragments per manually annotated call. Gruden and White (2016) then slightly improved on this methodology using a multi target tracking algorithm (Gaussian mixture probability hypothesis density filter) to achieve a precision of 85% and recall of 71.8% with a similar fragmentation (1.2). Neither Roch et al. (2011) or Gruden and White (2016) attempted species classification.

More recently, deep learning methods have been applied to the detection and classification of tonal vocalisations. Initial approaches usually involved passing a raw snippet of sound, in the form a spectrogram image, directly to a deep learning model; this resulted in remarkably high performance e.g. orca calls ~95% precision and recall (Bergler et al. 2019) or orca/pilot whale (>95% precision and recall) (Jiang et al. 2019). Although these preliminary studies showed significant promise, they required extensive training datasets and were unable to trace whistle contours, potentially limiting their efficacy for some PAM applications. However, recently, the first deep learning implementation of a contour tracing algorithm has been tested on the DCLDE 2011 dataset and achieved a 25% increase in performance over the previously mentioned contour tracing algorithms (Li et al. 2020 preprint). Interestingly, this deep learning approach to contour tracing required minimal annotated data, instead relying on the generation of synthetic training data to generate substantial performance gains; minimising the requirement for large quantities of training data likely makes this method far more practical to deploy widely in PAM applications. However, despite this rapid progress, in general, from the literature to date, it is still unclear how robust deep learning algorithms are to inconsistencies in data for which they have not been trained. Thus, it remains unclear how stable deep learning based approaches are for more expanded general use in PAM. This will undoubtedly be a focus of further research into what is a promising methodology and likely future direction of PAM detection and classification algorithms.

1.2.1.2 Echolocation clicks and PAM

The detection and classification of echolocation clicks often involves the extraction of any transient sounds from acoustic data which could possibly be echolocation clicks, followed by the classification of these sounds to species level. The differences in the acoustic properties of clicks between different species and the behaviour encoded within the timing of the click sequences mean that PAM

for echolocation clicks has the potential to be used to both identify species and categorise some behaviour of toothed whales. However, narrow beam profiles and variation in output levels introduce significant complexity in interpreting received acoustic data. A physical consequence of producing a narrow echolocation beam is the angle-dependent distortion in both the waveform and the spectra in off-axis clicks (Au et al. 2012, Ladegaard et al. 2015), something which is further confounded by frequency-dependent attenuation in seawater (Ainslie and Mccolm 1998, Ainslie 2013). Thus, as an animal scans across a PAM receiver, the waveform, spectra, and received amplitude (and thus signal-to-noise ratio (SNR)) of clicks vary significantly as a function of both the received angle, the range to the animal, and its current behavioural state. This variability is further confounded by the overlap of acoustic features of clicks with other co-occurring sources of transients (e.g. anthropogenic, snapping shrimp, sediment movement) (from now on termed *transient noise*) and in some circumstances, the echolocation clicks of other non-target species, posing a significant analysis challenge.

An automated algorithm designed to detect and classify echolocating animals must be able to deal with large variations in the waveform, spectra, and SNR of clicks received on a PAM device. Even for taxa with highly stereotyped clicks, such as porpoises and beaked whales, this can be a substantial challenge, with the performance of different types of automated algorithms (often called 'detectors') varying significantly (Yack et al. 2010, Sarnocinska et al. 2016). For delphinids, which generally have less stereotyped clicks that share many acoustic characteristics with different types of transient noise, species classification is a considerable and ongoing analytical challenge (Gillespie and Caillat 2008, Roch et al. 2008, 2011a, Frasier et al. 2017, Luo et al. 2017). One potential option to aid in acoustic classification of echolocation clicks is to exploit our understanding of the acoustic behaviour and foraging ecology of echolocators. The slowly varying click sequences of odontocetes received on a PAM device, as well as the identification of behavioural states, are potentially very useful indicators for the identification of clicks or click trains within a complex soundscape (e.g. Gerard et al. 2008, Roberts and Read 2015, Le Bot et al. 2015), primarily because confounding transient noise usually does not occur in regular, slowly varying sequences (an exception being the regular pulsed tones produced by boat echosounders). By grouping clicks together, the spectra can be averaged which has the advantage of averaging and smoothing the spectrum which will likely improve the performance of classification algorithms. Additionally, in some taxa, where species-

specific features are only distinguishable once many clicks have been averaged, grouping clicks may aid in species classification. For example, dolphin spectra averaged over many clicks show specific peaks and troughs (Soldevilla et al. 2008) which can be used to classify individual dolphin species (Frasier et al. 2017).

Thus, the automated extraction of both whistles and echolocation clicks represents a complex, context dependent and ongoing analysis challenge. The difficulties in designing and training algorithms which are sophisticated enough to deal with the myriad of biological and environmental variation in received PAM data is further confounded by a lack of co-ordination in testing the efficacy of new methods. It is a general trend in the literature that the there is almost no consistency in the data used to test novel detection and classification algorithms for both clicks and whistles (with a few of the exceptions noted above) and thus comparison between different algorithms is difficult. Even if detection and classification algorithms could be easily compared, their usefulness for PAM can only truly be determined once they have been exposed to a large variety of data of different contexts. This is often time prohibitive, however, can be somewhat facilitated by making the algorithms open source and crucially, accessible, so that they can be used and tested in other studies (e.g. Rankin et al. 2017, Erbs et al. 2017). It should also be noted that in most of the above studies, the training data has been manually annotated by an expert. In many cases, the data has been categorised to species or group of species based purely on acoustic properties (e.g. Frasier et al. 2017) and has not been ground-truthed using, for example, visual studies. Acquiring ground-truthed data at sea, especially around long-term recorders, is not always feasible and thus using training or testing data based on expert opinion is required to enable further progress in developing automated analysis methods.

1.2.2 Localisation

Localisation is the process by which PAM data are used to obtain some type of location information of a soniferous animal (such as bearing or range to the animal, depth and/or precise 3D location). This can be used to study diving behaviour (e.g. Miller & Dawson 2009), acquire source levels and beam profile measurements (e.g. Ladegaard et al. 2017), investigate social interactions (e.g. Quick & Janik 2012) or determine distance for density estimation (e.g. Barlow & Taylor 2005).

Relatively simple localisation methods can be used to determine bearings to animals, for example utilising simple directional hydrophones to track sperm whales (e.g. Whitehead & Gordon 1986) or hydrophones coupled with particle velocity sensors, such as DIFAR Sonobuoys, to locate baleen whales (e.g. Miller 2012).

The most analytically complex localisation methods take advantage of the fact that acoustic signals do not necessarily travel in a straight line. They are warped by sound speed, depth and salinity gradients and reflect off the seabed and sea surface (Porter and Bucker 1987). If detailed oceanographic information of an environment is known (such as bathymetry, bottom type, and sound speed profile) then the predicted propagation of acoustic signals can be exploited to provide location information. For example Tiemann et al. (2006) used received multipath sperm whale clicks, ray tracing models and knowledge of complex bathymetry to track sperm whale dives in three dimensions using a single hydrophone, and Thode (2005) exploited bottom echoes and ray refraction to enhance the capabilities of a towed hydrophone array, allowing sperm whale foraging depths to be calculated. As acoustic signals propagate, they are subject to frequency and environment dependent interference and attenuation often resulting in a received vocalisation being both dispersed in time and distorted in frequency. If the source signal and surrounding acoustic environment are accurately known then, for a source at a given location, the likely dispersion and distortion of a signal at the location of a receiver can be computed; therefore by comparing simulated and received acoustic data, a source location can be estimated, a method known as matched field processing (Baggeroer et al. 1988, Thode et al. 2000, 2006, Wiggins et al. 2004). Matched field processing has practical application, e.g. for density estimation of right whales (Marques et al. 2011), however, it is difficult to use with toothed whales because the distortion in a received signal is confounded by the distortion due to the beam profile of animals.

However, by far the most common method for acoustic localisation is to use multi hydrophone arrays (multiple hydrophones at known locations). The time delays between a given vocalisation arriving at different receivers within an array can be used to calculate the location of an animal (Watkins and Schevill 1972). This method has the advantage of not requiring specialised direction-finding sensors or detailed information on acoustic propagation conditions (although this can improve accuracy). The most widespread type of PAM array is the linear towed hydrophone array, which can only measure bearings to a single received vocalisation (with left/right ambiguity) but is capable of determining a

range to a continuously vocalising animal over time using target motion analysis (Leaper et al. 2000). Since towed arrays can calculate a range to an animal, they are ideal for distance sampling (a statistical framework to determine animal abundance (Buckland et al. 2001)). Therefore, when used as part of well-designed line transect survey, and usually combined with a concurrent visual study, towed hydrophone arrays can be used to calculate the absolute density of cetaceans in a surveyed area (e.g. Barlow & Taylor 2005; Lewis et al. 2007; Gordon et al. 2011). However, simple linear towed hydrophone array systems usually calculate distances with large uncertainties (von Benda-Beckmann et al. 2013), and therefore are not suitable for studies where detailed data on the behaviour or movements of individual animals is required. An alternate methodology is the use of large aperture arrays which utilise multiple widely spaced hydrophones to precisely locate individual vocalisations and thus can be used to track the fine scale movements of animals underwater (as opposed to towed arrays which usually require multiple received vocalisations to determine distance).

There are multiple approaches to designing and deploying large aperture arrays. For example, groups of autonomous clusters of hydrophones placed on the seabed have been used to track the diving behaviour and movements of beaked whales (Wiggins et al. 2012) and harbour porpoises (Malinka et al. 2018) whilst floating time-synced buoys have been employed to determine the spiral 3D dive profile of sperm whales (Miller and Dawson 2009). Vertical arrays, where hydrophones are arranged in a rigid or flexible linear vertical configuration, are perhaps the most commonly employed design of large aperture array. These are usually deployed from drifting research vessels or buoys and have been has been used in a large number of studies, for example to study sperm whales (Møhl et al. 2000, Wahlberg 2002, Heerfordt et al. 2007), Risso's dolphins (Madsen et al. 2004), killer whales (*Orcinus orca*) (Holt et al. 2009), bottlenose dolphins *(Tursiops truncatus)* (Hastie et al. 2006), Indo-Pacific bottlenose dolphins (*Tursiops aduncus*), humpback dolphins (de Freitas et al. 2015), narwhals (*Monodon monoceros*) (Koblitz et al. 2016), finless porpoises *(Neophocaena phocaenoides)* (Ural et al. 2006), and harbour porpoises (Villadsgaard et al. 2007, Kyhn et al. 2013). Vertical arrays have the advantage of being both relatively compact and are usually able to be deployed and recovered relatively quickly from research vessels.

As with detection and classification, it is important to consider aspects of the biosonar properties of a study species, primarily it's beam profile, before designing a large aperture array for acoustically localising echolocation clicks. In general, the more widely separated the hydrophones are, the more

accurate localisations will be because any fixed error in time delay measurements (e.g. ambiguity in cross correlation (Gillespie and Macaulay 2019)) will be proportionally smaller. An often-used rule of thumb is that a large aperture array can only localise to ten times the array aperture (the distance between outermost elements), although this is heavily caveated and dependent on the number and distribution of receivers (see Chapter 3). For a 2D location (depth and range) to be determined, a minimum of 3 hydrophone elements must detect a vocalisation, and for an unambiguous a 3D location, at least 4 elements, distributed in three dimensions, are required (assuming only time delay measurements between receivers are utilised) (Wahlberg et al. 2001). The ensonification of multiple elements in an array can be problematic when studying toothed whales due to the narrow beam profile of their echolocation clicks, and the high attenuation of high frequency clicks in seawater (e.g. harbour porpoises) (Ainslie and Mccolm 1998). If hydrophone elements are too widely spaced, these factors can mean that an insufficient number of hydrophones are ensonified by a given click. Thus the spacing of hydrophones in arrays is a trade-off; hydrophones must be spaced sufficiently close together for a minimum number to be *consistently* ensonified by highly directional vocalisations, but sufficiently separated to allow accurate localisation at useful ranges (Wahlberg et al. 2001).

Typical biosonar behaviour is also important in localisation and particularly in the design of large aperture arrays. Most clicks are effectively indistinguishable between different individuals, so far as is currently known. Therefore, if the ICI of any one animal is very low and/or two or more individuals are vocalising at the same time, and/or a hydrophone array is deployed in a highly reverberant environment, then matching clicks from the same animal on different hydrophones can be difficult, a problem from now on termed "click aliasing". Mismatching clicks on different hydrophones introduces large errors in localisation and hence it is important that either robust *click matching* algorithms are used, or that all hydrophones in the array are spaced closely together to minimise click aliasing. Specifically, the typical ICI of an animal should be more than half the maximum spacing between hydrophones divided by the sound speed. The issue of click aliasing has previously been addressed for data collected on large aperture arrays for some species or taxa; Baggenstoss (2013) proposed a method to track beaked whale clicks by using a 'correlelogram' (analogous to a spectrogram but replacing spectra with cross correlation functions) of time delay measurements to create time delay contours for pairs of hydrophones. These contours were then associated by comparing different pairs of hydrophones which share the same hydrophone. Nosal (2013) proposed

a method whereby a likelihood surface is created for every possible time delay measurement between hydrophone pairs. The surfaces between all pairs are then multiplied together and persistent peaks over multiple calls above a threshold are clustered and extracted, allowing for the positions of multiple whales to be determined. The detection and classification of click trains, rather than individual clicks can also be advantageous for click matching. For example, Baggenstoss (2011a) developed algorithms to remove echoes and obtain click trains of individual sperm whales on different hydrophones within an array. Baggenstoss (2011b) then correlated these click trains and used the resulting time delay measurements to create multiple localisation solutions, applied weights to each, and began a pruning process to remove unlikely solutions, thus ending up with correct positions of one or more animals.

Many of the localisation methods above are taxa dependent. For example, the matched field processing only works well for low frequency less directional vocalisations of baleen whales and directional hydrophone systems usually do not record at sample rates high enough for the clicks of many species of toothed whales. Any localisation method requiring detailed propagation modelling will become problematic at high frequencies: for example, although harbour porpoises clicks can be refracted by sound speed gradients (DeRuiter et al. 2010) and will reflect off the sea surface and seabed, the high frequency of their clicks means that small surface waves and fine scale changes in bathymetry will significantly affect propagation. Thus, accurate propagation modelling of porpoise clicks requires highly detailed environmental information. Click matching methods can also be species dependent; the click matching algorithms mentioned above have only been tested with seabed mounted wide baseline arrays on sperm whales and beaked whales, and may not be applicable to other types of clicks and/or arrays (e.g. vertical arrays). For example the cross correlation function of two porpoise clicks has many similarly sized peaks (Gillespie and Macaulay 2019) and so NBHF clicks used with the click matching methods proposed by Baggenstoss (2013) could produce noisy correlograms which would make contour extraction difficult.

1.2.3 Density Estimation

PAM can be used to calculate animal density in a given area - a key metric for conservation and regulatory frameworks. There are several analytical approaches to density estimation using PAM

which are usually dependent on the type of survey performed (Buckland et al. 2005, Marques et al. 2013).

The most common PAM density estimation method is to use localising towed hydrophone arrays, as described in the previous section. Towed arrays have the great advantage in that they often increase sample size compared to visualise studies (e.g. Barlow & Taylor 2005), and like visual studies, can calculate the distances to detected animals. These distances allow the probability of acoustically detecting an animal or group of animals to be calculated, a key parameter in estimating density that accounts for animals which go undetected during the survey (e.g. Lewis et al. 2007; Gordon et al. 2011). However, towed array surveys require a vessel to survey on pre-defined track lines, and therefore, primarily due to the cost of using dedicated research vessels over extended periods of time, they often only provide a snapshot of animal abundance.

Fixed or drifting acoustic sensors can cost-effectively survey an area over much longer time scales compared to towed arrays, potentially allowing temporal trends in abundance to also be calculated (Gerrodette et al. 2011, Thomas et al. 2017, Barlow et al. 2018). Such sensors are advantageous because they are less likely to disturb animals compared to a research vessel (e.g. Palka & Hammond 2001; Wisniewska et al. 2018) but usually require some additional information to estimate the probability of detecting a vocalisation if they cannot calculate distances to animals. In distance sampling, this can be achieved by performing additional studies where the locations of animals are tracked (e.g. using visual or acoustic localisation) around a PAM device and then used to calculate a probability of detection. This may subsequently be applied to data collected on other devices or at other times (e.g. Kyhn et al. 2012; Carlén et al. 2018). If no such auxiliary location data are available to directly measure the detection probability, another approach is to use Monte Carlo simulations to model a value for the probability of detection. These simulations require inputs such as accurate source level distributions, the beam profile and diving behaviour of a given species to produce accurate results (Küsel et al. 2011, Frasier et al. 2016, Hildebrand et al. 2019).

An alternative option for determining animal density acoustically is to use spatially explicit capture recapture (SECR) which uses a different statistical framework to distance sampling and does not require direct estimations of the probability of detection as an input (Efford et al. 2009, Borchers et al. 2015). Applying SECR to acoustic data requires the same signal to be received on multiple

receivers but additional data can also be incorporated, such as bearing information to animals, to improve results (Stevenson et al. 2015, Kidney et al. 2016). Acoustic SECR is relatively novel and only simple approximations of highly directional vocalisations have so far been incorporated into the framework (Stevenson 2016), thus more work is needed for application to toothed whales. Despite this, SECR shows significant potential for acoustic density estimation in the future.

Both distance sampling and SECR, when used in conjunction with PAM data, require an estimation of either cue rate (in this case the average number of clicks per second) or group size, as well as quantification of the performance of automated classifiers (e.g. Marques et al. 2009). Thus, no acoustic method of density estimation for toothed whales can be conducted accurately without some auxiliary information on the echolocation behaviour of the target species, and in some cases, such as in the use of Monte Carlo simulations methods for detection probability, a comprehensive understanding of aspects of toothed whales biosonar (e.g. fully described beam profiles) and acoustic and diving behaviour.

1.3 TIDAL RAPIDS

The effectiveness of using PAM to detect echolocation clicks and subsequently calculate animal density is predicated on the use of effective automated algorithms for detection, classification and potentially localisation, all of which require knowledge on varying aspects of a target species biosonar and acoustic behaviour. If all these aspects are used in conjunction properly, PAM has the potential to be a highly cost-effective methodology for both studying animal behaviour and density estimation.

However, PAM is still a fast-developing field; there has been substantial progress but still little agreement amongst researchers on optimal automated detection algorithms, there are few off-the-shelf hardware packages capable of localisation, and density estimation continues to evolve with emerging statistical methods. This PhD develops detection, classification and localisation algorithms and studies aspects of the biosonar of a captive harbour porpoise, in order to apply PAM density estimation methods to a particularly difficult to-study habitat, tidal rapids. These methods are used to determine the fine scale behaviour, distribution and density of harbour porpoises in tidal rapid habitats.

Tidal rapid habitats are areas in which bathymetry and large tidal ranges generate fast moving currents, usually around headlands or in narrow channels between islands. Fast currents interact with the topography of the seabed, creating upwellings, eddies, and standing waves, creating an area with a generally higher sea state than surrounding areas (Davies et al. 2012). This creates a predictable structure to a tidal rapid area, with different eddies, boils, fronts, *etc.*, appearing at set times within the tidal cycle (Benjamins et al. 2015). These unique and highly energetic environments are thought to increase foraging opportunities for marine predators and aggregate marine species, with correlations with tidal phase reported in many tidal rapid habitats (e.g. Zamon 2003, Waggit et al. 2017, Hastie et al. 2016)

A narrow corridor of fast moving water will result in the number of prey passing over a particular area per unit time increasing, however, water is an incompressible fluid in which both predator and prey (marine mammals and fish in this instance) are immersed and interact with and are subject to the same currents *etc.*; therefore it does not necessarily follow that a tidal rapid should confer any advantage to a predator. The exact motivation behind the increased numbers of large megafauna in some tidal rapids remains uncertain. It has been suggested that animals can place themselves in certain positions of the eddies and currents in order to optimise foraging success by targeting prey which may have been displaced or disorientated due to the strong tidal flows. For example, several studies have suggested that schools of fish may be disorientated or broken up by eddies, leading to increased vulnerability to predators (Enstipp et al. 2007, Crook and Davoren 2014). It has also been suggested that fish in tidal rapids are pushed to the surface by strong currents which could reduce the energetic cost of foraging dives for predators. Hall (2011) proposed that prey pass through small area at specific times, leading to a 'conveyor belt' of predictable and abundant food, however, for this to be effective predators, they would need to balance the energetics of swimming in high current areas with the advantages offered by increased foraging success. One obvious strategy would be to utilise a lower current area, e.g. an eddy, to lay in wait as prey pass by. None of these hypotheses have been thoroughly empirically tested; however, several studies have demonstrated what is likely unique foraging behaviour of marine mammals in tidal rapids.

Hastie et al. (2016) showed that 19 tagged harbour seals spent a high proportion of their time in narrowest part of a tidal rapid channel and observed multiple surfacing where seals had caught Atlantic mackerel (*Scomber scombrus*), not a usual part of their diet. Active sonar methods were later

utilised to demonstrate that seals favoured mid water column dives, suggesting a different foraging strategy compared to non-tidal areas where seals generally dive to, or close to, the seabed (Hastie et al. 2019). Passive acoustic localisation has also been used to study the fine scale behaviour of marine mammals in tidal rapids. Hastie et al. (2006) used a drifting vertical hydrophone array to study bottlenose dolphin behaviour in a narrow channel at the entrance to the Cromarty Firth, Scotland. Here, dolphins were observed consistently diving near the seabed whilst foraging and emitting isolated instances of characteristic acoustic behaviour ('brays') Janik (2000) suggesting that the dolphins were feeding on large fish, probably Atlantic salmon.

There is limited evidence suggesting harbour porpoises both frequent and forage in tidal habitats. Larger scale surveys of harbour porpoises have shown that density is best described by slope and *low* current areas (Embling et al. 2010, Booth et al. 2013), however, these analyses were performed at large spatial scales, and so it is likely that the importance of geographically small areas, such as tidal habitats, would have been missed. More focused studies note a habitat preference, larger group sizes, and/or unusually high concentrations of harbour porpoises in high energy tidal sites (Goodwin 2008, Marubini et al. 2009), with Gordon et al. (2011) reporting one of the highest ever recorded densities of harbour porpoises in the UK near the Bishops and Clerks rocks in Wales. An array of seafloor moored passive acoustic loggers has been used to show that harbour porpoise presence in tidal areas changes at very small spatio-temporal scales (Benjamins et al. 2017). Additionally, there have been attempts to use drifting PAM systems to determine the presence and absence of animals, however, there is currently no statistical framework to calculate absolute animal densities using these drifters (Wilson et al. 2013).

There have been no comprehensive sub-surface studies of harbour porpoise behaviour in tidal rapid sites. Studies performed so far of the fine scale behaviour of toothed whales in tidal rapids have primarily used visual methods; porpoises have been observed maintaining station within tidal races in the UK (Pierpoint 2008), Canada (Hall 2011), and Japan (Akamatsu et al. 2010) with the suggestion that animals may be intercepting or ambushing prey carried in fast moving water. However, in one of the few PAM studies taking place in a tidal rapid, Benjamins et al. (2016) suggest that harbour porpoises may move with the tide, rather than against it, in the Great Race, off Jura in Scotland.

Many of the previous studies on toothed whale behaviour in tidal rapids have been limited by relatively rudimentary metrics such as sighting rates at the surface, and/or using acoustic click loggers to measure presence/absence. A comprehensive understanding of the importance of tidal rapid habitats requires detailed information on both *sub-surface behaviour*, *distribution* and *density* of harbour porpoises. However, there are currently very few studies in which these have been measured (with an exception being (Gordon et al. 2011) which measured density). This lack of information on the basic biology of top predators in tidal rapid areas holds true for other cetacean species, and it is perhaps therefore fitting for a comprehensive review on the subject to be titled "Confusion Reigns" (Benjamins et al. 2015).

One of the primary reasons underlying the absence of these data and use of more rudimentary data collection methods is the technical and practical challenges of deploying scientific equipment in fast moving currents and harsh sea conditions. Furthermore, the analytical challenges associated with measuring fine-scale behaviour and density of harbour porpoises (and other marine mammals) in tidal rapids are not trivial. Visual studies cannot provide information on sub surface behaviour and are limited by higher sea states. Tagging animals with bio-loggers that track the movements of the tagged animal is a possible means of understanding underwater fine-scale behaviour. However, tagging is likely not a cost-effective or appropriate option when the habitat of interest is a geographically restricted area, as in a tidal rapids, in which a tagged animal may spend only a small proportion or none of its time (Hastie et al. 2014). PAM has the advantage of being relatively unaffected by sea state or light conditions, and can detect vocalising animals within an area of interest; however, methods to obtain fine scale behaviour from PAM are not well developed and using any sort of PAM device in tidal areas - whether bottom mounted, towed or drifting - likely requires some adaptions to existing density estimation methods and/or modifications to the survey methodology. For example, towed arrays will not stream directly behind a vessel in a tidal stream due to the strong and chaotic surface currents and engine noise by a surveying vessel may affect the behaviour of animals, which can be in close proximity in geographically restricted tidal habitats (Wisniewska et al. 2018). All PAM systems are likely affected by the large variations of noise in tidal stream habitats (Carter, 2013; Malinka et al., 2015) which will alter the probability of detecting animals. Bottom-mounted PAM systems will additionally suffer from highly variable flow noise at different states of the tide and so may have a significantly reduced probability of detecting clicks.

Although drifting PAM systems minimise flow noise, it may be difficult to design a survey which samples an area evenly with respect to the distribution of animals. Despite these analysis challenges, PAM likely still represents the most efficient survey methodology to obtain detailed information on toothed whale behaviour and density in tidal rapids (Gordon et al. 2011).

1.4 HARBOUR PORPOISE

This PhD focuses on harbour porpoises, one of the most common marine mammals found in European and North American waters (Hammond et al. 2013, Waring et al. 2015). In Europe, harbour porpoises are listed under Annex II and IV of the EU Habitats Directive (European Commission 1992) which requires EU Member States to assess and address potential conservation threats, and in the USA and Canada, they are protected by the Marine Mammal Protection Act and the Species At Risk Act (*U.S. Marine Mammal Protection Act of 1972. 16 U.S. Code Sections 1362 and 1372 (2000).* 1972), respectively. Harbour porpoises are small, undemonstrative animals making many visual research methods difficult to apply, especially in higher sea states, such as occur in tidal rapids. However, they are also very vocal animals, producing characteristic narrow band high frequency (NBHF) clicks. NBHF clicks are relatively long for echolocation clicks (~77 µs), narrow band (16 kHz -3 dB bandwidth) and centred around 130 kHz (Mohl and Andersen 1973, Teilmann et al. 2002). *(Note: Some mistaken studies have noted low frequency signals in harbour porpoises, however, these are now considered artefacts from now out of date recording devices* (Hansen et al. 2008)*).*

A combination of factors, including the availability of captive animals, consistent incidental live bycatch in a Danish herring weir fishery (see Wisniewska et al. (2016) supplemenatry materials) and the overlap in distribution with the waters of mostly highly developed nations mean that harbour porpoise biosonar is amongst the most well studied of any toothed whale species.

The source levels of porpoise clicks recorded from captive animals range from 120 to 177 dB re 1µPa pp at 1m (Mohl and Andersen 1973, Akamatsu et al. 1994), however, a study of wild Danish harbour porpoise using a small vertical hydrophone array showed that click source levels could reach 205 dB re 1µPa pp at 1m (although this was an outlier and possibly due to an error in their localisation calculations) with an average value of 191 re 1µPa pp at 1m (Villadsgaard et al. 2007). This has significant implications for the detection range on PAM systems and has subsequently been verified

in a similar study by Kyhn et al. (2013) who found an average source level of 189 dB re 1µPa pp at 1m, although no individual clicks were recorded above 200 dB re 1µPa pp at 1m.

The forward beam profile of harbour porpoises has been measured in multiple studies from stationary, captive harbour porpoises. Au et al. (1999) recorded a 16° half power (-3 dB) beam which was confirmed using suction cup hydrophones attached directly to the harbour porpoise's melon (Au 2006). Koblitz et al. (2012) measured a narrower -3 dB horizontal beam width of 13.1° and a vertically compressed beam width of 10.7°. The only measurement of porpoise beam beyond 30° was by (Hansen et al. 2008), however, this was not the focus of the study and only used a 5 hydrophones resulting in poor angular resolution. Adaptive widening of the porpoise beam was suggested in Madsen et al. (2010), speculated upon by Wisniewska et al. (2012) and later demonstrated and quantified by Wisniewska et al. (2015), who showed a dramatic widening of the half-power beam width during the buzz phase, in some trials increasing the half power -3 dB beam width by up to 20° (the porpoise increased its half power beam width from 9.1° to a maximum of 30°).

As harbour porpoises produce no vocalisations other than NBHF clicks, acoustic behaviour is characterised solely by changes in the amplitude of and interval between echolocation clicks. When a porpoise closes in on a prey item it changes from standard range locking behaviour, maintains a constant ICI and then produces a buzz, a short burst of around 600 lower amplitude clicks per second (Verfuß et al. 2007, Deruiter et al. 2009). Verfuß et al. (2009) used synchronised video and audio recordings of two captive animals to investigate this foraging behaviour in detail. They noted the distinct 'approach phase' after detection of a prey item. In the initial approach phase porpoises moved towards the prey item while maintaining a near constant ICI with similar studies demonstrated the same animals lowered their source levels by ~ 20log(*R*) (where *R i*s distance to prey) so that the incident received levels at the prey item remained near constant (Beedholm and Miller 2007, Carolina et al. 2009). Verfuß et al. (2009) theorised that, if prey could hear NBHF clicks, a constant received sound pressure from echolocation clicks and ICI could acoustically mask a porpoises approach, allowing for the prey to be effectively ambushed. Deuiter et al. (2009) used an alternate method, acoustic tags (DTAGs), to record the acoustic behaviour and movement of two captive porpoises. They found very similar behaviour, a constant ICI as the animal approaches, followed by a buzz of up to 640 clicks per second or an ICI of ~1.6 ms but found that the ~20log(*R*) did not provide a clear fit to received levels versus ICI, suggesting that harbour porpoise may not follow the automatic gain

control mechanism proposed by Au & Benoit-Bird (2003). This has recently been confirmed by Ladegaard et al. (2019) who noted that captive animals in differing reverberant environment adjust their output levels independently of ICI and thus, as is being consistently confirmed with other toothed whale species, harbour porpoise appear to have some degree of cognitive controls over their output levels and thus source levels are context dependent.

Studies of *wild* harbour porpoises with acoustic tags have confirmed many of the same results as in captivity and yielded important information on their foraging ecology. Akamatsu et al. (2007) and Linnenschmidt et al. (2013) both tagged four wild harbour porpoises in Danish waters and showed large variations in echolocation behaviour. Both studies noted that all wild animals echolocated almost continually and demonstrated characteristic foraging behaviour observed in captive studies, however, their data also showed that the porpoises occasionally ceased echolocation behaviour altogether, for periods of up to 20 minutes. Wright et al. (2016) recorded parabolic dives of wild tagged animals during these periods, suggesting that this silence may indicate sleeping behaviour and that individual animals could actually be silent 5 to 10% of their time. Wright et al. (2016) noted this may have significant implications for PAM based monitoring methods which so far, have assumed porpoises produce clicks almost continuously. However, the tags used in these studies were not sensitive enough to detect lower amplitude buzzes so animals may have just been switching acoustic behaviour, rather than remaining completely silent.

Currently, in Danish waters, there is an ongoing program to tag harbour porpoises with a new generation of highly sensitive sound and movement (DTAGs) (Johnson and Tyack 2003). DTAGs record acoustic data and can be equipped with a variety of additional sensors, such as GPS and heart rate monitors. The tags register outgoing clicks and buzzes and, because they have a very low noise floor, will also record the much fainter returning echoes from prey items and surroundings. Wisniewska et al. (2016) was able to use the acoustic data on DTAGS to construct echograms (a visualisation of a harbour porpoises' acoustic scene) during target approaches. Remarkably, the tailbeat frequency of fish was visible in these echograms which Wisniewska et al. (2016) then used to estimate prey size during foraging attempts. Results showed that harbour porpoises were feeding on smaller prey with up to 200-500 prey capture events per hour. The energetic aspects of this ultra-high feeding rate were investigated by Rojano-Doñate et al. (2018) who recorded high field metabolic

rates of wild harbour porpoises, however, there is some debate on whether this behaviour is representative of the species as a whole (Hoekendijk et al., 2018; Wisniewska et al., 2018) and differing energy content of prey could drive very different foraging rates (Booth 2020). The use of DTAGs has provided an unparalleled information on the sensory ecology and foraging behaviour of harbour porpoises, however, the data they provide can also be used to assess behavioural responses to anthropogenic impacts e.g. noise (Wisniewska et al. 2018) and for investigating acoustic social behaviour.

Most studies to date have focused on the sensory component of harbour porpoises clicks. However, because they produce no other type of vocalization, any communication must also be encoded in clicks. Communication and social interaction between harbour porpoises has not been widely studied. Clausen et al. (2010), proposed that the buzz-like calls observed from captive porpoises serve an additional social function. Certain amplitudes and patterns in the ICI of buzzes were attributed to specific behavioural patterns, e.g. aggression was characterised by a rapid decreases in ICI, very low final ICI and high received levels. Sørensen et al. (2018) confirmed the existence of call buzzes in tag data from wild harbour porpoises in which a specific subset of buzz ICIs seems to be used for calling rather than foraging. Thus, communication appears to be encoded in some types of high repetition click sequences; these should be identifiable on PAM instruments.

Despite these numerous studies, as for all toothed whales, there are still significant data gaps. Social interaction between harbour porpoises is still poorly understood and underwater fine scale behavioural responses to noise have only been studied in the wild once (Wisniewska et al. 2018). Despite much work on beam profiles, the entire 4π beam profile (360° horizontal and 180° vertical measurements) of a harbour porpoise has not yet been measured, and the distortion in off-axis clicks has not been fully quantified; these are potentially important parameters in detection classification, localisation and density estimation, especially if using Monte Carlo simulation methods to determine detection probability (Frasier et al. 2016).

1.5 THESIS STRUCTURE

This thesis focuses on the further development of PAM analysis methods and studies of the beam profile and fine scale diving behaviour of harbour porpoises to inform a distance sampling framework for density estimation. These methods are demonstrated on PAM survey data collected in a tidal

rapid habitat in Kylerhea, off Skye in Scotland, a particularly unique and difficult environment to study. New detection, classification and localisation algorithms were combined to analyse the large quantities of acoustic data collected on drifting PAM recorders and more complex vertical hydrophone arrays. The fine scale acoustic and diving behaviour of harbour porpoise in different areas of the tidal stream were calculated and used to determine the probability of detecting clicks and buzzes at small spatial and temporal scales within the tidal stream. This is then incorporated into distance sampling to estimate the number of animals and foraging rates. The PAM and density estimation methods are, to varying degrees, informed by aspects of the biosonar properties and acoustic behaviour of harbour porpoises, either from existing literature, or from further acoustic studies of captive animals. The structure of the thesis is as follow.

Chapter 2 discusses the implementation of an open source multi species click train classifier and whether there are advantages to using such a detector and classifier for sperm whales, delphinids and harbour porpoises.

Chapter 3 develops drifting vertical hydrophone arrays which can be deployed in tidal rapids to record the 3D positions of harbour porpoises and other echolocating toothed whales. Algorithms to automatically address the issue of spatial aliasing and interpolate the tracks of multiple diving animals are discussed.

Chapter 4 measures the full 4π radian beam of a captive harbour porpoise and discusses the implications of beam profile measurement for density estimation when using Monte Carlo simulations to calculate the probability of detection.

Chapter 5 uses the new detection and localisation algorithms and the measured 4π beam profile in previous chapters to develop a statistical framework to measure the fine scale diving behaviour density and foraging rates of harbour porpoises using drifters in a tidal rapid site (Kylerhea, Scotland).

Chapter 6 presents a general discussion of results from the previous chapters.

1.6 REFERENCES

Aguilar de Soto, N., P. T. Madsen, P. Tyack, P. Arranz, J. Marrero, A. Fais, E. Revelli, and M. Johnson. 2012. No shallow talk: Cryptic strategy in the vocal communication of Blainville's beaked

whales. Marine Mammal Science 28:E75–E92.

Von Ahn, L., B. Maurer, C. McMillen, D. Abraham, and M. Blum. 2008. recaptcha: Human-based character recognition via web security measures. Science 321:1465–1468.

Ainslie, M. A. 2013. Neglect of bandwidth of Odontocetes echo location clicks biases propagation loss and single hydrophone population estimates. The Journal of the Acoustical Society of America 134:3506–3512.

Ainslie, M. A., and J. G. Mccolm. 1998. A simplified formula for viscous and chemical absorption in sea water. The Journal of the Acoustical Society of America 103:1671.

Akamatsu, T., Y. Hatakeyama, T. Kojima, and H. Soeda. 1994. Echolocation rates of two harbor porpoises (*Phocoena phocoena*). Marine Mammal Science 10:401–411.

Akamatsu, T., K. Nakamura, R. Kawabe, S. Furukawa, H. Murata, A. Kawakubo, and M. Komaba. 2010. Seasonal and diurnal presence of finless porpoises at a corridor to the ocean from their habitat. Marine Biology 157:1879–1887.

Akamatsu, T., J. Teilmann, L. A. Miller, J. Tougaard, R. Dietz, D. Wang, K. Wang, U. Siebert, and Y. Naito. 2007. Comparison of echolocation behaviour between coastal and riverine porpoises. Deep Sea Research Part II: Topical Studies in Oceanography 54:290–297.

Mac Aodha, O., R. Gibb, K. E. Barlow, E. Browning, M. Firman, R. Freeman, B. Harder, L. Kinsey, G. R. Mead, S. E. Newson, I. Pandourski, S. Parsons, J. Russ, A. Szodoray-Paradi, F. Szodoray-Paradi, E. Tilova, M. Girolami, G. Brostow, and K. E. Jones. 2018. Bat detective—Deep learning tools for bat acoustic signal detection. PLOS Computational Biology 14:e1005995.

Aroyan, J. L., T. W. Cranford, J. Kent, and K. S. Norris. 1992. Computer modeling of acoustic beam formation in Delphinusdelphis. The Journal of the Acoustical Society of America 92:2539–2545.

Au, W. W. L. 1980. Echolocation Signals of the Atlantic Bottlenose Dolphin (Tursiops truncatus) in Open Waters. Pages 251–282 Animal Sonar Systems. Springer US, Boston, MA.

Au, W. W. L. 1993. The Sonar of Dolphins. Page Acoustics Australia. Springer New York, New York, NY.

Au, W. W. L. 2006. Acoustic radiation from the head of echolocating harbor porpoises (Phocoena phocoena). Journal of Experimental Biology 209:2726–2733.

Au, W. W. L., and K. J. Benoit-Bird. 2003. Automatic gain control in the echolocation system of dolphins. Nature 423:861–863.

Au, W. W. L., B. Branstetter, P. W. Moore, and J. J. Finneran. 2012. Dolphin biosonar signals measured at extreme off-axis angles: Insights to sound propagation in the head. The Journal of the Acoustical Society of America 132:1199–1206.

Au, W. W. L., R. W. Floyd, R. H. Penner, and A. E. Murchison. 1974. Measurement of echolocation signals of the Atlantic bottlenose dolphin, Tursiops truncatus Montagu, in open waters. The Journal of the Acoustical Society of America 56:1280–1290.

Au, W. W. L., R. A. Kastelein, T. Rippe, and N. M. Schooneman. 1999. Transmission beam pattern and echolocation signals of a harbor porpoise (Phocoena phocoena). The Journal of the Acoustical Society of America 106:3699–3705.

Au, W. W., and P. M. Scheifele. 1994. The Sonar of Dolphins. The Journal of the Acoustical Society of America 95:585–586.

Baggenstoss, P. M. 2011a. An algorithm for the localization of multiple interfering sperm whales using multi-sensor time difference of arrival. The Journal of the Acoustical Society of America 130:102–112.

Baggenstoss, P. M. 2011b. Separation of sperm whale click trains for multipath rejection. The Journal of the Acoustical Society of America 129:3598–3609.

Baggenstoss, P. M. 2013. Processing advances for localization of beaked whales using time difference of arrival. Journal of the Acoustical Society of America 133:4065–76.

Baggeroer, A. B., W. A. Kuperman, and H. Schmidt. 1988. Matched field processing: Source localization in correlated noise as an optimum parameter esimation problem. The Journal of the Acoustical Society of America 83:571–587.

Barlow, J., E. T. Griffiths, H. Klinck, and D. V. Harris. 2018. Diving behavior of Cuvier's beaked whales inferred from three-dimensional acoustic localization and tracking using a nested array of drifting hydrophone recorders. The Journal of the Acoustical Society of America 144:2030–2041.

Barlow, J., and B. L. Taylor. 2005. Estimates of sperm whale abundance in the northeastern temperate pacific from a combined acoustic and visual survey. Marine Mammal Science 21:429–445.

Barlow, K. E., P. A. Briggs, K. A. Haysom, A. M. Hutson, N. L. Lechiara, P. A. Racey, A. L. Walsh, and S. D. Langton. 2015. Citizen science reveals trends in bat populations: The National Bat Monitoring Programme in Great Britain. Biological Conservation 182:14–26.

Bassett, H. R., S. Baumann, G. S. Campbell, S. M. Wiggins, and J. A. Hildebrand. 2009. Dall's porpoise (Phocoenoides dalli) echolocation click spectral structure. The Journal of the Acoustical Society of America 125:2677–2677.

Beedholm, K., and L. A. Miller. 2007. Automatic Gain Control in Harbor Porpoises (Phocoena phocoena)? Central Versus Peripheral Mechanisms. Aquatic Mammals 33:69–75.

von Benda-Beckmann, A. M., S. P. Beerens, and S. P. van IJsselmuide. 2013. Effect of towed array stability on instantaneous localization of marine mammals. The Journal of the Acoustical

Society of America 134:2409–2417.

Benjamins, S., A. Dale, N. van Geel, and B. Wilson. 2016. Riding the tide: use of a moving tidal-stream habitat by harbour porpoises. Marine Ecology Progress Series 549:275–288.

Benjamins, S., A. Dale, G. Hastie, J. Waggitt, M.-A. Lea, B. Scott, and B. Wilson. 2015. Confusion Reigns? A Review of Marine Megafauna Interactions with Tidal-Stream Environments. Pages 1–54 Oceanography and Marine Biology: An Annual Review.

Benjamins, S., N. van Geel, G. Hastie, J. Elliott, and B. Wilson. 2017. Harbour porpoise distribution can vary at small spatiotemporal scales in energetic habitats. Deep Sea Research Part II: Topical Studies in Oceanography 141:191–202.

Bergler, C., H. Schröter, R. X. Cheng, V. Barth, M. Weber, E. Nöth, H. Hofer, and A. Maier. 2019. ORCA-SPOT: An Automatic Killer Whale Sound Detection Toolkit Using Deep Learning. Scientific Reports 9:10997.

Bittencourt, L., W. Soares-Filho, I. M. S. de Lima, S. Pai, J. Lailson-Brito, L. M. Barreira, A. F. Azevedo, and L. A. A. Guerra. 2018. Mapping cetacean sounds using a passive acoustic monitoring system towed by an autonomous Wave Glider in the Southwestern Atlantic Ocean. Deep Sea Research Part I: Oceanographic Research Papers 142:58–68.

Booth, C., C. Embling, J. Gordon, S. Calderan, and P. Hammond. 2013. Habitat preferences and distribution of the harbour porpoise Phocoena phocoena west of Scotland. Marine Ecology Progress Series 478:273–285.

Booth, C. G. 2020. Food for thought: Harbor porpoise foraging behavior and diet inform vulnerability to disturbance. Marine Mammal Science 36:195–208.

Booth, C. G., C. S. Oedekoven, D. Gillespie, J. Macaulay, R. Plunkett, R. Joy, D. Harris, J. Wood, T. A. Marques, L. Marshall, U. K. Verfuss, P. Tyack, M. Johnson, and L. Thomas. 2017. Assessing the Viability of Density Estimation for Cetaceans from passive Acoustic Fixed sensors throughout the Life Cycle of an Offshore E & P Field Development. Page Assessing the Viability of Density Estimation for Cetaceans from Passive Acoustic Fixed Sensors throughout the Life Cycle of an Offshore E&P Field Development.

Borchers, D. L., B. C. Stevenson, D. Kidney, L. Thomas, and T. A. Marques. 2015. A Unifying Model for Capture–Recapture and Distance Sampling Surveys of Wildlife Populations. Journal of the American Statistical Association 110:195–204.

Bossart, G. D. 2011. Marine Mammals as Sentinel Species for Oceans and Human Health. Veterinary Pathology 48:676–690.

Le Bot, O., J. I. Mars, C. Gervaise, and Y. Simard. 2015. Rhythmic analysis for click train detection and source separation with examples on beluga whales. Applied Acoustics 95:37–49.

Branstetter, B. K., P. W. Moore, J. J. Finneran, M. N. Tormey, and H. Aihara. 2012. Directional

properties of bottlenose dolphin (Tursiops truncatus) clicks, burst-pulse, and whistle sounds. The Journal of the Acoustical Society of America 131:1613–1621.

Brinkløv, S., M. B. Fenton, and J. M. Ratcliffe. 2013. Echolocation in Oilbirds and swiftlets. Frontiers in Physiology 4.

Buckland, S. T., D. R. Anderson, K. P. Burnham, and J. L. Laake. 2005. Distance Sampling. Page Encyclopedia of Biostatistics. John Wiley & Sons, Ltd, Chichester, UK.

Buckland, S. T., D. R. Anderson, K. P. Burnham, J. L. Laake, D. L. Borchers, and L. Thomas. 2001. Introduction to Distance sampling: estimating abundance of biological populations. Page New York USA. New York.

Caillat, M., L. Thomas, and D. Gillespie. 2013. The effects of acoustic misclassification on cetacean species abundance estimation. The Journal of the Acoustical Society of America 134:2469–2476.

Carlén, I., L. Thomas, J. Carlström, M. Amundin, J. Teilmann, N. Tregenza, J. Tougaard, J. C. Koblitz, S. Sveegaard, D. Wennerberg, O. Loisa, M. Dähne, K. Brundiers, M. Kosecka, L. A. Kyhn, C. T. Ljungqvist, I. Pawliczka, R. Koza, B. Arciszewski, A. Galatius, M. Jabbusch, J. Laaksonlaita, J. Niemi, S. Lyytinen, A. Gallus, H. Benke, P. Blankett, K. E. Skóra, and A. Acevedo-Gutiérrez. 2018. Basin-scale distribution of harbour porpoises in the Baltic Sea provides basis for effective conservation actions. Biological Conservation 226:42–53.

Carolina, A. G., M. H. Rasmussen, M. Wahlberg, H. C. Petersen, and L. A. Miller. 2009. Changes in Click Source Levels With Distance To Targets : Studies of Free-Ranging White-Beaked Dolphins Lagenorhynchus Albirostris and Captive Harbour Porpoises Phocoena Phocoena. Bioacoustics 19:49–65.

Carter, C. J. 2013. Tidal Energy, Underwater Noise & Marine Mammals. University of Aberdeen.

Clausen, K. T., M. Wahlberg, K. Beedholm, S. Deruiter, and P. T. Madsen. 2010. Click communication in harbour porpoises Phocoena phocoena. Bioacoustics 20:1–28.

Cranford, T. W. 2000. In Search of Impulse Sound Sources in Odontocetes. Pages 109–155.

Cranford, T. W., M. Amundin, and K. S. Norris. 1996. Functional morphology and homology in the odontocete nasal complex: Implications for sound generation. Journal of Morphology 228:223–285.

Crook, K., and G. Davoren. 2014. Underwater behaviour of common murres foraging on capelin: influences of prey density and antipredator behaviour. Marine Ecology Progress Series 501:279–290.

Davies IM, Gubbins M, Watret R (2012) Scoping study for tidal-stream energy development in Scottish waters. Scottish Marine and Freshwater Science Report 3(1). Available at www. scotland. gov. uk/ Publications/ 2012/ 04/ 2639 (accessed 23 October 2014)

Dawson, S. M. 2010. Clicks and Communication: The Behavioural and Social Contexts of Hector's Dolphin Vocalizations. Ethology 88:265–276.

Deruiter, S. L., A. Bahr, M.-A. Blanchet, S. F. Hansen, J. H. Kristensen, P. T. Madsen, P. L. Tyack, and M. Wahlberg. 2009. Acoustic behaviour of echolocating porpoises during prey capture. The Journal of experimental biology 212:3100–3107.

DeRuiter, S. L., M. Hansen, H. N. Koopman, A. J. Westgate, P. L. Tyack, and P. T. Madsen. 2010. Propagation of narrow-band-high-frequency clicks: measured and modeled transmission loss of porpoise-like clicks in porpoise habitats. The Journal of the Acoustical Society of America 127:560–567.

Douglas, L. A., S. M. Dawson, and N. Jaquet. 2005. Click rates and silences of sperm whales at Kaikoura, New Zealand. The Journal of the Acoustical Society of America 118:523–529.

Efford, M. G., D. K. Dawson, and D. L. Borchers. 2009. Population density estimated from locations of individuals on a passive detector array. Ecology 90:2676–2682.

Embling, C. B., P. a. Gillibrand, J. Gordon, J. Shrimpton, P. T. Stevick, and P. S. Hammond. 2010. Using habitat models to identify suitable sites for marine protected areas for harbour porpoises (Phocoena phocoena). Biological Conservation 143:267–279.

Enstipp, M. R., D. Grémillet, and D. R. Jones. 2007. Investigating the functional link between prey abundance and seabird predatory performance. Marine Ecology Progress Series 331:267–279.

Erbs, F., S. H. Elwen, and T. Gridley. 2017. Automatic classification of whistles from coastal dolphins of the southern African subregion. The Journal of the Acoustical Society of America 141:2489–2500.

European Commission. 1992. Council Directive 92/43/EEC of 21 May 1992 on the conservation of natural habitats and of wild fauna and flora L 269:1–15.

Fais, A., M. Johnson, M. Wilson, N. Aguilar Soto, and P. T. Madsen. 2016. Sperm whale predator-prey interactions involve chasing and buzzing, but no acoustic stunning. Scientific Reports 6:28562.

Forsman, K. A., and M. G. Malmquist. 1988. Evidence for echolocation in the common shrew, Sorex araneus. Journal of Zoology 216:655–662.

Frasier, K. E., M. A. Roch, M. S. Soldevilla, S. M. Wiggins, L. P. Garrison, and J. A. Hildebrand. 2017. Automated classification of dolphin echolocation click types from the Gulf of Mexico. PLoS Computational Biology 13:1–23.

Frasier, K. E., S. M. Wiggins, D. Harris, T. A. Marques, L. Thomas, and J. A. Hildebrand. 2016. Delphinid echolocation click detection probability on near-seafloor sensors. The Journal of the Acoustical Society of America 140:1918–1930.

de Freitas, M., F. H. Jensen, J. Tyne, L. Bejder, and P. T. Madsen. 2015. Echolocation parameters of

Australian humpback dolphins (Sousa sahulensis) and Indo-Pacific bottlenose dolphins (Tursiops aduncus) in the wild. The Journal of the Acoustical Society of America 137:3033–3041.

Galatius, A., M. T. Olsen, M. E. Steeman, R. A. Racicot, C. D. Bradshaw, L. A. Kyhn, and L. A. Miller. 2019. Raising your voice: evolution of narrow-band high-frequency signals in toothed whales (Odontoceti). Biological Journal of the Linnean Society 126:213–224.

Gassmann, M., S. M. Wiggins, and J. A. Hildebrand. 2015. Three-dimensional tracking of Cuvier ' s beaked whales ' echolocation sounds using nested hydrophone arrays. Journal of the Acoustical Society of America 138:2483–2494.

Gerard, O., C. Carthel, and S. Coraluppi. 2008. Estimating the number of beaked whales using an MHT tracker. Pages 1–6 2008 New Trends for Environmental Monitoring Using Passive Systems. IEEE.

Gerrodette, T., B. L. Taylor, R. Swift, S. Rankin, A. M. Jaramillo-Legorreta, and L. Rojas-Bracho. 2011. A combined visual and acoustic estimate of 2008 abundance, and change in abundance since 1997, for the vaquita, Phocoena sinus. Marine Mammal Science 27:E79–E100.

Gillespie, D., P. Berggren, S. Brown, I. Kuklik, C. Lacey, T. Lewis, J. Matthews, R. Mclanaghan, A. Moscrop, and N. Tregenza. 2005. Relative abundance of harbour porpoises (Phocoena phocoena) from acoustic and visual surveys of the Baltic Sea and adjacent waters during 2001 and 2002. Journal of Cetacean Research and Management 7:51.

Gillespie, D., and M. Caillat. 2008. Statistical Classification of Odontocete Clicks. Canadian Acoustics 36:20–26.

Gillespie, D., M. Caillat, J. Gordon, and P. White. 2013. Automatic detection and classification of odontocete whistles. The Journal of the Acoustical Society of America 134:2427–2437.

Gillespie, D., and J. Macaulay. 2019. Time of arrival difference estimation for narrow band high frequency echolocation clicks. The Journal of the Acoustical Society of America 146:EL387–EL392.

Goodwin, L. 2008. Diurnal and tidal variations in habitat use of the harbour porpoise (Phocoena phocoena) in Southwest Britain. Aquatic Mammals 34:44–53.

Goold, J. C., and S. E. Jones. 1995. Time and frequency domain characteristics of sperm whale clicks. The Journal of the Acoustical Society of America 98:1279–1291.

Gordon, J., D. Thompson, R. Leaper, D. Gillespie, C. Pierpoint, S. Calderan, J. Macaulay, T. Gordon, and N. Simpson. 2011. Assessment of risk to marine mammals from underwater marine renewable devices in Welsh waters - Phase 2 - Studies of marine mammals in Welsh high tidal waters. Page Welsh Government Assembly Report.

Götz, T., R. Antunes, and S. Heinrich. 2010. Echolocation clicks of free-ranging Chilean dolphins (

Cephalorhynchus eutropia). The Journal of the Acoustical Society of America 128:563–566.

Gruden, P., and P. R. White. 2016. Automated tracking of dolphin whistles using Gaussian mixture probability hypothesis density filters. The Journal of the Acoustical Society of America 140:1981–1991.

Hall, A. 2011. Foraging behaviour and reproductive season habitat selection of Northeast Pacific porpoises. University of British Columbia.

Hammond, P. S., K. Macleod, P. Berggren, D. L. Borchers, L. Burt, A. Cañadas, G. Desportes, G. P. Donovan, A. Gilles, D. Gillespie, J. Gordon, L. Hiby, I. Kuklik, R. Leaper, K. Lehnert, M. Leopold, P. Lovell, N. Øien, C. G. M. Paxton, V. Ridoux, E. Rogan, F. Samarra, M. Scheidat, M. Sequeira, U. Siebert, H. Skov, R. Swift, M. L. Tasker, J. Teilmann, O. Van Canneyt, and J. A. Vázquez. 2013. Cetacean abundance and distribution in European Atlantic shelf waters to inform conservation and management. Biological Conservation 164:107–122.

Hansen, M., M. Wahlberg, and P. T. Madsen. 2008. Low-frequency components in harbor porpoise (Phocoena phocoena) clicks: communication signal, by-products, or artifacts? The Journal of the Acoustical Society of America 124:4059.

Hastie, G. D., M. Bivins, A. Coram, J. Gordon, P. Jepp, J. MacAulay, C. Sparling, and D. Gillespie. 2019. Three-dimensional movements of harbour seals in a tidally energetic channel: Application of a novel sonar tracking system. Aquatic Conservation: Marine and Freshwater Ecosystems 29:564–575.

Hastie, G. D., D. M. Gillespie, J. C. D. Gordon, J. D. J. Macaulay, B. J. McConnell, and C. E. Sparling. 2014. Tracking Technologies for Quantifying Marine Mammal Interactions with Tidal Turbines: Pitfalls and Possibilities. Pages 127–139.

Hastie, G. D., D. J. F. Russell, S. Benjamins, S. Moss, B. Wilson, and D. Thompson. 2016. Dynamic habitat corridors for marine predators; intensive use of a coastal channel by harbour seals is modulated by tidal currents. Behavioral Ecology and Sociobiology 70:2161–2174.

Hastie, G. D., B. Wilson, and P. M. Thompson. 2006. Diving deep in a foraging hotspot: acoustic insights into bottlenose dolphin dive depths and feeding behaviour. Marine Biology 148:1181–1188.

Heerfordt, A., B. Møhl, and M. Wahlberg. 2007. A wideband connection to sperm whales: A fiber-optic, deep-sea hydrophone array. Deep Sea Research Part I: Oceanographic Research Papers 54:428–436.

Hildebrand, J. A., K. E. Frasier, S. Baumann-Pickering, S. M. Wiggins, K. P. Merkens, L. P. Garrison, M. S. Soldevilla, and M. A. McDonald. 2019. Assessing Seasonality and Density From Passive Acoustic Monitoring of Signals Presumed to be From Pygmy and Dwarf Sperm Whales in the Gulf of Mexico. Frontiers in Marine Science 6:1–17.

Hoekendijk, J. P. A., J. Spitz, A. J. Read, M. F. Leopold, and M. C. Fontaine. 2018. Resilience of harbor porpoises to anthropogenic disturbance: Must they really feed continuously? Marine Mammal Science 34:258–264.

Holt, M. M., D. P. Noren, V. Veirs, C. K. Emmons, and S. Veirs. 2009. Speaking up: Killer whales (Orcinus orca) increase their call amplitude in response to vessel noise. The Journal of the Acoustical Society of America 125:EL27-L32.

Jakobsen, L., M. N. Olsen, and A. Surlykke. 2015. Dynamics of the echolocation beam during prey pursuit in aerial hawking bats. Proceedings of the National Academy of Sciences of the United States of America 112:8118–8123.

Janik, V. M. 2000. Food-related bray calls in wild bottlenose dolphins (Tursiops truncatus). Proceedings of the Royal Society B: Biological Sciences 267:923–927.

Jensen, F. H., L. Bejder, M. Wahlberg, and P. T. Madsen. 2009. Biosonar adjustments to target range of echolocating bottlenose dolphins (Tursiops sp.) in the wild. Journal of Experimental Biology 212:1078–1086.

Jensen, F. H., M. Johnson, M. Ladegaard, D. M. Wisniewska, and P. T. Madsen. 2018. Narrow Acoustic Field of View Drives Frequency Scaling in Toothed Whale Biosonar. Current Biology 28:3878-3885.e3.

Jensen, F. H., O. A. Keller, P. L. Tyack, and F. Visser. 2020. Dynamic biosonar adjustment strategies in deep-diving Risso's dolphins driven partly by prey evasion. The Journal of Experimental Biology 223:jeb216283.

Jensen, F. H., J. M. Perez, M. Johnson, N. A. Soto, and P. T. Madsen. 2011. Calling under pressure: short-finned pilot whales make social calls during deep foraging dives. Proceedings of the Royal Society B: Biological Sciences 278:3017–3025.

Jensen, F. H., A. Rocco, R. M. Mansur, B. D. Smith, V. M. Janik, and P. T. Madsen. 2013. Clicking in shallow rivers: short-range echolocation of Irrawaddy and Ganges River dolphins in a shallow, acoustically complex habitat. PloS one 8:e59284.

Jensen, F. H., M. Wahlberg, K. Beedholm, M. Johnson, N. A. de Soto, and P. T. Madsen. 2015. Single-click beam patterns suggest dynamic changes to the field of view of echolocating Atlantic spotted dolphins (Stenella frontalis) in the wild. Journal of Experimental Biology 218:1314–1324.

Jiang, J., L. Bu, F. Duan, X. Wang, W. Liu, Z. Sun, and C. Li. 2019. Whistle detection and classification for whales based on convolutional neural networks. Applied Acoustics 150:169–178.

Johansson, A. T., and P. R. White. 2011. An adaptive filter-based method for robust, automatic detection and frequency estimation of whistles. The Journal of the Acoustical Society of America 130:893–903.

Johnson, M., P. T. Madsen, W. M. X. Zimmer, N. A. de Soto, and P. L. Tyack. 2006. Foraging Blainville's beaked whales (Mesoplodon densirostris) produce distinct click types matched to different phases of echolocation. Journal of Experimental Biology 209:5038–5050.

Johnson, M., P. T. Madsen, W. M. X. X. Zimmer, N. Aguilar de Soto, and P. L. Tyack. 2004. Beaked whales echolocate on prey. Proceedings of the Royal Society of London. Series B: Biological Sciences 271:S383–S386.

Johnson, M. P., and P. L. Tyack. 2003. A digital acoustic recording tag for measuring the response of wild marine mammals to sound. IEEE Journal of Oceanic Engineering 28:3–12.

Kershenbaum, A., and M. A. Roch. 2013. An image processing based paradigm for the extraction of tonal sounds in cetacean communications. The Journal of the Acoustical Society of America 134:4435–4445.

Kidney, D., B. M. Rawson, D. L. Borchers, B. C. Stevenson, T. A. Marques, and L. Thomas. 2016. An efficient acoustic density estimation method with human detectors applied to gibbons in Cambodia. PLOS ONE 11:e0155066.

Koblitz, J. C., P. Stilz, M. H. Rasmussen, and K. L. Laidre. 2016. Highly Directional Sonar Beam of Narwhals (Monodon monoceros) Measured with a Vertical 16 Hydrophone Array. PLOS ONE 11:e0162069.

Koblitz, J. C., M. Wahlberg, P. Stilz, P. T. Madsen, K. Beedholm, and H.-U. Schnitzler. 2012. Asymmetry and dynamics of a narrow sonar beam in an echolocating harbor porpoise. The Journal of the Acoustical Society of America 131:2315.

Küsel, E. T., D. K. Mellinger, L. Thomas, T. A. Marques, D. Moretti, and J. Ward. 2011. Cetacean population density estimation from single fixed sensors using passive acoustics. The Journal of the Acoustical Society of America 129:3610–3622.

Kyhn, L. A., J. Tougaard, K. Beedholm, F. H. Jensen, E. Ashe, R. Williams, and P. T. Madsen. 2013. Clicking in a Killer Whale Habitat: Narrow-Band, High-Frequency Biosonar Clicks of Harbour Porpoise (Phocoena phocoena) and Dall's Porpoise (Phocoenoides dalli). PLoS ONE 8:e63763.

Kyhn, L. a., J. Tougaard, L. Thomas, L. R. Duve, J. Stenback, M. Amundin, G. Desportes, and J. Teilmann. 2012. From echolocation clicks to animal density—Acoustic sampling of harbor porpoises with static dataloggers. The Journal of the Acoustical Society of America 131:550.

Ladegaard, M., F. H. Jensen, K. Beedholm, V. M. F. Da Silva, and P. T. Madsen. 2017. Amazon river dolphins (Inia geoffrensis) modify biosonar output level and directivity during prey interception in the wild. Journal of Experimental Biology 220:2654–2665.

Ladegaard, M., F. H. Jensen, M. de Freitas, V. M. Ferreira da Silva, and P. T. Madsen. 2015. Amazon river dolphins (Inia geoffrensis) use a high-frequency short-range biosonar. Journal of Experimental Biology 218:3091–3101.

Ladegaard, M., and P. T. Madsen. 2019. Context-dependent biosonar adjustments during active target approaches in echolocating harbour porpoises. The Journal of Experimental Biology 222:jeb206169.

Ladegaard, M., J. Mulsow, D. S. Houser, F. H. Jensen, M. Johnson, P. T. Madsen, and J. J. Finneran. 2019. Dolphin echolocation behaviour during active long-range target approaches. The Journal of Experimental Biology 222:jeb189217.

Lammers, M. O., W. W. L. Au, and D. L. Herzing. 2003. The broadband social acoustic signaling behavior of spinner and spotted dolphins. The Journal of the Acoustical Society of America 114:1629–1639.

Lavery, T. J., B. Roudnew, P. Gill, J. Seymour, L. Seuront, G. Johnson, J. G. Mitchell, and V. Smetacek. 2010. Iron defecation by sperm whales stimulates carbon export in the Southern Ocean. Proceedings of the Royal Society B: Biological Sciences 277:3527–3531.

Leaper, R., D. Gillespie, and V. Papastavrou. 2000. Results of passive acoustic surveys for odontocetes in the Southern Ocean. Journal of Cetacean Research and Management 2:187–196.

Lewis, T., D. Gillespie, C. Lacey, J. Matthews, M. Danbolt, R. Leaper, R. McLanaghan, and A. Moscrop. 2007. Sperm whale abundance estimates from acoustic surveys of the Ionian Sea and Straits of Sicily in 2003. Journal of the Marine Biological Association of the United Kingdom 87:353–357.

Li, P., X. Liua, K. J. Palmer, E. Fleishman, D. Gillespie, E.-M. Nosal, Y. Shiu, H. Klinck, D. Cholewiak, T. Helble, and M. A. Roch. 2020. Learning Deep Models from Synthetic Data for Extracting Dolphin Whistle Contours.

Li, S., D. Wang, K. Wang, T. Akamatsu, Z. Ma, and J. Han. 2007. Echolocation click sounds from wild inshore finless porpoise (Neophocaena phocaenoides sunameri) with comparisons to the sonar of riverine N. p. asiaeorientalis. The Journal of the Acoustical Society of America 121:3938.

Linnenschmidt, M., J. Teilmann, T. Akamatsu, R. Dietz, and L. A. Miller. 2013. Biosonar, dive, and foraging activity of satellite tracked harbor porpoises (*Phocoena phocoena*). Marine Mammal Science 29:E77–E97.

Luo, W., W. Yang, Z. Song, and Y. Zhang. 2017. Automatic species recognition using echolocation clicks from odontocetes. Pages 1–5 2017 IEEE International Conference on Signal Processing, Communications and Computing (ICSPCC). IEEE.

Madsen, P. T. 2005. Biosonar performance of foraging beaked whales (Mesoplodon densirostris). Journal of Experimental Biology 208:181–194.

Madsen, P. T., D. A. Carder, K. Bedholm, and S. H. Ridgway. 2005. Porpoise Clicks From a Sperm Whale Nose—Convergent Evolution of 130 Khz Pulses in Toothed Whale Sonars? Bioacoustics

15:195–206.

Madsen, P. T., I. Kerr, and R. Payne. 2004. Echolocation clicks of two free-ranging, oceanic delphinids with different food preferences: false killer whales Pseudorca crassidens and Risso's dolphins Grampus griseus. The Journal of experimental biology 207:1811–1823.

Madsen, P. T., M. Lammers, D. Wisniewska, and K. Beedholm. 2013a. Nasal sound production in echolocating delphinids (Tursiops truncatus and Pseudorca crassidens) is dynamic, but unilateral: clicking on the right side and whistling on the left side. Journal of Experimental Biology 216:4091–4102.

Madsen, P. T., N. A. de Soto, P. Arranz, and M. Johnson. 2013b. Echolocation in Blainville's beaked whales (Mesoplodon densirostris). Journal of Comparative Physiology A: Neuroethology, Sensory, Neural, and Behavioral Physiology 199:451–469.

Madsen, P. T., and A. Surlykke. 2013. Functional Convergence in Bat and Toothed Whale Biosonars. Physiology 28:276–283.

Madsen, P. T., and M. Wahlberg. 2007. Recording and quantification of ultrasonic echolocation clicks from free-ranging toothed whales. Deep Sea Research Part I: Oceanographic Research Papers 54:1421–1444.

Madsen, P. T., D. Wisniewska, and K. Beedholm. 2010. Single source sound production and dynamic beam formation in echolocating harbour porpoises (Phocoena phocoena). Journal of Experimental Biology 213:3105–3110.

Malinka, C. E., A. E. Hay, and R. Cheel. 2015. Towards acoustic monitoring of marine mammals at a tidal energy site: Grand Passage, NS, Canada. Proceedings of the 11th European Wave and Tidal Energy Conference:1–10.

Malinka, C., D. Gillespie, J. Macaulay, R. Joy, and C. Sparling. 2018. First in situ passive acoustic monitoring for marine mammals during operation of a tidal turbine in Ramsey Sound, Wales. Marine Ecology Progress Series 590:247–266.

Mallawaarachchi, A., S. H. Ong, M. Chitre, and E. Taylor. 2008. Spectrogram denoising and automated extraction of the fundamental frequency variation of dolphin whistles. The Journal of the Acoustical Society of America 124:1159–1170.

Marques, T. A., L. Thomas, S. W. Martin, D. K. Mellinger, J. A. Ward, D. J. Moretti, D. Harris, and P. L. Tyack. 2013. Estimating animal population density using passive acoustics. Biological reviews of the Cambridge Philosophical Society 88:287–309.

Marques, T. A., L. Thomas, J. Ward, N. DiMarzio, and P. L. Tyack. 2009. Estimating cetacean population density using fixed passive acoustic sensors: An example with Blainville's beaked whales. The Journal of the Acoustical Society of America 125:1982–1994.

Marques, T., L. Munger, L. Thomas, S. Wiggins, and J. Hildebrand. 2011. Estimating North Pacific

right whale Eubalaena japonica density using passive acoustic cue counting. Endangered Species Research 13:163–172.

Martin, M. J., T. Gridley, S. H. Elwen, and F. H. Jensen. 2018. Heaviside's dolphins (Cephalorhynchus heavisidii) relax acoustic crypsis to increase communication range. Proceedings of the Royal Society B: Biological Sciences 285:20181178.

Marubini, F., A. Gimona, P. G. H. Evans, P. J. Wright, and G. J. Pierce. 2009. Habitat Preferences and Interannual Variability in Occurrence of the Harbour Porpoise Phocoena phocoena off Northwest Scotland. Marine Ecology Progress Series 381:297–310.

Melcón, M. L., M. Failla, and M. a. Iñíguez. 2012. Echolocation behavior of franciscana dolphins (Pontoporia blainvillei) in the wild. The Journal of the Acoustical Society of America 131:EL448.

Miller, B., and S. Dawson. 2009. A large-aperture low-cost hydrophone array for tracking whales from small boats. The Journal of the Acoustical Society of America 126:2248–2256.

Miller, B. S. B. 2012. Real-time tracking of blue whales using DIFAR sonobuoys. Proceedings of Acoustics 2012:7.

Mohl, B., and S. Andersen. 1973. Echolocation: high-frequency component in the click of the harbour porpoise (Phocoena ph. L.). The Journal of the Acoustical Society of America 54:1368–1379.

Møhl, B., M. Wahlberg, P. T. Madsen, A. Heerfordt, and A. Lund. 2003. The monopulsed nature of sperm whale clicks. The Journal of the Acoustical Society of America 114:1143–1154.

Møhl, B., M. Wahlberg, P. T. Madsen, L. a Miller, and a Surlykke. 2000. Sperm whale clicks: directionality and source level revisited. The Journal of the Acoustical Society of America 107:638–648.

Moore, P. W., L. A. Dankiewicz, and D. S. Houser. 2008. Beamwidth control and angular target detection in an echolocating bottlenose dolphin (Tursiops truncatus). The Journal of the Acoustical Society of America 124:3324–3332.

Moore, S. E. 2008. Marine mammals as ecosystem sentinels. Journal of Mammalogy 89:534–540.

Morisaka, T., and R. C. Connor. 2007. Predation by killer whales (Orcinus orca) and the evolution of whistle loss and narrow-band high frequency clicks in odontocetes. Journal of Evolutionary Biology 20:1439–1458.

Morozov, V. P., A. I. Akopian, V. I. Burdin, K. A. Zaitseva, and Y. A. Sokovykh. 1972. Tracking frequency of the location signals of dolphins as a function of distance to the target. Biophysics 17:139–145.

Newson, S. E., H. E. Evans, and S. Gillings. 2015. A novel citizen science approach for large-scale standardised monitoring of bat activity and distribution, evaluated in eastern England.

Biological Conservation 191:38–49.

Nosal, E.-M. 2013. Methods for tracking multiple marine mammals with wide-baseline passive acoustic arrays. The Journal of the Acoustical Society of America 134:2383–92.

Oswald, J. N., S. Rankin, J. Barlow, and M. O. Lammers. 2007. A tool for real-time acoustic species identification of delphinid whistles. The Journal of the Acoustical Society of America 122:587.

Palka, D. L., and P. S. Hammond. 2001. Accounting for responsive movement in line transect estimates of abundance. Canadian Journal of Fisheries and Aquatic Sciences 58:777–787.

Penner, R. H. 1988. Attention and Detection in Dolphin Echolocation. Pages 707–713 Animal Sonar. Springer US, Boston, MA.

Pierpoint, C. 2008. Harbour porpoise (Phocoena phocoena) foraging strategy at a high energy, near-shore site in south-west Wales, UK. Journal of the Marine Biological Association of the United Kingdom 88:1167–1173.

Porter, M. B., and H. P. Bucker. 1987. Gaussian beam tracing for computing ocean acoustic fields. The Journal of the Acoustical Society of America 82:1349–1359.

Price, J., K. P. Johnson, and D. H. Clayton. 2004. The evolution of echolocation in swiftlets. Journal of Avian Biology 35:135–143.

Quick, N. J., and V. M. Janik. 2008. Whistle rates of wild bottlenose dolphins (Tursiops truncatus): Influences of group size and behavior. Journal of Comparative Psychology 122:305–311.

Quick, N. J., and V. M. Janik. 2012. Bottlenose dolphins exchange signature whistles when meeting at sea. Proceedings of the Royal Society B: Biological Sciences 279:2539–2545.

Rankin, S., F. Archer, J. L. Keating, J. N. Oswald, M. Oswald, A. Curtis, and J. Barlow. 2017. Acoustic classification of dolphins in the California Current using whistles, echolocation clicks, and burst pulses. Marine Mammal Science 33:520–540.

Rasmussen, M. H., L. A. Miller, and W. W. L. Au. 2002. Source levels of clicks from free-ranging white-beaked dolphins (Lagenorhynchus albirostris Gray 1846) recorded in Icelandic waters. The Journal of the Acoustical Society of America 111:1122–1125.

Rendell, L. E., and H. Whitehead. 2003. Vocal clans in sperm whales (Physeter macrocephalus). Proceedings of the Royal Society of London. Series B: Biological Sciences 270:225–231.

Roberts, B. L., and A. J. Read. 2015. Field assessment of C-POD performance in detecting echolocation click trains of bottlenose dolphins (Tursiops truncatus). Marine Mammal Science 31:169–190.

Roch, M. A., H. Klinck, S. Baumann-Pickering, D. K. Mellinger, S. Qui, M. S. Soldevilla, and J. A. Hildebrand. 2011a. Classification of echolocation clicks from odontocetes in the Southern California Bight. The Journal of the Acoustical Society of America 129:467–475.

Roch, M. A., T. Scott Brandes, B. Patel, Y. Barkley, S. Baumann-Pickering, and M. S. Soldevilla. 2011b. Automated extraction of odontocete whistle contours. The Journal of the Acoustical Society of America 130:2212–2223.

Roch, M. A., M. S. Soldevilla, R. Hoenigman, S. M. Wiggins, and J. A. Hildebrand. 2008. Comparison of machine learning techniques for the classification of echolocation clicks from three species of odontocetes. Canadian Acoustics - Acoustique Canadienne 36:41–47.

Rojano-Doñate, L., B. I. McDonald, D. M. Wisniewska, M. Johnson, J. Teilmann, M. Wahlberg, J. Højer-Kristensen, and P. T. Madsen. 2018. High field metabolic rates of wild harbour porpoises. The Journal of Experimental Biology 221:jeb185827.

Sarnocinska, J., J. Tougaard, M. Johnson, P. T. Madsen, and M. Wahlberg. 2016. Comparing the performance of C-PODs and SoundTrap/PAMGUARD in detecting the acoustic activity of harbor porpoises (Phocoena phocoena). Page 070013 Proceedings of Meetings on Acoustics.

Schrøder, A. E. M., K. Beedholm, and P. T. Madsen. 2017. Time-varying auditory gain control in response to double-pulse stimuli in harbour porpoises is not mediated by a stapedial reflex. Biology Open 6:525–529.

Shapiro, A. D., J. Tougaard, P. B. Jørgensen, L. a. Kyhn, J. D. Balle, C. Bernardez, A. Fjälling, J. Karlsen, and M. Wahlberg. 2009. Transmission loss patterns from acoustic harassment and deterrent devices do not always follow geometrical spreading predictions. Marine Mammal Science 25:53–67.

Soldevilla, M. S., E. E. Henderson, G. S. Campbell, S. M. Wiggins, J. a Hildebrand, and M. a Roch. 2008. Classification of Risso's and Pacific white-sided dolphins using spectral properties of echolocation clicks. The Journal of the Acoustical Society of America 124:609–24.

Sørensen, P. M., D. M. Wisniewska, F. H. Jensen, M. Johnson, J. Teilmann, and P. T. Madsen. 2018. Click communication in wild harbour porpoises (Phocoena phocoena). Scientific Reports 8:9702.

Steiner, W. W. 1981. Species-specific differences in pure tonal whistle vocalizations of five western North Atlantic dolphin species. Behavioral Ecology and Sociobiology 9:241–246.

Stevenson, B. C. 2016. Methods in spatially explicit capture-recapture. University of St Andrews.

Stevenson, B. C., D. L. Borchers, R. Altwegg, R. J. Swift, D. M. Gillespie, and G. J. Measey. 2015. A general framework for animal density estimation from acoustic detections across a fixed microphone array. Methods in Ecology and Evolution 6:38–48.

Surlykke, A., S. Boel Pedersen, and L. Jakobsen. 2009. Echolocating bats emit a highly directional sonar sound beam in the field. Proceedings of the Royal Society B: Biological Sciences 276:853–860.

Surlykke, A., L. Jakobsen, E. K. V. Kalko, and R. A. Page. 2013. Echolocation intensity and

directionality of perching and flying fringe-lipped bats, Trachops cirrhosus (Phyllostomidae). Frontiers in Physiology 4:1–9.

Surlykke, A., P. E. Nachtigall, R. R. Fay, and A. N. Popper. 2014. Biosonar. Page (A. Surlykke, P. E. Nachtigall, R. R. Fay, and A. N. Popper, Eds.) Springer Handbook of Auditory Research. Springer New York, New York, NY.

Teilmann, J., L. a Miller, T. Kirketerp, R. a Kastelein, P. T. Madsen, B. K. Nielsen, and W. W. L. Au. 2002. Characteristics of echolocation signals used by a harbour porpoise (*Phocoena phocoena*) in a target detection experiment. Aquatic Mammals 28:275–284.

Thode, A. 2005. Three-dimensional passive acoustic tracking of sperm whales (Physeter macrocephalus) in ray-refracting environments. The Journal of the Acoustical Society of America 118:3575–3584.

Thode, A. M., G. L. D'Spain, and W. A. Kuperman. 2000. Matched-field processing, geoacoustic inversion, and source signature recovery of blue whale vocalizations. The Journal of the Acoustical Society of America 107:1286–1300.

Thode, A. M., P. Gerstoft, W. C. Burgess, K. G. Sabra, M. Guerra, M. D. Stokes, M. Noad, and D. H. Cato. 2006. A portable matched-field processing system using passive acoustic time synchronization. IEEE Journal of Oceanic Engineering 31:696–710.

Thomas, L., A. Jaramillo-Legorreta, G. Cardenas-Hinojosa, E. Nieto-Garcia, L. Rojas-Bracho, J. M. Ver Hoef, J. Moore, B. Taylor, J. Barlow, and N. Tregenza. 2017. Last call: Passive acoustic monitoring shows continued rapid decline of critically endangered vaquita. The Journal of the Acoustical Society of America 142:EL512–EL517.

Tiemann, C. O., A. M. Thode, J. Straley, V. O'Connell, and K. Folkert. 2006. Three-dimensional localization of sperm whales using a single hydrophone. The Journal of the Acoustical Society of America 120:2355–2365.

U.S. Marine Mammal Protection Act of 1972. 16 U.S. Code Sections 1362 and 1372 (2000). 1972. .

Ural, T., R. Bahli, M. Yano, T. Inoue, T. Sakamaki, and T. Fukuchi. 2006. Results From A High-Resolution Acoustic Device For Monitoring Finless Porpoises In Coastal Precincts Off Japan. Pages 1–5 OCEANS 2006 - Asia Pacific. IEEE.

Urick, R. J. 1983. Principles of underwater sound. 3rd Edition. Peninsula Publishing, New York, NY.

Verfuß, U. K., C. G. Honnef, A. Meding, M. Dähne, R. Mundry, and H. Benke. 2007. Geographical and seasonal variation of harbour porpoise (*Phocoena phocoena*) presence in the German Baltic Sea revealed by passive acoustic monitoring. Journal of the Marine Biological Association of the UK 87:165–176.

Verfuß, U. K., L. A. Miller, P. K. D. Pilz, and H. U. Schnitzler. 2009. Echolocation by two foraging harbour porpoises (Phocoena phocoena). Journal of Experimental Biology 212:823–834.

Villadsgaard, A., M. Wahlberg, and J. Tougaard. 2007. Echolocation signals of wild harbour porpoises, Phocoena phocoena. Journal of Experimental Biology 210:56–64.

Wahlberg, M. 2002. The acoustic behaviour of diving sperm whales observed with a hydrophone array. Journal of Experimental Marine Biology and Ecology 281:53–62.

Wahlberg, M., B. Møhl, and P. Teglberg Madsen. 2001. Estimating source position accuracy of a large-aperture hydrophone array for bioacoustics. The Journal of the Acoustical Society of America 109:397.

Waring, G. T., E. Josephson, and K. Maze-foley. 2015. NOAA Technical Memorandum NMFS-US Atlantic and Gulf of Mexico Marine Mammal Stock Assessments -- 2014. NOAA Tech Memo NMFS NE 231; 361 p.

Watkins, W. a., and W. E. Schevill. 1972. Sound source location by arrival-times on a non-rigid three-dimensional hydrophone array. Deep Sea Research 19:691–706.

White, P. R., and M. L. Hadley. 2008. Introduction to particle filters for tracking applications in the passive acoustic monitoring of cetaceans. Canadian Acoustics - Acoustique Canadienne 36:146-152.

Whitehead, H., and J. Gordon. 1986. Methods of obtaining data for assessing and modelling sperm whale populations which do not depend on catches. Reports of the International Whaling Commission 8:149–166.

Whitehead, H., and L. Weilgart. 1990. Click rates from sperm whales. The Journal of the Acoustical Society of America 87:1798–1806.

Wiggins, S. M., M. a. McDonald, and J. a. Hildebrand. 2012. Beaked whale and dolphin tracking using a multichannel autonomous acoustic recorder. The Journal of the Acoustical Society of America 131:156.

Wiggins, S. M., M. A. McDonald, L. M. Munger, S. E. Moore, and J. A. Hildebrand. 2004. Waveguide propagation allows range estimates for north pacific right whales in the bering sea. Page Canadian Acoustics - Acoustique Canadienne.

Wilson, B., S. Benjamins, and J. Elliott. 2013. Using drifting passive echolocation loggers to study harbour porpoises in tidal-stream habitats. Endangered Species Research 22:125–143.

Wisniewska, D. M., M. Johnson, K. Beedholm, M. Wahlberg, and P. T. Madsen. 2012. Acoustic gaze adjustments during active target selection in echolocating porpoises. The Journal of experimental biology 215:4358–73.

Wisniewska, D. M., M. Johnson, J. Teilmann, L. Rojano-Doñate, J. Shearer, S. Sveegaard, L. A. Miller, U. Siebert, and P. T. Madsen. 2018a. Response to “Resilience of harbor porpoises to anthropogenic disturbance: Must they really feed continuously?” Marine Mammal Science 34:265–270.

Wisniewska, D. M., M. Johnson, J. Teilmann, U. Siebert, A. Galatius, R. Dietz, and P. T. Madsen. 2018b. High rates of vessel noise disrupt foraging in wild harbour porpoises (Phocoena phocoena). Proceedings of the Royal Society B: Biological Sciences 285:20172314.

Wisniewska, D. M. M., M. Johnson, J. Teilmann, L. Rojano-Doñate, J. Shearer, S. Sveegaard, L. A. A. Miller, U. Siebert, and P. T. T. Madsen. 2016. Ultra-High Foraging Rates of Harbor Porpoises Make Them Vulnerable to Anthropogenic Disturbance. Current Biology 26:1441–1446.

Wisniewska, D. M., J. M. Ratcliffe, K. Beedholm, C. B. Christensen, M. Johnson, J. C. Koblitz, M. Wahlberg, and P. T. Madsen. 2015. Range-dependent flexibility in the acoustic field of view of echolocating porpoises (Phocoena phocoena). eLife 4:1–16.

Wright, A. J., T. Akamatsu, K. N. Mouritsen, S. Sveegaard, R. Dietz, and J. Teilmann. 2016. Review of Low-Level Bioacoustic Behavior in Wild Cetaceans: Conservation Implications of Possible Sleeping Behavior. Pages 1251–1258.

Yack, T. M., J. Barlow, M. A. Roch, H. Klinck, S. Martin, D. K. Mellinger, and D. Gillespie. 2010. Comparison of beaked whale detection algorithms. Applied Acoustics 71:1043–1049.

Yovel, Y., B. Falk, C. F. Moss, and N. Ulanovsky. 2010. Optimal Localization by Pointing Off Axis. Science 327:701–704.

Zamon, J. E. 2003. Mixed species aggregations feeding upon herring and sandlance schools in a nearshore archipelago depend on flooding tidal currents. Marine Ecology Progress Series 261:243–255.

Zimmer, W. M. X., M. P. Johnson, P. T. Madsen, and P. L. Tyack. 2005. Echolocation clicks of free-ranging Cuvier's beaked whales (Ziphius cavirostris). The Journal of the Acoustical Society of America 117:3919–3927.

Chapter 2: Open source click train detector for toothed whales

Sperm whale surfacing near Kruzof Island, Alaska, US

Chapter 2: Open source click train detector for toothed whales

ABSTRACT

Toothed whales (for example sperm whales, delphinids, river dolphins, porpoises and beaked whales) produce sequences of echolocation clicks (click trains) with varying amplitudes and inter click intervals to sense their surroundings and locate prey. Click trains detected on passive acoustic monitoring equipment contain information on both the likely species and behavioural state of the source animal. Thus, the contextual detection of these sequences has the potential to improve species classification compared to identifying individual transients and provides an automated means to obtain behavioural information. There are, however, very few accessible and open source click train algorithms available for analysis of passive acoustic data. Here a multi hypothesis tracking pattern recognition algorithm is used to identify sperm whale, delphinid and harbour porpoise click trains. The algorithm shows promise for all three taxa, significantly lowering false positive rates compared to an individual click by click classification approach and particularly improves performance in delphinid click identification. The algorithm is open source and has been integrated into PAMGuard, a widely used passive acoustic software suite.

INTRODUCTION

Toothed whales produce echolocation clicks which differ in frequency, amplitude and waveform depending on species. These can vary from the multi pulsed 15 kHz transients produced by sperm whales (Møhl et al. 2003) to short broadband clicks used by most delphinids (Au 1993, Ladegaard et al. 2015), the longer frequency-modulated pulses of beaked whales (Johnson et al. 2004, 2006) and narrow band high frequency clicks (NBHF) which are utilised by harbour porpoises (Li et al. 2007, Villadsgaard et al. 2007, Bassett et al. 2009, Kyhn et al. 2013), *Kogia* (Madsen et al. 2005, Merkens et al. 2018), six species of delphinids (Kyhn et al. 2009, 2010, Götz et al. 2010) and a single species of river dolphin (Melcón, et al. 2012).

Whilst the acoustic properties of clicks vary across taxa, all toothed whale species measured so far echolocate using a highly directional beam profile with directivity indices which are remarkably similar across different species (Jensen et al. 2018). For the same distance, the amplitude of a click is therefore highest when recordings are made directly in front of the animal and reduces significantly (up to -50 dB) with increasing off-axis angles (Zimmer et al. 2005, Au et al. 2012a, Finneran et al. 2014). A physical consequence of this type of sound production is that the waveform and frequency content of clicks also vary as a function of off-axis angle, with off-axis waveforms often highly distorted compared to direct on-axis clicks (Au et al. 2012b, Finneran et al. 2014, Ladegaard et al. 2015).

The distribution of inter click intervals (ICI) broadly scale with species size (Jensen et al. 2018) and can be additionally affected by behaviour . For example, sperm whales, the largest toothed whale, produce clicks every 0.5-2 s on average e.g. (Douglas et al. 2005, Fais et al. 2016) and harbour porpoises, amongst the smallest species, appear to have more variable clicks rates with an ICI between 20-300 ms (Verfuß et al. 2009, Linnenschmidt et al. 2013). Although the average ICI of click trains varies significantly across species, there are several behavioural modes which are broadly shared between different toothed whale groups. Sperm whales (e.g. Gordon 1987; Miller et al. 2004; Fais et al. 2016), dolphins (e.g. Wisniewska et al. 2014), beaked whales (Johnson et al. 2004) and porpoises (e.g. Deruiter et al. 2009) have all been recorded increasing click rates preceding prey capture (beaked whales and most deep divers only do so at very close range), with the final few

seconds ending in a buzz; a sequence of rapid clicks produced at lower source levels. Many delphinid species have also been recorded producing brief bursts of ultra-high click rates (<20 µs), termed 'burst pulses', likely used in social interaction (Dawson 2010), and harbour porpoises have been observed producing buzz-like sounds with specific ICI modes in communication contexts (Clausen et al. 2010, Sørensen et al. 2018).

Useful information about species (or species group) identity and behaviour is therefore contained both in the acoustic properties of individual clicks *and* the sequences of click intervals within click trains. Passive acoustic monitoring (PAM) is widely used to detect, classify, localise, estimate the density of, and, in some cases, infer the behaviour of cetaceans. The directional beam profile of toothed whales and the range and frequency-dependent attenuation as clicks propagate through the water column (Ainslie and Mccolm 1998) means clicks received on a hydrophone will vary significantly in amplitude, waveform, and frequency content. The acoustic features of clicks are thus highly variable and often overlap with other transients (e.g. anthropogenic, snapping shrimp, sediment movement – from now on termed *transient noise*) and, in many circumstances, the echolocation clicks of other species.

A number of automated detectors and classifiers based on the analysis of the waveform of individual clicks have been developed for PAM. These range from relatively simple and computationally efficient energy band detectors (Klinck and Mellinger 2011) and Taeger energy operator-based algorithms e.g. (Kandia and Stylianou 2006, Glotin et al. 2008, Baumann-Pickering et al. 2010) to a range of statistical and machine learning methods, such as logistic regression models (Cosentino et al. 2019), decision trees (Gillespie and Caillat 2008), Gaussian mixture models (Roch et al. 2011), support vector machines (Jarvis et al. 2008) and neural net based approaches (Jiang et al. 2018). The performance of classifiers varies significantly with the signal to noise ratio (SNR) (Klinck and Mellinger 2011) and whilst some methods have reported remarkably accurate results in species identification (e.g. Luo et al. 2017; Kandia & Stylianou 2006; Cosentino et al. 2019) others can show relatively high false positive rates, especially in distinguishing between species with similar click types e.g. (Roch et al. 2011). The variety of training and analysis datasets used in these different studies means that it is difficult to quantify the comparative performance of these methods, and thus determine whether accurate results are due to an effective analysis approach, over-training and/or using training data that underrepresents the full range of possible confounding noise sources. In one

study, where different beaked whale click classification algorithms were compared, simple individual click classifiers performed nearly as well as more complex machine learning based methodologies (Yack et al. 2010).

The contextual information provided by click trains has the potential to improve classification in several ways compared with individual click-by-click based algorithms. Slowly varying ICI is a strong indication that a group of clicks is from a biological source (often an odontocete); noise from transients is often more random or, when man-made, has a very uniform ICI (e.g. echo sounders). Slowly varying sequences of clicks are therefore a good indicator that signals are of interest. If a sequence of transients is successfully detected then the spectra of individual clicks within the click train can be averaged, giving a more consistent and smoothed average spectrum which generally improves the performance of most types of species classification algorithms. In some taxa, such as dolphins, similar click features and distortion resulting from highly directional beam profiles means that species-specific features are often only discernible when multiple clicks are combined into average spectra or concatenated spectrograms (Soldevilla et al. 2008). The advantages of grouping clicks together for species classification has been demonstrated by Frasier et al. (2017) who used unsupervised machine learning methods based on averaging the spectra of detected delphinid clicks within 5-minute bins to successfully identify individual dolphin species. Thus click train detection has the potential to improve classification by averaging multiple clicks, enable classification of species with similar click features, provide detailed information on acoustic behaviour and can be used to determine the likely number of animals in a recording – a parameter that can be important for group size estimates used in density estimation.

The challenge for an automated click train detection algorithm is to group clicks from the same echolocating animal including in situations where there are significant levels of transient noise and/or where multiple animals are generating interleaving click trains. Several different approaches to automated click train analysis have been attempted. Rhythmic analysis uses the time between successive clicks to create a time versus ICI surface (ICI-gram) in which click trains appear as slowly changing contours, analogous to tonal sounds on a spectrogram (Le Bot et al. 2015). This method has the advantage of requiring only the time of each received click, however, the ICI-grams can become noisy when transient noise is present and thus extraction of ICI contours and association of clicks into click trains introduces a further pattern recognition problem. A number of more bespoke algorithms,

usually based on tracking a subset of temporal or acoustic features, have been developed for sperm whales (Lepper et al. 2005, Baggenstoss 2011) and dolphins (Starkhammar et al. 2011), however, none provide a generalised framework for click train detection of different species. Multi-hypothesis tracking (MHT) algorithms consider a large set of hypotheses for possible click trains and, although processor intensive, have been demonstrated to be effective when applied to beaked whale and pilot whale data (Gerard et al 2008a; Gerard et al. 2008b; Gerard et al. 2009). This approach appears to be the most promising because it's a generalised pattern recognition algorithm and can incorporate multiple click parameters, e.g. ICI, waveform, bearing etc.

Whilst each type of algorithm has been appropriate for their bespoke analyses, as with individual-based click classifiers, all the aforementioned studies have used disparate datasets and there are no standardised performance metrics for accurate comparison of these algorithms. In addition, many of the methods are complex to implement and none have have provided well documented programming libraries to allow other researchers to assess the performance of each method on other datasets. Thus, despite the potential efficacy of click train detection, this lack of accessibility would usually preclude the wide-scale adoption of click train analysis methods in PAM studies. However, in marine mammal PAM applications, click train based analysis is widely used for some species but is based almost entirely on one proprietary algorithm used in conjunction with specific PAM hardware (FPODs, CPODs and TPODs) developed by a private company (Chelonia Ltd.). This hardware/system has shown to be effective in detecting numerous delphinid and NBHF species e.g. (Roberts and Read 2015, Sostres Alonso and Nuuttila 2015) and has been used as an analysis methodology in dozens of academic papers and by many private consulting firms (e.g. Wilson et al. 2013, Garrod et al. 2018, Wright and Tregenza 2020). The wide-scale adoption of this proprietary and hardware specific algorithm highlights the need for a more generally applicable click train classification system, which can be used with acoustic recording devices.

Here an open source and computationally efficient click train detector is presented based on multi-hypothesis tracking first proposed for click train detection by Gerard et al. (2008a). Their algorithm has been improved and integrated into PAMGuard, a widely used bioacoustics software package (Gillespie *et al.*, 2008; www.pamguard.org). The efficacy of the MHT click train detector is tested by comparing its performance to several manually annotated datasets of sperm whales, delphinids, and

harbour porpoises, and additionally tested its performance against an individual click-by-click classifier.

2.1 MATERIALS AND METHODS

The data input for both the click train detector and the individual click-by-click classifier is a list of detected transients extracted from raw acoustic recordings using the PAMGuard click detector module (version 2.00.18b). The click detector module detects all transients which are a pre-specified threshold (in this case 10 dB) over continuously sampled background noise levels (see section 5.9.3 for a detailed description of the click detection algorithm). Each transient detection triggers the collection of a short waveform snippet of raw acoustic data containing the transient waveform and a pre- and post-detection buffer of 100 samples. Detected transients are also tagged with metadata such as time, sample number, and, where available, bearing estimated from the time delays between closely spaced receivers. Generally, the click detector module is used to detect all transients within a frequency band at a relatively low threshold above background noise levels and thus will typically run at a high false positive rate, detecting a range of direct and multi-path transients which can originate from biological, anthropogenic and stochastic noise sources. Downstream classification algorithms can then be used to identify transients of interest.

2.1.1 Multi-Hypothesis Tracking Click Train Analysis

2.1.1.1 MHT Click Train detector Introduction

The task for any click train detection algorithm is to associate transients over time which are from the same click train (e.g. from an individual dolphin, or a single echosounder, etc.). An MHT click train detector approaches this problem by creating large numbers of possible associations of clicks (track hypothesis) and tests each possible association for the likelihood it is from the same source and thus represents a valid click train. As the number of clicks (n) increases over time, the number of track hypothesis increases by 2^n, and so associations which are of the lowest likelihood are pruned, leaving only the highest likelihood click trains to continue over time.

The MHT algorithm thus consists of two components; first, a set of tentative click associations, which expands and contracts over time as clicks are added to the hypothesis mix and lowest likelihood click trains are pruned, and second, a model which determines the likelihood of an association of clicks

being from the same click train. Here the likelihood is represented by a χ^2 value, where the lower the value, the more likely a click train is from a single source.

2.1.1.2 Track Hypothesis

The multiple track hypothesis are represented by a large binary matrix. This "hypothesis matrix" has dimensions equal to the current position in the click time series $k=1,2,3\ldots n$ and the current number of possible track hypotheses N. Each entry is either 0 or 1, with 1 indicating that click k is contained within a possible train.

Each time a new click is added, the size of the hypothesis matrix doubles as each track hypothesis has both a 1 and 0 added to it i.e. the new click is both included and not included in the possible click train. Thus, the number of hypotheses rapidly increases with each subsequent click in the series and so, to prevent the number of hypotheses reaching computational limits, for every added click, a pruning process is undertaken (Figure 1). First, a χ^2 value for every click train in the hypothesis matrix is calculated. Then, starting at the track hypothesis with the lowest χ^2 (highest likelihood), the algorithm moves back a number of clicks defined by a prune back constant, Np. All hypothesis branches which contain the same association of clicks defined from click $1,2,3\ldots n- Np$ are kept. Any other track hypothesis with conflicting associations, i.e. that contain some but not all of the same clicks in the association from $1,2,3...n- Np$, are discarded. The pruning process is then repeated for the remaining unkept click train associations in the hypothesis matrix. This is continued until either there are no more unkept track hypotheses, or the number of pruning iterations reaches a set limit. If that limit is reached, then all remaining track hypotheses are discarded. In addition, a single track hypothesis which contains no clicks is always kept in the hypothesis matrix, allowing a completely new click train to start at any iteration. The remaining matrix contains a set of track hypotheses each of which contains a unique set of clicks up to click $n- Np$ i.e. there are no clicks which are part of two trains.

Once pruning has taken place, click trains are tested to determine whether they are complete. Click train completeness is based on the ICI. If a click train in the hypothesis matrix "coasts", whereby it acknowledges that it has likely missed a click based on previous ICI measurements, for a set number of inter-click intervals, then it saved and removed from the hypothesis matrix.

Eventually, the trailing end of the hypothesis matrix will contain no clicks, i.e. is filled with zeros. To save memory, this part of the hypothesis matrix is checked every 100 clicks and the hypothesis matrix is trimmed up to the first active click in the track hypothesis matrix.

Thus, over time, many thousands of track hypotheses (i.e. possible click trains) are considered, many removed from the hypothesis matrix and some saved. The algorithm therefore can track multiple clicks trains simultaneously and considers new hypotheses on every iteration, allowing it to generate new trains at any time.

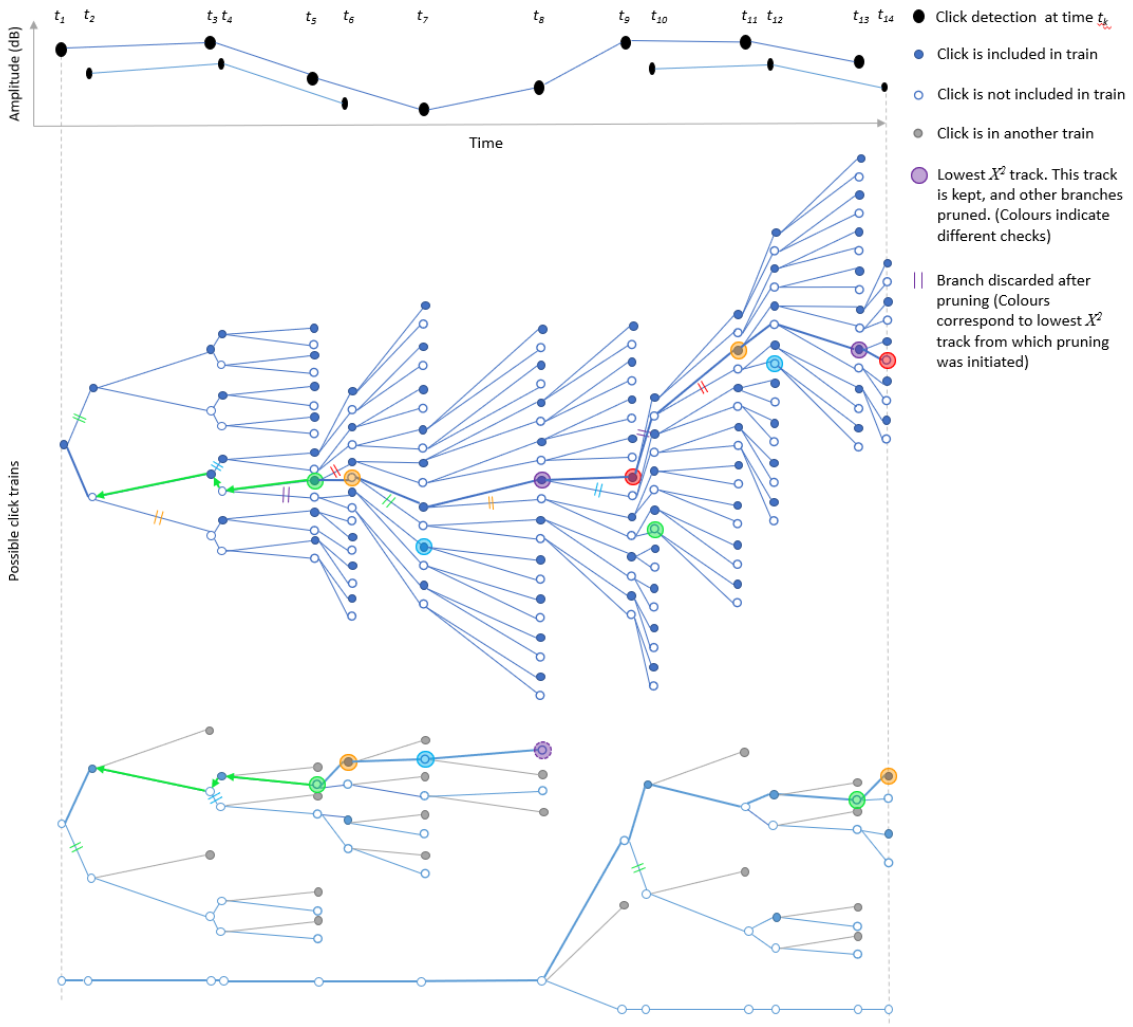

Figure 1. Diagram demonstrating the methodology of the click train algorithm. Black dots are a set of 14 detected clicks at times t_1 to t_{14}. The click train algorithm begins at click 1 and creates two possible clicks trains, one that includes the first click (filled circle) and the other in which the click is not part of the click train (non-filled circle). The algorithm then moves to the next click and adds it to the hypothesis matrix. As the number of clicks increases, the hypothesis matrix exponentially expands in size and must be pruned. After a minimum of N_{pmin} clicks (in this case 4) each track hypothesis (possible click train) is assigned a χ^2 score. The track hypothesis with lowest score (defined by larger coloured circles) has its branch traced back N_p (in this case 3) clicks. Any track hypothesis which does not include the click N_p steps back are pruned (defined by the double lines). Clicks which share no click associations with the first track hypothesis are then pruned and the process repeats until all clicks are part of a track or a maximum number of tracks have been considered (in this example there are two tracks). The algorithm then moves to the next click, adds it to the hypothesis matrix, assigns χ^2 scores and traces the lowest χ^2 branch N_p steps back, pruning the hypothesis matrix again; the process repeats until the last click. Note that there is always a track hypothesis with no associated clicks (i.e. the bottom-most branch where no clicks belong to a click train). If a track hypothesis is confirmed and thus removed from the hypothesis matrix, then this track can be used to start another click train.

2.1.1.3 Click Train Likelihood Model

An MHT algorithm is only effective if the χ^2 model accurately reflects the likelihood that a click train is from a single biological source. The model here is based on the likely properties of toothed whale click trains. The acoustic behaviour and narrow beam profile of toothed whales mean that clicks detected on hydrophones generally share a number of slowly varying stereotyped properties. Specifically, the ICIs generally change slowly over time and the amplitude and spectral properties of click trains slowly varies with both distance and, due to highly directional beam profiles, the relative angle of the animal to the receiver. If an acoustic sensor is capable of calculating the bearing to an animal, i.e. using two or more hydrophones or specialised sensors (e.g. Miller 2012) then the received time delays between hydrophones and/or bearing to animals will also change gradually over time.

The rate at which these click train *descriptors* change is dependent on several factors. An animal swimming closer to the hydrophone will result in a greater relative change in bearing between the animal and a hydrophone. The apparent source level due to a toothed whale's narrow beam profile is a function of the relative angle of an animal to the receiver and standard spherical spreading models mean that amplitude changes more rapidly at closer ranges. Thus, as range decreases, bearing and received amplitude changes will likely increase. This is also true for swim speed. A faster swimming animal will mean that changes in amplitude and bearing are greater. In order not to bias detection efficiency with distance and swim speed it is therefore important that a model considers the rate in rate of change . For example, a click train with large but consistent bearing changes, as an animal swims closely and/or more slowly past a sensor, should not be penalised compared to a distant click train with slowly changing bearings. One solution is to consider the 2nd derivative of bearing and amplitude measurements. The 2nd derivative should not penalise large changes in bearing, amplitude or other descriptors as long the changes are consistent, thus should minimise bias due to range and swim speed.

The χ^2 model used here considered both the slowly varying properties of click trains, as well as bonus and penalty factors to discourage fragmentation and aliasing (selecting a multiple of the true ICI) of detected click trains.

The initial basis of the model is:

$$\chi^2 = \sum_{i=1}^{m} \left(\left(\sum_{k=2}^{n-1} \frac{\left((y_{i,k} - y_{i,k-1}) - (y_{i,k+1} - y_{i,k})\right)^2}{max\left(q_i(t_{k+1} - t_k), qt_i\right)^2} \right) \Big/ n \right) \Big/ m \qquad \text{Eq. 2.1}$$

where m is the number of selected descriptors, e.g. ICI, amplitude, bearing *etc.*, and $y_{i,k}$ is the measurement of descriptor i for click k in a click train with n associated clicks. t_{k+1} is the measured time of a click k. Each descriptor is divided by q_i which is a user tuneable parameter that alters the importance each descriptor has on the total χ^2. Ideally it should correspond to a prediction of the likely variance in the second derivative of the descriptor measurements, however, this can be difficult to quantify and there may be reasons to favour some descriptors over others. Furthermore, because the hypothesis matrix considers only the relative magnitudes of the χ^2 value between possible tracks, the absolute value of q_i for each descriptor makes no difference to the tracking algorithm; instead it is the ratio of q_i between different descriptors which is important. qt_i is a minimum divisor allowed which prevents very small ICIs close to zero from assigning very large contributions to the ${\chi_r}^2$ value.

An example of the model, if only amplitude and ICI descriptors of click trains are considered, is:

$$\chi^2 = \left(\sum_{k=1}^{n-1} \frac{\left(20\left(\log_{10}\left(\frac{x_k}{x_{k-1}}\right) - \log_{10}\left(\frac{x_{k+1}}{x_k}\right)\right)\right)^2}{max(q_a(t_{k+1} - t_k),\ qt_a)^2} + \sum_{k=2}^{n-1} \frac{((t_k - t_{k-1}) - (t_{k+1} - t_k))^2}{max(q_c(t_{k+1} - t_k),\ qt_c)^2} \right) \Big/ 2n \qquad \text{Eq. 2.2}$$

where x_k is the linear peak to peak amplitude of a click, q_a is the amplitude specific divisor, and q_c is the ICI specific divisor .

χ^2 is a measurement of the consistency of descriptors within a click train, however, there are several weaknesses in this model. χ^2 will be the same value if it selects every second, third etc. click in a uniform click train (click train aliasing). Thus, using this model alone often results in overlapping aliased click trains. The χ^2 value is also independent of the length of a click trains. As a tracked click train becomes longer there is a higher chance of inconsistencies in click train descriptors which will

increase the value of χ^2 and thus the hypothesis matrix will favour shorter fragmented rather than continuous click trains

To minimise this, a number of bonus/penalty factors are added to χ^2; these are:

- Add a penalty for "coasting" i.e. when an expected click, based on ICI, is not present in the click train. This penalty is a constant C multiplied by the number of coasts i.e. the likely number of missed clicks based on ICI
- If the median ICI of the possible click train is above a specified maximum value, add a large penalty which effectively makes it one of the least likely click trains in the hypothesis matrix. If the median ICI is below the maximum value then $\chi^2 = \chi^2(\frac{\tilde{I}}{\max_k I_k})$ where $\tilde{I}$ is the median ICI, $\max_k I_k$ is the maximum ICI in the possible click train. This bonus term favours lower ICI values preventing aliased click trains.
- Add a bonus factor for longer click trains to prevent fragmentation. This is the length of click train divided by the total number of clicks added to the hypothesis matrix.
- If a track hypothesis is newly added in the hypothesis matrix, then add a minor penalty factor Tp (in this case, a penalty of 100).

An example of the MHT click train algorithm is graphically illustrated in Figure 1, and a summary of the algorithm is follows:

1. Add a click to the hypothesis matrix and calculate a new set of possible click trains based on the existing previous trains.
2. If the number of clicks in the time series is less than Np, then *repeat* step 1.
3. If the number of clicks is greater than Np, then calculate χ^2 for all click trains in the hypothesis matrix using Eq. 2.1 and adding bonus and penalty factors.
4. Select the lowest χ^2 and count backwards to position $k\text{-}Np$ in the hypothesis matrix. Remove all track hypotheses which have the same combination of clicks from $0 \ldots k\text{-}Np$ and save to a new hypothesis matrix.
5. Repeat step 4 until all click trains have been removed, or until the maximum number of new hypotheses has been reached.

6. Scan the new hypothesis matrix and remove and save any click trains which have over C allowed coasts. These become confirmed click trains.
7. If the next click in the time series is greater than the maximum number of permissible coasts, then save all active track hypotheses in the hypothesis matrix and reset.
8. If there are more than a user defined number of trailing zeros, then trim the hypothesis matrix.
9. Move to next click in time series and repeat until the end of the dataset.

2.1.2 Click Train Classification

The MHT click train detector is based on associating clicks with slowly varying descriptors; this detects click trains from echolocating toothed whales but will also detect false positives from any other regular transient sources. For example, if there is a significant number of transients from noise sources then it is likely there is some set of transients that will meet the criteria for a low χ^2 value, generating spurious click trains. Echo sounders from boats and any other source of repetitive transient sounds will also be detected. There is therefore a requirement for a secondary classification stage to both remove false positive click trains and discriminate between toothed whale species.

The MHT click train detector implements a basic binary classifier based on the click train's χ^2 value, ICI measurements and average spectrum. A maximum threshold is set for a click train's final χ^2 value, and minimum and maximum limits set for the medians and standard deviation of ICI. This ensures that a click train is indeed from a sequence of transients with slowly varying descriptors and sets broad limits for ICI pertaining to species or groups.

To identify species, the normalised average spectrum of clicks within a click train is correlated with species spectrum template. The spectra are multiplied together to obtain a spectral correlation match value between 0 and 1. A threshold is set on the correlation value. If χ^2, ICI, and correlation match value all pass the threshold for a specified classifier, then the click train is classified as belonging to that species.

2.1.2.1 Individual Click-by-Click Classifier

Several algorithms have been developed for individual click-by-click based classification. To compare against the click train detector, one possible algorithm would be to use the same spectral correlation templates used in click train classification but apply them to the spectrum of individual clicks.

However, this negates an advantage of classifying clicks on an individual basis. Individual clicks contain waveform as well as spectral information, whilst the average spectrum of a click train contains only spectral information, because a changing waveform, due to distortion from propagation, noise and off-axis distortion, is difficult to accurately average over many clicks. Therefore, to provide a fairer comparison, a matched click classification algorithm was selected for comparison to the click train detector.

The matched click classifier classifies clicks based on a set of accept and reject waveform templates, where the match template is an idealised example of the echolocation click that should be detected and the reject template is an example waveform which should not be classified. The classifier can accept multiple sets of templates. A transient is correlated with each set of match and reject templates. A click is classified if the ratio in correlation between the accept/reject template for any template set is above a pre-defined threshold value. This classifier is designed to minimise false positives from another echolocating species and is therefore especially suited to situations in which the number of potentially confounding click detections from one species (e.g. dolphins) is much greater than that of another species (e.g. harbour porpoises or beaked whales).

2.1.3 Java Implementation

The MHT click train detector is implemented in Java as a discrete application programming interface (API). Each track hypothesis is described by a list of integers, where each bit within the integer represents whether a click is used within the click train or not. Thus, one integer represents a consecutive sequence of 32 clicks. This optimises memory usage and allows the algorithm to consider many possible click associations.

The MHT API is integrated into both PAMGuard and MATLAB (The Mathworks, Natick, MA). A new click train detector module with a graphical user interface was created in PAMGuard to allow users to change click train detector parameters and visualise results. The algorithm can be used in real time monitoring applications and/or in post analysis of acoustic data. The MATLAB library calls the Java API directly. It is therefore comparable in computational speed to PAMGuard and allows users to incorporate the algorithm into custom scripts. The matched click classifier is also a module in PAMGuard.

2.2 TEST DATA SETS

Harbour porpoise and sperm whale datasets were used to assess the performance of the click train classifier. Both datasets contained at least one delphinid species and various anthropogenic and natural noise sources.

2.2.1 Harbour Porpoise Dataset

Data were collected in Cornwall, UK, in December 2018. A 4-channel SoundTrap (Ocean Instruments, New Zealand) was deployed on a gill net in ~25 m of water. Custom made hydrophones (sensitivity -201 dB re 1 V/ µPa) with 20dB 040527D ETEC (ETEC, Denmark) pre-amplifiers were arranged in a 5 cm aperture tetrahedral configuration, allowing 3D bearings to the clicks to be resolved. The clip level of the system was ~181 dB re 1 µPa. Each channel was sampled at 384 kHz, and raw data was saved as compressed X3 files on an internal SD card. The total recording time was 48 hours.

An initial band-pass detection filter band (80-150 kHz) was applied which removed many lower frequency transient sounds allowing the detection of harbour porpoise and broadband delphinid clicks. 3D bearings for each detected transient were calculated in the PAMGuard click detector module. The accuracy of time delay calculations for NBHF are greatly improved for NBHF clicks if up-sampling is used (Gillespie and Macaulay 2019) and so all transients were up-sampled 4 times before time delay measurements and subsequent bearings calculations were performed.

There were no visual observations during the deployment.

2.2.2 Sperm Whale Dataset

Data on sperm whales were collected along the shelf edge off Sitka, Alaska, USA, during 4 cruises in May and June 2019. A stereo towed array with 3 m aperture was towed 200 m behind three different long line fishing vessels ranging in length from 13.7 to 16.8 meters. The towed array contained Magrec HS/ 150 (sensitivity ~ -204 dB re 1 V/ µPa) hydrophones paired with 28dB Magrec HP03 pre-amplifiers and data were digitised at 192 kHz sample rate using a Behringer UMC 202 ASIO SoundCard (24-bit). The clip level of the system was estimated to be ~180 dB re 1µPa, however, it was not properly calibrated. Acoustic data were saved as stereo WAV files to the hard drive of an Intel NUC PC (8th generation i7U processor and 8 GB of RAM) using PAMGuard. During these surveys, the MHT click train detector ran as a PAMGuard module in real time.

A high-pass detection filter of 2 kHz was used to minimise false transients from vessel noise. Bearings between 0 and 180° were calculated automatically in the PAMGuard click detector module. No up-sampling was used in time delay calculations because sperm whale and delphinid clicks are broadband enough not to require it.

There were very high levels of transient noise in this dataset, partly due to electrical noise. This was received on both channels but with the phase inversed between channels. On initial data analysis runs, this swamped both the individual click-by-click and click train classifier resulting in very poor performance. To compensate for this a pre click classification stage was added. Clicks between 80° and 100° bearing were removed if the maximum peak of the cross-correlation function was less than the absolute value of the minimum peak and the saved waveform snippet was <3ms; this eliminated most inverse phase electrical noise whilst preserving acoustic transients.

However, at specific times, despite the initial click pre-filtering stage, high levels of noise occurred at 90° bearing causing large spikes in false positives for both algorithms. This again significantly reduced performance, particularly on a click-by-click basis because of the large numbers of transient present. To compensate for this and provide a more useful comparison, all data between 88° and 92° degrees was removed.

There was fragmented visual effort during the survey. The only delphinids observed were killer whales and visual observations coincided with detections of the typical broadband transients of delphinid echolocation clicks. Sperm whales were visually observed throughout the survey.

2.3 MANUAL ANALYSIS AND TRAINING DATA

Both datasets were manually annotated by an expert analysts. Click trains identified from the spectral properties of clicks and by consistent bearings and ICI and then marked out using the PAMGuard click detector module and annotation tools. The manual dataset was considered “truth” for testing the automated algorithms. Relatively low source levels, high attenuation in seawater and directional click production mean that harbour porpoise detections are often fragmented. Thus, a single click train was defined as a group of clicks with no gap greater than two seconds. The same rules were applied to delphinid click trains.

Sperm whale click trains were marked out in the same manner, however, because of their much larger ICI, a click train was considered to have ended after a gap of ten seconds. Delphinid detections within this dataset were annotated in the same way as in the harbour porpoise dataset.

Several subsections of each dataset, containing examples of each species and anthropogenic noise, were used to train the click train detector. The training data used were 10% of each dataset. q_i in Eq. 1.1 can be considered a measure of how much each descriptor type influences the decision to include clicks into a click train. For example, a higher q_i for bearing means that consistent bearing measurements over time contribute less to deciding whether clicks are associated into a train.

A manual analyst determined a set of reasonable initial values for each parameter by assessing the performance of the click train detector while varying q_i parameters for each descriptor. The values for q_i selected for each descriptor were those that resulted in both reasonable tracking of click trains and the χ^2 value for all descriptors being roughly equal, indicating similar importance for each parameter.

Once satisfactory initial descriptor values had been determined for a dataset, optimised values were determined by an iterative process. The click train algorithm was run through a sensitivity analysis. Each descriptor value was assigned a new value chosen from a flat distribution of values within one order of magnitude of the current default value. The click train detector was then run on the sample dataset using the new descriptor values and performance compared to manual annotations. This process was repeated 100 times and if performance was significantly improved by a particular set of descriptor values, then the new values were selected as new defaults and the training process was repeated until a set of descriptors with optimum and stable performance were established.

2.4 ALGORITHM PERFORMANCE

Two performance measures of the automated click train detector were considered: the ability to determine whether a species or taxa is present within a one-minute time bin (a commonly used metric e.g. Jacobson et al. 2015), and the capability in associating clicks from a single click train (i.e. a single animal). Individual click-by-click classifiers have no ability to associate clicks and thus they were only compared to the click train detector for species presence.

Species presence was tested by splitting each dataset into one-minute bins. A bin was considered a species positive minute (SPM) if there were a minimum number of individual clicks classified as the

target species or taxa. In the harbour porpoise dataset the three classes considered were harbour porpoise, delphinid and unclassified (e.g. transient noise, boat cavitation etc.). In the sperm whale dataset the three classes were sperm whale, delphinid and unclassified.

The efficacy of the detector was measured by generating a precision-recall curve (Roch et al. 2011). *Recall* is the proportion of true manually annotated calls that are detected (i.e. how efficient the detector is), and *precision* is the number of true divided by the total number of automated detections. In this case true call refers to a one-minute bin that contains a manually annotated detection. A perfect detector has a precision and recall value of 1. The curve was generated by measuring precision and recall for a range of detector thresholds. The detector threshold for the click train detector is the minimum spectral correlation value required (between 0 and 1) before a click train is classified. For the matched click classifier, the detection threshold is the minimum ratio between accept and reject templates before a click is positively classified.

Two metrics - fragment size and association crossover - were used to measure the ability of the click train detector to associate clicks from the same animal. Fragment size is the percentage of clicks included within a manually annotated click train which are automatically classified by the click train detector. If all clicks in a click train are classified as the target species, then the fragment size is 1. Association crossover is when a single automatically detected click train contains clicks from two separate manually annotated trains. It is defined as the percentage of automatically detected clicks trains which include clicks from two or more manually annotated click trains.

2.5 RESULTS

2.5.1 Harbour Porpoise Dataset

1.2 million transients were detected from acoustic data collected on the SoundTrap in section 2.3.1. Of these, 27,472 were classified as harbour porpoise clicks, 52,289 were classified as dolphin clicks, and 128,453 were classified as transients in trains produced by the cavitation of passing boat propellers. The remaining transients broadly occurred at a steady rate and with dispersed bearings.

Table 1. Descriptor values used in click train detection for the harbour porpoise dataset.

Descriptor	q_i
ICI	0.05 s
Amplitude	30 dB
Bearing	8°
Correlation	10

Figure 2 shows a one-minute clip of data containing click trains from both harbour porpoise and delphinids (likely common dolphins, this species being regularly sighted in the area). The click train detector using descriptor values in Table 1 was capable of tracking multiple click trains from harbour porpoises and delphinids at the same time and extracting single trains from transient noise.

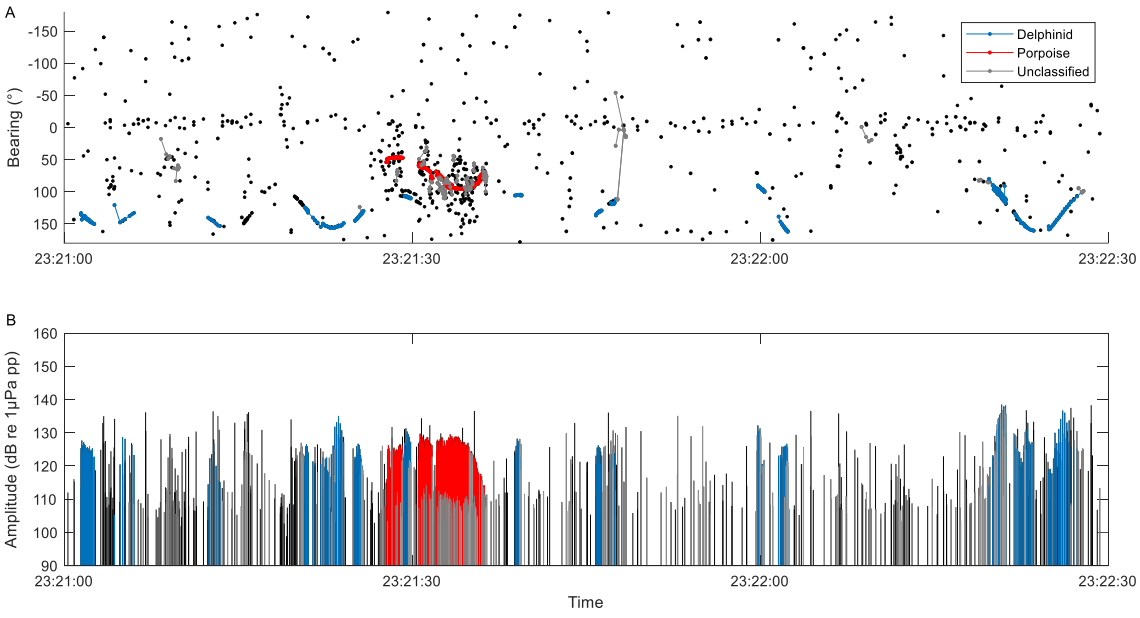

Figure 2. Example of the click train detector working on a harbour porpoise and dolphin dataset. Plot A shows a bearing-time display with each dot showing a detected transient. Blue dots indicate a click train classified as dolphin, and red dots indicate clicks classified as harbour porpoise. Grey indicates that a click train has been detected but not classified to either harbour porpoise or delphind. Plot B shows a received amplitude time stem plot of received click peak-to-peak amplitudes – each line is a transient and coloured lines indicate transients which have been classified. Note that within the harbour porpoise detection, the click train detector has de-interleaved click trains and then classified them to harbour porpoise and delphinid.

Figure 3 is a summary of the entire dataset and compares the click train detector and matched click classifier to manually annotated click trains. The long-term spectral average (LTSA) in plot A shows an overview of the soundscape; this contains high levels of low frequency noise and some broadband noise where small vessels pass close by the hydrophone. Echosounders and a faint electrical noise band are also visible. Plots B and C show the detector outputs; each vertical line on each plot is a one-minute bin coloured according to the number of classified clicks within that bin. Annotated data (A) is considered truth. The plots indicate that both the automated click train classifier (CT) and the matched click classifier (MT) perform well for harbour porpoises, since the results from both classifiers closely align with the manual annotations. The click train detector also performs well for dolphins, however, the matched click classifier runs at a high false positive rate, as indicated by the generally higher background rate in click detections.

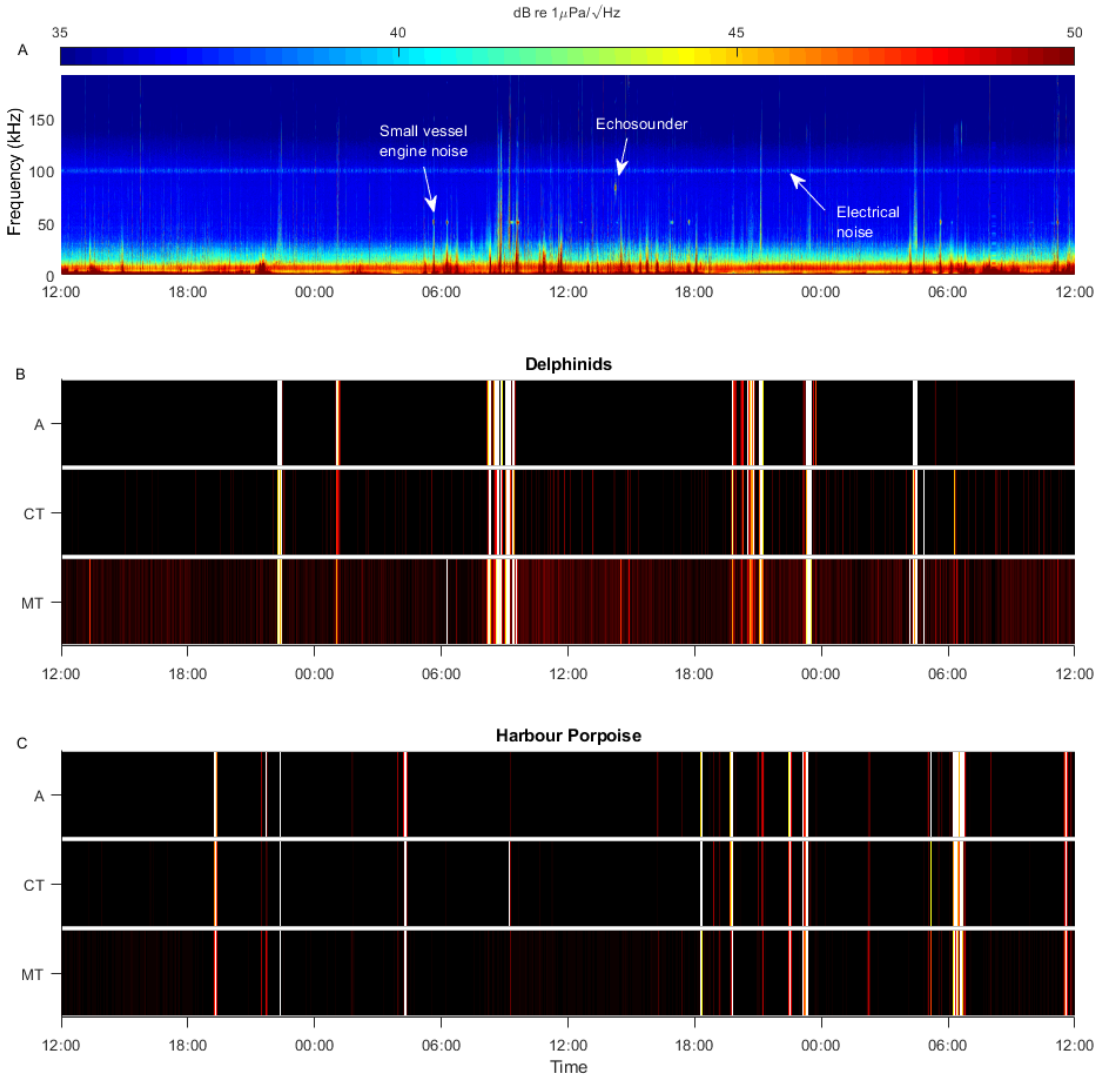

Figure 3. An overview of the soundscape and detector performance for the harbour porpoise dataset. Plot A shows a long term spectral average for the 48 hour deployment period. Plot B shows three plots comparing the click train detector (CT) and matched click classifier (MT) to manually annotated data (A) for dolphin clicks (top) and porpoise clicks (bottom). Each line on the ribbon plot indicates a one-minute bin. The colour of the line is the number of classified clicks within the bin, with black indicating no clicks and then a colour scale of red (<50 clicks) , yellow (50-100 clicks) , and white (over 100 clicks).

2.5.2 Sperm Whale Dataset

In total, 42.8 hours of towed hydrophone data were collected in SE Alaskan waters. 1.6 million transients were detected in these data; manual annotation identified 42,250 were sperm whale clicks, 3,420 killer whales clicks and 1,110 transients from a passing vessel. The remaining transients were propeller, electrical and echosounder noise from the survey vessel and unknown sources.

Figure 4 shows an example of a large group of killer whales passing the survey vessel with more distant sperm whales detected astern and forward of the vessel. This example demonstrates a complex multi-species situation where the click train algorithm using descriptor values in Table 2 is concurrently tracking multiple individuals whilst also dealing with a complex transient noise field. There was some cross-talk between hydrophones resulted in many transients near 90°.

Table 2 Descriptor values used in click train detection for the sperm whale dataset.

Descriptor	**q_i**
ICI	0.2 s
Amplitude	15 dB
Bearing	0.5 °
Correlation	10

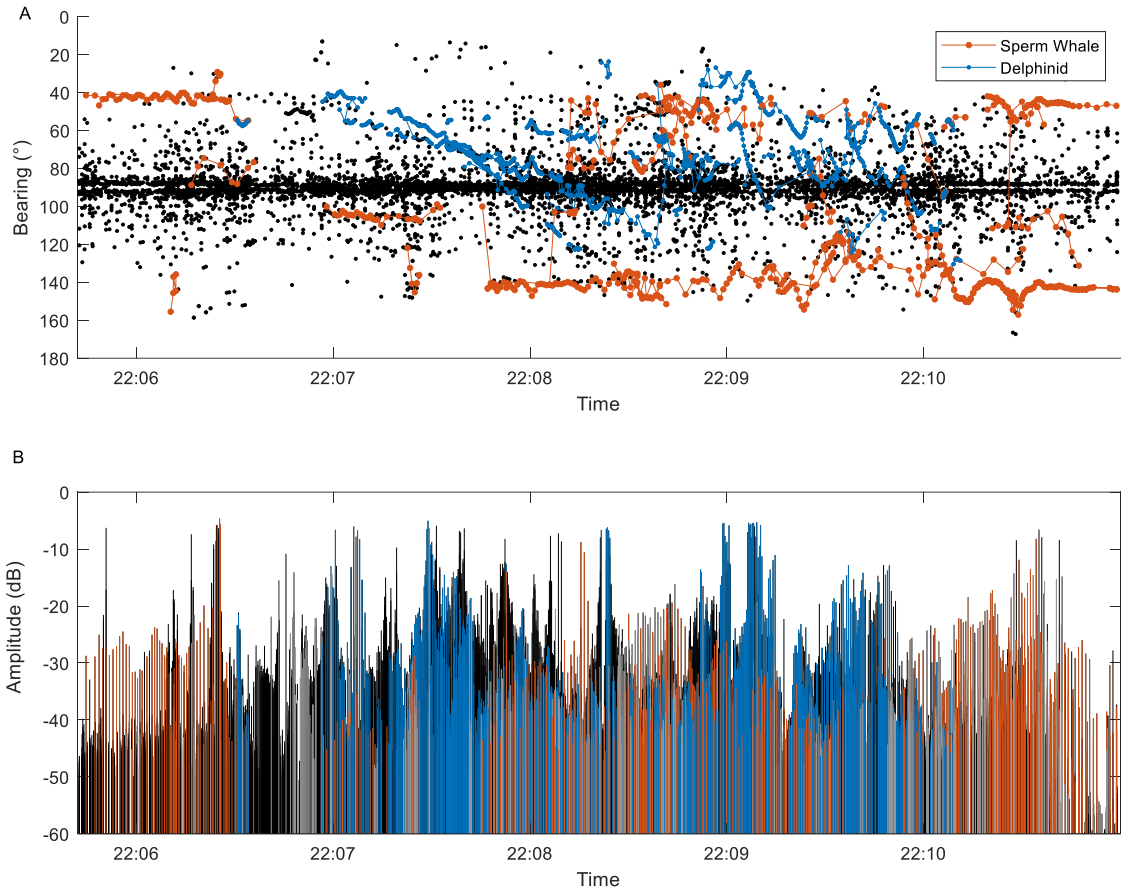

Figure 4. Example of the click train applied to towed array data. Here, there is a large pod of killer whales passing the research vessel. Sperm whales are present at a farther distance from the vessel. Plot A shows a bearing time plot with each dot representing a detected transient and plot B is a received amplitude time stem plot where each vertical line represents a transient. Blue represents clicks trains classified as delphinids (killer whales) and orange shows click trains classified as sperm whales. There is a lot of transient noise and echoes at 90°. Note that the towed array was not calibrated and thus the dB values are relative to the clipping level of the recording chain.

Figure 5 is a concatenation of all towed array surveys in the sperm whale dataset. It is clear from the LTSA that the acoustic and electrical noise profiles varied significantly between surveys due to different vessel being used in each survey.

The click train detector performed well for delphinids (almost certainly killer whales), with fewer false positives compared to the matched click classifier. Performance between the matched click classifier and click train detector in determining SPM was similar for sperm whale clicks.

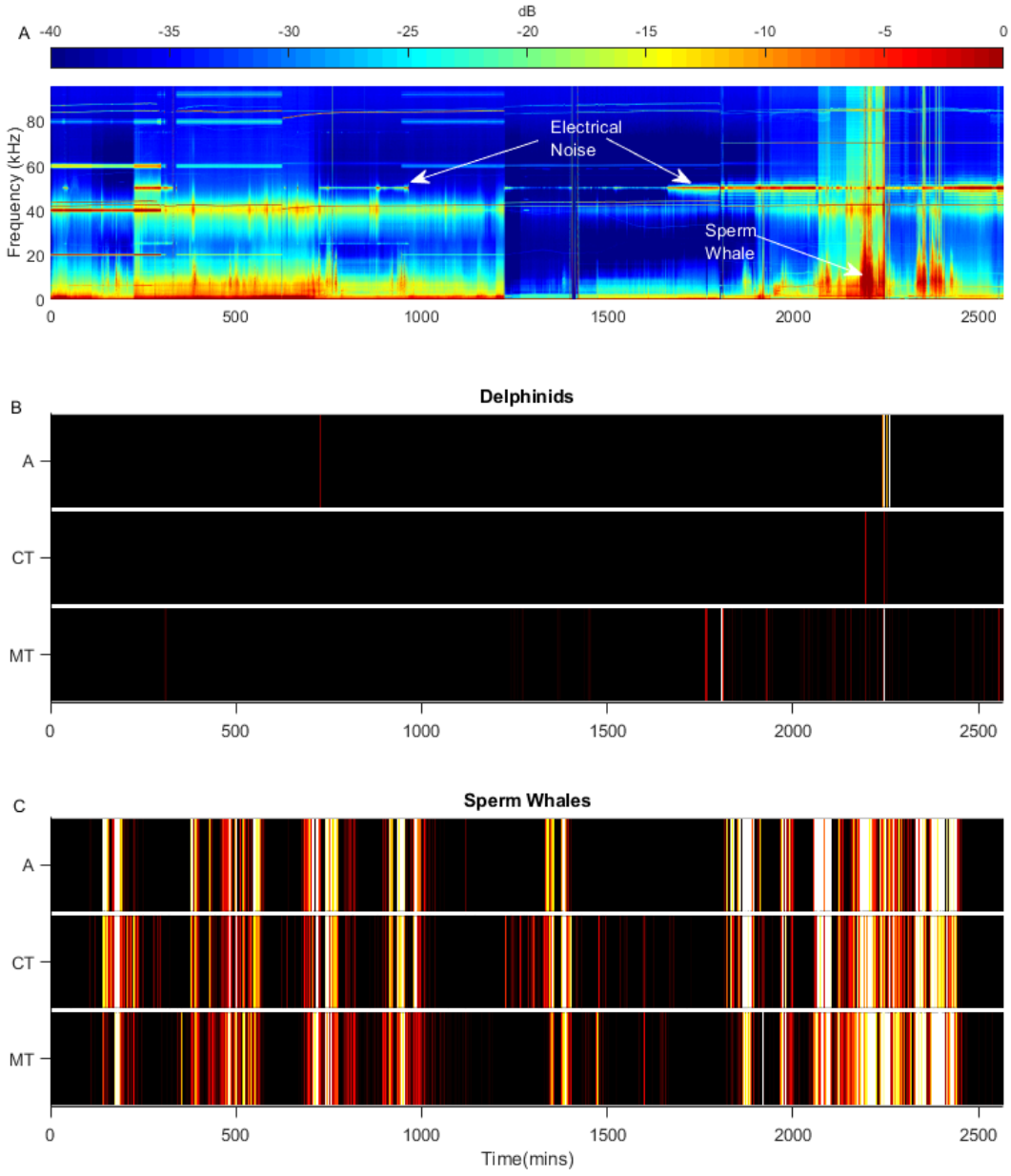

Figure 5. An overview of the soundscape and detector performance for the Alaskan dataset. Plot A shows a concatenated long-term spectral average for all surveys. Note that the dB scale is relative to the clip level as the towed array had not been calibrated. Plot B shows three ribbon plots comparing the click train detector (CT) and matched click classifier (MT) to manually annotated data (A) for killer whale clicks (delphinids). Each vertical line on the ribbon plot indicates a one-minute bin. Plot C shows the detector comparative detector performance for sperm whale clicks.

2.5.3 Precision Recall Curves

Precision and recall curves shown in Figure 6 compare the performance of the click train detector and matched click classifier for harbour porpoise, delphinids and sperm whales. For harbour porpoises, which have relatively stereotyped clicks, the matched click classifier performed on par, or better than the click train detector in determining species positive minutes. However, the matched click classifier tended to have a significantly higher false positive rate at lower SNR levels, but a higher overall detection efficiency when identifying individual clicks. The detection of the less stereotyped clicks of sperm whales marginally benefited from using a click train detection algorithm with the matched click classifier performing similar on species positives minutes but poorly on an individual click by clicks basis with both a significantly higher false positive rate and lower detection efficiency at low SNR. The detection of delphinids, which also have less stereotyped clicks, was significantly improved when using a click train algorithm. The matched click classifier performed adequately on species positive minutes but had a much higher false positive rate and lower detection efficiency at all SNR values.

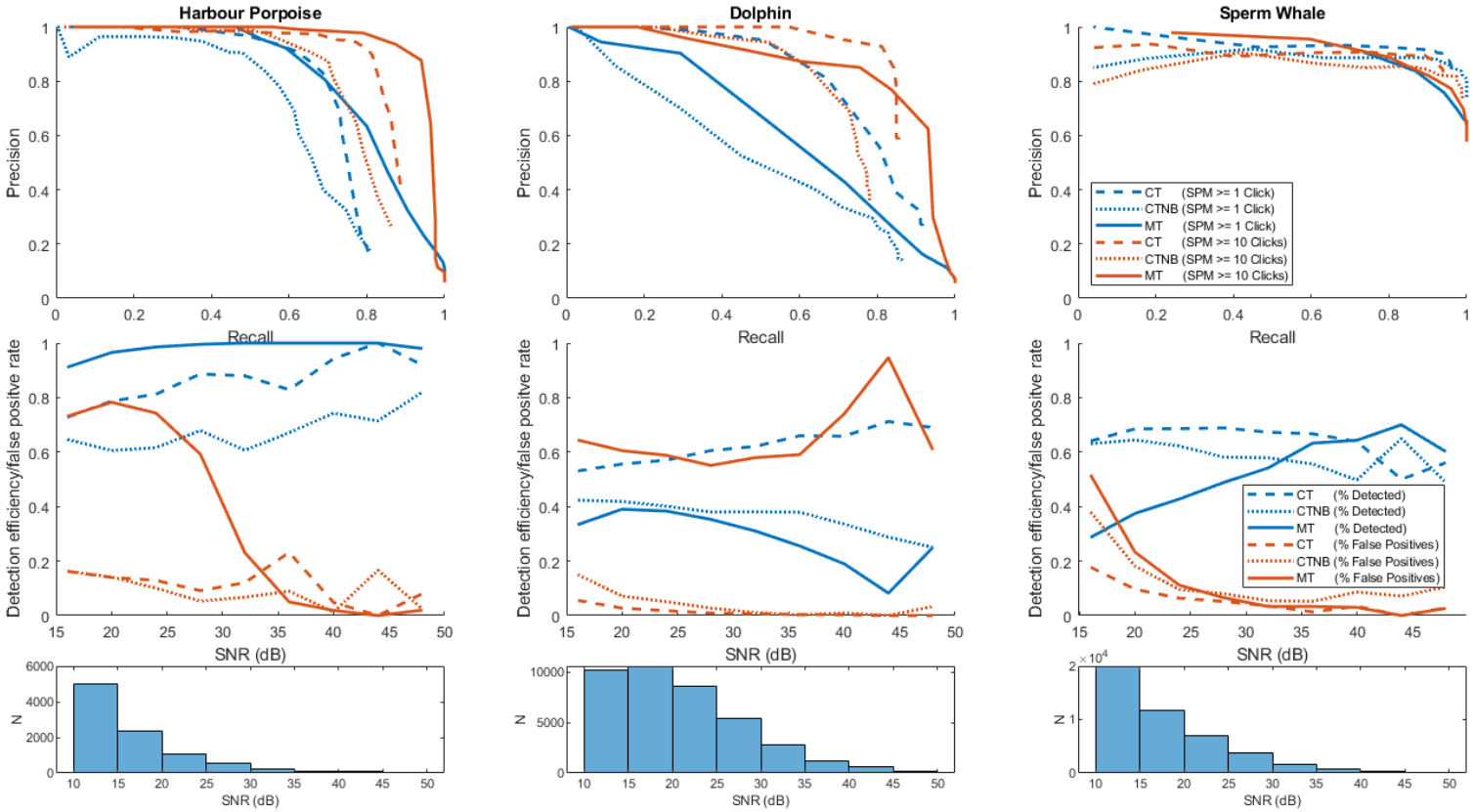

Figure 6. Performance metrics for the click train detector and matched click classifier for harbour porpoise, delphinids and sperm whales. MT is matched click classifier, CT is the click train detector and CTNB is the click train detector without considering bearing information. Precision-recall curves consider the ability of each algorithm to identify species positive minutes (SPM). Two thresholds, at least 1 classified click (blue) and 10 *classified clicks (orange), to define a positive species minute are considered. The curves are generated for different thresholds of the species classifiers. In the case of the click train detector the classifier threshold is the spectral template correlation value and in the case of the matched click classifier it is the ratio between the match and reject templates. The second row of plots show the detection efficiency (blue) and false positive rate (orange) in classifying individual clicks. The third row shows the distribution of SNR of manually annotated clicks for each species.*

2.5.4 Sensitivity

The sensitivity of the click train detector to changes in descriptor values (e.g. ICI, amplitude, bearing, *etc.*) for a subset of each dataset is shown in precision recall curves in Figure 7. The colours of each dot indicate the spectrum correlation threshold value used to classify a click train. In most cases, relatively large changes in the descriptor values, up to an order of magnitude above and below default values used in the previous results, cause only minor changes to performance i.e. the same coloured dots stay at a similar precision and recall. At very low spectral correlation thresholds (blue dots), precision is poor because there is a high false positive rate, however, at higher thresholds precisions and recall are acceptable for almost all user settings. Thus, the click train detector is relatively robust to user settings.

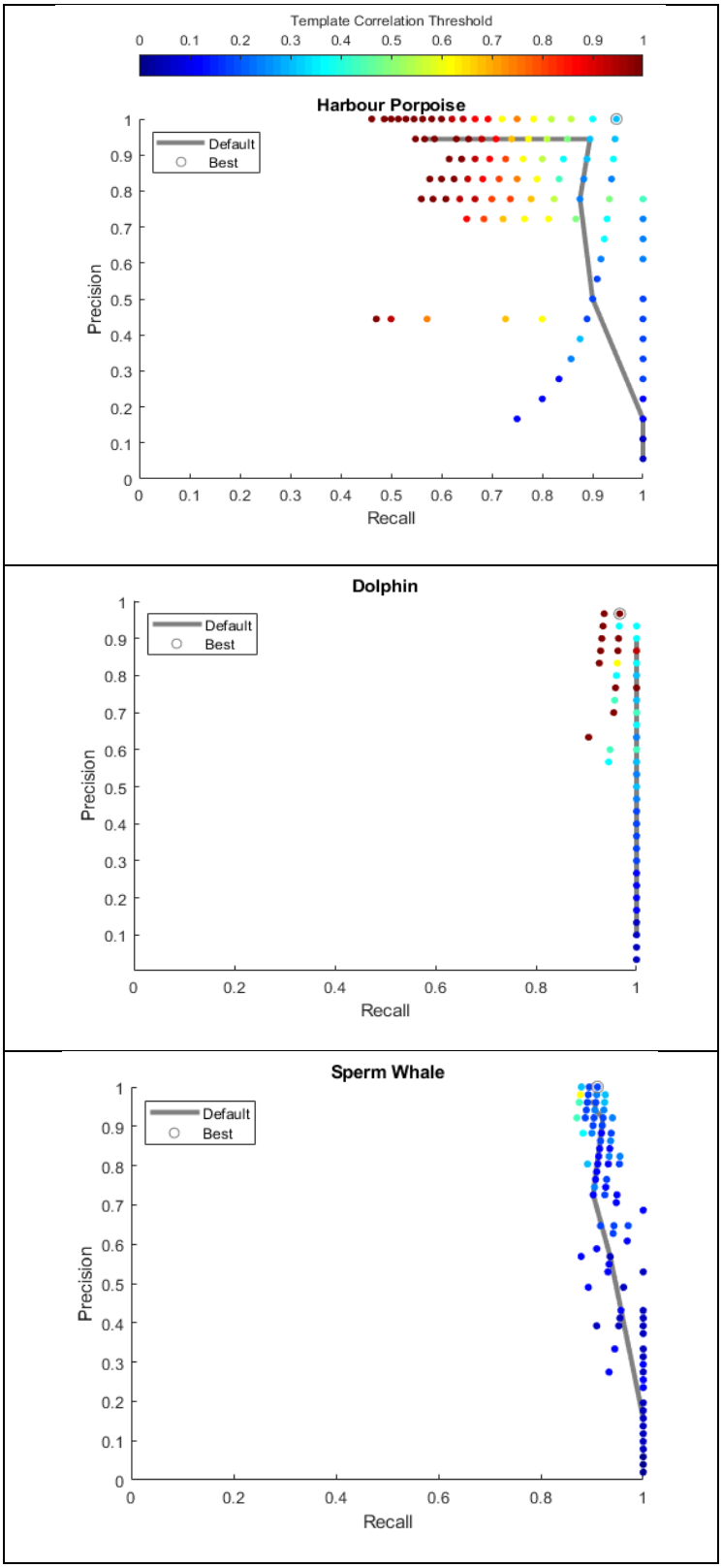

Figure 7. Sensitivity plots for changes in the click train descriptor values. Each point represents the precision and recall values for a set of descriptors with randomised values up to an order of magnitude above or below the default values. For each set of descriptors, multiple template correlation thresholds are applied to generate points on a precision recall curve as shown in Figure 6. The colour of each dot represents the value of the correlation template threshold. Thus, if the settings are relatively robust to changes in the user settings then the same coloured dots should cluster around the same precision recall.

2.5.5 Association

Figure 8 shows an example of manually annotated click trains, detected click trains and classified click trains. This shows that the click train detector does a good job at tracking individual clicks trains, however, in general, it tends to fragment click trains compared to a manual analyst. It should also be noted that the click train detector will track a continuous series of echoes, thus for one animal there can occasionally be two overlapping trains.

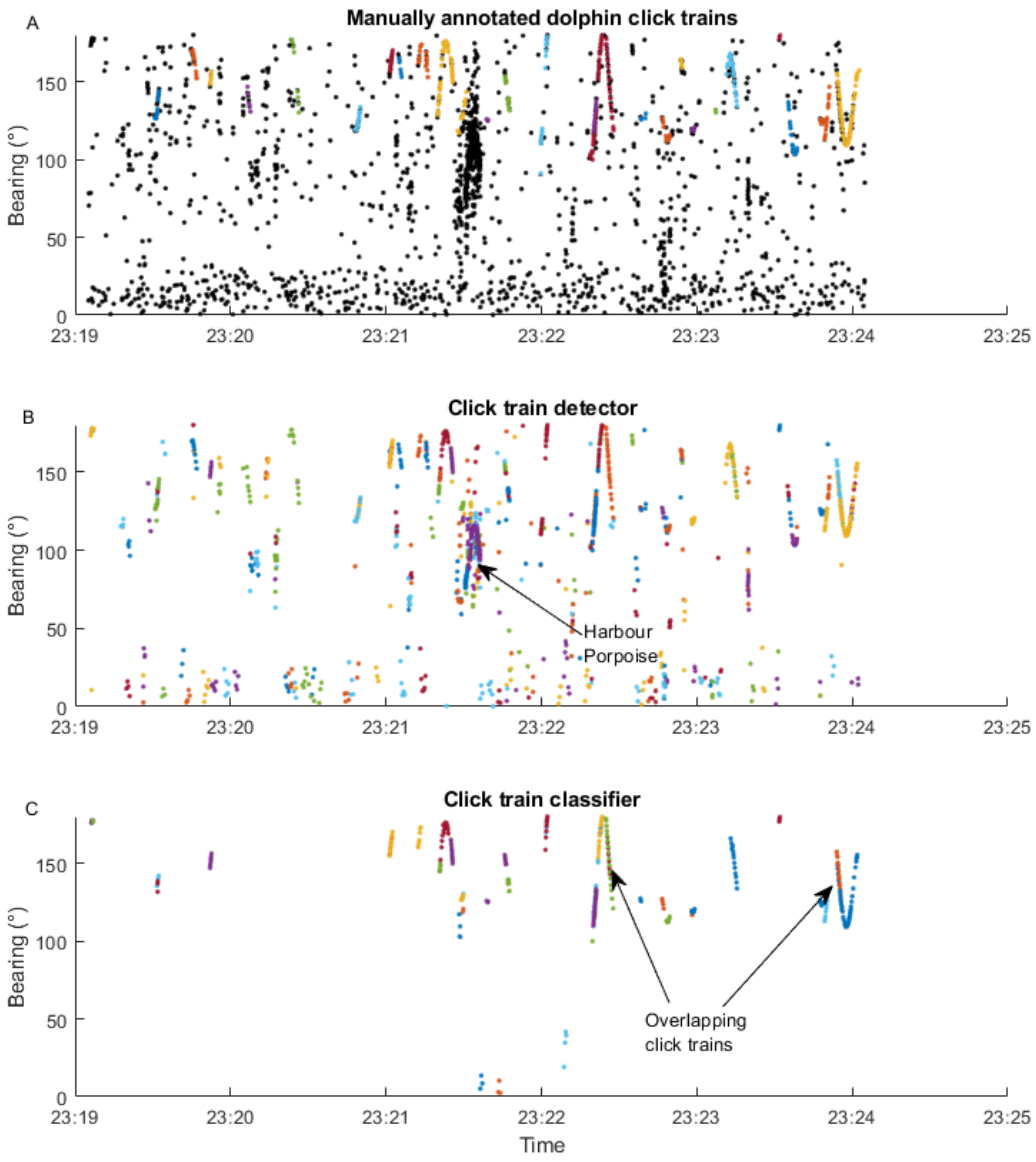

Figure 8. Example of click train association. Plot A shows manually annotated delphinid click trains with each colour representing a different click train. Black dots are unclassified clicks. Note that the cluster of black dots at 23:21:30 is a harbour porpoise. Plot B shows results from the click train detector without any post-filtering of clicks trains. Plot C shows the remaining click trains after species classification. Note that the annotated click trains do not contain echoes, however, the click train detector will track consistent echoes in a click train. For example, note the click trains at around 23:22:20 which show overlapping colours.

Figure 9 shows a histogram of the maximum percentage of each manually annotated click train that was tracked by the click train detector e.g. it shows the largest tracked click train fragment. This indicates a large variation in fragment sizes, with some click trains completely tracked and other highly fragmented. In general, many of the smaller fragments came from click trains with fewer clicks and/or occurred because the click train detector tracked echoes instead of direct path clicks. For all species, less than 5% of detected click trains resulted in association crossover, and when this occurred it was usually due to multiple clicks trains simultaneously present in a complex transient noise field

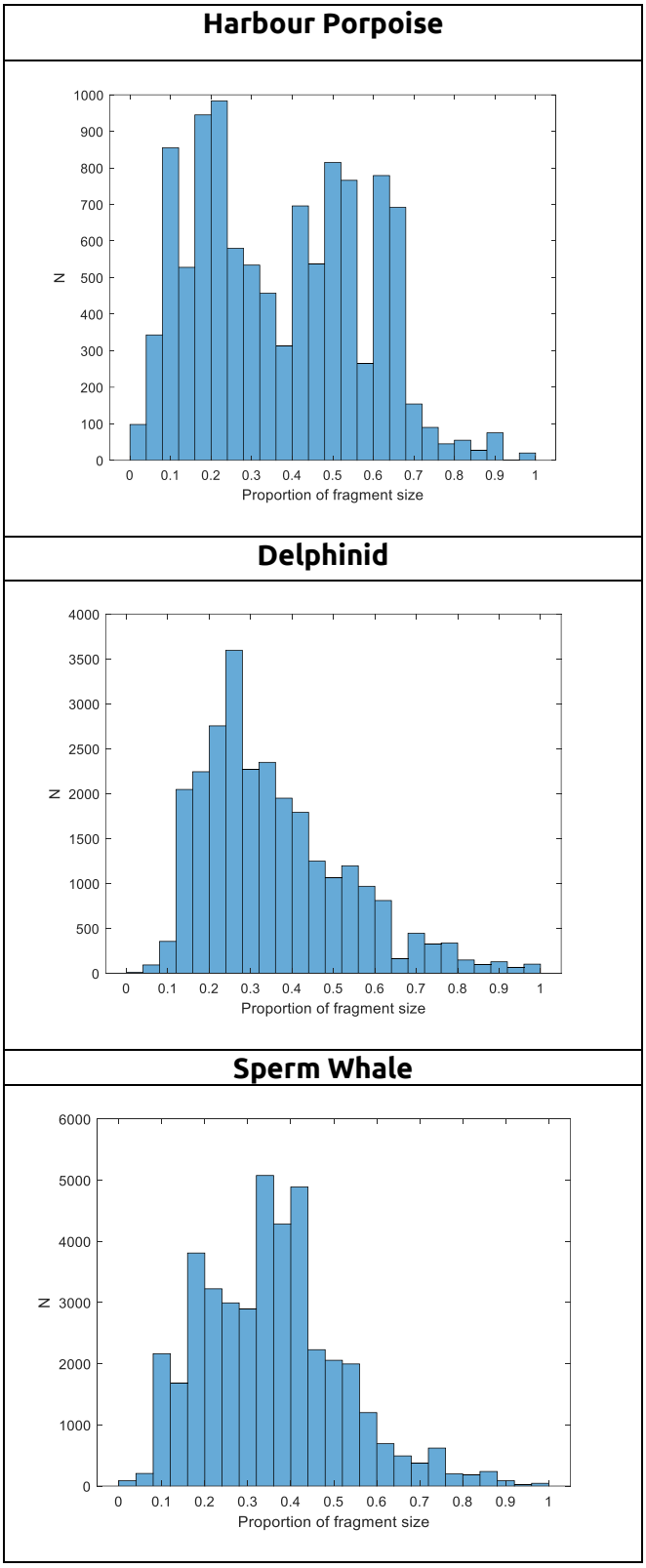

Figure 9. The distribution of click train fragment sizes for each species. The fragment size proportion refers to the proportion of clicks a detected click train formed of a manually annotated click train. 1 indicates all clicks were detected and 0 indicates no clicks were detected. The smaller fragment sizes tended to occur in lower SNR click trains.

2.6 DISCUSSION

The multi hypothesis based open source click train detector was capable of efficiently detecting and classifying three different toothed whale groups. These had widely varying acoustic and behavioural parameters and were recorded on a variety of hardware in differing transient noise fields.

The efficacy in using a click train based approach compared to an individual click-by-click approach for species or taxa classification was dependent on both the analysis metric (species positive minutes or individual clicks) and how stereotyped the target clicks were. The matched click classifier was often similar in performance to the click train detector when determining species positive minutes (Figure 6A), however. on an individual click-by-click basis it ran at significantly higher false positive rates, especially for lower SNR clicks (Figure 6B). This difference between SPM and individual click classification in the matched click classifier was due to a consistent background rate of false detections, i.e. low SNR transients will consistently trigger the matched click detector over time. When comparing all clicks in a large dataset, this can result in a very high false positive rate. The click train detector had a consistently lower false positive rate because is it less vulnerable to these random false positives due to requiring a consistent pattern of clicks to register a detection which generally only occurs when there is a biological source or high levels of transient noise present. However, when a very simple filter is applied to the matched click classifier, in this case a minimum number of clicks per minute, then the background false positive rate is negated which results in higher performance determining species positive minutes.

In the case of harbour porpoise clicks, the matched click classifier clearly outperformed the click train detector when a minimum number of clicks per minute filter was applied Figure 6A. Harbour porpoise have highly stereotyped clicks which generally reduces false positives and increases detection efficiency of individual click-by-click classifiers. However, there were also many instances of disparate harbour porpoise click detections, when only a few high SNR clicks were detected without any preceding or following click trains. It is unknown why these types of detections occurred, however, it is an anecdotally common pattern in PAM studies of harbour porpoises. The click train detector is not capable of registering these disparate detections and thus had a significantly higher false negative rate (reduced recall) compared to the matched click classifier. However, at low SNR levels the click train detector, on a click-by-click basis, outperformed the match clicks classifier with a much lower false positive rate.

Delphinid clicks are much less stereotyped than harbour porpoise clicks, and so the matched click classifier performed poorly compared to the click train detector (Figure 3B and Figure 6B), running at a much higher false positive background rate and low detection efficiency.

However, for sperm whales, which also have less stereotyped clicks, there was a more marginal improvement when using the click train detector; the matched click classifier performed similarly for SPM (Figure 4B) and on an individual basis for higher SNR clicks (Figure 6). The waveform template used by the matched click classifier was based on a high SNR click, likely to be close to on-axis. On-axis sperm whale clicks are somewhat stereotyped multi modal pulses and so the matched click classifier likely performed well at higher SNR because high SNR clicks are more likely to be closer to on-axis and thus less distorted. However, this was also a particularly difficult dataset for the click train detector due to the high levels of electric and environmental transient noise which resulted in significant numbers of spurious tracks.

Although in some cases the relatively simple click-by-click approach worked well for stereotyped clicks, i.e. in determining species positive minutes, there are also various additional advantages to using a click train approach. The ability to associate clicks also has the potential to significantly improve classification. Here, the average spectra of all clicks was correlated with a spectral template creating a relatively basic binary classifier to assign a classification ID. Previous studies have shown that average spectra of dolphins can, for some species, contain consistent and stable peaks and notches (Soldevilla et al. 2008). Machine learning methods have further utilised the properties of the average spectra of large groups of clicks to successfully classify the presence of different delphinid species (Frasier et al. 2017, Rankin et al. 2017). The application of a click train detection algorithm could further improve these classification methods; the association of clicks from single individuals, rather than grouping all clicks in a time bin, creates cleaner average spectra inputs which would likely result in better performing and more stable classifiers. Representation of the average spectra of clicks trains (e.g. concatenated spectrograms of clicks) could potentially be used with the latest deep learning classifiers. Such spectra are computationally low in size compared to raw acoustic data and so lend themselves to cloud storage for accessible data access in addition to training and running new machine learning models.

Click train detection also potentially has implication for density estimation. The click train algorithm was able to associate clicks from an individual animal (Figure 8). This can be used to estimate group size and so could be potentially integrated into density estimation methods. Click trains detected on a moving towed hydrophone array, as in the Alaskan dataset shown here, could potentially be used to determine the range (a vital metric in distance sampling (Marques et al. 2013)) to the animal via target motion analysis e.g. (Leaper et al. 2000). However, this will require a secondary analysis stage to join up click train fragments, either by developing tools for manual analyst to efficiently do so or by developing an automated click train fusion algorithm. The lower false positive rates of the click train detector could also have implications for density estimation. Caillat et al. (2013) showed that, in the case of rare species, even if the performance of a classifier has been accurately determined, a high false positive rate can lead to large errors in density estimation. Thus, building classifiers which minimise false positives can be important in situations were rare species are studied. The click train detection algorithm could form the basis of such a detector/classifier, however, should be used with caution. The probability of classifying a click is entangled with the number of clicks detected previously. Thus, the detection probability of an individual clicks is related to both the probability of detecting the click and the number, amplitude, timing bearing etc. of previously detected clicks. Modelling these detection probabilities is likely very complex compared to individual click by click classifiers (e.g. Küsel et al. 2011)) and thus click train detection (and any such contextual based algorithms) may be more suited to species positive minutes and estimates of group size rather than cue counting when used within a distance sampling framework.

Whilst this multi hypothesis click train detector approach shows promise, the algorithm has by no means been exhaustively tested and there may be instances where using a click train detector has performance advantages over a click-by-click approach not considered in the datasets used here (or vice versa). By making the code open source, well annotated, and extensible, it is hoped that other researchers will test this MHT based approach on additional datasets. The code base has also been designed to be easily modified; for example, adding a new type of χ^2 model would be straightforward. In all cases, the click train-based approach was more processor intensive than individual click-by-click classification however, it consistently ran faster than real time on standard computer hardware (Intel i7U 8th generation processor, 8GB RAM) and is therefore suitable for most real time PAM applications, such as mitigation exercises. If increased computational performance is

required, then reducing the prune back constant Np (by one or two) results in large increases in speed with only minimal decrease in detection efficiency. Thus, the algorithm could be applied to lower power or embedded processors.

2.7 CONCLUSION

A multi hypothesis click train-based algorithm was capable of efficiently detecting and classifying click trains from multiple odontocete species. For stereotyped clicks, the application of a basic post analysis metric, e.g. a minimum number of clicks in a one-minute bin, allowed an individual click-by-click algorithm to perform as well or better than a click train based approach when calculating species positive minutes but maintained a high false positive rate at low SNR. For less stereotyped clicks, i.e. delphinids and sperm whales, the click train detector significantly improved performance, and in all cases the click train detector had a lower false positive rate, which can be useful in some density estimation applications were a rare species is present. The average spectra of detected click trains may be useful for more sophisticated machine learning classification approaches. The click train detection algorithm has been made both accessible by integrating into commonly used PAM software (PAMGuard) and the API is fully open source and available online. It is hoped this will allow other researchers to further test and improve the click train detection algorithm.

2.8 ACKNOWLEDGEMENTS

Thanks to Chloe Malinka Peter Madsen, Kristian Beedholm and for helpful comments. Thanks to Nation Oceanographic and Atmospheric Administration, USA and Alaska Longline Fishermen's Association, USA for assistance in collecting the sperm whale dataset. Thanks to Mikey Taylor-Firth and Al Kingston for collecting the Harbour Porpoise dataset.

2.9 CODING

All code, including the matched click classifier, the click train detector in PAMGuard, graphs, analysis scripts etc was written by me. Kristian Beedholm (University of Aarhus) came up with the idea for the matched click classifier and the idea for using MHT in click train detection came from Gerard et al. (2008). I made modifications to both algorithms and implemented them in Java.

2.10 REFERENCES

Ainslie, M. A., and J. G. Mccolm. 1998. A simplified formula for viscous and chemical absorption in sea water. The Journal of the Acoustical Society of America 103:1671.

Au, W. W. L. 1993. The Sonar of Dolphins. Page Acoustics Australia. Springer New York, New York, NY.

Au, W. W. L., B. Branstetter, P. W. Moore, and J. J. Finneran. 2012a. The biosonar field around an Atlantic bottlenose dolphin (Tursiops truncatus). The Journal of the Acoustical Society of America 131:569–576.

Au, W. W. L., B. Branstetter, P. W. Moore, and J. J. Finneran. 2012b. Dolphin biosonar signals measured at extreme off-axis angles: Insights to sound propagation in the head. The Journal of the Acoustical Society of America 132:1199–1206.

Baggenstoss, P. M. 2011. Separation of sperm whale click trains for multipath rejection. The Journal of the Acoustical Society of America 129:3598–3609.

Bassett, H. R., S. Baumann, G. S. Campbell, S. M. Wiggins, and J. A. Hildebrand. 2009. Dall's porpoise (Phocoenoides dalli) echolocation click spectral structure. The Journal of the Acoustical Society of America 125:2677–2677.

Baumann-Pickering, S., S. M. Wiggins, E. H. Roth, M. A. Roch, H.-U. Schnitzler, and J. A. Hildebrand. 2010. Echolocation signals of a beaked whale at Palmyra Atoll. The Journal of the Acoustical Society of America 127:3790–3799.

Le Bot, O., J. I. Mars, C. Gervaise, and Y. Simard. 2015. Rhythmic analysis for click train detection and source separation with examples on beluga whales. Applied Acoustics 95:37–49.

Caillat, M., L. Thomas, and D. Gillespie. 2013. The effects of acoustic misclassification on cetacean species abundance estimation. The Journal of the Acoustical Society of America 134:2469–2476.

Clausen, K. T., M. Wahlberg, K. Beedholm, S. Deruiter, and P. T. Madsen. 2010. Click communication in harbour porpoises Phocoena phocoena. Bioacoustics 20:1–28.

Cosentino, M., F. Guarato, J. Tougaard, D. Nairn, J. C. Jackson, and J. F. C. Windmill. 2019. Porpoise click classifier (PorCC): A high-accuracy classifier to study harbour porpoises (Phocoena phocoena) in the wild. The Journal of the Acoustical Society of America 145:3427–3434.

Dawson, S. M. 2010. Clicks and Communication: The Behavioural and Social Contexts of Hector's Dolphin Vocalizations. Ethology 88:265–276.

Deruiter, S. L., A. Bahr, M.-A. Blanchet, S. F. Hansen, J. H. Kristensen, P. T. Madsen, P. L. Tyack, and M. Wahlberg. 2009. Acoustic behaviour of echolocating porpoises during prey capture. The Journal of experimental biology 212:3100–3107.

Douglas, L. A., S. M. Dawson, and N. Jaquet. 2005. Click rates and silences of sperm whales at Kaikoura, New Zealand. The Journal of the Acoustical Society of America 118:523–529.

Fais, A., M. Johnson, M. Wilson, N. Aguilar Soto, and P. T. Madsen. 2016. Sperm whale predator-prey interactions involve chasing and buzzing, but no acoustic stunning. Scientific Reports 6:28562.

Finneran, J. J., B. K. Branstetter, D. S. Houser, P. W. Moore, J. Mulsow, C. Martin, and S. Perisho. 2014. High-resolution measurement of a bottlenose dolphin's (Tursiops truncatus) biosonar transmission beam pattern in the horizontal plane. The Journal of the Acoustical Society of America 136:2025–2038.

Frasier, K. E., M. A. Roch, M. S. Soldevilla, S. M. Wiggins, L. P. Garrison, and J. A. Hildebrand. 2017. Automated classification of dolphin echolocation click types from the Gulf of Mexico. PLoS Computational Biology 13:1–23.

Gerard, O., C. Carthel, and S. Coraluppi. 2008a. Estimating the number of beaked whales using an MHT tracker. Pages 1–6 2008 New Trends for Environmental Monitoring Using Passive Systems. IEEE.

Gerard, O., C. Carthel, and S. Coraluppi. 2009. Classification of odontocete buzz clicks using a multi-hypothesis tracker. Pages 1–7 OCEANS 2009-EUROPE. IEEE.

Gerard, O., C. Carthel, S. Coraluppi, and P. Willett. 2008b. Feature-Aided Tracking for Marine Mammal Detection and Classification. Canadian Acoustics 36:13–19.

Gillespie, D., and M. Caillat. 2008. Statistical Classification of Odontocete Clicks. Canadian Acoustics 36:20–26.

Gillespie, D., J. Gordon, R. Mchugh, D. Mclaren, D. Mellinger, P. Redmond, A. Thode, P. Trinder, and X. Y. Deng. 2008. PAMGUARD: Semiautomated, open source software for real-time acoustic detection and localisation of cetaceans. Proceedings of the Institute of Acoustics 30:2547.

Gillespie, D., and J. Macaulay. 2019. Time of arrival difference estimation for narrow band high frequency echolocation clicks. The Journal of the Acoustical Society of America 146:EL387–EL392.

Glotin, H., F. Caudal, and P. Giraudet. 2008. Whale cocktail party: Real-time multiple tracking and signal analyses. Canadian Acoustics - Acoustique Canadienne 36:139–145.

Gordon, J. 1987. The Behaviour and Ecology of Sperm Whales off Sri Lanka. University of Cambridge.

Götz, T., R. Antunes, and S. Heinrich. 2010. Echolocation clicks of free-ranging Chilean dolphins (Cephalorhynchus eutropia). The Journal of the Acoustical Society of America 128:563–566.

Jacobson, E. K., K. A. Forney, and J. T. Harvey. 2015. Acoustic evidence that harbor porpoises (Phocoena phocoena) avoid bottlenose dolphins (Tursiops truncatus). Marine Mammal

Science 31:386–397.

Jarvis, S., N. DiMarzio, R. Morrissey, and D. Moretti. 2008. A novel multi-class support vector machine classifier for automated classification of beaked whales and other small odontocetes. Canadian Acoustics - Acoustique Canadienne 36:34–40.

Jensen, F. H., M. Johnson, M. Ladegaard, D. M. Wisniewska, and P. T. Madsen. 2018. Narrow Acoustic Field of View Drives Frequency Scaling in Toothed Whale Biosonar. Current Biology 28:3878-3885.e3.

Jiang, J. jia, L. ran Bu, X. quan Wang, C. yue Li, Z. bo Sun, H. Yan, B. Hua, F. jie Duan, and J. Yang. 2018. Clicks classification of sperm whale and long-finned pilot whale based on continuous wavelet transform and artificial neural network. Applied Acoustics 141:26–34.

Johnson, M., P. T. Madsen, W. M. X. Zimmer, N. A. de Soto, and P. L. Tyack. 2006. Foraging Blainville's beaked whales (Mesoplodon densirostris) produce distinct click types matched to different phases of echolocation. Journal of Experimental Biology 209:5038–5050.

Johnson, M., P. T. Madsen, W. M. X. X. Zimmer, N. Aguilar de Soto, and P. L. Tyack. 2004. Beaked whales echolocate on prey. Proceedings of the Royal Society of London. Series B: Biological Sciences 271:S383–S386.

Kandia, V., and Y. Stylianou. 2006. Detection of sperm whale clicks based on the Teager–Kaiser energy operator. Applied Acoustics 67:1144–1163.

Klinck, H., and D. K. Mellinger. 2011. The energy ratio mapping algorithm: A tool to improve the energy-based detection of odontocete echolocation clicks. The Journal of the Acoustical Society of America 129:1807–1812.

Küsel, E. T., D. K. Mellinger, L. Thomas, T. A. Marques, D. Moretti, and J. Ward. 2011. Cetacean population density estimation from single fixed sensors using passive acoustics. The Journal of the Acoustical Society of America 129:3610–3622.

Kyhn, L. A., F. H. Jensen, K. Beedholm, J. Tougaard, M. Hansen, and P. T. Madsen. 2010. Echolocation in sympatric Peale's dolphins (Lagenorhynchus australis) and Commerson's dolphins (Cephalorhynchus commersonii) producing narrow-band high-frequency clicks. Journal of Experimental Biology 213:1940–1949.

Kyhn, L. A., J. Tougaard, K. Beedholm, F. H. Jensen, E. Ashe, R. Williams, and P. T. Madsen. 2013. Clicking in a Killer Whale Habitat: Narrow-Band, High-Frequency Biosonar Clicks of Harbour Porpoise (Phocoena phocoena) and Dall's Porpoise (Phocoenoides dalli). PLoS ONE 8:e63763.

Kyhn, L. A., J. Tougaard, F. Jensen, M. Wahlberg, G. Stone, A. Yoshinaga, K. Beedholm, and P. T. Madsen. 2009. Feeding at a high pitch: source parameters of narrow band, high-frequency clicks from echolocating off-shore hourglass dolphins and coastal Hector's dolphins. The Journal of the Acoustical Society of America 125:1783–1791.

Ladegaard, M., F. H. Jensen, M. de Freitas, V. M. Ferreira da Silva, and P. T. Madsen. 2015. Amazon river dolphins (Inia geoffrensis) use a high-frequency short-range biosonar. Journal of Experimental Biology 218:3091–3101.

Leaper, R., D. Gillespie, and V. Papastavrou. 2000. Results of passive acoustic surveys for odontocetes in the Southern Ocean. Journal of Cetacean Research and Management 2:187–196.

Lepper, P., N. Dümortier, K. Dudzinski, and S. Datta. 2005. Separation of Complex Echolocation Signal ' Trains ' From Multiple Bio-Sonar Sources. Proceedings of the International Conference "Underwater Acoustic Measurements: Technologies &Results" Heraklion, Crete, Greece, 28th June – 1st July 2005:1–6.

Li, S., D. Wang, K. Wang, T. Akamatsu, Z. Ma, and J. Han. 2007. Echolocation click sounds from wild inshore finless porpoise (Neophocaena phocaenoides sunameri) with comparisons to the sonar of riverine N. p. asiaeorientalis. The Journal of the Acoustical Society of America 121:3938.

Linnenschmidt, M., J. Teilmann, T. Akamatsu, R. Dietz, and L. A. Miller. 2013. Biosonar, dive, and foraging activity of satellite tracked harbor porpoises (*Phocoena phocoena*). Marine Mammal Science 29:E77–E97.

Luo, W., W. Yang, Z. Song, and Y. Zhang. 2017. Automatic species recognition using echolocation clicks from odontocetes. 2017 IEEE International Conference on Signal Processing, Communications and Computing, ICSPCC 2017 2017-Janua:1–5.

Madsen, P. T., D. A. Carder, K. Bedholm, and S. H. Ridgway. 2005. Porpoise Clicks From a Sperm Whale Nose—Convergent Evolution of 130 Khz Pulses in Toothed Whale Sonars? Bioacoustics 15:195–206.

Marques, T. A., L. Thomas, S. W. Martin, D. K. Mellinger, J. A. Ward, D. J. Moretti, D. Harris, and P. L. Tyack. 2013. Estimating animal population density using passive acoustics. Biological reviews of the Cambridge Philosophical Society 88:287–309.

Melcón, M. L., M. Failla, and M. a. Iñíguez. 2012. Echolocation behavior of franciscana dolphins (Pontoporia blainvillei) in the wild. The Journal of the Acoustical Society of America 131:EL448.

Merkens, K., D. Mann, V. M. Janik, D. Claridge, M. Hill, and E. Oleson. 2018. Clicks of dwarf sperm whales (Kogia sima). Marine Mammal Science 34:963–978.

Miller, B. S. B. 2012. Real-time tracking of blue whales using DIFAR sonobuoys. Proceedings of Acoustics 2012:7.

Miller, P. J. O., M. P. Johnson, and P. L. Tyack. 2004. Sperm whale behaviour indicates the use of echolocation click buzzes 'creaks' in prey capture. Proceedings of the Royal Society of London.

Series B: Biological Sciences 271:2239–2247.

Møhl, B., M. Wahlberg, P. T. Madsen, A. Heerfordt, and A. Lund. 2003. The monopulsed nature of sperm whale clicks. The Journal of the Acoustical Society of America 114:1143–1154.

Rankin, S., F. Archer, J. L. Keating, J. N. Oswald, M. Oswald, A. Curtis, and J. Barlow. 2017. Acoustic classification of dolphins in the California Current using whistles, echolocation clicks, and burst pulses. Marine Mammal Science 33:520–540.

Roberts, B. L., and A. J. Read. 2015. Field assessment of C-POD performance in detecting echolocation click trains of bottlenose dolphins (Tursiops truncatus). Marine Mammal Science 31:169–190.

Roch, M. A., H. Klinck, S. Baumann-Pickering, D. K. Mellinger, S. Qui, M. S. Soldevilla, and J. A. Hildebrand. 2011a. Classification of echolocation clicks from odontocetes in the Southern California Bight. The Journal of the Acoustical Society of America 129:467–475.

Roch, M. A., T. Scott Brandes, B. Patel, Y. Barkley, S. Baumann-Pickering, and M. S. Soldevilla. 2011b. Automated extraction of odontocete whistle contours. The Journal of the Acoustical Society of America 130:2212–2223.

Soldevilla, M. S., E. E. Henderson, G. S. Campbell, S. M. Wiggins, J. a Hildebrand, and M. a Roch. 2008. Classification of Risso's and Pacific white-sided dolphins using spectral properties of echolocation clicks. The Journal of the Acoustical Society of America 124:609–24.

Sørensen, P. M., D. M. Wisniewska, F. H. Jensen, M. Johnson, J. Teilmann, and P. T. Madsen. 2018. Click communication in wild harbour porpoises (Phocoena phocoena). Scientific Reports 8:9702.

Sostres Alonso, M., and H. K. Nuuttila. 2015. Detection rates of wild harbour porpoises and bottlenose dolphins using static acoustic click loggers vary with depth. Bioacoustics 24:101–110.

Starkhammar, J., J. Nilsson, M. Amundin, S. a Kuczaj, M. Almqvist, and H. W. Persson. 2011. Separating overlapping click trains originating from multiple individuals in echolocation recordings. The Journal of the Acoustical Society of America 129:458–466.

Verfuß, U. K., L. A. Miller, P. K. D. Pilz, and H. U. Schnitzler. 2009. Echolocation by two foraging harbour porpoises (Phocoena phocoena). Journal of Experimental Biology 212:823–834.

Villadsgaard, A., M. Wahlberg, and J. Tougaard. 2007. Echolocation signals of wild harbour porpoises, Phocoena phocoena. Journal of Experimental Biology 210:56–64.

Wisniewska, D. M., M. Johnson, P. E. Nachtigall, and P. T. Madsen. 2014. Buzzing during biosonar-based interception of prey in the delphinids Tursiops truncatus and Pseudorca crassidens. Journal of Experimental Biology 217:4279–4282.

Yack, T. M., J. Barlow, M. A. Roch, H. Klinck, S. Martin, D. K. Mellinger, and D. Gillespie. 2010. Comparison of beaked whale detection algorithms. Applied Acoustics 71:1043–1049.

Zimmer, W. M. X., P. L. Tyack, M. P. Johnson, and P. T. Madsen. 2005. Three-dimensional beam pattern of regular sperm whale clicks confirms bent-horn hypothesis. The Journal of the Acoustical Society of America 117:1473–1485.A

Chapter 3: Passive acoustic methods for fine-scale tracking of harbour porpoises in tidal rapids.

Silurian in a tidal race with 35m vertical hydrophone array deployed

Chapter 3: Passive acoustic methods for fine-scale tracking of harbour porpoises in tidal rapids.

ABSTRACT

The growing interest in generating electrical power from tidal currents using tidal turbine generators raises a number of environmental concerns, including the risk that marine mammals might be injured or killed through collision with rotating turbine blades. To understand this risk, information on how marine mammals use tidal rapid habitats and in particular their underwater movements and dive behaviour is required. Porpoises, which are the most abundant small cetacean at most European tidal sites, are difficult animals to tag, and the limited size of tidal habitats means that any telemetered animal would be likely to spend only a small proportion of time within them. Here, an alternative approach is explored, whereby passive acoustic monitoring (PAM) is used to obtain fine scale geo-referenced tracks of harbour porpoises in tidal rapid areas. Large aperture hydrophone arrays are required to obtain accurate locations of animals from PAM data and automated algorithms are necessary to process the large quantities of acoustic data collected on such systems during a typical survey. Methods to automate localisation, including a method to match porpoise detections on different hydrophones and separate different vocalising animals, and an assessment of the localisation accuracy of the large aperture hydrophone array are presented.

3.1 INTRODUCTION

In many parts of the world, there is an increasing interest in generating renewable, low-carbon electricity in the marine environment. The prospect of harnessing power from tidal flows, which have the great advantage of being highly predictable, is being pursued in several regions with large tidal ranges and strong currents (Toke 2011). Most proposed tidal generators have large, exposed, freely rotating blades and tip speeds may reach up to 12.5 ms^{-1}. The potential risk for fish, birds and marine mammals to collide with these blades, resulting in possible injury or death, is poorly understood and therefore considered by most regulators a primary conservation and welfare concern (Wilson et al. 2007). If the tidal turbine industry expands, the large scale deployment of tidal turbines and resulting inevitable increase in anthropogenic activity could also displace such animals (Frid et al. 2012). Little information exists on the interactions between tidal rapid areas and marine megafauna and thus the potential consequences of such habitat exclusion are not known (Benjamins et al. 2015). Of the multiple information gaps which exist in this area, the fine scale underwater movements and depth distributions of marine megafauna is perhaps least understood, yet forms a key parameter in assessing both collision risk (Thompson and Lonergan 2015) and habitat usage.

Recording fine scale geo-referenced positions of marine mammals underwater is not a trivial problem. Animal-borne tags with depth and orientation sensors and/or GPS (global positioning systems) are an initial obvious choice (e.g. Linnenschmidt et al. 2013; Wisniewska et al. 2016). However, when such methods are applied to a geographically restricted and atypical habitat, the likelihood that any tagged animal will spend a large proportion of their time in the study area is low. Thus, a tagging programme to collect a significant volume of data on diving behaviour of porpoises in tidal rapid areas would be likely to be prohibitively expensive. PAM has the potential to provide an alternative approach to obtain fine scale information on behaviour, targeting animals within a specific geographic area of interest, such as tidal rapids.

Widely spaced (or 'large aperture') hydrophone arrays have been used for decades to track the movements of cetaceans underwater (e.g. Watkins & Schevill 1972; Møhl et al. 2000; Miller & Dawson 2009; Wiggins et al. 2012). By analysing the time of arrival differences (TOADs) between a vocalisation detected on several dispersed hydrophones, it is possible to determine the position of the vocalising animal. Such systems have been used to determine locations of NBHF species (e.g. Ural

et al. 2006, Villadsgaard et al. 2007, Kyhn et al. 2013), however these studies all used rigid hydrophone arrays with dimensions of a few meters and therefore the range at which accurate localisations were possible was restricted to tens of meters. Although these arrays were appropriate for their respective studies, for this application, a PAM system capable of providing accurate animal locations at ranges up to a few hundred meters was required and thus a significantly larger hydrophone array which could be deployed in strong currents was required.

Large aperture vertical linear hydrophone arrays can be deployed from a drifting vessel and have been used in the past to localise the depth of bottlenose dolphins in tidal areas (Hastie et al. 2006). Crucially, such systems can be of the order of tens or hundreds of meters long (e.g. Heerfordt et al. 2007, Holt et al. 2009) providing accurate localisations at larger ranges. Any linear array can only provide locations in two dimensions (Au & Hastings 2008) and in the case of a vertical linear array, these would be the range and depth of a vocalising cetacean. However, information such as the orientation of animals in a tidal stream and fine-scale movements in relation to bottom topography is important in understanding how tidal habitats are utilised and this is lost if animals are only located in two dimensions. In addition, significant errors in localisation can be introduced if a linear vertical array moves off the vertical axis - a circumstance which is likely to occur when the supporting vessel or buoy drifts with the wind and/or if currents vary with depths.

This chapter explores the use of a large aperture vertical hydrophone array drifting in tidal rapids to obtain fine scale 3D geo-referenced porpoise tracks. The accuracy of the system is extensively tested by broadcasting simulated porpoise clicks from known locations and depths. Automated methods to analyse the large quantities of data collected by the array during a typical survey are presented.

3.2 MATERIALS AND METHODS

3.2.1 Using Large Aperture Hydrophone Arrays in Tidal Rapids

There are several practical difficulties which must be considered when designing a large aperture array to localise harbour porpoises.

Strong and differential currents in tidal rapids mean that large and heavy structures would be required to deploy an array rigidly on the seabed. Anchoring a buoy or vessel in strong currents would be difficult, introduce significant flow noise and the array configuration may be hugely distorted by

the current. A drifting array is therefore a much more cost effective and practical option. However, any drifting array in tidal rapids must be capable of being quickly deployed and recovered as fast currents are likely to carry it into dangerous and/or shallow-water areas. Free hanging weighted vertical cable arrays are a practical option as they can be quickly recovered either by hand or using a winch.

Wave action, strong differential currents and wind moving the research vessel against tide can cause a free hanging array, even if substantially weighted, to move through the water. This can cause significant deformation of the array creating uncertainty in the position of hydrophone elements. To maintain localisation accuracy the locations of all the hydrophones in the array must be measured with fine temporal resolution i.e. multiple measurements per second.

A simple linear vertical system which moves off the vertical axis will lose resolution in depth, even if the angle of the array and therefore the position of hydrophones are known accurately. This is because a localisation from any linear hydrophone array restricts the position of a source to a circle of possible locations. The circle is centred on and perpendicular to the linear array. In the case of a vertical linear array, the radius of the circle represents the horizontal range and the depth directly corresponds to the depth of a source. If a vertical array moves off the vertical angle, even if the position of all hydrophone is known, a fundamental uncertainty is introduced in depth and range i.e. the source is still located on a circle but that circle is now at an angle. Thus, any linear array must remain close to vertical to provide accurate depth information. Therefore, for any deployment in tidal rapids an array must be designed in such a way that the depth information can still be calculated if the array moves off the vertical axis, which is inevitable in an environment with high flow. This is achieved by ensuring at least some hydrophone elements are not in a straight line i.e. breaking the linearity of the array.

Perhaps the most significant design consideration is determining the optimal spacing between hydrophone elements in the array. Generally, an array with larger spacings between hydrophones will provide more accurate locations as the errors due to uncertainty in hydrophone positions, and time of arrival measurements, are proportionally smaller. However, echolocating cetaceans,

including harbour porpoises, produce highly directional clicks (Au et al. 1999, Koblitz et al. 2012) and click source amplitudes are under behavioural control and can vary substantially (DeRuiter et al. 2009). Porpoise clicks might thus be thought of as a narrow beam flashlight constantly varying in intensity and width, rather than a uniform spherical pulse (Wisniewska et al. 2015). This narrow beamwidth presents several challenges when large aperture hydrophone arrays are used because it is likely that only a subset of hydrophones will be ensonified by an animal's directional sonar beam at any one time. Assuming only time delays from single direct path sounds are considered (i.e. without utilising echoes or multiple vocalisations), for a 2D location (depth and range) to be determined, a minimum of 3 hydrophone elements must detect a vocalisation and for a 3D location at least 4 elements, distributed in three dimensions, are required . The spacing of hydrophones in arrays is therefore a trade-off. Hydrophone elements must be spaced sufficiently close together for a minimum number to be *consistently* ensonified by directional vocalisations, but sufficiently separated to allow accurate localisation at useful ranges.

3.2.2 Vertical Array Design

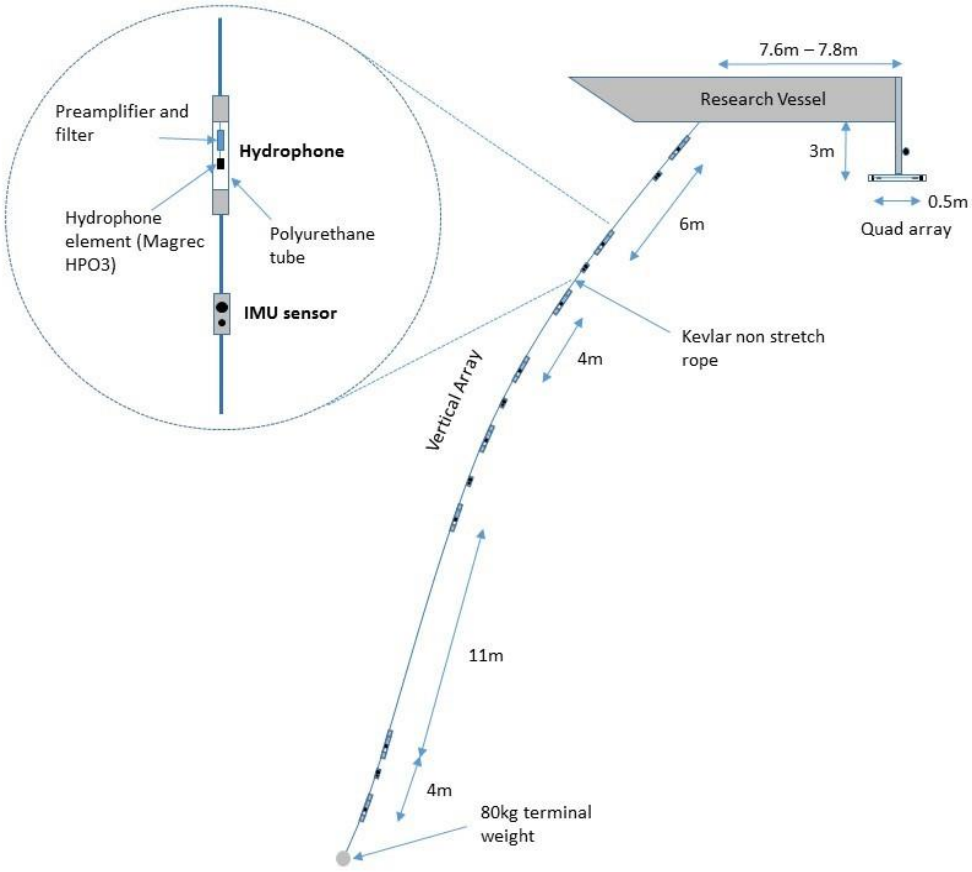

Figure 1. Diagram (not to scale) of the 10 hydrophone large aperture array. The system consisted of both a flexible vertically orientated array with eight dispersed hydrophone elements and an additional rigid tetrahedral cluster (the quad array) which allowed the bearing to an animal to be calculated. When combined with information collected by a vector GPS and orientation sensors on the vertical array, this allowed geo-referenced positions of harbour porpoises to be determined. The array is shown at an angle to illustrate potential movement in a tidal stream. Unless otherwise indicated on the diagram, the distance between hydrophone elements on the vertical array was 4m.

Several designs of hydrophone array were tested; however, only the final iteration is discussed here. This consisted of a 30-45 m vertical array with 6-8 hydrophones spaced between 4 and 11 m apart and a tetrahedral cluster of 4 hydrophones with elements separated by 50 cm (the "quad array") mounted rigidly on the vessel with an offset of ~7.5 - 8m from the vertical array. The quad array provided an unambiguous vector which, when combined with the range and depth from the vertical array, allowed 3D coordinates to be determined. To minimise flow noise and provide mechanical protection the hydrophone elements were housed individually inside small oil-filled polyurethane

tubes, each of which was attached to a non-stretch Kevlar rope that was kept taut by a terminal weight (80 kg).

Both the quad array and vertical array could be quickly deployed and recovered (<3 minutes). The vertical array sections were hung from the side of a vessel and the windlass on the anchor winch was used to recover the weight whilst the array itself was brought on board by hand. The quad array was rigidly attached to the boat's hull with a quick release mechanism that allowed for rapid recovery. OpenTag™ IMUs (inertial measurement units) from Loggerhead Instruments (www.loggerhead.com), equipped with a 3D accelerometer, 3D magnetometer, and 3D gyroscope, as well as sensors for pressure and temperature, were attached at regular intervals along the vertical array. These measured heading and pitch at each location, allowing the shape of the vertical array to be reconstructed, and so the position of hydrophones to be determined. A Hemisphere VS101 vector GPS (www.hemispheregnss.com) was used to record the heading and position of the vessel and an IS-2-30 inclinometer (www.leveldevelopments.com) was used to measure the vessel's pitch and roll. The combined data from these sensors allowed a time series of the 3D location of all hydrophones to be calculated every 0.5 seconds.

Both arrays used Magrec HPO3 hydrophones (*Magrec*, Devon, UK). Each of these consisted of a spherical 9 mm diameter ceramic with a sensitivity of -218.to -194 dB re 1V/1µPa @ 150 kHz, connected to a Magrec HPO2 pre-amplifier (with gains of either 28 or 40 dB and 20 kHz high pass filter). Signals from hydrophones were further amplified and filtered on the vessel using a custom four-channel ETEC (www.etec.dk) and two stereo Magrec HP27 amplifiers; high-pass filters with cut-on frequency of 20 kHz were typically applied to reduce low and medium frequency noise. National Instruments (NI) data acquisition (DAQ) cards (6251, 6351 and 6356) were used to digitise the signals at sample rates ranging between 500 and 1000 kHz (www.ni.com). NI cards were used in a master-slave configuration, whereby all acquisition was from a single clock pulse (the master) guaranteeing synchronisation over-all channels. In 2014, both the amplifiers and NI DAQ cards were replaced with three synchronised four-channel SAIL DAQ cards (St Andrews Instrumentation Limited, www.sa-instrumentation.com). These have inbuilt software adjustable amplifiers, filters and DAQ abilities. All recordings were saved as WAV files using PAMGuard (version 1.15.11) (www.pamguard.org).

3.2.3 Localisation Accuracy Trials

The location accuracy that could be achieved with the acoustic array was tested by broadcasting simulated porpoise clicks at known locations and depths.

A MATLAB (The Mathworks Inc.) script was written to produce a single channel WAV file containing bursts of 25 simulated porpoise clicks (length: 0.1 ms, frequency: 140 kHz, envelope: Gaussian). This was output through an NI 6252 DAQ card at 1 V_{p-p} using PAMGuard. The signal was amplified by a Sony XPLOD 1200x stereo amplifier (www.sony.co.uk) and then projected from a transmit transducer, Neptune Sonar HS150 hydrophone (Neptune Sonar Ltd., www.neptune-sonar.co.uk), on a 30 m cable. The broadcast system was operated from an inflatable boat which could then drift at different ranges from the array while the deployment depth of the transducer was adjusted. An Aladin dive computer (www.scubapro.com) and OpenTag™ were used to record the depth of the transmit hydrophone and a GlobalSat BU-353-S4 GPS (www.globalsat.co.uk) logged by PAMGuard provided a record of the position of the boat carrying the sound source.

3.2.4 Hydrophone Calibration

All hydrophones on the array were calibrated by comparing received RMS voltages from a broadcast source to a calibrated Reson TC4013 hydrophone and Reson VP2000 amplifier (http://www.teledyne-reson.com/). The calibrated hydrophone was mounted next to each hydrophone and series of tones, from 20-200 kHz, were output at a range of 20 m using the broadcast system described above.

3.3 ANALYSIS

3.3.1 Localisation Algorithms

The theory underpinning the process of localising a vocalising animal using an array of receivers is relatively straightforward. A sound (porpoise click) is detected on multiple receivers (hydrophones), the time delays between the click arriving at different hydrophone are measured, and from this, a location can be determined, either by direct calculation or using an iterative search algorithm.

3.3.1.1 Hyperbolic Localisation

The most common way to calculate the position of a sound source from a set of time delays is via hyperbolic localisation, i.e. to directly calculate from observed time delays via a set equation . This method has the great advantage of being computationally efficient. However, it cannot automatically deal with ambiguous results, propagating errors can be complex (Wahlberg et al. 2001)

and different equations have to be constructed for linear, planar and volumetric arrays (Au and Hastings 2008).

3.3.1.2 Iterative Search Algorithms

With the advance of modern computing, it is now practical to use localisation algorithms based on what is commonly termed as 'the forward problem'. Instead of trying to directly calculate parameters (the source location) from given observables (time delays), the problem is approached from the other direction; by answering the question, what time delays would be produced from a source in a given location?

Assuming a refraction free environment, it is straightforward to calculate the time it would take for a sound wave produced by a source at $s=(s_x,s_y,s_z)$, travelling at a speed of c to reach a hydrophone i located at $r=(r_x,r_y,r_z)$ using;

$$T(i) = \sqrt{\frac{(r_x(i) - s_x(i))^2 + (r_y(i) - s_y(i))^2 + (r_z(i) - s_z(i))^2}{c^2}} \qquad \text{Eq. 3.1}$$

From this, the expected time delay between two hydrophones can be found by calculating the time from the source to each hydrophone and subtracting one from the other. Thus, it is possible to calculate all the time delays expected between all elements on an array for a source at a given location. A χ^2 value can determine the extent to which these time delays match time delays from a real set of observed data by the function:

$$\chi^2 = \sum \frac{(\tau_{obs}(i,j) - \tau_{calc}(i,j))^2}{\varepsilon^2} \qquad \text{Eq. 3.2}$$

were $\tau_{obs}(i,j)$ is the actual observed time delay between hydrophones i and j, $\tau_{calc}(i,j)$ is the calculated time delay between hydrophones i and j from an acoustic source at some point in space and ε represents the expected standard deviation in observed data (White et al. 2006). For example, for a four hydrophone array, i=1,1,1,2,2,3 and j=2,3,4,3,4,4.

Various algorithms exist to sample large spatial volumes to find a location (or locations) which minimise the χ^2 value i.e. find the most likely location of the acoustic source. Such algorithms are generally more computationally intensive than directly solving via set equations but can also provide more reliable information on potential errors and ambiguities. Two such algorithms are discussed below.

3.3.1.2.1 Simplex

The downhill simplex optimisation method (Nelder and Mead 1965) is a common optimisation function which can be used to minimise the χ^2 value in any number of dimensions. In three dimensional space, the simplex can be visualised as a tetrahedron which, at each stage in the search process, can stretch, contract and reflect through its own centre until it surrounds the most likely solution and contracts to a point. Once the size of that point reaches a predetermined minimum size, the algorithm stops. Although it is fast, a disadvantage of the simplex algorithm is that it returns no error estimate. A good description of the simplex algorithm can be found in (Press et al. 1988).

3.3.1.2.2 Markov chain Monte Carlo

Markov chain Monte Carlo (MCMC) is a simulation technique which can be used to solve a wide variety of problems. For localisation, a random walk MCMC algorithm, Metropolis-Hastings algorithm (Metropolis et al. 1953), was implemented. This utilises a series of random jumps in space to arrive at the most likely source location. From an initial random point, a jump is made to a new point via a random jump function; in this case, a random Gaussian number generator determines new *x*, *y*, and *z* co-ordinates to jump to. After each new jump, χ^2 is calculated for the time delays that would be generated by an animal at the new jump location. If χ^2 is lower than the previous point in space, the jump is executed. If it is not, then the jump is only executed with a probability of:

$$p = e^{-\left(\frac{\Delta\chi^2}{2}\right)} \qquad \text{Eq. 3.3}$$

where $\Delta\chi^2$ represents the difference in χ^2 values between the previous and new jump point. If a jump is unsuccessful, a new random jump is calculated and the process repeats. As the number of iterations grows, a chain of jumps is created, which converges to a volume in space where parameter values result in a low χ^2 value, i.e. where observed and calculated data are similar. Thus, in an acoustic

localisation, a chain will converge in space to the most likely position of the acoustic source and create a 'cloud' around the likely source location. For a linear vertical array, this should be a doughnut-shaped cloud of points with a well-defined depth and range. For a 3D array, the cloud will be centred on a specific point. The mean position of points within the cloud represents the location, and the standard deviation of points directly corresponds to the standard error in location (Chib and Greenberg 1995).

A typical MCMC localisation algorithm will run many chains, each starting at a different random location. The convergence of multiple chains to the same location is a good indication of a valid result, however, random start locations also allow for different chains to converge to different possible localisation positions if ambiguities exist. If such ambiguities do exist, then the average location of points will simply give the average positions of different ambiguous results. Therefore, a clustering algorithm is required. A *k means square* (MacQueen 1967) clustering algorithm was used which assumed no more than 5 possible clusters and set a minimum value of 5m absolute distance between different clusters before they were considered a single result.

MCMC methods provide a useful visualisation of localisation results, accurately propagate errors and create clusters of results if ambiguities in location exist. It therefore provides a flexible and informative, albeit computationally demanding, method to localise sound sources.

3.3.2 Practical Issues in localising Harbour Porpoises in Tidal Rapids.

There are a number of general environmental and physical factors which must be considered when using PAM to detect, classify and localise marine mammals and these have been discussed in many publications e.g. (Au and Hastings 2008, Zimmer 2011). Localizing harbour porpoises with large aperture hydrophone arrays in energetic tidal habitats presents some additional practical and analytical challenges.

3.3.2.1 Click Match Uncertainty

Any TOAD based localisation method requires the same signal to be identified on all or a subset of elements within an array. When the distance between elements is small and potential signals arrive relatively infrequently, it is comparatively straight forward to identify the same signal on all the hydrophones in an array. However, there is the potential for *match uncertainty* when the time between potential signals becomes similar to or less than the time of flight between elements in an

array. Match uncertainty occurs when a detection of a transient on one hydrophone channel may be wrongly matched with a detection of a different transient on another hydrophone channel. This problem increases as arrays get larger and the time of flight between elements increases. A number of factors which are particularly relevant to harbour porpoises in tidal rapids habitats contribute to the problem of match uncertainty. These are:

1) High vocalization rates. Many tidal rapid areas are thought to be important areas for foraging (Pierpoint 2008, Benjamins et al. 2015). During foraging harbour porpoises click rates increase and in the final phase of prey capture reach ~600 clicks per second (an inter click interval (ICI) of 1.67 ms) (Verfuß et al. 2009)
2) Two or more individuals vocalising at the same time. Harbour porpoise show a habitat preference and/or are aggregate in unusually high numbers in at least some high energy tidal sites (Goodwin 2008, Marubini et al. 2009, Gordon et al. 2011) and therefore simultaneously detecting multiple individuals is likely.
3) Reverberation. Tidal habitats are often shallow and therefore reverberant environments resulting in strong echoes detected from the sea surface and seabed.

An initial intuitive approach might be to match detections on different hydrophone based on the waveform, amplitude and/or spectral characteristics of detected clicks. In the case of harbour porpoises, due to their narrow beam profiles, the same click detected at different angles relative to the porpoise can have very different waveforms and amplitudes and clicks from different individuals very rarely show consistent differences. Thus, an approach based on spectral or temporal characteristics will do little to match clicks on different hydrophones.

Instead a different approach is required. It is obvious that detections on different hydrophones are only potential matches if they occur within a time window determined by the distance between the hydrophones, d, and the speed of sound, c i.e. a detection is only a possible match if it is d/c seconds before or after a primary detection. If there are multiple detections within a time window on different hydrophones, then there are many possible combinations of transient detections any of which could be the direct arrival of the primary detected signal. An example of this is shown in Figure 2.

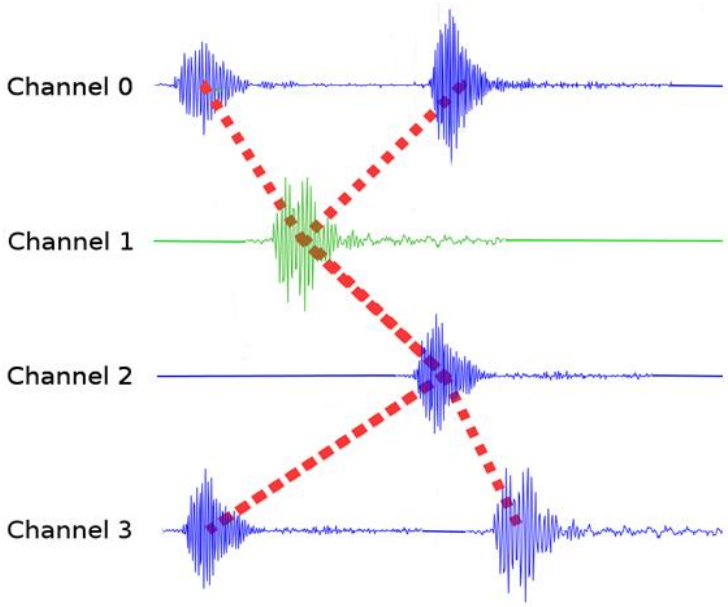

Figure 2. Example of match uncertainty. A detected click on channel 1 should also be detected on channels 0, 2 and 3. As the position of the animal is unknown, to find the same click on another channel it is necessary to look t seconds before and after the primary click were t is a time related to the distance between hydrophones. In this time window there may be several clicks detected due to a variety of factors including echoes, high click rates or other vocalising animals. As porpoise clicks from different individuals and echoes are essentially indistinguishable, finding the correct combination of clicks is difficult. One solution is to localise every possible combination, shown here by dashed lines. Incorrect combinations will either be localised to unrealsitic locations, e.g. above the sea surface, or poorly fit the localisation algorithm used, resulting in a high χ^2 value.

To solve match uncertainty, the correct combination of time delays needs to be determined. One approach is simply to calculate the sound source location for every possible combination of detections. The combination of TOADs which produce a source location with the lowest χ^2 value (best fit to the localisation model) is selected as the most likely location. Many of the calculated positions resulting from incorrect combinations and/or localisation of echoes will be unrealistic, located above the sea surface or at an improbable range and/or depth; these are discarded.

This method requires a position to be calculated for every combination of detections. The number of combinations for a 10 channel system can quickly reach thousands of locations, and therefore computationally efficient methods of localisation are required. Hyperbolic and simplex algorithms are fast enough to allow for many thousands of combinations to be calculated in a few seconds, however, using these methods alone precludes some of the advantages from the more processor intensive iterative approaches, such as MCMC. Therefore, a hybrid algorithm was developed: faster

algorithms were used to calculate the most likely combination of detections and then those combinations were localised with an MCMC based algorithm. This approach was named 'mimplex'.

The mimplex algorithm works as follows.

1) For a given porpoise click, find all possible matching clicks on different hydrophones.
2) Calculate all possible time delay combinations.
3) Localise every time delay combination using hyperbolic and simplex algorithms.
4) Using Eq. 2 calculate the χ^2 value for each localisation. The time delay combination with the lowest χ^2 is deemed the correct combination and localised with MCMC.
5) The result is saved and the algorithm moves to the next click. Select the next click in the series and go to step 1.
6) After processing has finished, discard results if above sea level or at an unrealistic range or depth or if χ^2 is higher than a predefined threshold.

For each localisation, the mimplex algorithm requires a primary channel. In this case, there are two approaches. The first is to use predefined channel on the array as the primary channel. If a click is not detected on that channel then it is not localised and therefore some useful localisations are potentially missed. The second approach is to use a dynamic primary channel. However, this requires that matched clicks are removed from further localisation attempts. This involves a decision on whether a localisation is valid *during,* rather than after, processing (e.g. it is not advisable to remove matched clicks from further localisation if the current localisation is 500 m above sea level and therefore invalid) and so introduces a significant extra level of complexity.

Here, for simplicity, a hydrophone midway on the vertical array was used as the predefined primary channel under the assumption that most clicks which ensonified a minimum number of hydrophones on the vertical array for a successful localisation would most likely be detected on a mid-array hydrophone. This assumption would not hold for a significantly longer array with more hydrophones and thus developing a robust dynamic primary channel system is a focus of further work.

3.3.3 Tracking dives

Having calculated the locations for individual clicks the next step is to join these into a series of tracks showing the movement and behaviour of individual animals. The high frequency and therefore rapid

attenuation of NBHF clicks combined with highly directional vocalisations means that the probability of a harbour porpoise ensonifying a sufficient number of hydrophones on a large aperture array for a successful localisation (3 for a 2D location and 4 for a 3D location), is dependent on an individual animal's range, depth and orientation. This and the fact that porpoises may not vocalise continuously mean that a typical acoustic encounter with a porpoise will at best provide a scatter of localisation points representing only *fragments* of a complete dive. In addition, these localisation points are not evenly distributed in time; changes in ICI will result in more or fewer localisations per second. A tracking algorithm is therefore required to perform the following tasks.

1) Separate the clicks and tracks of different animals vocalising at the same time.
2) Interpolate the tracks of individual animals.
3) Smooth interpolated tracks to compensate for localisation errors and gain more accurate insights into animal swim speed and orientation.

This is relatively simple for a single animal, merely requiring a 'joining of dots' and then smoothing and interpolation of the resulting track. However, the problem is more complex when localisations of clicks of several animals are calculated at the same time. As discussed above, clicks of different individuals cannot be distinguished by their acoustic characteristics and therefore tracks must be identified based on location rather than acoustic information. This type of pattern recognition problem, often referred to as multi target tracking, is common and several solutions exist e.g. (Berclaz et al. 2011); the approach adopted here was to use a state estimation technique, a 3D Kalman filter (Kalman 1960) combined with a matching algorithm, Hungarian method (Kuhn 1955), to track multiple animals simultaneously (Luetteke et al. 2012, Yussiff et al. 2014). In this model, the movement of a porpoise is described by:

$$\begin{bmatrix} x_k \\ y_k \\ z_k \\ \dot{x}_k \\ \dot{y}_k \\ \dot{z}_k \end{bmatrix} = \begin{bmatrix} 1 & 0 & 0 & t & 0 & 0 \\ 0 & 1 & 0 & 0 & t & 0 \\ 0 & 0 & 1 & 0 & 0 & t \\ 0 & 0 & 0 & 1 & 0 & 0 \\ 0 & 0 & 0 & 0 & 1 & 0 \\ 0 & 0 & 0 & 0 & 0 & 1 \end{bmatrix} \begin{bmatrix} x_{k-1} \\ y_{k-1} \\ z_{k-1} \\ \dot{x}_{k-1} \\ \dot{y}_{k-1} \\ \dot{z}_{k-1} \end{bmatrix} + \begin{bmatrix} t^2/2 \\ t^2/2 \\ t^2/2 \\ t \\ t \\ t \end{bmatrix} a + w_k \qquad \text{Eq. 3.4}$$

where x, y, z are the independent Cartesian co-ordinates of the porpoise and $\dot{x}$, $\dot{y}$, $\dot{z}$ are the velocity, or the derivative of x, y, z with respect to time. t is time, a is a normally distributed acceleration of a

typical harbour porpoise with a mean of 0 and a standard deviation of σ_a and k represents concurrent time steps. w_k is the process error/noise with a covariance matrix:

$$Ex = {\sigma_a}^2 \begin{bmatrix} t^4/2 & 0 & 0 & t^3/2 & 0 & 0 \\ 0 & t^4/2 & 0 & 0 & t^3/2 & 0 \\ 0 & 0 & t^4/2 & 0 & 0 & t^3/2 \\ t^3/2 & 0 & 0 & t^2 & 0 & 0 \\ 0 & t^3/2 & 0 & 0 & t^2 & 0 \\ 0 & 0 & t^3/2 & 0 & 0 & t^2 \end{bmatrix} \quad \text{Eq. 3.5}$$

Eq. 3.4 can be rewritten as:

$$\bar{x}_k = F\bar{x}_{k-1} + Ga_k + w_k \quad \text{Eq. 3.6}$$

where F is defined as the state transition matrix and G is the control input matrix and $\bar{x}_k$ is the position, velocity vector.

As position is the only measurement which can be made from localisation results, the measurement update model is:

$$z_k = \begin{bmatrix} 1 & 0 & 0 & 0 & 0 & 0 \\ 0 & 1 & 0 & 0 & 0 & 0 \\ 0 & 0 & 1 & 0 & 0 & 0 \end{bmatrix} \begin{bmatrix} x_k \\ y_k \\ z_k \\ \dot{x}_k \\ \dot{y}_k \\ \dot{z}_k \end{bmatrix} + v_k \quad \text{Eq. 3.7}$$

where v_k is the measurement error/observation noise with a covariance matrix of:

$$Ez = \begin{bmatrix} \sigma_x^2 & 0 & 0 \\ 0 & \sigma_y^2 & 0 \\ 0 & 0 & \sigma_z^2 \end{bmatrix} \quad \text{Eq. 3.8}$$

where $\sigma_x, \sigma_y, \sigma_z$ are the standard deviations in position measurements (x, y, z); these are calculated automatically by the mimplex algorithm for each localisation point.

Eq. 3.7 can be rewritten as:

$$z_k = H\bar{x}_k + v_k \quad \text{Eq. 3.9}$$

where H is defined as the observation matrix.

F, G, H, Ex and Ez form the basis of the Kalman filter which can be constructed as shown in Kalman (1960). On its own, the Kalman filter simply smooths a single animal track and will not perform well if multiple tracks are present. However, the predictive component of a Kalman filter allows multiple instances to be used in conjunction with a Hungarian matching algorithm (Kuhn 1955) to track multiple animals simultaneously. The algorithm works as follows:

1) Data are binned into 0.5 second intervals. All positions are clustered by x,y and depth via agglomerative hierarchical clustering using the MATLAB 'cluster' function. This initial stage has two functions.
    a. It averages out stochasticity in the localisation positions the thus provides cleaner input data for the Kalman filter.
    b. It reduces the number of possibilities the matching algorithm must consider and thus helps prevent aliased tracks i.e. were the algorithm tracks the same animal simultaneously with multiple tracks.
2) A Kalman filter is started from each cluster in the first bin.
3) Move to the next time bin.
4) For all current tracks the next predicated state is calculated by $\overline{x}_k = F\bar{x}_{k-1} + Ga_k$.
5) All possible distances between observed animal positions and predicated states are calculated and input into a cost matrix. Localised positions are then assigned to predictions via a Hungarian matching algorithm.
6) If a track has not been assigned to a new localisation, it is tagged with a 'strike'. If the number of strikes reaches a pre-defined number, it is stopped in step 10.
7) If a track has been assigned to a localisation which is greater than a defined maximum distance (in this case 15 m + 10% of the localisation depth) from the end of the track, that detection is ignored and the track is given a strike.
8) If a localised detection has not been assigned a track, or has been ignored because it is greater than the maximum allowed distance, a new track is started from that detection.
9) For any track successfully assigned a detection, all strikes are removed.
10) Any track which has more than the allowed number of strikes is stopped. The end of that track which is formed only by predictions is removed and the remaining section added to a list of completed track fragments.

11) The Kalman filter for each current track is updated.
12) Go back to step 3 and continue to last time bin.

Using this algorithm, it is possible to automatically generate track fragments from large quantities of data, a sample of which is shown in Figure 6. The standard deviation in acceleration (σ_a in Eq. 3.5) was 0.12ms^{-2}, a likely high estimate based on (Teilmann et al. 2006) and the maximum number of strikes allowed for each track was 15.

3.3.3.1 Array Movement Error

In any localisation calculation, error in receiver positions will propagate to an error in the localised positions of animals. Receiver movement is a major concern in flexible vertical array systems used in tidal currents. Arrays can deform substantially as a result of differential currents at different depths and the effects of wind on the surface supporting vessel. Therefore, simply assuming that an array remains vertical could introduce large errors in the localised positions under some conditions.

The five OpenTag™ orientation sensors on the array were attached with roughly regular spacing (Figure 1). The orientation of the vertical array was therefore known at each orientation sensor. These data were used to reconstruct the most likely 'shape' of the vertical array underwater and thus determine the most likely position of each hydrophone. To model the array shape the vertical array was spilt into *n* (in this case *n*=100) sections. Section *0* starting where the array connects to the vessel at (x_0,y_0,z_0)=(0,0,0) and section *n* ending at the deepest hydrophone. Each orientation sensor was located on a section between 0 and *n*. The unit vector of that section was provided by the angle recorded by the orientation tags. For the other sections without a sensor, the unit vector was defined as:

$$\hat{\mathbf{u}}_i = \frac{\mathbf{u}_i}{|\mathbf{u}_i|} \qquad \text{Eq. 3.10}$$

where:

$$\mathbf{u}_i = \frac{(i - i_A)}{(i_B - i_A)}(\hat{\mathbf{u}}_B - \hat{\mathbf{u}}_A) \qquad \text{Eq. 3.11}$$

$\hat{\mathbf{u}}_i$ is the unit vector of section *i* with *i*=1,2,3….*n*. i_A is the number of the first section above i which holds a tag and i_B is the number of the first section below i which holds a tag. $\hat{\mathbf{u}}_B$ is the recorded unit vector of the tag on section i_B and $\hat{\mathbf{u}}_A$ is the recorded unit vector of the tag on section i_A. Sections which have no tag above have a unit vector $\hat{\mathbf{u}}_B$ and sections which have no tag between them at the end of the array have a unit vector $\hat{\mathbf{u}}_A$

Once the orientation angles for each section have been calculated, (*x, y, z*) positions can be determined using the unit vector and length of each section.

$$\boldsymbol{v}_i = \hat{\mathbf{u}}_i \times C + \boldsymbol{v}_{i-1} \qquad \text{Eq. 3.12}$$

where $\boldsymbol{v}_i$ is the *(x,y,z)* position of the end of each section and C is the length of a section. This process is carried out for sections 0-*n* to determine the shape and orientation of the array. Data from the ship based inclinometer and vector GPS are then used to calculate the real world location (latitude, longitude and height) of each (x_0,y_0,z_0), and thus the real world location of all hydrophones on the array.

3.3.3.2 Refraction

Refraction of sound due to temperature and salinity gradients in underwater environments has the potential to introduce large errors into localisation. Strong turbulent water flows in tidal rapids usually results in well mixed water masses. Sound speed profiles were calculated for all survey locations using CTD profiles from the British Oceanographic Data Centre (BODC) database and potential refraction modelled using ACTUP Software (Duncan and Maggi 2006). Refraction was insignificant and variation in speed of sound was no greater than 5.68ms^{-1}. This is negligible (0.4%) and thus a conservative error estimate of 10ms^{-1} was integrated into the MCMC localisation model rather than using more complex refraction models for localisation (e.g. Thode 2005).

3.3.3.3 Noise

To detect a harbour porpoise click, the received signal must be greater than the background noise level. Sediments moving in strong currents are thought to be a major source of noise in tidal areas (Bassett et al. 2013). There is no solution to high levels of noise if present in a frequency band of interest, however, all hydrophones were calibrated, allowing for an assessment of the potential impacts on harbour porpoise detectability.

The maximum range at which an on-axis click with a source level of 191 dB re 1µPa pp at 1m (the average source level of wild porpoise clicks (Villadsgaard et al. 2007)) would be detected was calculated using a simple spherical propagation model:

$$TL = 20\log_{10}(R) + \alpha R \quad \text{Eq. 3.13}$$

where TL is the transmission loss R is the range in meters and α is the absorption coefficient. α was calculated to be 0.041 dBm^{-1} at 130 kHz (Ainslie and Mccolm 1998). The maximum detection range can be assumed to be the range R, at which

$$SL - TL = NL + SNR_{min} \quad \text{Eq. 3.14}$$

where SL is the source level (191 dB re 1µPa pp at 1m), NL is the noise level in the 100 to 160 kHz frequency band and SNR_{min} is the minimum signal to noise ratio at which clicks can be detected. This equation was solved for R to assess the impact on porpoise detectability of variable noise conditions in tidal areas. See section 5.9.3 on how noise and click amplitude are compared.

3.3.4 Software

3.3.4.1 Click Detection

Raw acoustic data was passed through the PAMGuard click detector module (version 1.15.11c) with a signal to noise ratio (SNR_{min}) threshold set to 10 dB. All detected clicks were classified as likely to be from a harbour porpoise or unidentified based on their spectral content and length using the PAMGuard click classifier (Gillespie et al. 2008).

3.3.4.2 Localisation and Tracking

A time series of hydrophone positions, calculated in MATLAB using the methods detailed in section 3.3.3.1, were then imported into PAMGuard. Detected porpoise clicks and hydrophone positions were used to calculate animal locations using a new PAMGuard localisation module (version 1.15.11c) which implemented the mimplex methods described above. The localisation modules assumed a sound speed of 1500 ms^{-1} with a standard error of 10 ms^{-1}, the standard error in hydrophone positions was 1 cm if on a flexible array i.e. vertical array and 1 mm if rigid i.e. between quad array hydrophones and the cross correlation error was assumed to be 2 µs (1 sample).

Localisation results were filtered to remove any points above the sea surface and at ranges greater than 200 m as accuracy trials showed localised positions clearly broke down after this range. Finally, only results with a χ^2 value of less than 250 were used in further analyses. This value was chosen as

manual inspection of results showed it provided a good balance between excluding obviously incorrect localisations and removing too many correct values.

Harbour porpoise track fragments were then calculated in MATLAB from the filtered localisation results using the Kalman filter algorithm described in section 3.3.3.

3.3.4.3 Simulation of Errors

Error surfaces were generated to simulate the localisation accuracy of both the arrays at different ranges. The PAMGuard Sound Acquisition and Click Detector modules were used to generate simulated clicks in a 100 m x 100 m grid around both arrays at 5 depths, 0, 10, 20 30 and 40 m. A simulated click on each of the hydrophones was generated assuming a source was located at every grid point and then localised using exactly the same methods applied to real data. The errors predicted were then used to estimate the average localization error with respect to range.

3.3.4.4 Noise

In order to assess realistic detection ranges in tidal environments, noise measurements were performed for several example drifts using the PAMGuard Filtered Noise Measurement module. A bandpass 100 kHz to 160 kHz, 6th order Butterworth filter (Butterworth 1930) was used, with a measurement period of 10 seconds. The RMS noise calculated by the noise module was assumed to be equivalent to the click detector's noise floor (the click detector trigger used the same filter) and thus $NL{+}SNR_{min}$ in Eq. 3.14 could be calculated using methods in section 5.9.3. For visualisation purposes, long term spectral averages (LTSA) were calculated using the PAMGuard LTSA modules.

3.4 FIELD TRIALS

Field work was carried out in coastal waters off the west of Scotland, in the Sound of Islay, the Great Race and Gulf of Corryvreckan in 2013 and in Kyle Rhea and the Sound of Sleat in 2014. The research vessel used was Silurian, a 16m motor sailing vessel. Broadcast trials occurred in 2013.

3.5 RESULTS

3.5.1 Localisation Accuracy and Mimplex performance

During localisation accuracy trials, 39% of detected broadcast clicks were successfully localised. If it is assumed that, with an omnidirectional sound source, half of the clicks detected are likely to be surface echoes, the proportion of direct path clicks localised accurately is likely to be between 70 to 80%.

Figure *3*A and 3B show the localised depth and range of the sound source plotted against true depth and range. Figure 3C shows a summary of real and simulated errors; the median error in the field trials (difference between true and localised position) is plotted alongside simulated errors in 25 m range bins. The mean error in angle to the sound source was 3.06°. This was not affected by range.

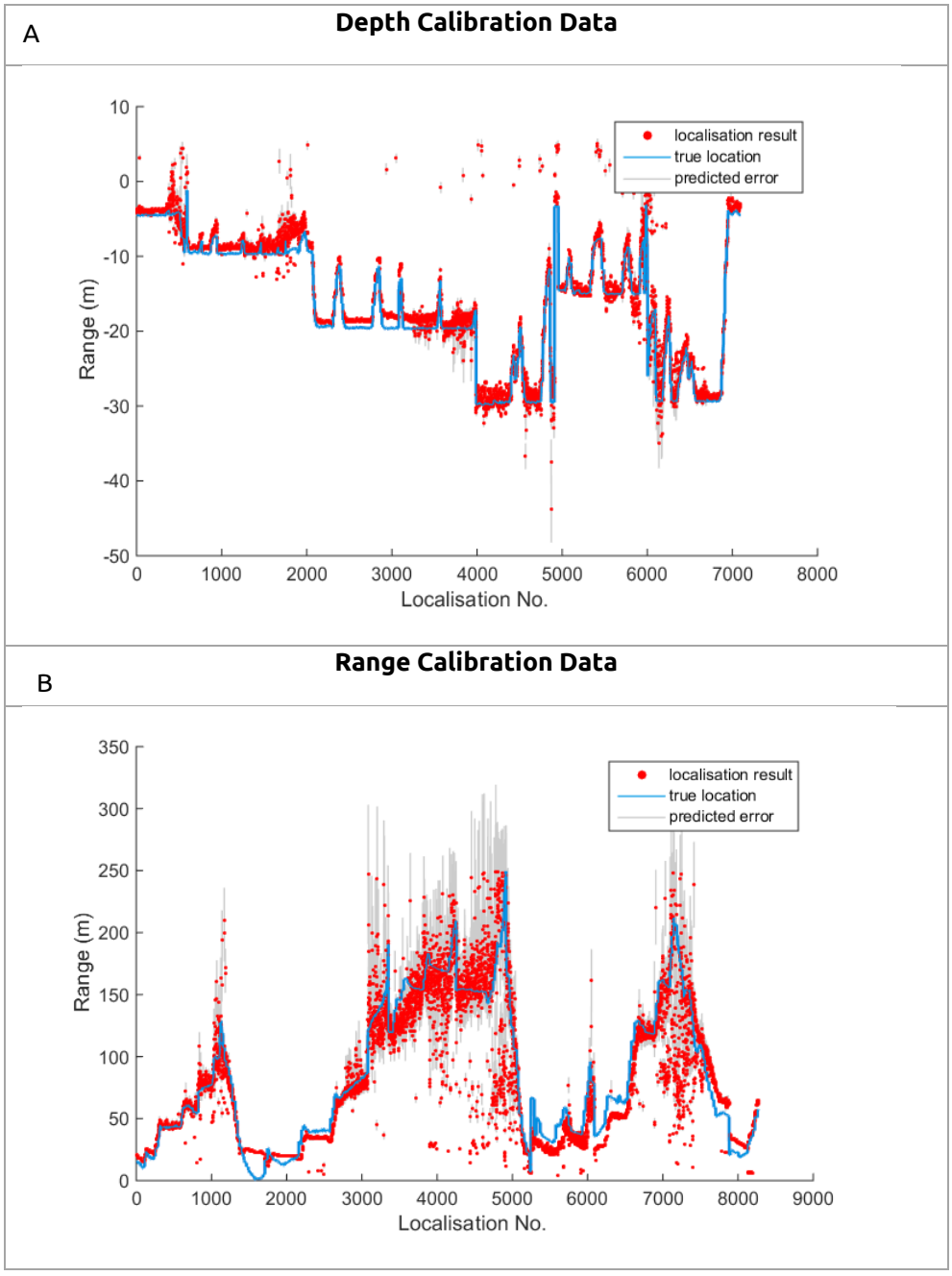

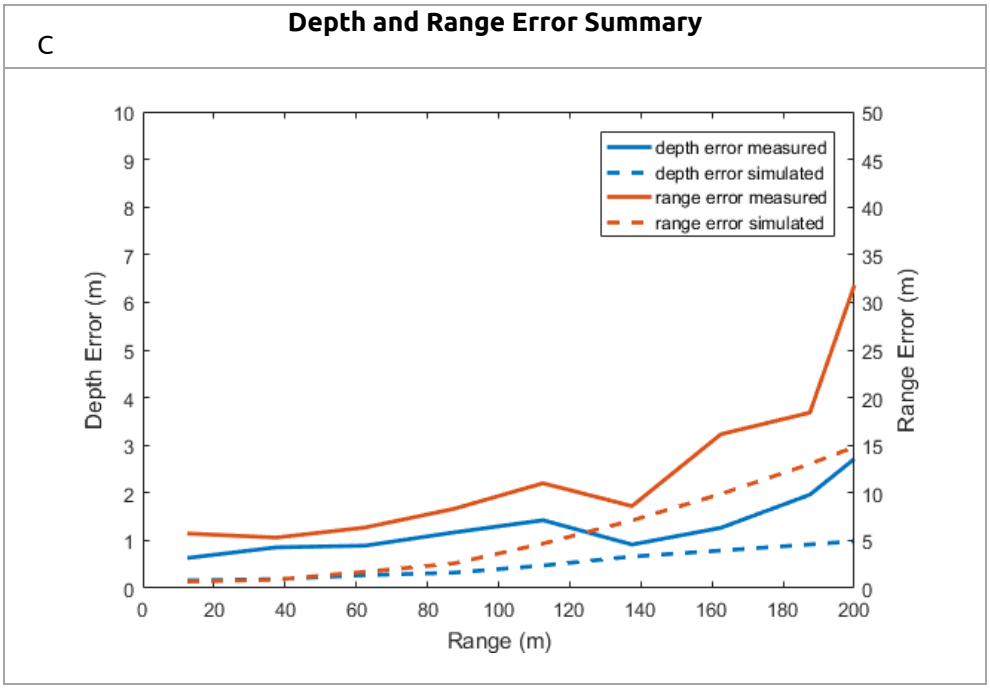

Figure 3 The localised depth and range of the sound source compared to the true location of the pinger and summary of errors. Graphs 3A and 3B show the depth and range of the localised clicks compared to the true depth and range of the sound source. Error bars are 95% confidence intervals calculated by the MCMC algorithm. Graph 3C is a plot of errors in depth and range against range and also shows predicted errors calculated from simulations. Errors in field measurements are the median difference between true location and calculated location and in simulation are the 95% confidence interval calculated by MCMC.

3.5.2 Noise

Figure 4 shows an example of long term spectral averages over two ~8 hour long tidal surveys in the Sound of Islay and the Great Race with detection range overlaid. The green line shows the expected on-axis detection range for a 191 dB re 1 µPa peak to peak at 1 m porpoise click (the highest average recorded in the wild) assuming that detection is possible at an SNR of 15dB; this was the SNR used in the click detection algorithm. In the Sound of Islay, large broad band noise spikes are present, whilst in the Great Race the majority of ambient noise remains well below the porpoise frequency band.

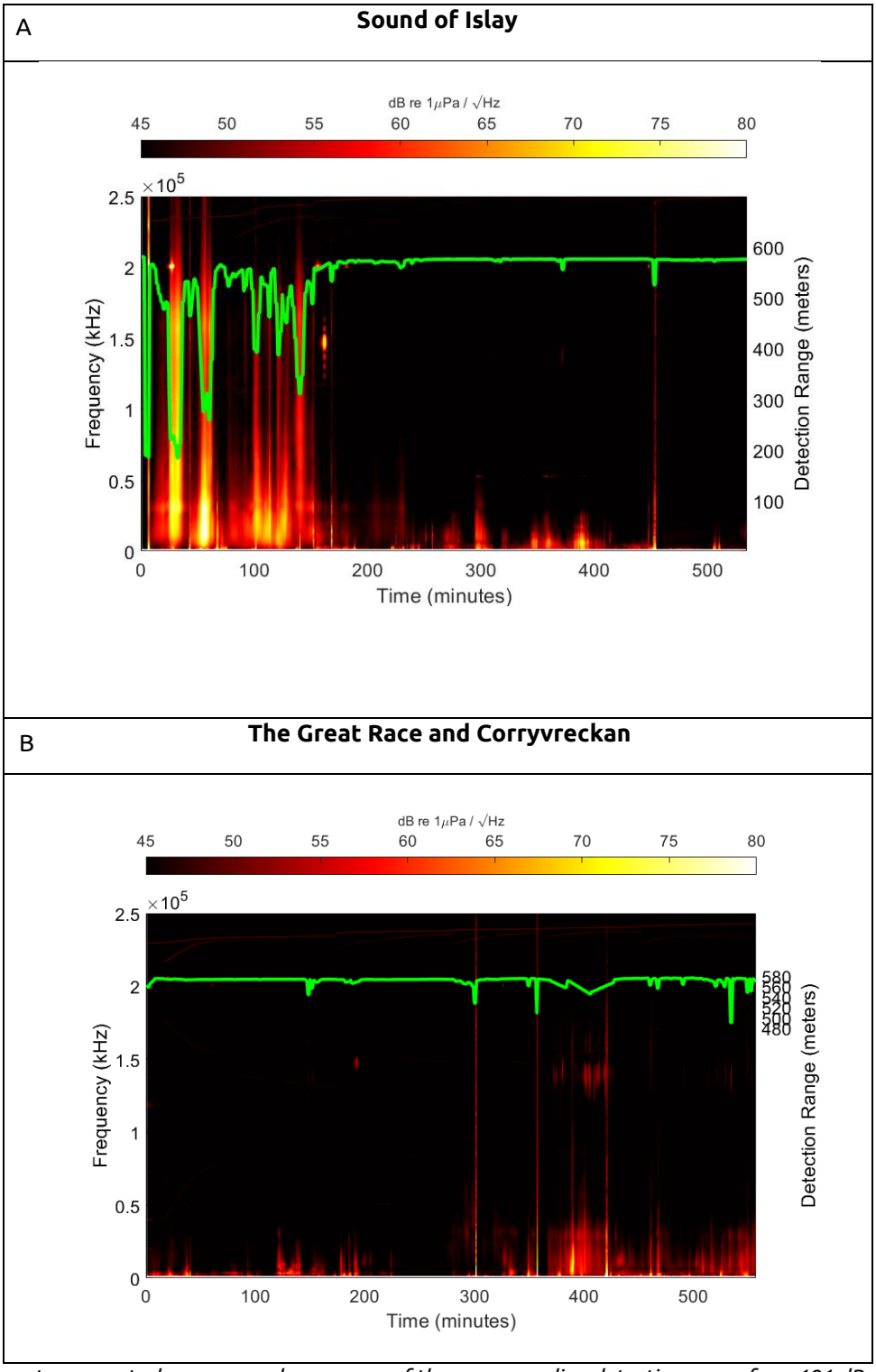

Figure 4. Long term spectral average and a measure of the corresponding detection range for a 191 dB re 1 µPa at 1m peak to peak on-axis porpoise click. Two full survey days in the Sound of Islay and the Great Race are shown as examples. The noise levels in the Sound of Islay were highly variable and broadband which resulted in large changes in the detection range during periods of noise, as shown with corresponding decreases in detection range. Noise was generally well below the porpoise frequency band in the Great Race, resulting in a much less variable detection range.

3.5.3 Click Detection Distribution

A minimum of three true duplicated clicks must be detected on the vertical section of the array to allow the mimplex algorithm to calculate a location. For every successful localisation, the distance between the two most widely separated hydrophones on which the click was detected click was calculated. The results (Figure 5) clearly show that for most localisations clicks were detected on widely separated hydrophones.

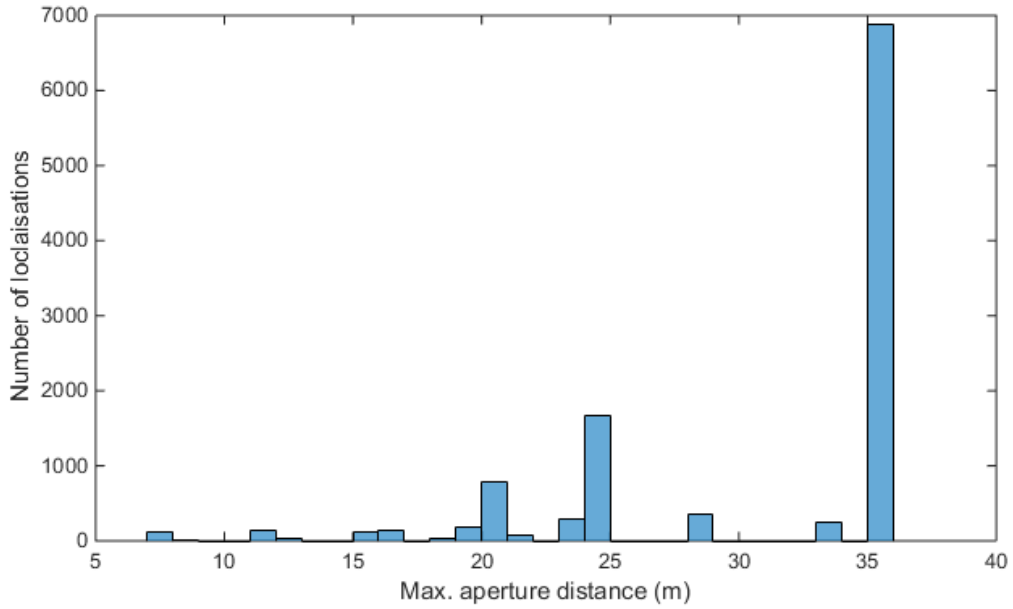

Figure 5. Histogram showing the distance between the two most widely seperated hydrophones on the array (max aperure distance) on which a localised click was detected. The majority of porpoise detections which could be localised (i.e. detected on a minimum of 3 hydrophones) involve detections on widely spaced hydrophone elements.

3.5.4 Tracks

Figure 6 shows an example of porpoise dive tracks from the Sound of Sleat, calculated using the mimplex and tracking algorithms. In total, 171 hours of data was recorded and an average of 822,170 porpoise clicks per hydrophone were detected. This resulted in 5,206 geo-referenced track fragments. 89% of localised clicks were grouped into tracks consisting of at least 3 clicks and 67% of localised clicks were grouped into tracks consisting of at least 10 clicks.

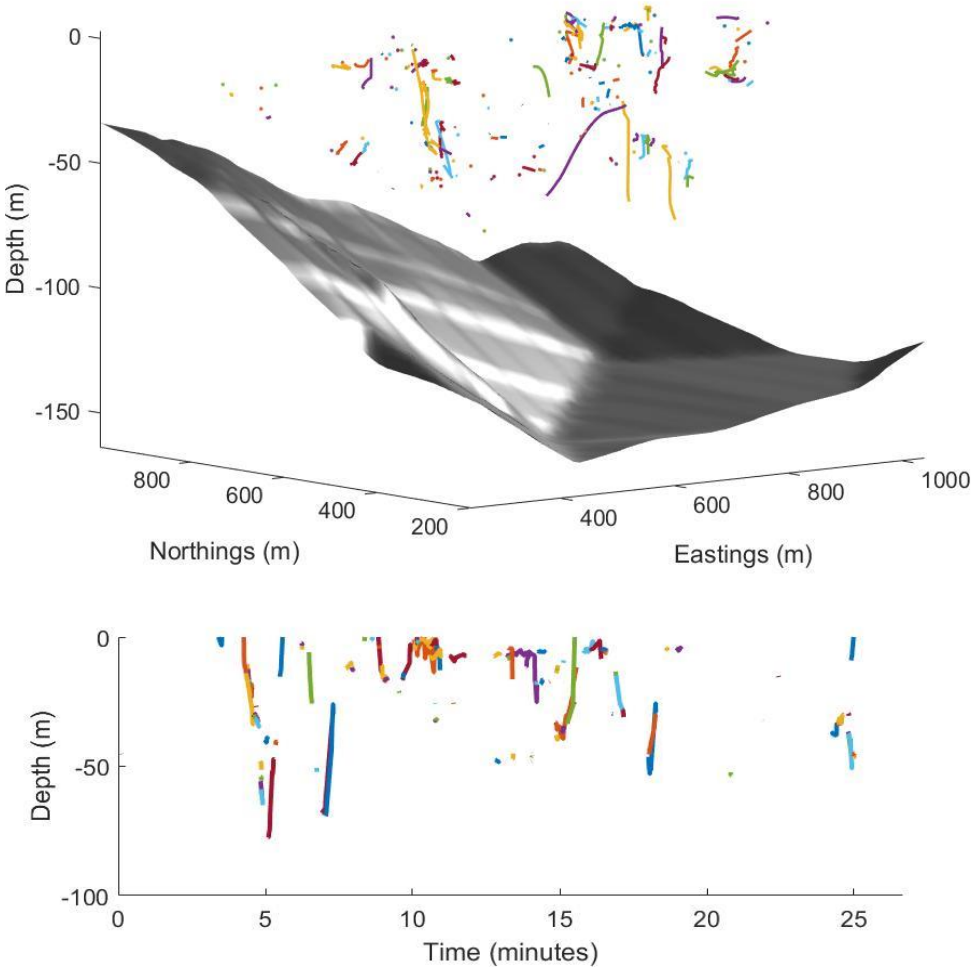

Figure 6. Example of dive fragments of harbour porpoises in the Sound of Sleat, Scotland. Figure 6a shows an example of geo referenced tracks and bathymetry. Figure 6b shows an example of track fragments in depth and time. Note size differences in fragments in both graphs. Tracks can be tens of seconds long, forming a significant portion of an animal's dive, or can be just a few seconds long, providing a 'snapshot' location of an animal.

3.6 DISCUSSION

The large aperture hydrophone array developed here was designed specifically to obtain detailed behavioural information on harbour porpoises within tidal rapid sites and over the typical time scale of a survey (>1 week). Results from field trials and surveys demonstrate that 1) large aperture arrays can coherently detect porpoise NBHF clicks on a sufficient number of hydrophones to attempt localisation, 2) large aperture arrays are capable of providing accurate information on 3D animal locations in high current areas and 3) effective automated methods can be used to analyse data.

The majority of published studies which have used PAM to determine the location of harbour porpoises have utilised small rigid hydrophone arrays with aperture sizes on the order of a few meters (e.g. Ural et al. 2006, Villadsgaard et al. 2007, Kyhn et al. 2013). Although appropriate for those studies, small hydrophone apertures significantly reduce the range at which accurate localisations are possible and therefore the efficacy of adopting such systems to measure dive profiles is limited. Results presented in this manuscript show that, despite the narrow beam profile and high attenuation of NBHF clicks, much larger hydrophone apertures can be used for localising wild harbour porpoises. The ability to do so greatly increases the potential range at which animals can be localised (here ~200m) allowing these methods to be applied as an effective survey methodology to collect data on the fine scale behaviour of echolocating animals.

Many designs of vertical arrays were tested in tidal rapids while developing the array configuration described here. It became apparent during the development process that movement of the hydrophone array, due to the windage of the survey vessel and differential underwater currents, was introducing large localisation errors. Any movement of the vertical array results in uncertainties in hydrophone positions which then propagate to large errors in the localised positions of animals. To solve this, the shape of the array underwater was reconstructed using orientation units, allowing the positions of hydrophones to be accurately calculated. However, any vertical linear array which sits off the vertical angle also introduces fundamental ambiguities in localisation which cannot be resolved by knowledge of hydrophone positions. The addition of the quad array broke the linearity of the vertical array and so removed this fundamental ambiguity, recovering localisation accuracy and so allowing 3D positions of animals to be calculated. The localisation accuracy of the system was extensively tested both in the field during broadcast trials and using simulation tools. The field trials showed similar increases in error with range but, in general, average errors were around twice that of simulations (Figure 3). Realistic estimates of errors were input into the localisation model (perhaps even slightly small for hydrophone positions) and thus these localisation errors could be caused by un-modelled errors in the array geometry calculations or the use of a constant or incorrect sound speed profile, which were not included in simulations but are almost certainly present when equipment is deployed in the field. Simulated data can therefore provide an initial estimate of the errors around an array but is not a substitute for testing in the field. Despite the increase in error, field trials demonstrated that, when combined with data from a vector GPS and orientation sensors,

it was possible to obtain accurate geo-referenced localisations of the broadcast pinger, with sub-meter accuracy in depth at ranges <60 m. The vertical array is therefore capable of resolving the fine scale behaviour of animals, however, to maintain such accuracy in high current areas it is vital that both the movement of the array is accurately measured *and,* crucially, the array is designed in such a way that any linear symmetry is broken.

To make this a viable survey methodology, *automated* tools were required to analyse the large quantities of acoustic data collected over significant time periods (e.g. 14 days). Without running experiments with a tagged animal and accompanying PAM array, it is difficult to quantify the effectiveness of some aspects of the automated tracking system (hydrophone array + automated algorithms) e.g. how accurate the tracking algorithm is at separating multiple animals and what proportion of porpoise tracks are recorded at different ranges. However, it was possible to test the performance of the mimplex algorithm. Results from the click broadcast trials demonstrated the automated mimplex algorithm was likely able to accurately localise ~70 to 80% of individual clicks. Considering that the average click rate of a wild harbour porpoises in the areas studies was ~14 clicks per second, this should allow measurement of fine scale movements of detected animals. The omni-directional source created multiple reverberations and echoes so the broadcast trials were a good test of the mimplex algorithm's ability to successfully match clicks on different hydrophones. Since the output source did not move like a porpoise, or simulate typical acoustic behaviour, the broadcast trials could not be used to test the tracking algorithm. Assessing tracking performance will be the focus of further research, however, visual inspection of tracking results indicated the algorithm produced realistic tracks from localised points. The ability of the mimplex algorithm to match clicks and the tracking algorithm to separate and interpolate individual dive fragments was particularly useful during the tidal rapid surveys. Patches of high frequency noise, shallow water leading to reverberation, and high densities of vocalizing porpoises produced a particularly complex soundscape in the porpoise frequency band and meant that simultaneous tracking of multiple individuals was often required. The automated nature of these methods is vital for surveys; manual attempts at matching and localising 822,170 porpoise clicks would be both costly and prohibitively time consuming.

Although these methods provide an effective system for tracking animals, there are several limitations which must be considered. Noise is a major concern for any PAM survey and could conceivably reduce the average detection range of animals to an extent that makes PAM arrays ineffective in some areas. The tidal sites surveyed here had variable noise profiles. The most extreme example, the Sound of Islay (Figure 4A), shows the maximum detection range of an on-axis click being reduced to 150m in some parts of the tidal stream, a reduction of over 2/3. This would reduce the number of detections by approximately $(2/3)^2$, a factor of 2.25. Other studies have noted localised and often geographically consistent increases in high frequency noise levels in tidal rapids (Gordon et al. 2011, Malinka et al. 2015). The experience with these surveys is much the same, with occasional localised patches of high frequency noise in which porpoise detection probability will be substantially reduced. Therefore, a prudent approach before considering the use of complex drifting arrays or any other PAM system in a tidal rapid area would be to make measurements of ambient noise levels in the areas of interest, especially when tidal currents are strongest, to determine whether PAM surveys are a viable option.

The other significant consideration when employing this system, and indeed with PAM in general, is the strong association between the detectability of any animal with a narrow beam profile and its orientation, range and depth. An animal facing away from the array is far less likely to be detected than one facing towards the array. This problem is exacerbated when localisation, which requires detections on a number of hydrophones, is being attempted. Consequently, it is very rare for an entire dive to be recorded; instead fragments of animal tracks are produced. However, this is somewhat tempered by the ability of the system to collect large quantities of data on multiple animals which can be analysed to produce statistically meaningful measures of harbour porpoise behaviour and use of the water column.

A primary driver for this work was to better quantify the collision risk tidal turbines might pose to harbour porpoises. For this to be determined, substantial datasets on underwater behaviour must be collected from many animals, in multiple tidal areas and over full tidal and diel cycles. The drifting system and automated algorithms described in this chapter can be targeted at specific geographic areas such as tidal rapids, provide accurate information on animal behaviour and is cost effective, so is well suited to this task. Although developed primarily for tracking harbour porpoises in tidal rapids,

the methods developed here are relatively general and could be applied to other echolocating species, other habitats and/or array types. Indeed, the relatively high attenuation and directionality of NBHF clicks makes the harbour porpoise a particularly poor candidate species for localisation; it is therefore to be expected that this methodology may work more effectively with other echolocating species in less energetic habitats.

3.7 CONCLUSION

Information on the fine-scale movements of animals underwater has primarily been the preserve of tagging, and indeed the information that tagged animals have provided has been instrumental in our understanding of animal behaviour. However, in the specific case of a small geographic area of interest, such as tidal streams, the cost/data ratio of tagging animals, which may spend the majority of their time outside these areas, is less favourable. It has been shown that, in these situations, localisation using large aperture drifting arrays is a viable alternative methodology and can be used effectively in tidal rapid habitats. It provides a targeted, cost-effective and non-invasive platform to provide high resolution data on animal behaviour and can be utilised in adverse conditions during both day and night.

3.8 ACKNOWEDGEMENTS

Thanks to Carol Sparling and Gordon Hastie of SMRU, and Ben Wilson and Steven Benjamins of SAMS for input and helpful discussions. Special thanks to Alex Coram (SMRU) for practical input, field assistance and discussion throughout this project, as well as other field assistants over the years. I am grateful to Jay Barlow for suggesting the use of the Sony XPLOD for this application. Thanks to 'Student Dave Tutorials' for code resources and instructive tutorials and BODC for supplying CTD profiles. This work was funded by the Scottish Government through the Marine Mammal Scientific Support Research Programme MMSS/001/11.

3.9 REFERENCES

Ainslie, M. A., and J. G. Mccolm. 1998. A simplified formula for viscous and chemical absorption in sea water. The Journal of the Acoustical Society of America 103:1671.

Au, W. W. L., and M. C. Hastings. 2008. Principles of Marine Bioacoustics. Springer US, New York, NY.

Au, W. W. L., R. A. Kastelein, T. Rippe, and N. M. Schooneman. 1999. Transmission beam pattern and echolocation signals of a harbor porpoise (Phocoena phocoena). The Journal of the Acoustical Society of America 106:3699–3705.

Bassett, C., J. Thomson, and B. Polagye. 2013. Sediment-generated noise and bed stress in a tidal channel. Journal of Geophysical Research: Oceans 118:2249–2265.

Benjamins, S., A. Dale, G. Hastie, J. Waggitt, M.-A. Lea, B. Scott, and B. Wilson. 2015. Confusion Reigns? A Review of Marine Megafauna Interactions with Tidal-Stream Environments. Pages 1–54 Oceanography and Marine Biology: An Annual Review.

Berclaz, J., F. Fleuret, E. Türetken, and P. Fua. 2011. Multiple object tracking using k-shortest paths optimization. IEEE Transactions on Pattern Analysis and Machine Intelligence 33:1806–1819.

Butterworth, S. 1930. On the theory of filter amplifiers. Experimental Wireless and the Wireless Engineer 7:536–541.

Chib, S., and E. Greenberg. 1995. Understanding the Metropolis-Hastings Algorithm. The American Statistician 49:327–335.

Deruiter, S. L., A. Bahr, M.-A. Blanchet, S. F. Hansen, J. H. Kristensen, P. T. Madsen, P. L. Tyack, and M. Wahlberg. 2009. Acoustic behaviour of echolocating porpoises during prey capture. The Journal of experimental biology 212:3100–3107.

Duncan, A. J., and A. L. Maggi. 2006. A Consistent, User Friendly Interface for Running a Variety of Underwater Acoustic Propagation Codes. Pages 471–477 Proceedings of the First Australasian Acoustical Societies' Conference. Christchurch, New Zealand.

Frid, C., E. Andonegi, J. Depestele, A. Judd, D. Rihan, S. I. Rogers, and E. Kenchington. 2012. The environmental interactions of tidal and wave energy generation devices. Environmental Impact Assessment Review 32:133–139.

Gillespie, D., J. Gordon, R. Mchugh, D. Mclaren, D. Mellinger, P. Redmond, A. Thode, P. Trinder, and X. Y. Deng. 2008. PAMGUARD: Semiautomated, open source software for real-time acoustic detection and localisation of cetaceans. Proceedings of the Institute of Acoustics 30:2547.

Goodwin, L. 2008. Diurnal and tidal variations in habitat use of the harbour porpoise (Phocoena phocoena) in Southwest Britain. Aquatic Mammals 34:44–53.

Gordon, J., D. Thompson, R. Leaper, D. Gillespie, C. Pierpoint, S. Calderan, J. Macaulay, T. Gordon, and N. Simpson. 2011. Assessment of risk to marine mammals from underwater marine renewable devices in Welsh waters - Phase 2 - Studies of marine mammals in Welsh high tidal waters. Page Welsh Government Assembly Report.

Hastie, G. D., B. Wilson, and P. M. Thompson. 2006. Diving deep in a foraging hotspot: acoustic insights into bottlenose dolphin dive depths and feeding behaviour. Marine Biology 148:1181–1188.

Heerfordt, A., B. Møhl, and M. Wahlberg. 2007. A wideband connection to sperm whales: A fiber-optic, deep-sea hydrophone array. Deep Sea Research Part I: Oceanographic Research Papers

54:428–436.

Holt, M. M., D. P. Noren, V. Veirs, C. K. Emmons, and S. Veirs. 2009. Speaking up: Killer whales (Orcinus orca) increase their call amplitude in response to vessel noise. The Journal of the Acoustical Society of America 125:EL27-L32.

Kalman, R. E. 1960. A New Approach to Linear Filtering and Prediction Problems. Transactions of the ASME-Journal of Basic Engineering 82:35–45.

Koblitz, J. C., M. Wahlberg, P. Stilz, P. T. Madsen, K. Beedholm, and H.-U. Schnitzler. 2012. Asymmetry and dynamics of a narrow sonar beam in an echolocating harbor porpoise. The Journal of the Acoustical Society of America 131:2315.

Kuhn, H. W. 1955. The Hungarian method for the assignment problem. Naval Research Logistics Quarterly 2:83–97.

Kyhn, L. A., J. Tougaard, K. Beedholm, F. H. Jensen, E. Ashe, R. Williams, and P. T. Madsen. 2013. Clicking in a Killer Whale Habitat: Narrow-Band, High-Frequency Biosonar Clicks of Harbour Porpoise (Phocoena phocoena) and Dall's Porpoise (Phocoenoides dalli). PLoS ONE 8:e63763.

Linnenschmidt, M., J. Teilmann, T. Akamatsu, R. Dietz, and L. A. Miller. 2013. Biosonar, dive, and foraging activity of satellite tracked harbor porpoises (*Phocoena phocoena*). Marine Mammal Science 29:E77–E97.

Luetteke, F., X. Zhang, and J. Franke. 2012. Implementation of the Hungarian Method for object tracking on a camera monitored transportation system. 7th German Conference on Robotics:1–6.

MacQueen, J. B. 1967. Kmeans Some Methods for classification and Analysis of Multivariate Observations. 5th Berkeley Symposium on Mathematical Statistics and Probability 1967 1:281–297.

Malinka, C. E., A. E. Hay, and R. Cheel. 2015. Towards acoustic monitoring of marine mammals at a tidal energy site: Grand Passage, NS, Canada. Proceedings of the 11th European Wave and Tidal Energy Conference:1–10.

Marubini, F., A. Gimona, P. G. H. Evans, P. J. Wright, and G. J. Pierce. 2009. Habitat Preferences and Interannual Variability in Occurrence of the Harbour Porpoise Phocoena phocoena off Northwest Scotland. Marine Ecology Progress Series 381:297–310.

Metropolis, N., A. W. Rosenbluth, M. N. Rosenbluth, A. H. Teller, and E. Teller. 1953. Equation of State Calculations by Fast Computing Machines. The Journal of Chemical Physics 21:1087–1092.

Miller, B., and S. Dawson. 2009. A large-aperture low-cost hydrophone array for tracking whales from small boats. The Journal of the Acoustical Society of America 126:2248–2256.

Møhl, B., M. Wahlberg, P. T. Madsen, L. a Miller, and a Surlykke. 2000. Sperm whale clicks: directionality and source level revisited. The Journal of the Acoustical Society of America 107:638–648.

Nelder, J. A., and R. Mead. 1965. A Simplex Method for Function Minimization. The Computer Journal 7:308–313.

Pierpoint, C. 2008. Harbour porpoise (Phocoena phocoena) foraging strategy at a high energy, near-shore site in south-west Wales, UK. Journal of the Marine Biological Association of the United Kingdom 88:1167–1173.

Press, W. H., S. A. Teukolsky, W. T. Vetterling, and B. P. Flannery. 1988. Numerical Recipes: The Art of Scientific Computing. Cambridge University Press New York, Second Edition.

Teilmann, J., J. Tougaard, L. A. Miller, T. Kirketerp, K. Hansen, and S. Brando. 2006. Reactions of captive harbor porpoises (Phocoena phocoena) to pinger-like sounds. Marine Mammal Science 22:240–260.

Thode, A. 2005. Three-dimensional passive acoustic tracking of sperm whales (Physeter macrocephalus) in ray-refracting environments. The Journal of the Acoustical Society of America 118:3575–3584.

Thompson, D., and M. Lonergan. 2015. Collision risk and impact Study: Examination of models for estimating the risk of collisions between seals and tidal turbines. Sea Mammal Research Unit, University of St Andrews, Report to Scottish Government, no. MR 7.2.2. St Andrews.

Toke, D. 2011. The UK offshore wind power programme: A sea-change in UK energy policy? Energy Policy 39:526–534.

Ural, T., R. Bahli, M. Yano, T. Inoue, T. Sakamaki, and T. Fukuchi. 2006. Results From A High-Resolution Acoustic Device For Monitoring Finless Porpoises In Coastal Precincts Off Japan. Pages 1–5 OCEANS 2006 - Asia Pacific. IEEE.

Verfuß, U. K., L. A. Miller, P. K. D. Pilz, and H. U. Schnitzler. 2009. Echolocation by two foraging harbour porpoises (Phocoena phocoena). Journal of Experimental Biology 212:823–834.

Villadsgaard, A., M. Wahlberg, and J. Tougaard. 2007. Echolocation signals of wild harbour porpoises, Phocoena phocoena. Journal of Experimental Biology 210:56–64.

Wahlberg, M., B. Møhl, and P. Teglberg Madsen. 2001. Estimating source position accuracy of a large-aperture hydrophone array for bioacoustics. The Journal of the Acoustical Society of America 109:397.

Watkins, W. a., and W. E. Schevill. 1972. Sound source location by arrival-times on a non-rigid three-dimensional hydrophone array. Deep Sea Research 19:691–706.

White, P. R., T. G. Leighton, D. C. Finfer, C. Powles, and O. N. Baumann. 2006. Localisation of sperm

whales using bottom-mounted sensors. Applied Acoustics 67:1074–1090.

Wiggins, S. M., M. a. McDonald, and J. a. Hildebrand. 2012. Beaked whale and dolphin tracking using a multichannel autonomous acoustic recorder. The Journal of the Acoustical Society of America 131:156.

Wilson, B., R. S. Batty, F. Daunt, and C. Carter. 2007. Collision risks between marine renewable energy devices and mammals, fish and diving birds. Page Report to the Scottish Executive.

Wisniewska, D. M. M., M. Johnson, J. Teilmann, L. Rojano-Doñate, J. Shearer, S. Sveegaard, L. A. A. Miller, U. Siebert, and P. T. T. Madsen. 2016. Ultra-High Foraging Rates of Harbor Porpoises Make Them Vulnerable to Anthropogenic Disturbance. Current Biology 26:1441–1446.

Wisniewska, D. M., J. M. Ratcliffe, K. Beedholm, C. B. Christensen, M. Johnson, J. C. Koblitz, M. Wahlberg, and P. T. Madsen. 2015. Range-dependent flexibility in the acoustic field of view of echolocating porpoises (Phocoena phocoena). eLife 4:1–16.

Yussiff, A.-L., S.-P. Yong, and B. B. Baharudin. 2014. Parallel Kalman filter-based multi-human tracking in surveillance video. Pages 1–6 2014 International Conference on Computer and Information Sciences (ICCOINS). IEEE.

Zimmer, W. 2011. Passive Acoustic Monitoring of Cetaceans. Cambridge University Press, Cambridge.

Chapter 4: High resolution 3D beam radiation pattern of harbour porpoise NBHF clicks with implications for biology and passive acoustic monitoring

Measuring 3D beam profiles in Fjord and Baelt, Denmark during a snowstorm.

Chapter 4: High resolution 3D beam radiation pattern of harbour porpoise NBHF clicks with implications for biology and passive acoustic monitoring

ABSTRACT

The source properties and radiation patterns of animal vocalizations define, along with propagation and noise conditions, the active space in which they can be detected by conspecifics, predators, prey and by humans in passive acoustic monitoring (PAM). Here the full 4π (360° horizontal and vertical) beam profile of a free-swimming, trained harbour porpoise was measured using a 27-element hydrophone array. The forward beam is highly directional as predicted by a piston model and previous empirical measurements. However, at off axis angles greater than ± 30°, the beam attenuates more rapidly than the piston model and no side lobes are present. A diffuse back beam is also present with levels about -30 dB relative to on-axis. In PAM around 65% of detections can be from portions of the beam profile with distorted click spectra and waveforms, although this drops substantially for lower source levels. Monte Carlo simulations of the probability of detecting a harbour porpoise show that a piston model can significantly underestimate the probability of detection compared to the actual 3D radiation pattern documented here. This highlights the importance of empirical 4π measurements of beam profiles of toothed whales both to improve understanding of their biology and to inform PAM studies.

4.1 INTRODUCTION

All toothed whales studied so far produce highly directional echolocation clicks with directivity indices which are remarkably similar between species (Jensen et al. 2018). Directing acoustic energy in this way generates higher source levels along the acoustic axis for the same power, which increases the range at which prey can be detected in a noise-limited environment whilst also limiting clutter (Madsen and Surlykke 2013). A directional biosonar beam may also serve as a spatial filter of information, aid localization of prey targets via a steep intensity gradient, and direct sound energy away from their acute auditory system that must detect and process weak echoes milliseconds after the emission of a powerful click (Schrøder et al. 2017).

Directional beam profiles have significant implications for PAM, in that detectability of clicks is highly dependent on the orientation of the animal relative to the receiver and thus accurate knowledge of the beam profile is key in understanding the detectability of echolocation clicks. In an initial data exploration of harbour porpoise tracks collected from the vertical hydrophone arrays in Chapter 3, it was observed that a larger number of tracks were recorded when harbour porpoises were facing the array but there was also a small increase in the number of tracks at 180°, i.e. when animals were moving away from the array (see Figure 1) (Malinka et al. 2015). If all the energy in harbour porpoise beam profile is directed forward then there should be very few tracks at off-axis angles, which was not the case in the localised track data. This prompted speculation that the beam profile of a harbour porpoise may have more side and back energy than had been previously been assumed.

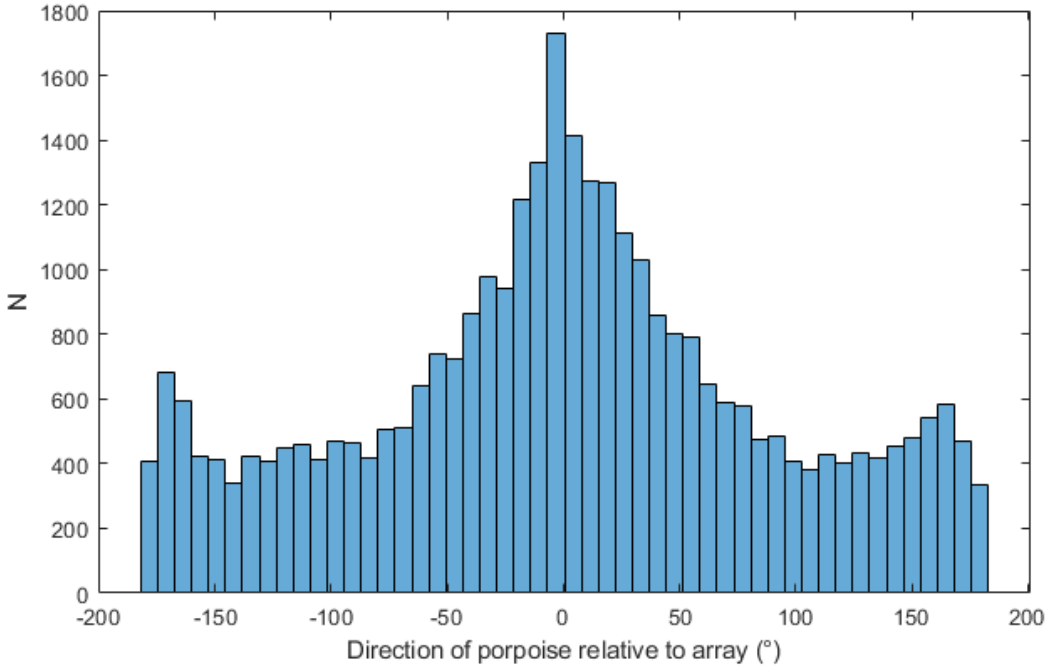

Figure 1. Angles from localised harbour porpoise tracks relative to the hydrophone array. 0° indicates a porpoise approaching the hydrophone array and -180°/180° indicates an animal moving away. Note that there are many more tracks facing towards the array. This is because the narrow beam profile of harbour porpoises means that it is more likely that a click is detected when the animal facing the array. However, there is also a slight increase in track numbers at -180°/180° when animals are moving away from the array. This suggests that that there is previously unrecorded energy in the beam profile of harbour porpoise beam profiles at larger off-axis angles.

Quantifying toothed whale beam profiles usually involves the use of a compact array of hydrophones in a star or linear, vertical configuration to record clicks from captive animals in controlled environments (e.g. Koblitz et al. 2012; Finneran et al. 2014; Smith et al. 2016) or wild animals in close proximity (e.g. Rasmussen et al. 2002, 2004; Au & Herzing 2003; Zimmer *et al.*, 2005; Kyhn *et al.*, 2013; Jensen et al. 2015; Ladegaard *et al.*, 2015; Koblitz *et al.*, 2016). In most studies, only the narrow forward aspect of a beam (~±30°) is measured because the vast majority of the energy is contained in this small section of the beam profile, and it is that part that serves the animal in echolocation. Another attractive feature of using near on-axis apparent source levels (ASL, (Møhl et al. 2000)) for beam estimation is that they can be conveniently fitted to a flat piston model to explain how most of the sound energy is radiated from the toothed whale forehead (Au 1993). The piston model describes the beam attenuation with respect to angle relative to the acoustic axis and depends entirely on only two parameters: the waveform of an on-axis echolocation click and the functional aperture of the emitter (Strother and Mogus 1970, Au et al. 1978). The piston model refers to a circular

piston of a specified radius which is placed flush on an infinite baffle. The piston moves in a motion which represents the signal of interest; for example it would undergo simple harmonic motion for a uniform sine wave and more complex motion to simulate a porpoise or dolphin click. The received amplitude of the signal output from the piston can then be modelled using a first order Bessel function which forms the basis of a transfer function that can be multiplied by the Fourier transform of an echolocation click , creating a beam profile (Au 1993, p. 110). The possible distortion of an off-axis click can also be modelled by considering the piston as a two point source, whereby the two clicks are emitted at opposing edges of the piston (i.e. separated by the aperture). At a large distance from the piston, these clicks will arrive with some phase delay; the convolution of the two signals then provides the distorted waveform.

When the on-axis waveform is known for a given species, the equivalent aperture can be back-calculated by fitting the piston model to an empirically measured beam profile (e.g. Beedholm & Møhl 2006; Koblitz et al. 2012). For some applications, the equivalent aperture can be used to generate beam profiles of morphologically similar species for which directly measured beam data have not been collected. However, while the piston model works well for beam profile estimations ~$\pm$30° around the acoustic axis, it may not offer accurate measures of ASL farther off-axis. In particular, the piston model will, by definition, not work beyond 90°.

While the consequences for biosonar operation may fully be explained within angles of $\pm$30° off-axis and thus successfully covered by the piston model, an understanding of the levels and waveforms of clicks farther off-axis is relevant for studies of other aspects of toothed whale biology; in particular management via passive acoustic monitoring (PAM). In the correct circumstances, PAM can be used to calculate animal density - a key metric for conservation regulatory frameworks. There are multiple analytic approaches to density estimation using PAM which are usually dependent on the type of survey performed (Marques et al. 2013). One possibility is to simulate the probability of detecting animals using a Monte Carlo simulation based on pre-determined auxiliary information on diving and acoustic behaviour. The efficacy of this approach is predicated on the accuracy of the model inputs, one of which is the beam profile (Küsel et al. 2011, Frasier et al. 2016). Another density estimation technique is the acoustic adaptation of spatially explicit capture/recapture (SECR) which is based on animals ensonifying different numbers of receivers within a widely spaced hydrophone array (Stevenson et al. 2015); this is a relatively novel density estimation

approach but if used with toothed whale clicks or other directional vocalisations requires a model of an animal's beam profile (Stevenson 2016). Knowledge of an animal's beam profile is also a factor when designing hydrophone arrays to localise different species (Zimmer et al. 2008).

The potential importance of beam profiles, both in understanding the sensory ecology of animals and for informing PAM, has prompted several studies on the wider radiation of sound around toothed whales. The full or near-full horizontal beam profiles of clicks (±180°), burst pulses and/or whistles have been measured for bottlenose dolphins (Au et al. 2012a, Branstetter et al. 2012, Finneran et al. 2014) and for a harbour porpoise (out to 130°) (Hansen et al. 2008). Whilst appropriate for their respective aims, these studies placed only a small number of hydrophones (5 to 8) around a stationary animal leading to relatively poor spatial resolution (with the exception Finneran *et al.*, 2014, who used 35 hydrophones) and limited measurements to one horizontal and/or vertical slice of the beam profile. The full 4π beam (all vertical and horizontal angles around a sphere) has been measured only once for a wild sperm whale using data from an acoustic tag deployed in tandem with a towed hydrophone array, although the nature of the equipment and sperm whale behaviour meant that on-axis beam measurements were rare and clipped (Zimmer et al. 2005).

This chapter measures the full 4π beam profile of a harbour porpoise (*Phocoena phocoena*). The forward beam profile of harbour porpoises has been measured multiple times on stationary, captive harbour porpoises. Au et al. (1999) recorded a 16° half power (-3 dB) beam which was confirmed using suction cup hydrophones attached directly to the harbour porpoise's melon (Au 2006). Koblitz et al. (2012) measured a narrower -3 dB horizontal beam width of 13.1° and a vertically compressed beam width of 10.7°. The shy nature of harbour porpoises makes them difficult to study visually but they are a good candidate for PAM because, despite high attenuation in seawater (Ainslie and Mccolm 1998), NBHF clicks are relatively unique within most soundscapes (although can be shared by overlapping species (e.g. Kyhn et al. 2013)). As PAM hardware becomes more cost-effective, acoustic density estimation methods are likely to be more widely used to study harbour porpoises (e.g. Carlén et al. 2018). Knowledge of the full 4π beam profile is an important aspect in both interpreting data and potentially for density estimation calculations but has not been measured before. Here, a 27-channel hydrophone array is used to measure the full 4π beam pattern of a free-swimming captive harbour porpoise. The implications for the probability of detecting animals using

PAM are explored by comparing the piston model measurements from previous literature and the empirically measured 4π beam pattern.

4.2 MATERIAL AND METHODS

4.2.1 Recording System

A total of 27 hydrophones were arranged around the periphery of a rectangular research sea pen (3 m deep x 8 m x 13 m; Fig. 1). This included eight TC 4034 hydrophones (Teledyne RESON A/S, Slangerup, Denmark) and 12 high-frequency, autonomous digital sound recorders (SoundTraps, Ocean Instruments, NZ). Additionally, seven TC 4013 hydrophones (Teledyne RESON A/S, Slangerup, Denmark), arranged in a star-array (used in Ladegaard et al. (2017)) were placed near one corner of the sea pen (Figure 2).

SoundTraps were mounted above each TC 4034 hydrophone on steel poles (1 cm diameter) at depths of 1 m and 1.3 m respectively. These poles were mounted on floating pontoons. The centre hydrophone in the star array was at a depth of 1.2 m. The other six hydrophones in the star-array were located at even spaced angles (every 60°) around the centre hydrophone at alternating radial distances of 37.5 cm and 77.5 cm. The star array was constructed from PVC and the solid poles holding hydrophones in place were 2cmin diameter.

Outputs from hydrophones on the star-array were amplified by 60 dB using a custom-built amplifier box with low cut (1 kHz 1-pole high pass) and anti-aliasing (200 kHz 4-pole low pass) filters (both Butterworth) before digitization at 16-bit resolution using two synchronised 8-channel analogue to digital converters (NI 6356 USB data acquisition cards, National Instruments, USA), providing 15 synchronised channels with a 4 V peak-to-peak range and a 500 kHz sample rate. This resulted in an overall clip levels of 164 and 157 dB re 1µPa for the TC 4034 and TC 4013 hydrophones, respectively. Data from the NI cards were saved as 16 channel WAV files using PAMGuard (version 2.00.13) ((Gillespie et al. 2008); www.pamguard.org). The SoundTraps were programmed to record on high gain mode, for an overall average clip level of 174 dB re 1 µPa at 125 kHz. Note that SoundTraps are autonomous single-channel units, and therefore time-synchronisation to channels on the array was completed after data collection.

4.2.2 Experimental Procedure

Data were collected in February 2018 at Fjord & Bælt in Kerteminde, Denmark, where one harbour porpoise, Freja, 62 kg and 22 years old, was housed in an outdoor sea pen. The weather during the three days of data collection was fair, with no rain during data collection.

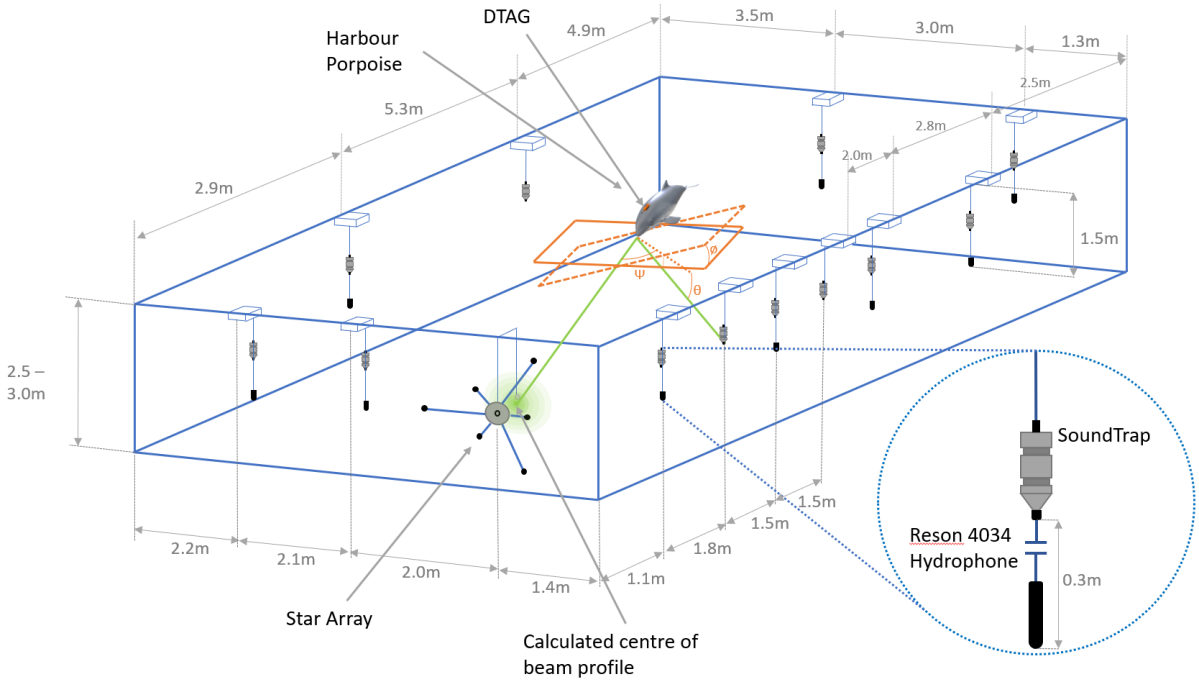

Figure 2. Diagram of the experimental setup (not to scale). The porpoise approached the 7-channel star array. The received levels on the star array were used to calculate the locations of centre of the porpoise beam. The (x,y,z) position of the porpoise was localised using the star array. The centre of the beam and the localised porpoise position allowed for a vector to be calculated which was the acoustic axis of the animal. DTAG data then provided the roll angle of the porpoise. This created a full set of Euler angles (heading, pitch and roll). For every hydrophone (Reson and SoundTrap), the received level was measured. A vector from each hydrophone to porpoise was calculated which was then projected onto the porpoise roll frame of reference, providing both the vertical and horizontal angle with the respect to the on-axis beam. The source level for this horizontal and vertical angle was then calculated using the sonar equation, assuming spherical spreading. This process was repeated for every detected click to build up a picture of the beam profile.

Freja was trained with positive food reinforcement to swim towards a familiar target and touch it, as she has done in several previous studies (e.g. (Wisniewska et al. 2015, Ladegaard and Madsen 2019). The target, a 50 mm diameter aluminium sphere (TS -39 dB), was suspended on a monofilament line and placed in front of the centre of the star array, at distances of ~5-30 cm. One trial comprised a target approach over 10-14 meters that concluded with the porpoise putting the tip of her rostrum on the target, at which point the porpoise was then bridged with a whistle and received a fish reward. The porpoise was not specifically trained to produce echolocation clicks while performing these tasks, but consistently did so as part of its normal behaviour. There was a stereotypical reduction in SL and ICIs during the approach, and a terminal

buzz while moving up to the sphere to touch it, consistent with previous studies (Deruiter et al. 2009, Ladegaard and Madsen 2019) showing that she was echolocating to solve the task.

Target approaches were either completed with regular swimming or whilst rolling. Freja was given an audible and tactile signal to directly approach the target (n = 21), or was given a visual hand signal to actively roll while swimming in the direction of the target (n = 18) to provide for full 4π sampling of the acoustic radiation pattern. During rolling trials, one target approach comprised 1-3 rolls. 39 trials were run over four sessions over two consecutive days, with each session comprising up to 12 trials.

The porpoise sometimes wore opaque suction-cup eyecups during direct target-approach trials (on 7/21 target approach trials), so as to maximize the number of clicks produced since porpoises have been observed to produce more clicks when blindfolded (Verfuß et al. 2009). No eyecups were used during trials in which the porpoise was instructed to roll due to the visual cue used to request rolling.

The porpoise was equipped with a sound and movement tag (DTAG-4; (Johnson and Tyack 2003)), mounted dorsally behind the blowhole. Tag audio data were recorded at a sample rate of 576 kHz in 16-bit resolution (~170 dB re 1 µPa clip level). The pitch and roll data recorded by the tag allowed for the full orientation of the porpoise to be calculated and thus enabled measurement of the full 4π beam whilst the porpoise was free swimming.

Two GoPro Hero 2 cameras (GoPro, San Mateo, California, USA), time-synched with acoustic recordings, documented the experiments with either a birds-eye or trainers-eye view.

4.2.3 Calibrations

The 3D positions of each hydrophone were measured to a centimetre accuracy using a laser range finder (Bosch GLM 50 C Professional). Additionally, prior to each experimental session, each hydrophone was pinged with porpoise-like clicks (130 kHz, 10 cycles, generated by an Agilent (33220A, Agilent Technologies, CA, USA) waveform generator) from the same reference distance using a B&K 8105 hydrophone (Brüel & Kjær Sound & Vibration Measurement A/S, Nærum, Denmark) as a transducer.

The pinging trials were used to calculate the relative sensitivity of all hydrophones. A manual analyst marked out all clicks detected from the output hydrophone using the PAMGuard click detector module (version 2.00.13) (www.pamguard.org); these were then imported into MATLAB (The Mathworks Inc., Natick, MA))

using the PAMGuard/MATLAB library (https://sourceforge.net/projects/pamguard/files/Matlab/). The relative peak-to-peak amplitude (pp) of the received clicks on each hydrophone was calculated and corrected for DAQ voltage, range to the output hydrophone (assuming spherical spreading and 0.04 dBm^{-1} absorption coefficient), gain and transmission loss. Absolute sensitivity values were then calculated by scaling the relative sensitivity of each hydrophone to the known sensitivity of the central star hydrophone (-210 dB re 1V/µPa). This ensured that the relative sensitivities of each receiver were accurately calculated (standard deviation of ~1dB in measurements) to ensure precise estimation of the beam profile whilst also allowing absolute levels to be determined.

SoundTrap and DTAG clocks can drift at a rate of ~2 seconds per day, and typical inter click intervals of a harbour porpoise are < 100 ms, and so clock drift in SoundTraps could potentially result in errors when matching clicks between different devices. SoundTrap clocks were therefore aligned with the synchronised hydrophone array at the beginning of each session. Time alignment was performed in MATLAB by cross correlating the first 2 seconds of a detected click train. Each session was around 10 minutes which equates to a maximum of 14ms of clock drift and thus this provided sufficient time alignment for matching clicks but did not allow for the SoundTraps to be used for acoustic localisation purposes. The DTAG clock was synchronised to the array in the same manner.

4.2.4 Method Validation

Trials were also run with a 'fake porpoise': a TC-2130 transducer (Teledyne RESON A/S, Slangerup, Denmark), with a known directivity index (Jensen et al. 2015) and equivalent aperture having a radius of 2.5 cm – which generated a beam with a directionality index similar to that of a harbour porpoise. This transducer emitted a series of simulated narrow-band high frequency (NBHF) clicks at 130 kHz generated by a waveform generator (model 33220A, Agilent Technologies, CA, USA). The TC-2130, mounted on a broomstick, was manually moved towards the star-array along the approximate swim path of the real porpoise while emitting clicks. The porpoise was not in the research pen while these trials were conducted. The data from this were analysed in the same manner as clicks from the real porpoise. Additionally, the beam profile of the TC-2130 was accurately measured in a calibration tank. Details of the method validation can be found in the supplementary materials 4.9.1.

4.2.5 Data Analysis

Porpoise positions were calculated using the known spatial hydrophone configuration and the time of arrival differences of the same click between the receivers. To minimise errors arising from echoes, only the star array was used for localisation calculations. For every click detected on the central channel of the star array, all possible combinations of porpoise clicks detected on other channels were determined. Time of arrival differences for each combination were calculated and a Simplex minimisation algorithm (Nelder and Mead 1965) was used to calculate the range and direction to the porpoise. The time delay combination with the best fit to the localisation algorithm (i.e. the set of time delays which made most physical sense) was selected as the correct position of the porpoise. If this position was outside of the bounds of the pen it was discarded. A Savitzky-Golay FIR smoothing filter (Press and Teukolsky 1990) (polynomial order: 3, window length: 9) was then applied to all localised positions within a specified trial to construct a 3D interpolated track of the harbour porpoise approach as shown in Figure 3. Localisation errors were estimated to be small (usually <5cm) and so were ignored for the subsequent analysis stages.

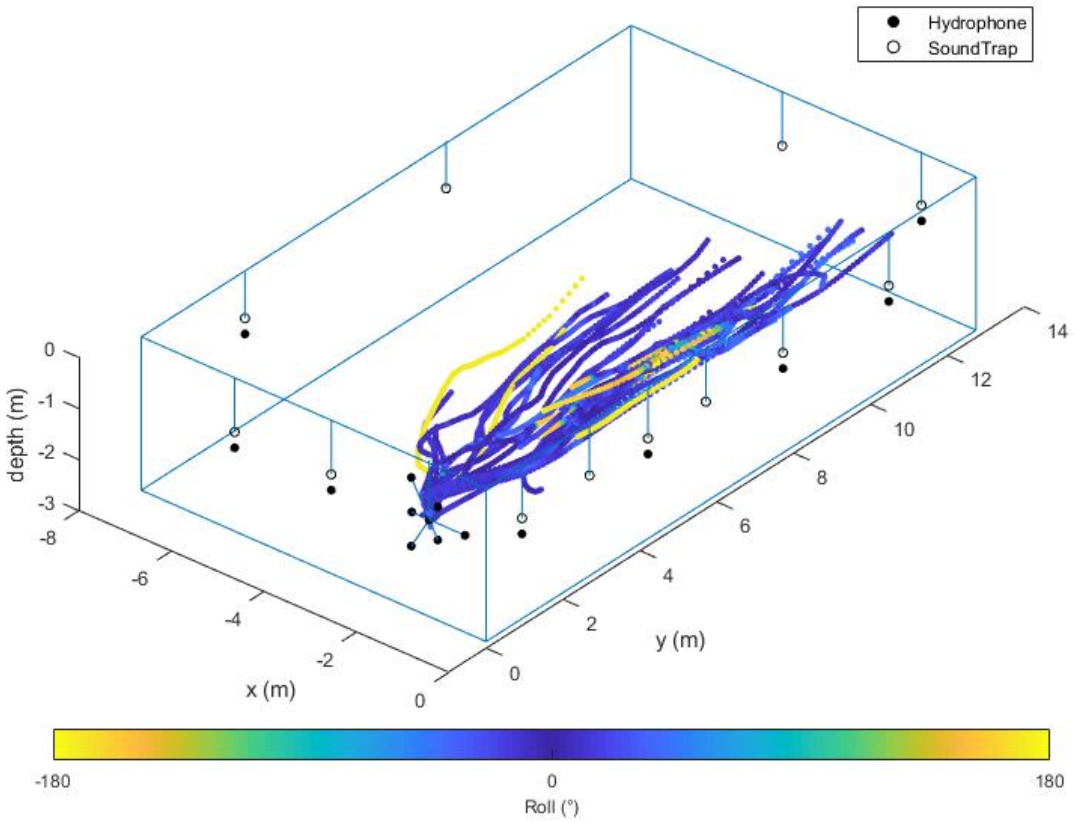

Figure 3 Plot of 40 localised trial tracks of the harbour porpoise, to scale. The harbour porpoise was tasked with swimming towards a target just in front of the star array. The colour of the track shows roll of the porpoise. Most roll values are near 0° because a single roll was a relatively brief event.

Given localised approach tracks (Figure 2) and properly time-aligned and calibrated hydrophones, it was possible to measure the beam profile. This involved a three-stage process for every detected click on the star array: First, clicks between the different hydrophones were matched. Second, the absolute orientation and position of the porpoise was calculated using the star array and DTAG. Finally, the received levels and range to the porpoise at each hydrophone was used to calculate the apparent source level (ASL) with respect to horizontal and vertical angles of the porpoise's own reference frame. The process was repeated for all detected clicks over multiple trials to build up a large number of measurements of the beam profile at different horizontal and vertical angles.

4.2.5.1 Matching Clicks

All detected clicks were imported into MATLAB. For every click received on the central channel of the star array, the same click was located on all other hydrophones around the sea pen. For each hydrophone, a time

window was calculated. The centre of the time window was based on the time for a click to travel from the track position of the porpoise to the hydrophone, assuming a sound speed of 1500 ms^{-1}. For synchronised hydrophones, the time window was then ±1 ms from this time; for SoundTraps, which were not as synchronised as accurately, the time window was ±10 ms. If multiple clicks were detected within the time window, then the first click was selected; the other clicks were likely echoes. For all clicks, the relative received levels (RLs, peak-to-peak and compensating for sensitivity differences) were calculated. RLs were measured by first filtering click waveforms with a 60 kHz high-pass filter to reduce any external noise, and then by up-sampling 3x using polynomial interpolation to a sample rate of 1500 kHz (1728kHz for SoundTraps) to more accurately measure the height of waveform peaks.

4.2.5.2 Calculating Orientation

The acoustic axis vector of the porpoise was then calculated using the star array. An interpolated surface (2nd order polynomial in both *x* and *y*) was constructed based on the received levels of the click and positions of the hydrophones within the star array using MATLAB curve fitting toolbox. The maximum peak of the surface was considered the received location of the central axis of the acoustic beam, and the height of the peak was the relative source level from which all beam loss measurements were calculated. A vector from the on-axis beam location to the position of the harbour porpoise on the approach track was then calculated and roll from the DTAG was extracted. The roll, combined with the acoustic axis vector, created a full set of Euler angles for the porpoise (heading, pitch and roll).

4.2.5.3 Calculating the ASL(φ, $\emptyset$)

A vector to the position of the porpoise on the approach track was then calculated for every hydrophone within the array, which detected the click. The vector was projected onto the rotational frame of reference of the porpoise using the Rodrigues rotation formula (Rodrigues 1840). The horizontal angle of the projected vector with respect to the acoustic axis vector was the horizontal beam angle, φ. The vertical angle from the plane of the acoustic axis to the hydrophone was the vertical beam angle, $\emptyset$.

The beam source level for this horizontal and vertical angle was calculated using the sonar (Eq. 4.1),

$$ASL_{pp}(\varphi, \emptyset) = RL_{pp} + 20\log_{10} R(t) + \alpha R(t) \qquad \text{Eq. 4.1}$$

where $ASL_{pp}(\varphi, \emptyset)$ is the apparent peak to peak source level measured at 1m range with respect to horizontal (φ) and vertical angles ($\emptyset$) (Møhl et al. 2000). $R(t)$ is the range from the hydrophone to the porpoise track at time t, RL_{pp} is the relative peak to peak received level, α is the absorption coefficient (0.04 dBm^{-1} for porpoise frequency; Ainslie & McColm 1998) and spreading loss is assumed to be spherical. The on-axis source level was calculated in the same manner by considering RL_{pp} to be the maxima of the received level surface on the star array. All ASL measurements were then normalised by subtracting the source level.

Every manually annotated click detected on the central star array hydrophone over all trials was analysed in this way. Data were then filtered to attempt to remove spurious results. All clicks which were detected when the acoustic axis was calculated to occur outside of the 40 cm radius from the central hydrophone on the star array were removed, as these often lead to inaccurate on-axis source level calculations. Measurements where the porpoise was within 0.5 m of a respective hydrophone were also removed as the log scale in equation Eq 1. means that small changes in the range at close ranges result in very large errors in ASL. Finally, the curve fitting algorithm occasionally registered a peak in the received level surface of the star array when the true peak of the beam was in fact outside the star array. These spurious results could be removed by setting an upper amplitude limit of 157dB re 1µPa pp to calculated on-axis source level.

4.2.6 Piston Model

The beam profile was compared to a piston model. The piston model was generated by calculating the first order Bessel function that makes up the spatial transfer function of a circular surface diameter 6.5 cm for horizontal angles and 8.3 cm for vertical angles (Koblitz et al. 2012). The Fourier transform (FT) of a porpoise click was multiplied by the Bessel function for a given angle and the peak-to-peak amplitude of the inverse Fourier transform of the result is the value of the piston model at that angle (Beedholm & Møhl 2006). The position of side lobes on the piston model can be sensitive to the exact input waveform. To account for variation within on-axis clicks, a piston model was generated for every porpoise click detected within 40 cm radius of the centre hydrophone of the star array. The linear power outputs of the piston models for all these clicks were averaged then converted to dB amplitude to give a final piston model. The standard deviation in directivity index was 0.15 dB and thus variation had little effect other than suppressing side lobes.

4.2.7 Probability of Detection Simulations

Monte Carlo simulations can be used to calculate the probability of detecting animals on PAM instruments (Küsel et al. 2011, Frasier et al. 2016). There are multiple input parameters to such simulations one of which is the beam profile of animals. To test the implications of using an empirically measured beam profile, as opposed to a piston model, a simple Monte Carlo simulation of a harbour porpoise was constructed using CetSim (https://github.com/macster110/cetacean_sim); an open source Java toolbox for probability of detection simulations.

The simulation placed an animal at a random x,y location with a total range from the hydrophone (array) between 0 and 750 m and maximum depth of 30 m. The simulated porpoises' source level, horizontal and vertical orientation and depth at each location were parametrised from pre-defined distributions/models. A received level was then calculated for a simulated hydrophone placed at the centre of the simulation x,y = (0,0) and thirty meters depth. A simulated click was detected (or not) if the received level was above a peak to peak threshold of 115 dB re 1 µPa pp (a typical value for PAM instruments). If detected, then the location was recorded as successful (coded 1), otherwise, the location was recorded as being unsuccessful (coded 0). 250000 random locations were considered and a probability of detection then calculated by dividing the total number of successful detections by the total number of attempts. Each simulation was bootstrapped 20 times and averaged to increase precision.

Simulations were run for a range of mean source levels and several different beam profiles. Source levels were varied between 160 and 200 dB re 1µPa pp at 1m, around the minimum and maximum source levels reported for wild harbour porpoises (Villadsgaard et al. 2007, Kyhn et al. 2012). Three beam profiles were tested for these source levels; the empirically measured beam, a full -90° to 90° piston model with the back beam set to -40 dB (the lowest value of the piston model), and the -30° to 30° piston model with all other values set to -200 dB beam attenuation (i.e. no side energy). The measured beam profile contained some holes at angles where no clicks were detected (see Figure 4), however, the Monte Carlo simulation requires these to have some value to function properly. Therefore any holes at the edge of the beam profile surface (near ±180° horizontal and ±90° vertical) were assumed to be -45dB (the lowest value of the measured beam profile) and any remaining holes were filled by interpolating the surrounding surface using Sibson interpolation (Park et al. 2006)

Other parameters remained constant across all simulations. The porpoise was assumed to have a normal distribution of vertical diving angles (mean = 0°, STD = 25°) a log normal depth distribution (shape = 2, scale = 3, max depth 30 m) and a standard deviation in source level of 5 dB (see section 5.4.6).

In the above simulations it was assumed that clicks were always correctly classified, however, it is a consequence of narrow beam profiles that off-axis angles clicks become highly distorted (Au et al. 2012b). Automated PAM detectors may perform less efficiently in detecting these clicks and so the assumption that all clicks are equally as detectible if above threshold does not necessarily hold. A 'beam volume' for the measured beam profile was constructed to test the number of distorted clicks that might be detected by a PAM device. The beam volume is the 3D space inside which a recorder with a detector threshold of 115 dB re 1 µPa pp would detect a porpoise click assuming a particular on-axis source level, spherical spreading loss and accounting for absorption. The proportion of the total volume in which distorted clicks would be detected can then be estimated and used as rough proxy for the percentage of distorted clicks a PAM device might detect.

4.3 RESULTS

In total, there were 40 successful trials in which 100,264 clicks were detected over all hydrophones in the array. Of these, 15,154 were collected when the harbour porpoise was on-axis to the star array, i.e. within a 40 cm radius of the central star array hydrophone. During trials in which the porpoise was instructed to roll (no eyecups) only 699 clicks were detected, however, all trials contained some on-axis clicks.

The maximum variation in source levels for on-axis clicks was 16 dB (minimum 156 dB re 1µPa and maximum 172 dB re 1µPa pp) with a mean of 161 dB re 1µPa pp at 1m and a 95% CI of ± 7 dB. This is slightly higher than other studies e.g. (Ladegaard and Madsen 2019), however, is biased by only higher source level clicks being selected for beam calculations as detailed in section 4.2.5.3.

Beam profile measurements consisted of many overlapping measurements at different horizontal and vertical angles. An average beam profile surface was calculated by taking the median of all results within 2° (horizontal) by 2°(vertical) bins. Larger bins (5° x 5°) were used for horizontal angles > ±30° off the acoustic axis because there were fewer results at increasing off axis angles. The median levels were plotted as a surface (Figure 4), demonstrating an intense forward beam and weaker diffuse energy behind the animal.

Note that clicks were not detected for all possible angles, and as such are represented as blank spaces in the surface.

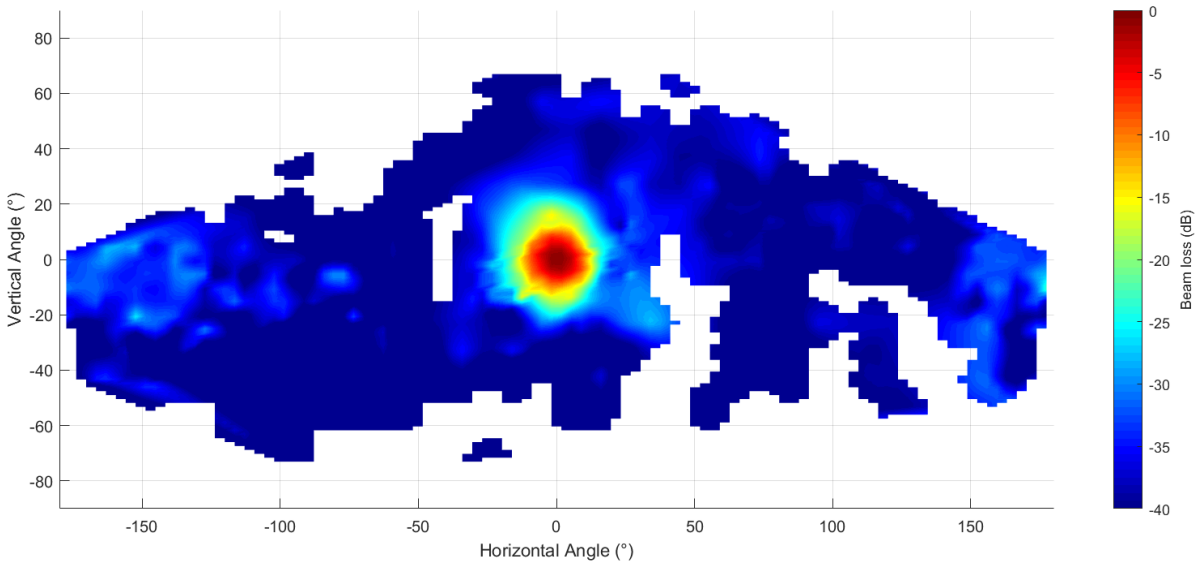

Figure 4. Porpoise beam profile showing full aspect coverage the beam. 2x2° grid bins used between ±30°, and 5x5° grids were used to take the median of the beam profile at all other angles. The intense forward beam is evident on-axis (0°, 0°). This attenuates rapidly towards ±90°. Behind the porpoise there is evidence of a diffuse acoustic energy which is ~30 dB less than the on-axis source level.

The spectra of clicks between ±3° vertical angle were plotted on a waterfall spectrogram with respect to horizontal angle. All clicks between within the vertical angle bounds were grouped into 5° horizontal angle bins. The FFTs of all clicks were calculated and plotted on a surface in angle order for each 5° bin. The 5° bin surfaces were then stretched or compressed to a uniform width and plotted together to create a waterfall angular spectrogram (Figure 5). This shows that the narrowband click spectrum breaks down at around 20° off the peak of the beam and is replaced by spectra with less predictable and more broadband components. It should be noted that the sensitivity of the hydrophones begins to drop off at around 150kHz and that it is likely that many of the broader band components outside 100 to 150kHz in Figure 4B are due to the much lower signal to noise ratio of clicks at larger off axis angles. At off-axis angles (>20°) some of the angle bins also contain very few clicks, which likely causes some of the variation in standard deviation and mean measurements.

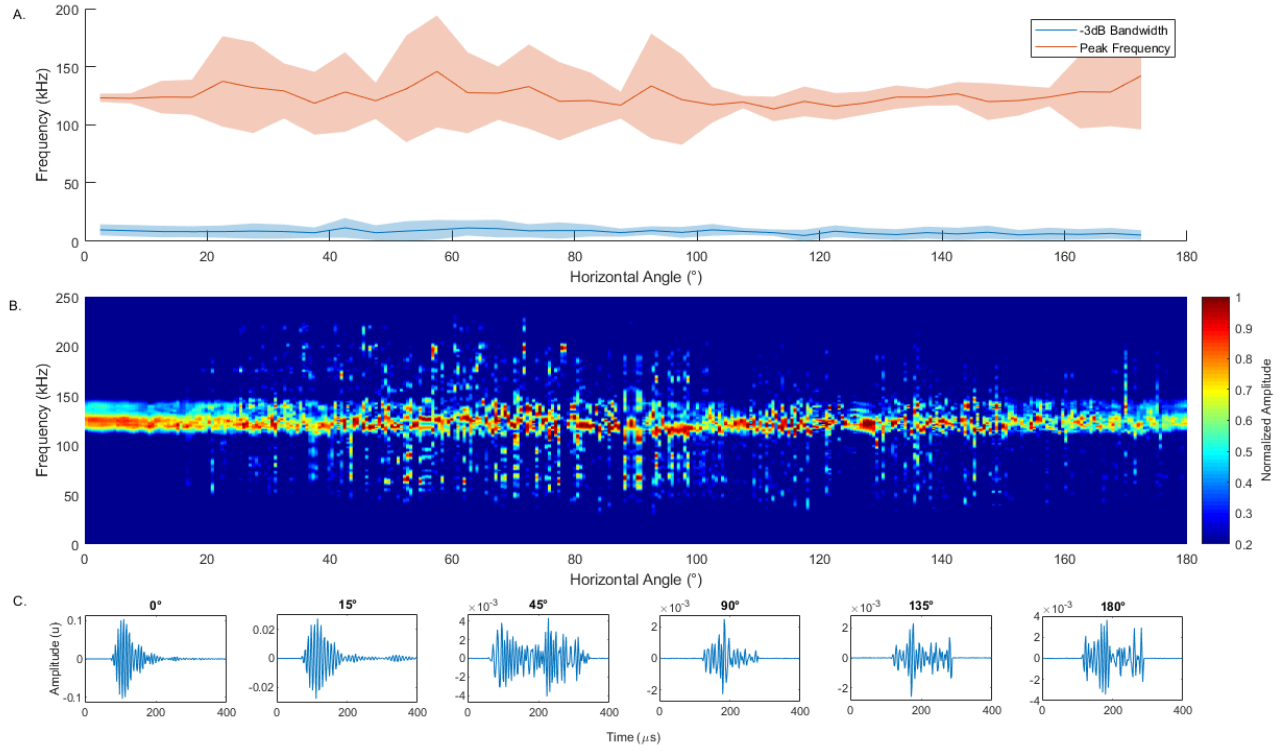

Figure 5. Frequency metrics, a waterfall spectrogram of clicks and examples of click waveforms with respect to horizontal axis. Clicks are split into 5° horizontal bins which contain all detected clicks within ±3° vertical angle sorted in order of horizontal angle. Plot A shows the mean peak frequency and -3 dB bandwidth, with standard deviation for each bin (Note that data points are plotted as the center of each bin). and plot B is a waterfall spectrogram of all clicks within each bin. The graphs show the break down in spectra beyond ~20° with peak frequency significantly more variable and with additional energy in higher and lower frequency components. It is likely that a portion of this distortion comes from the much lower signal to noise ratio of off-axis clicks, however, at off-axis angles and within the 100 to 150 kHz frequency band, there is clear structure to the spectra of sequential clicks that are not explained simply by lower SNR. Note that the frequency axis limits on the waterfall spectrogram are between 50 and 200 kHz. C shows an example of the waveforms of clicks extracted by PAMGuard at different angles. Note that some of these are zero padded to show a consistent time scale.

To assess how closely the piston model predicts off-axis beam attenuation, the empirically measured beam and a piston model were compared in two and three dimensions in Figure 6 and Figure 7. Figure 6 shows the raw beam for ±3° slices of the horizontal and vertical raw beam measurements plotted against a piston model with horizontal and vertical effective aperture diameters of 6.5 cm and 8.3 cm respectively (Koblitz et al. 2012).

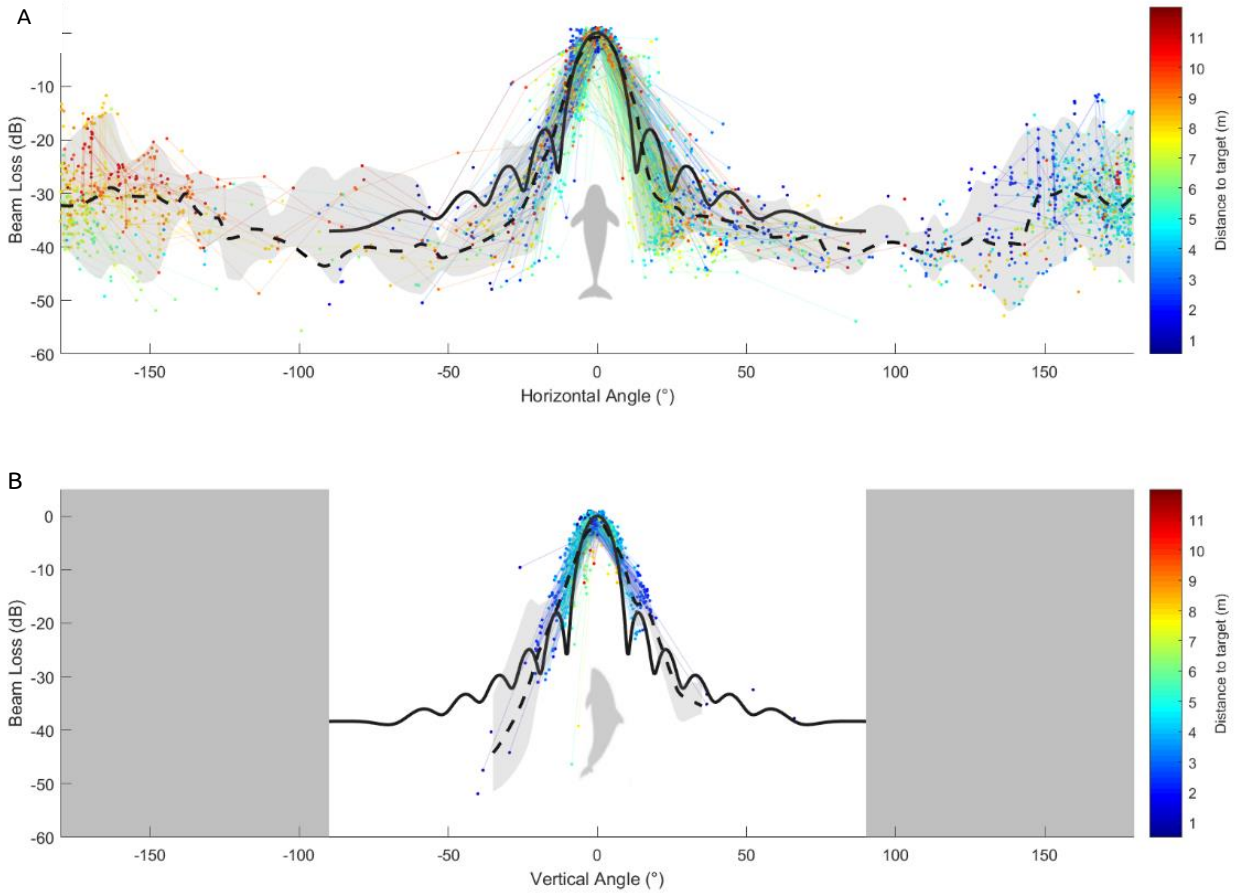

Figure 6. Raw beam data compared to the -90° to 90° piston model of an on-axis porpoise click for horizontal and vertical slices of the beam profile. Plot A shows all horizontal angles which have vertical angles between -3° to 3°. Plot B shows all vertical angles which have horizontal angles between of -3° and 3°. Scatter points show back-calculated beam source levels with respect to angle. The solid black line shows the average piston model results discussed in section 4.2.6. The dashed black line shows the average beam measurement with grey area indicating the 95% confidence interval. The thin coloured lines group single clicks detected on multiple hydrophones together. Scatter points and lines are coloured by the distance to the target.

Figure 7 shows the measured beam and piston model plotted on a surface plot of expected received level assuming spherical spreading laws with an absorption coefficient of 0.04 dBm^{-1} (Ainslie and Mccolm 1998) and an on-axis source level of 191 dB re 1 µPa pp at 1m (an average recorded in a study of wild porpoises (Villadsgaard et al. 2007)). For angles greater than 90°, the piston model assumed beam attenuation was constant and equal to the lowest value predicted at ±90°, in this case -40 dB. The plot shows the expected received level if a device were placed at (*x,y)* assuming a porpoise is facing in the +*y* direction at (0,0). This shows the typical acoustic space a wild animal might occupy in PAM studies.

A	B

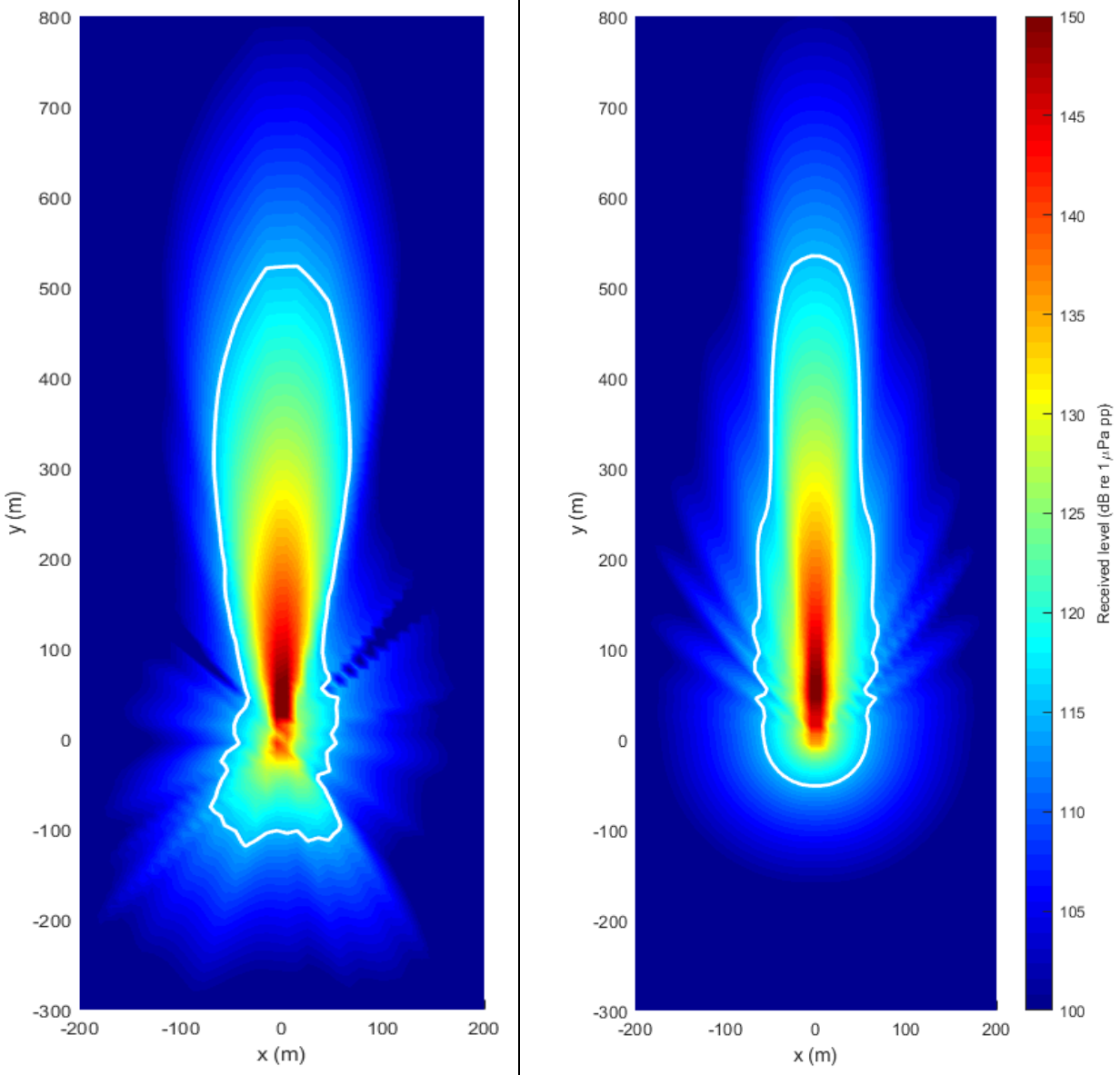

Figure 7. Beam profile detectability for an echolocation click with a SL of 191 dB re 1 µPa pp at 1m. Each point on plot is coloured by the expected received level if a porpoise were facing in the y direction and located at (0,0). Plot A shows the measured beam profile for a harbour porpoise and plot B shows piston model results, assuming a -40 dB uniform back beam (the lowest value of the piston model) using effective aperture diameter measurements. The lower colour limit of 100dB dB re 1 µPa pp was applied as this is below the usual limit (~115dB re 1 µPa) for automated detection of clicks in PAM studies; thus darker blue areas in which a PAM device is less likely to detect a click The white line in both plots indicates a 115dB received level which is the general received amplitude limit for automated detection of clicks in PAM studies

4.3.1 Implications for PAM

There are clear differences between the measured and piston model beam (Figure 6, 7), In the context of PAM, it is important to understand whether the assumption of a piston model will make any appreciable difference to density estimation. Figure 8 shows the results of three Monte Carlo simulations using the beam profiles in Figure 7 and an additional piston model beam profile which assumes a beam attenuation of -200 dB at all angles past ±30°, i.e. has energy only in the forward part of the beam. The probability ($\hat{P}$) is the probability of detection multiplied by a triangular step function to account for more animals as range increases (because the monitored area is larger). Hence $\hat{P}$ is probability of *encountering* a click from an animal at a given range, usually used when analysing data from a stationary or drifting PAM devices. The area under the graph therefore directly divides the density estimation equation (Marques et al. 2013). The results in Figure 7 show that, for a source level of 191 dB re 1µPa pp at 1m, the full -90° to 90° piston model makes little different to $\hat{P}$ and -30° to 30° piston model with no energy at other angles underestimates $\hat{P}$ by around half.

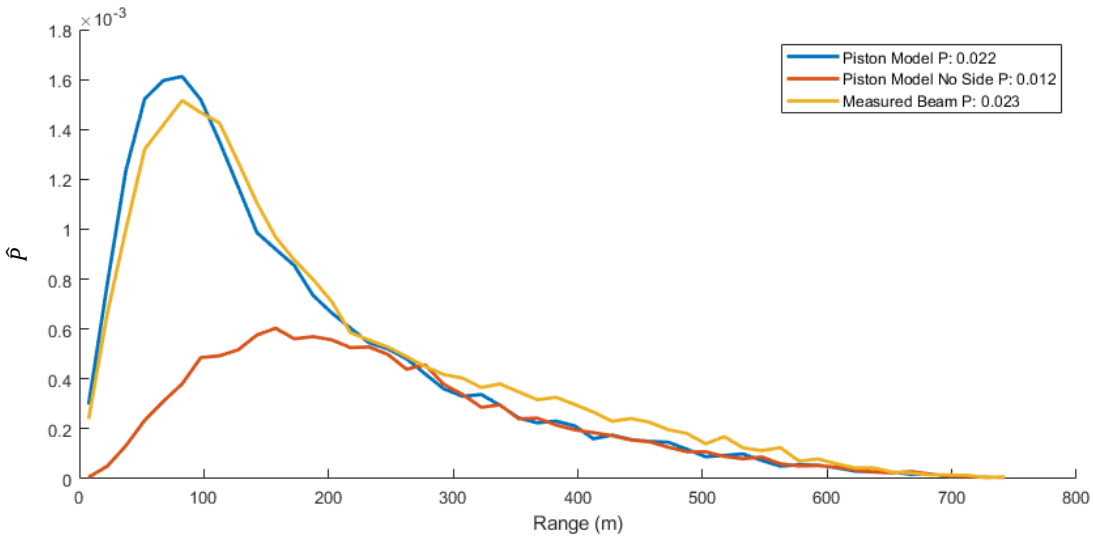

Figure 8. An example of the simulated probability of detection ($\hat{P}$) with range for different beam profiles assuming a mean source level of 191dB re 1µPa at 1m with a standard deviation of 5dB. This is the probability that an animal will be detected at a specified range assuming a homogenous distribution of animals around the sensor. The integral of these is the input into the density estimation equation for fixed sensors.

Figure 9 shows how the probability of encountering a click scales with different source levels and beam profiles. The ratio of the probability of encounter is not constant between beam profiles for different

source levels, with the piston model with side energy underestimating $\hat{P}$ by almost 40% at low source levels, but only by around 5% at the highest source levels. The piston model with no side energy consistently underestimates $\hat{P}$.

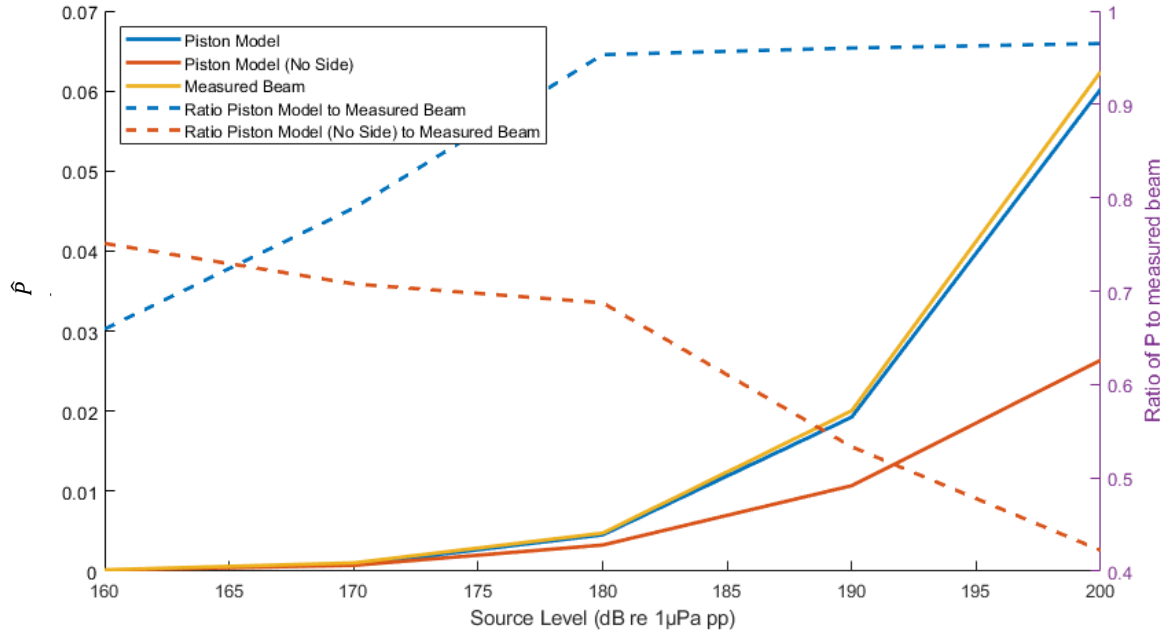

Figure 9. Probability of detection ($\hat{P}$) modelled for different beam profiles and source levels. As expected, the probability of detection increases with increasing source level for all beam profiles (left axis). The dotted lines show the ratio of the probability of detection of the piston model beam compared to the measured beam (right axis). This shows that the ratio of the beam profiles does not remain constant, i.e. at greater source levels, the piston model probability of detection is closer to the measured beam profile than at lower source levels if side energy assumed. However, if no side energy is assumed, then the piston model is closer to the measured beam at very low source levels.

In the above simulations it assumed that, as long a click is above a certain amplitude threshold, it is detected. Figure 5 indicates a breakdown in the stereotypical spectra of NBHF clicks after around 20°. To test the potential consequence of this for PAM, beam volumes for source levels between 160 and 200 dB re 1µPa pp at 1m were calculated. Figure 10 shows that, at low source levels, the percentage of distorted clicks that would be detected by a PAM receiver is very low <5%, however, at higher source levels the number of distorted clicks is much larger, reaching ~50% for 191 dB re 1µPa pp at 1m source levels. Thus, depending the behavioural state of a harbour porpoise, between 5% and 65% of click detections on PAM instruments would likely contain significant spectral distortion compared to on-axis clicks.

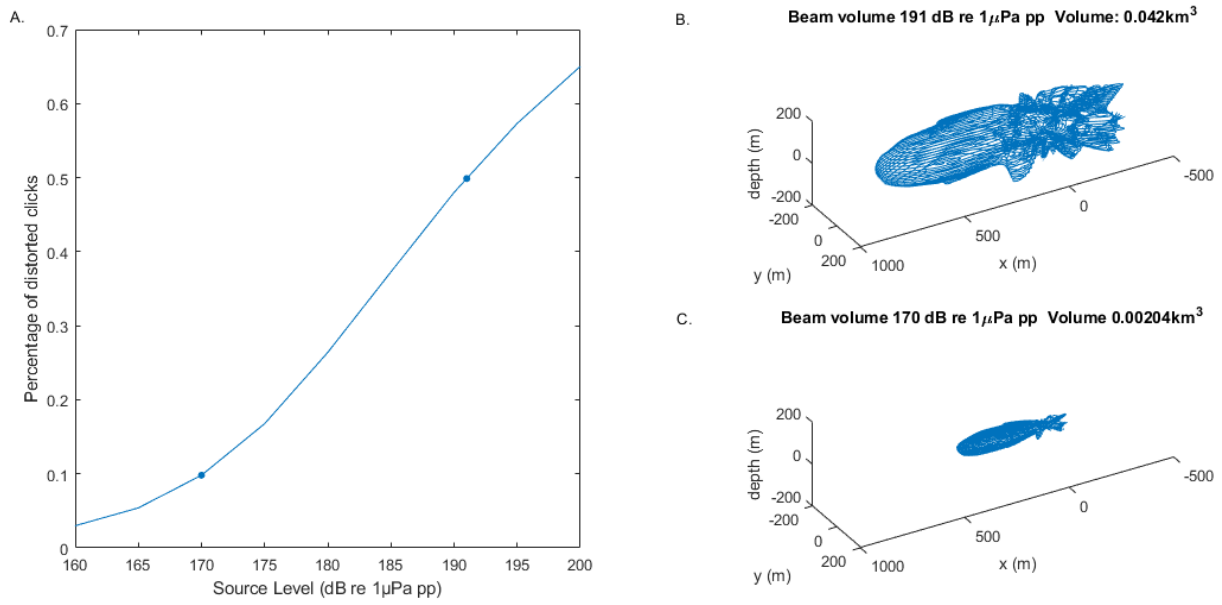

Figure 10. Plots showing the percentage of distorted clicks likely to be received by a PAM device and examples of beam volumes at differing source levels. Plot A shows the proportion of distorted clicks as a function of source level. The two points indicate the source levels of the example beam volumes shown in plots B and C, 190 and 160 dB re 1µPa pp at 1m respectively.

4.4 DISCUSSION

This chapter confirms the tightly focused forward beam profile (Figures 2, 5, 6) of a harbour porpoise can be successfully modelled with a flat piston for angles between ±30° (Au 2006, Koblitz et al. 2012, Wisniewska et al. 2015). However, at larger off-axis angles, the piston model underestimates the beam attenuation and creates a series of side lobes (Figures 5 and 6B) which were not evident in the measured beam profile. This directionality is likely formed through natural selection of harbour porpoise biosonars to i) increase the on axis source level for the same power, ii) reduce the amount of unwanted echoes in the form of clutter, iii) provide a spatial filter to aide localization, discrimination and tracking of targets of interest, and iv) to direct sound of the outgoing click away from the ears to minimize forward masking of faint echoes returning milliseconds after click emission (Schrøder et al. 2017). Thus, from an evolutionary perspective, it is perhaps not surprising that harbour porpoise biosonar has evolved both to minimise side lobes and to outperform the piston model in beam attenuation with angle. Side lobes are created from edge effects of the modelled piston aperture. However, there is no morphological structure which exactly mirrors the theoretical piston aperture in a porpoise. Thus, a more realistic equivalent aperture may be something which is not entirely radially symmetric and does not have a hard edge, minimising side lobes. There was also a possibility that

porpoises might be using their melon to change the effective piston aperture, which, when averaged over many clicks, would reduce side lobes. However, averaging out a piston model using the horizontal 5.5 to 7.4 cm (mean 6.5 cm) apertures, as reported by Koblitz et al. (2012), still leaves two small side lobes at ±17°. Even if clicks are filtered to almost pure tones (between 125 and 130 kHz), which should increase the size of any side lobes, no side lobes are evident in the data (see supplementary materials 4.9.2). This suggests that the piston model, at anything other than on-axis angles, does not fully account for the morphological complexity of toothed whales. Madsen et al. (2010) noted that clicks produced by the phonic lips in the porpoise are initially quite broadband before they are filtered by waveguide coupling with the melon to form the NBHF click. This notion is supported here, where the typical narrowband spectra of a NBHF click breaks down at about 20° (Figure 4), after which clicks are characterised by broader and less predictable spectra.

When measuring the ASL further off axis, it appears that porpoises produce a diffuse back beam at 180° off-axis, some 30 dB down from the SL. Madsen et al. (2010) have shown that harbour porpoises use their right pair phonic lips, which, in concert with air sacs and skull, collimate most of the produced sound energy through the melon to form a narrow forward beam. It is likely that some acoustic energy, especially when directed backwards, escapes this process, producing the back-end beam. Any baffled dipole source sound production system leads intrinsically to some diffuse waste acoustic energy, also demonstrated by the calibration experiments of the RESON TC2130 transducer (see supplementary material) that interestingly renders an ASL at 180° that is also about 30 dB down from the on-axis SL. Thus, the diffuse and weak back-end beam of a harbour porpoise may simply be the remnants of a natural selection process towards a directional dipole source to work efficiently in a biosonar system for navigation or feeding. Whether it also serves a purpose of, for example, facilitating eavesdropping by calves to better trail their mothers during biosonar-based foraging dives may be plausible (Hansen et al. 2008), but at this stage entirely speculative function for toothed whales at large. A similar weak back-end beam has also been reported in sperm whales (Zimmer et al., 2005) with a very different bauplan of their hypertrophied sound producing nose.

The difference between modelled and empirically measured beam profiles can significantly influence the probability of encountering clicks if side energy (>30°) is not taken into account. In Figure 7, the measured and full -90° to 90° piston beam model both have a significantly higher probability of encountering a click at shorter ranges compared to the piston model without side energy. There are two interacting factors

occurring here; the probability of *detecting* a click is increased slightly at shorter ranges because of the diffuse energy at the back of the measured and full piston beam profile. As the range increases the number of animals within each range bin also increases and thus small increases in the probability of *detecting* a click result in disproportionally larger increase in *encountering* a click. However, as range continues to increase, eventually any side and back beam energy becomes undetectable – at this stage the detectible energy is very similar for all beam profiles and thus at larger ranges $\hat{P}$ is almost identical. The point at which the back energy is no longer detected is therefore important in determining how different the overall value of $\hat{P}$ is. Thus, as is shown in Figure 7, at low source levels, the back energy quickly falls below threshold and so the ratio in $\hat{P}$ between the different beam profiles is more similar. At high source levels the point at which back energy is detectible is much larger and thus the ratio in $\hat{P}$ increases.

As click encounter rate is a direct divisor of the density estimation equation for static PAM devices, these differences in $\hat{P}$ directly translate to estimates of animal density. Compared to the measured beam profile, the piston model with side energy under-estimated the probability of encounter by between 5% to 30%, depending on the source level distribution of the animals in question. Assuming a piston model with no side energy and only a forward-facing beam resulted in an estimate of $\hat{P}$ which was consistently over 30% and up to 60% less than that of the measured beam profile. Thus, assuming a situation in which harbour porpoises are clicking at a source level of 191dB re 1µPa pp at 1m (the mean level recorded in the wild (Villadsgaard et al. 2007)), the piston model with no side energy would have more than doubled the density estimate but a piston model assuming both side and back energy would be roughly correct. Although the exact error in the modelling of the probability detection will be dependent on the survey type and combination of the many possible input model parameters used in a Monte Carlo simulation, this indicates that beam profiles are a potential significant source of error in these models. Thus, if using Monte Carlo methods for density estimation is required, direct measurements of the full 4π radiation pattern is preferential wherever possible; if these are not available then an accurate piston model assuming both side and back energy should be used.

4.5 CONCLUSION

Harbour porpoises produce an intense forward beam and much lower level diffuse acoustic energy to their rear. The beam profile of a porpoise can be modelled successfully with a piston model at ±30° around the

beam axis, but at off-axis angles of more than ±30°, the measured beam shows greater attenuation than the piston model predicts, and no distinct side lobes can be observed. Thus, porpoises have a slightly narrower acoustic field of view than predicted by the piston model. A weak and diffuse back beam with ASLs some 30 dB below SL, which is not predicted from the piston model, is also present. This chapter demonstrates that there can be a substantially higher probability of detection when using the empirically measured beam profile with a weak back-end beam, as opposed to the standard piston model, but this is dependent on source level and whether side and back energy in the piston model is assumed. As such, this study highlights the need for synergy between detailed biosonar studies, functional morphology and the continued development of PAM methodologies, especially density estimation. PAM is likely to form an increasing part of management strategies and conservation of cetacean species in the future and, as demonstrated by this study, an understanding of species biosonar, bioacoustics and acoustic behaviour are vital in interpreting and making best use of the data.

4.6 ACKNOWLEDGEMENTS

Thanks to the animal trainers J. Kristensen and F. Johansson for helping run the trials at Fjord & Bælt. Thanks to M. Wahlberg and J. Tougaard for lending hydrophones and SoundTraps, and to M. Johnson for access to a DTAG-4. Thanks to K. Beedholm, M. Wahlberg and J. Tougaard, M. Ladegaard and S. Northridge for helpful discussions. Equipment and training time was funded by a FNU grant to PTM.

4.7 ETHICS

The animals are maintained by Fjord&Bælt, Kerteminde, Denmark, under permit nos SN 343/FY-0014 and 1996-3446-0021 from the Danish Forest and Nature Agency, Danish Ministry of Environment.

4.8 REFERENCES

Ainslie, M. A., and J. G. Mccolm. 1998. A simplified formula for viscous and chemical absorption in sea water. The Journal of the Acoustical Society of America 103:1671.

Au, W. W. L. 1993. The Sonar of Dolphins. Page Acoustics Australia. Springer New York, New York, NY.

Au, W. W. L. 2006. Acoustic radiation from the head of echolocating harbor porpoises (Phocoena phocoena). Journal of Experimental Biology 209:2726–2733.

Au, W. W. L., B. Branstetter, P. W. Moore, and J. J. Finneran. 2012a. The biosonar field around an Atlantic bottlenose dolphin (Tursiops truncatus). The Journal of the Acoustical Society of America 131:569–576.

Au, W. W. L., B. Branstetter, P. W. Moore, and J. J. Finneran. 2012b. Dolphin biosonar signals measured at extreme off-axis angles: Insights to sound propagation in the head. The Journal of the Acoustical Society of America 132:1199–1206.

Au, W. W. L., R. W. Floyd, and J. E. Haun. 1978. Propagation of Atlantic bottlenose dolphin echolocation signals. The Journal of the Acoustical Society of America 64:411–422.

Au, W. W. L., R. A. Kastelein, T. Rippe, and N. M. Schooneman. 1999. Transmission beam pattern and echolocation signals of a harbor porpoise (Phocoena phocoena). The Journal of the Acoustical Society of America 106:3699–3705.

Beedholm, K., and B. Møhl. 2006. Directionality of sperm whale sonar clicks and its relation to piston radiation theory. The Journal of the Acoustical Society of America 119:EL14.

Branstetter, B. K., P. W. Moore, J. J. Finneran, M. N. Tormey, and H. Aihara. 2012. Directional properties of bottlenose dolphin (Tursiops truncatus) clicks, burst-pulse, and whistle sounds. The Journal of the Acoustical Society of America 131:1613–1621.

Carlén, I., L. Thomas, J. Carlström, M. Amundin, J. Teilmann, N. Tregenza, J. Tougaard, J. C. Koblitz, S. Sveegaard, D. Wennerberg, O. Loisa, M. Dähne, K. Brundiers, M. Kosecka, L. A. Kyhn, C. T. Ljungqvist, I. Pawliczka, R. Koza, B. Arciszewski, A. Galatius, M. Jabbusch, J. Laaksonlaita, J. Niemi, S. Lyytinen, A. Gallus, H. Benke, P. Blankett, K. E. Skóra, and A. Acevedo-Gutiérrez. 2018. Basin-scale distribution of harbour porpoises in the Baltic Sea provides basis for effective conservation actions. Biological Conservation 226:42–53.

Deruiter, S. L., A. Bahr, M.-A. Blanchet, S. F. Hansen, J. H. Kristensen, P. T. Madsen, P. L. Tyack, and M. Wahlberg. 2009. Acoustic behaviour of echolocating porpoises during prey capture. The Journal of experimental biology 212:3100–3107.

Finneran, J. J., B. K. Branstetter, D. S. Houser, P. W. Moore, J. Mulsow, C. Martin, and S. Perisho. 2014. High-resolution measurement of a bottlenose dolphin's (Tursiops truncatus) biosonar transmission beam pattern in the horizontal plane. The Journal of the Acoustical Society of America 136:2025–2038.

Frasier, K. E., S. M. Wiggins, D. Harris, T. A. Marques, L. Thomas, and J. A. Hildebrand. 2016. Delphinid echolocation click detection probability on near-seafloor sensors. The Journal of the Acoustical Society of America 140:1918–1930.

Gillespie, D., J. Gordon, R. Mchugh, D. Mclaren, D. Mellinger, P. Redmond, A. Thode, P. Trinder, and X. Y. Deng. 2008. PAMGUARD: Semiautomated, open source software for real-time acoustic detection and localisation of cetaceans. Proceedings of the Institute of Acoustics 30:2547.

Hansen, M., M. Wahlberg, and P. T. Madsen. 2008. Low-frequency components in harbor porpoise (Phocoena phocoena) clicks: communication signal, by-products, or artifacts? The Journal of the Acoustical Society of America 124:4059–4068.

Jensen, F. H., M. Johnson, M. Ladegaard, D. M. Wisniewska, and P. T. Madsen. 2018. Narrow Acoustic Field of View Drives Frequency Scaling in Toothed Whale Biosonar. Current Biology 28:3878-3885.e3.

Jensen, F. H., M. Wahlberg, K. Beedholm, M. Johnson, N. A. de Soto, and P. T. Madsen. 2015. Single-click beam patterns suggest dynamic changes to the field of view of echolocating Atlantic spotted dolphins (Stenella frontalis) in the wild. Journal of Experimental Biology 218:1314–1324.

Johnson, M. P., and P. L. Tyack. 2003. A digital acoustic recording tag for measuring the response of wild marine mammals to sound. IEEE Journal of Oceanic Engineering 28:3–12.

Koblitz, J. C., P. Stilz, M. H. Rasmussen, and K. L. Laidre. 2016. Highly Directional Sonar Beam of Narwhals (Monodon monoceros) Measured with a Vertical 16 Hydrophone Array. PLOS ONE 11:e0162069.

Koblitz, J. C., M. Wahlberg, P. Stilz, P. T. Madsen, K. Beedholm, and H.-U. Schnitzler. 2012. Asymmetry and dynamics of a narrow sonar beam in an echolocating harbor porpoise. The Journal of the Acoustical Society of America 131:2315.

Küsel, E. T., D. K. Mellinger, L. Thomas, T. A. Marques, D. Moretti, and J. Ward. 2011. Cetacean population density estimation from single fixed sensors using passive acoustics. The Journal of the Acoustical Society of America 129:3610–3622.

Kyhn, L. A., J. Tougaard, K. Beedholm, F. H. Jensen, E. Ashe, R. Williams, and P. T. Madsen. 2013. Clicking in a Killer Whale Habitat: Narrow-Band, High-Frequency Biosonar Clicks of Harbour Porpoise (Phocoena phocoena) and Dall's Porpoise (Phocoenoides dalli). PLoS ONE 8:e63763.

Kyhn, L. A., J. Tougaard, L. Thomas, L. R. Duve, J. Stenback, M. Amundin, G. Desportes, and J. Teilmann. 2012. From echolocation clicks to animal density—Acoustic sampling of harbor porpoises with static dataloggers. The Journal of the Acoustical Society of America 131:550.

Ladegaard, M., F. H. Jensen, K. Beedholm, V. M. F. Da Silva, and P. T. Madsen. 2017. Amazon river dolphins (Inia geoffrensis) modify biosonar output level and directivity during prey interception in the wild. Journal of Experimental Biology 220:2654–2665.

Ladegaard, M., F. H. Jensen, M. de Freitas, V. M. Ferreira da Silva, and P. T. Madsen. 2015. Amazon river dolphins (Inia geoffrensis) use a high-frequency short-range biosonar. Journal of Experimental Biology 218:3091–3101.

Ladegaard, M., and P. T. Madsen. 2019. Context-dependent biosonar adjustments during active target approaches in echolocating harbour porpoises. The Journal of Experimental Biology 222:jeb206169.

Madsen, P. T., and A. Surlykke. 2013. Functional Convergence in Bat and Toothed Whale Biosonars. Physiology 28:276–283.

Madsen, P. T., D. Wisniewska, and K. Beedholm. 2010. Single source sound production and dynamic beam formation in echolocating harbour porpoises (Phocoena phocoena). Journal of Experimental Biology

213:3105–3110.

Malinka, C. E., A. E. Hay, and R. Cheel. 2015. Towards acoustic monitoring of marine mammals at a tidal energy site: Grand Passage, NS, Canada. Proceedings of the 11th European Wave and Tidal Energy Conference:1–10.

Marques, T. A., L. Thomas, S. W. Martin, D. K. Mellinger, J. A. Ward, D. J. Moretti, D. Harris, and P. L. Tyack. 2013. Estimating animal population density using passive acoustics. Biological reviews of the Cambridge Philosophical Society 88:287–309.

Møhl, B., M. Wahlberg, P. T. Madsen, L. a Miller, and a Surlykke. 2000. Sperm whale clicks: directionality and source level revisited. The Journal of the Acoustical Society of America 107:638–648.

Nelder, J. A., and R. Mead. 1965. A Simplex Method for Function Minimization. The Computer Journal 7:308–313.

Park, S. W., L. Linsen, O. Kreylos, J. D. Owens, and B. Hamann. 2006. Discrete Sibson interpolation. IEEE Transactions on Visualization and Computer Graphics 12:243–253.

Press, W. H., and S. A. Teukolsky. 1990. Savitzky-Golay Smoothing Filters. Computers in Physics 4:669.

Rodrigues, O. 1840. es lois géometriques qui regissent les déplacements d' un systéme solide dans l' espace, et de la variation des coordonnées provenant de ces déplacement considérées indépendant des causes qui peuvent les produire. J. Math. Pures Appl. 5:380–440.

Schrøder, A. E. M., K. Beedholm, and P. T. Madsen. 2017. Time-varying auditory gain control in response to double-pulse stimuli in harbour porpoises is not mediated by a stapedial reflex. Biology Open 6:525–529.

Smith, A. B., L. N. Kloepper, W.-C. Yang, W.-H. Huang, I.-F. Jen, B. P. Rideout, and P. E. Nachtigall. 2016. Transmission beam characteristics of a Risso's dolphin (Grampus griseus). The Journal of the Acoustical Society of America 139:53–62.

Stevenson, B. C. 2016. Methods in spatially explicit capture-recapture. University of St Andrews.

Stevenson, B. C., D. L. Borchers, R. Altwegg, R. J. Swift, D. M. Gillespie, and G. J. Measey. 2015. A general framework for animal density estimation from acoustic detections across a fixed microphone array. Methods in Ecology and Evolution 6:38–48.

Strother, G. K., and M. Mogus. 1970. Acoustical Beam Patterns for Bats: Some Theoretical Considerations. The Journal of the Acoustical Society of America 48:1430–1432.

Verfuß, U. K., L. A. Miller, P. K. D. Pilz, and H. U. Schnitzler. 2009. Echolocation by two foraging harbour porpoises (Phocoena phocoena). Journal of Experimental Biology 212:823–834.

Villadsgaard, A., M. Wahlberg, and J. Tougaard. 2007. Echolocation signals of wild harbour porpoises,

Phocoena phocoena. Journal of Experimental Biology 210:56–64.

Wisniewska, D. M., J. M. Ratcliffe, K. Beedholm, C. B. Christensen, M. Johnson, J. C. Koblitz, M. Wahlberg, and P. T. Madsen. 2015. Range-dependent flexibility in the acoustic field of view of echolocating porpoises (Phocoena phocoena). eLife 4:1–16.

Zimmer, W. M. X., J. Harwood, P. L. Tyack, M. P. Johnson, and P. T. Madsen. 2008. Passive acoustic detection of deep-diving beaked whales. The Journal of the Acoustical Society of America 124:2823–2832.

Zimmer, W. M. X., P. L. Tyack, M. P. Johnson, and P. T. Madsen. 2005. Three-dimensional beam pattern of regular sperm whale clicks confirms bent-horn hypothesis. The Journal of the Acoustical Society of America 117:1473–1485.

4.9 SUPPLEMENTARY MATERIALS

4.9.1 Measuring the beam profile of a TC2130 direction Transducer

4.9.1.1 Introduction

A TC2130 is a directional transducer with a forward beam which can be approximated as a piston model with a 3cm radius circular aperture (Jensen et al. 2015). The transducer was used as a "fake" porpoise with a known beam shape to validate the accuracy of the pool hydrophone setup in measuring a harbour porpoises' 4π beam profile.

4.9.1.2 Method

Two experiments were performed. The transducer was measured in a calibration tank to accurately determine it's 360° beam profile and then measured using the same experimental setup as that used to measure the harbour porpoises beam.

4.9.1.3 Calibration Tank Experiment

The TC230 was mounted on an aluminium frame and attached to a 3D printed turntable which allowed it to be accurately rotated in 5° steps from 0° to 360° as shown in Figure 11S. Two full rotations were performed in a 3m diameter oak lined calibration tank. In the second experiment the transducer was rotated laterally 120° to check whether the beam profile was symmetric around the acoustic axis.

For each angle, a series of narrow-band high frequency (NBHF) clicks at 130 kHz with an inter click interval of 100ms were generated by a waveform generator (model 33220A, Agilent Technologies, CA, USA) and emitted through the transducer for 10 seconds. Clicks from the transducer were recorded on a compact

vertical array of six RESON hydrophones (10cm spacing between each) at ~1m distance. Data was amplified using a custom-built amplifier box with pre-whitening (1 kHz 1-pole high pass) and anti-aliasing (200 kHz 4-pole low pass) filters (both Butterworth). This was digitized with 16-bit resolution using an analogue to digital converter (NI 6356 USB soundcards, National Instruments, USA), providing up to 8 synchronised channels with a 4 V peak-to-peak range and 500 kHz sample rate. 6 channels were used to record data from the hydrophones and the 7th channel was directly connected to a second output channel on the agilent, which mirrored the output channel to the transducer.

Data from the NI card was recorded as 7 channel .wav files using PAMGuard (www.pamguard.org). Clicks were detected using the PAMGuard click detector (version 2.00.13). These were manually annotated by an analyst and imported into MATLAB using the PAMGuard MATLAB library. The calibration click from the agilent was used to determine the direct path click received on the hydrophones. The peak to peak amplitude and energy flux density of all detected direct path clicks was calculated and plotted against the angle of the transducer.

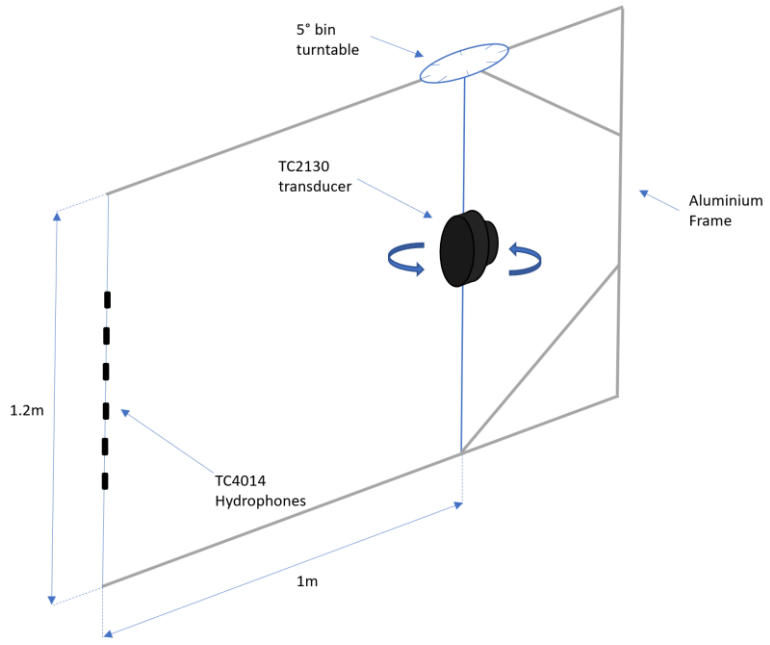

Figure 11S, Diagram of the calibration tank experiment. The frame was placed in the calibration tank and 10 second bursts of 130kHz clicks with an inter click interval of 100ms output through the TC2103 transducer. These were recorded on six hydrophones mounted 1 meter from the transducer. The transducer was rotated by 5 degrees and the experiment repeated. Rotation was continued in 5° bins for until the full 360° beam profile had been measured. The transducer was then rotated 120° about it's acoustic axis and the entire experiment performed again.

4.9.1.4 Harbour Porpoise Experiment Setup Test

The transducer was mounted on a broomstick and manually moved towards the star-array along the approximate swim path of the real porpoise whilst emitting 130kHz porpoise-like clicks. The output from the agilent was the same as in the calibration pool experiment. The porpoise was not in the research pen while these trials were conducted. The data from this were analysed in the same manner as clicks from the real porpoise and results compared to the calibration tank measurements.

4.9.1.5 Results

Three measurements were calculated for each click, the peak to peak amplitude, the root mean square (RMS) amplitude and the energy flux density. For each angle, amplitudes were averaged and the standard deviation considered to be the error. The factory calibration using a continuous 150kHz was extracted from the TC2130 datasheet. The average beam profile for both calibration experiments and factory calibration is shown in Figure 12S.

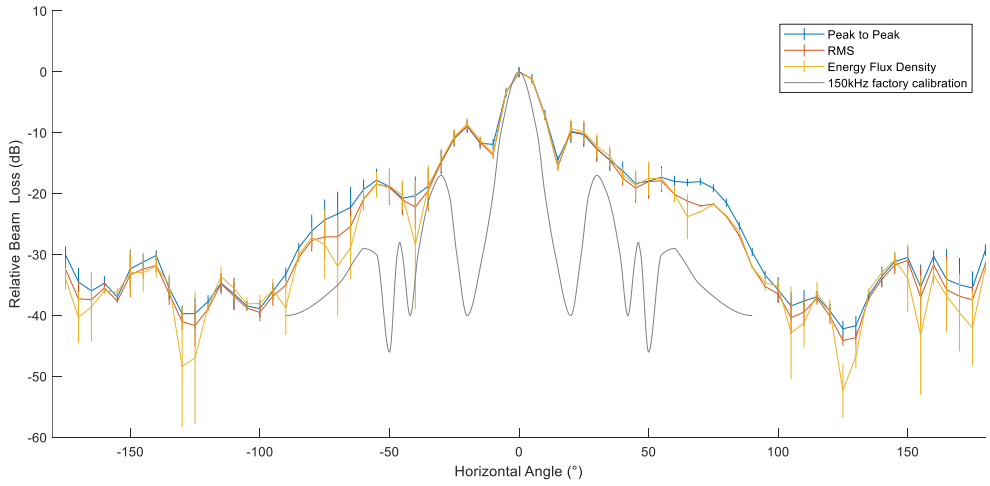

Figure 12S. Measurements of the transducer and error bars. Peak to peak, RMS and energy flux density were calculated for each detected clicks. These values were averaged for each angle and the standard deviation plotted as error bars.

The two calibration pool experiments were plotted separately in Figure 13. This shows that the transducer is not symmetric around it's acoustic axis i.e. there is some distortion of the beam laterally.

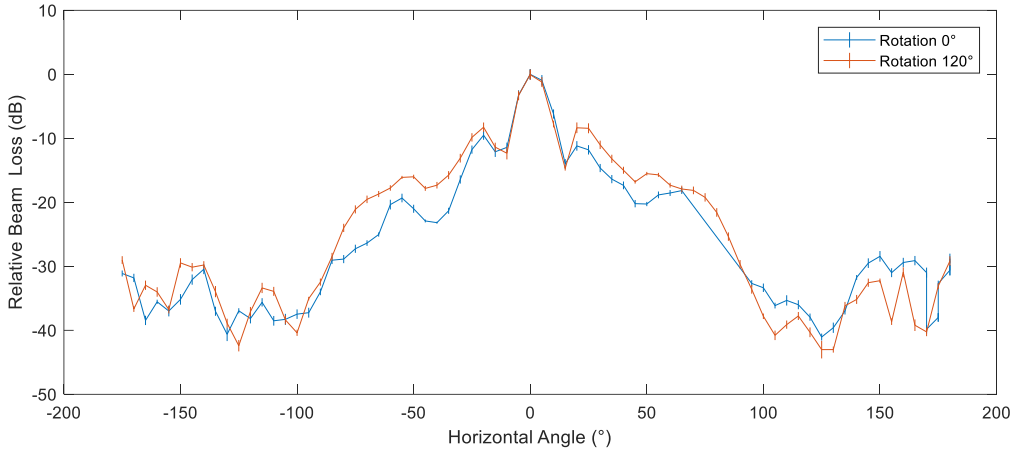

Figure 13S. Comparison of the peak to peak beam profile of the transducer when rotated 120° around it's acoustic axis.

The peak to peak and energy flux density measurements were compared to the beam profile calculated using the porpoise experimental setup as shown in Figure 14S. Only measurements from the porpoise experiment with vertical angles between -3° and 3° are shown to accurately depict the horizontal beam profile of the transducer.

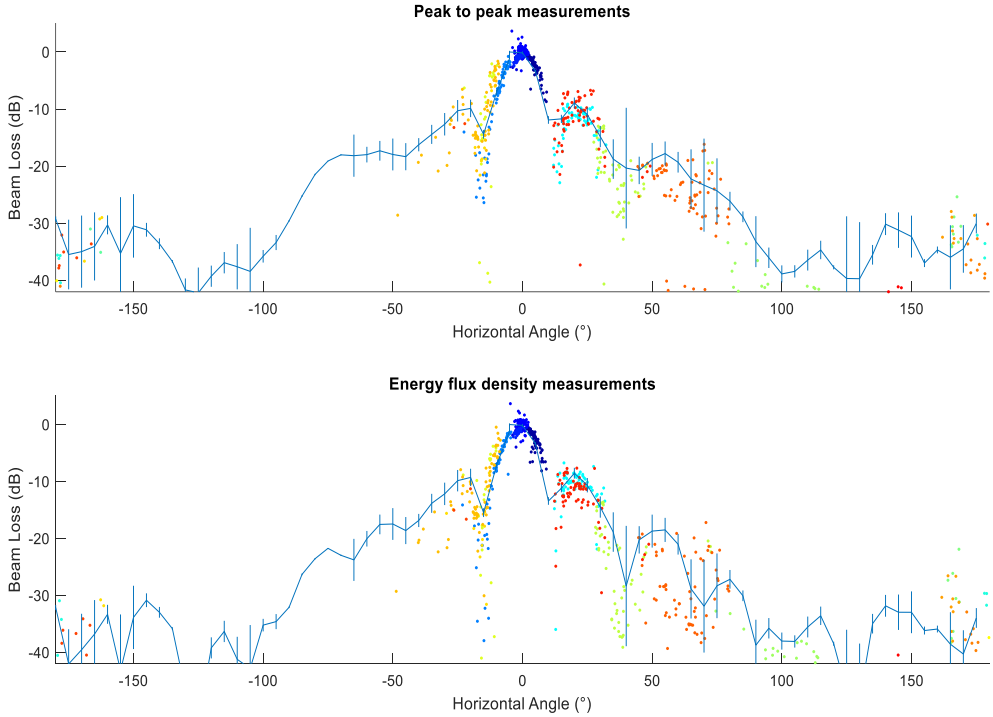

Figure 14S. Comparison of measurements from the harbour porpoise experimental setup (scatter points) and the calibration pool measurements (blue line). Both peak to peak and energy flux density measurements gave been plotted.

4.9.1.6 Discussion and Conclusion

The measurements of the TC2130 using the harbour porpoise experiment setup agreed with the measurements taken in the calibration pool.

During experiments using the harbour porpoise experimental setup, it was difficult to keep the transducer more than a meter from the side of the pool. The position of the transducer was acoustically localised using the hydrophone array which inevitably leads to some error in location. Hydrophones on the same side of the pool as the transducer were often very close to the transducer at angles close to 90° and therefore any small errors in acoustic localisation can lead to large errors in estimated transmission loss (because of the log scale) and thus large errors in estimates of the beam profile. To compensate for this beam profile measurements were only acquired from hydrophones which were at least 1.5m from the acoustic source. In harbour porpoise experiments, the porpoise was further into the centre of the pool and thus it was rare for hydrophones to be within 1.5m of the animal. However, in the TC2103 transducer experiment hydrophones on the same side of the pool were often within 1.5m. This is why there is a gap in the data from the porpoise experimental setup between around -50 to -150.

There are some troughs in the beam profile (~20°) measured using the harbour porpoise experimental setup which are not present in data from the calibration experiment. On closer inspection, these troughs are less than 5° in width and thus it is likely they were missed in the pool calibration experiment.

The TC2130 beam profile was not symmetric around it's acoustic axis, there was variation of up to 6dB as shown in Figure 13S. It is unknown what the rotation of the transducer was when being measured using the porpoise experimental setup, however, it did not change much during trials. This means that up to 6dB in difference between the calibration and porpoise experimental setup measurements are possible.

4.9.1.7 Conclusion

The experimental setup used to measure the harbour porpoise beam profile could produce accurate results of a beam profile.

4.9.2 Side lobes

4.9.2.1 Introduction

Side lobes were not apparent on the measured porpoise beam profile. To check that this was not due to stochasticity in the data, clicks were tightly filtered around their peak frequency, as this should exacerbate any side lobes which are present.

4.9.2.2 Results

Figure 15S shows exactly the same plot as Figure 6 in the chapter, except here, waveforms have been filtered using a 125-130 kHz Butterworth 4th order band-pass filter. There are no obvious side lobes present.

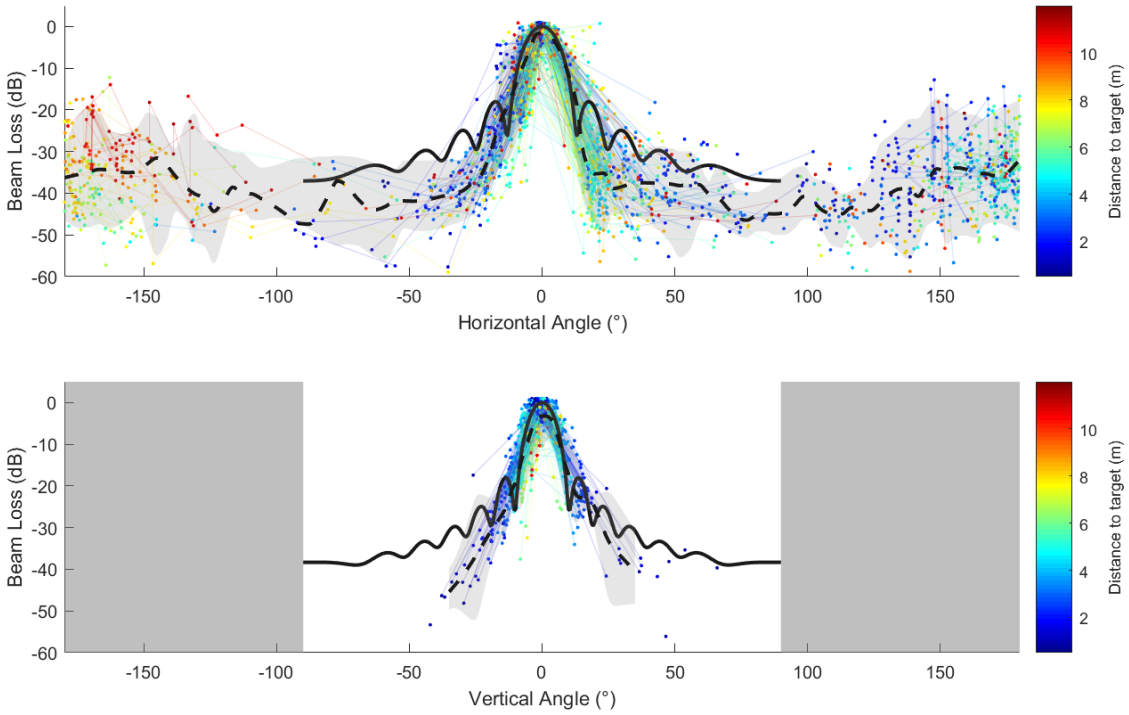

Figure 15S. Calculated beam profile compared to piston model for filtered data. Plot A shows all horizontal angles which have vertical angles between -3° to 3° are plotted. Plot B shows all vertical angles which have horizontal angles between of -3° and 3°. Scatter points show back calculated beam source levels with respect to angle. The solid black line shows the piston model results. The dashed black line shows the average beam measurement with grey area indicating the 95% confidence interval. The small grey lines group single clicks detected on multiple hydrophones together. Scatter points and lines are coloured by the distance to the target.

Figure 16S shows the beam surface for the highly filtered clicks. The beam profile is slightly narrower and less symmetric but there are still no obvious side lobes.

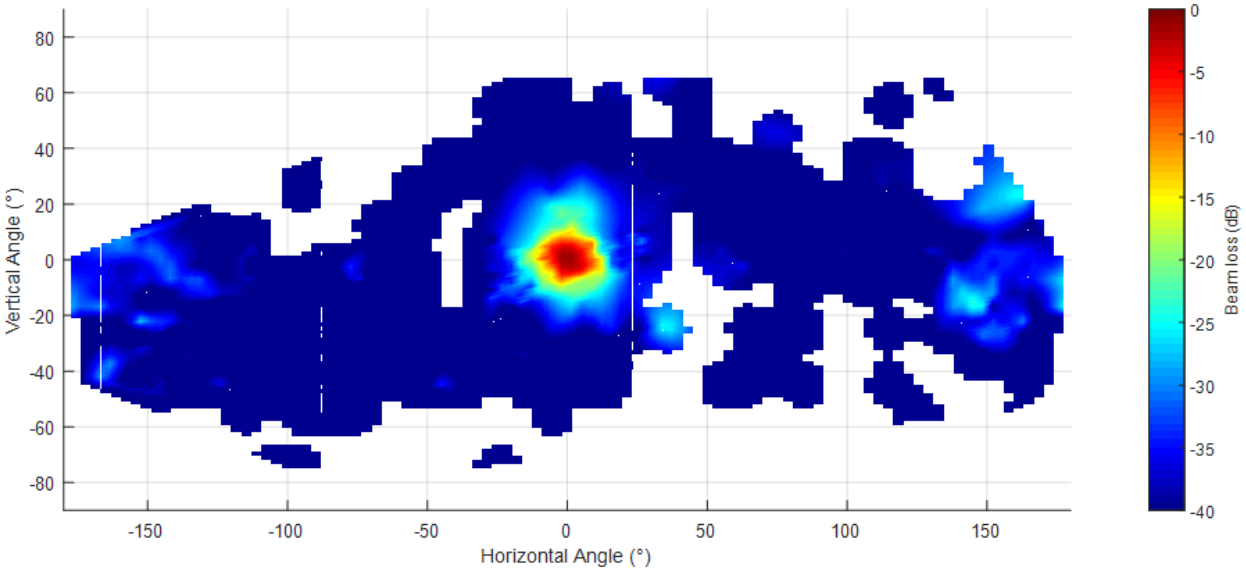

Figure 16S. Porpoise beam profile showing full aspect coverage the beam, as constructed using highly filtered clicks. 2x2° grid bins used between ±30°, and 5x5° grids were used to take the median of the beam profile at all other angles.

4.9.2.3 Conclusion

Even with filtering there does not appear to be any obvious side lobes and thus the lack of side lobes appears to be due to the fact the porpoise beam is not a perfect baffled piston, and not due to stochasticity in the data.

Chapter 5: Harbour Porpoise fine scale density, distribution and foraging behaviour in tidal rapids using drifting passive acoustics arrays

Kylerhea narrows and the entrance to the Sound of Sleat.

Chapter 5: Harbour Porpoise fine scale density, distribution and foraging behaviour in tidal rapids using drifting passive acoustics arrays

ABSTRACT

Tidal rapids are atypical and highly dynamic habitats which are known to attract harbour porpoises and other top predators. The reasons underlying why such tidal habitats confer an advantage to harbour porpoises is unknown although there are visual observations suggesting high rates of foraging. Understanding how harbour porpoises utilise tidal rapid habitats and how important these habitats might be, requires detailed information on the behaviour, distribution and density of animals. A combination of drifting vertical hydrophone arrays and single channel recorders were used to conduct a PAM survey of Kylerhea, a tidal rapid habitat in Scotland, in summer 2014 and 2015. The PAM systems were able to record echolocation clicks, foraging buzzes and communication calls of harbour porpoise. The vertical arrays could localise clicks, providing 3D geo referenced dive tracks of animals, and calculate on-axis source levels. The behavioural information collected by the vertical arrays was used to calculate a click and buzz detection probability using a Monte Carlo simulation method. This was then applied to all drifting PAM devices and a distance sampling approach was used to estimate density, distribution and foraging rates. Results show that there was a high density of porpoises in the area immediately south of the narrow highest current area of the tidal rapids but almost no porpoises in the narrows themselves. Distribution, depth distribution and foraging rates were highly coupled with tidal state with most of the foraging in the ebb tide concentrated in a fast spit of water that leaves the narrows and foraging during the flood tide more distributed across the habitat. Overall foraging rates are high, indicating that these habitats could provide a large portion of the energetic requirements of harbour porpoise.

5.1 INTRODUCTION

Tidal rapid habitats are areas in which bathymetry and large tidal ranges generate fast moving currents, usually around headlands or in narrow sounds between islands. Large volumes of water can move at high speed (~4 ms^{-1}), generating a range of surface features such as eddies, standing waves, boils, and a generally higher sea state than surrounding areas (Davies et al. 2012). These unique and highly energetic environments are thought to increase foraging opportunities for marine megafauna and aggregations of marine species, correlated with tidal phase, have been reported in many tidal rapid habitats (Zamon 2003, Waggit et al. 2017, Hastie et al. 2016).

Despite their relatively high abundance (Hammond et al. 2013, Waring et al. 2015), there is a paucity of data on the behaviour and density of harbour porpoises in tidal stream habitats. Although several studies have demonstrated that harbour porpoise presence is highly correlated with current speed, tidal height and hydrodynamic characteristics in tidally energetic habitats (IJsseldijk et al. 2015, Waggitt et al. 2018, Tollit et al. 2019), the reasons underlying this are poorly understood. Porpoises have been observed maintaining position within tidal races in the UK (Pierpoint 2008), Canada (Hall 2011) and Japan (finless porpoise; Akamatsu et al. 2010) with the suggestion that animals may be intercepting or ambushing prey carried in fast moving water. However, a passive acoustic study by Benjamins et al. (2016) in the Great Race, Scotland, suggests harbour porpoises move with the tide rather than against it, and some visual and acoustic studies have indicated porpoises may be more abundant in lower current areas of tidal streams (Waggitt et al. 2018) or that larger scale distribution of animals is best described by low current habitats (Embling et al. 2010, Booth et al. 2013).

Many of the previous studies have been limited by relatively rudimentary metrics such as sighting rates at the surface and/or using acoustic click loggers to measure presence/absence, a metric which provides no information on the area monitored or the number of animals that may be present. A comprehensive understanding of the importance of tidal rapid habitats requires detailed information on both sub surface behaviour, distribution and absolute density of harbour porpoises; however, there are currently very few studies in which these have been measured (an exception being Gordon et al. (2011)). This lack of information for tidal rapid areas is consistent across many cetacean species and marine top predators (see Benjamins et al. (2015) for a comprehensive review).

One of the primary reasons underlying the lack these data is the technical and practical challenges of deploying scientific equipment in fast moving currents and the complex analytical methods required to then use the collected data to quantify fine-scale behaviour and density of harbour porpoises (and other marine mammals). There are several potential methodological approaches that might be considered; visual studies are relatively straightforward but do not provide information on sub surface behaviour and are limited by higher sea states. Tagging animals with bio-loggers that track movement is possible but likely not a cost-effective option where the area of interest is geographically restricted and a tagged animal may spend only a small proportion of its time within it (Hastie et al. 2014). Active acoustic monitoring has been shown to be effective for monitoring the dive behaviour of seals in tidal rapids, however, the equipment is expensive, power hungry and has limited range (Hastie et al. 2019). For more soniferous animals (such as harbour porpoises), passive acoustic monitoring (PAM) has the great advantage of being relatively unaffected by sea state, light conditions and can detect any vocalising animals within a relatively large area of interest.

Density estimation of toothed whales using PAM has been achieved by several studies (e.g. Gordon et al. 2011; Thomas et al. 2017; Carlén et al. 2018). A key parameter to enable density estimation is the probability of acoustically detecting an animal or group of animals (Marques et al. 2013) for a review of density estimation using acoustic data). Estimating detection probability allows for animals to go undetected during a survey, as these missed animals can be accounted for during the density estimation analysis. Detection probability is typically estimated as a function of range between animal(s) and the acoustic recorder; the resulting statistical model is known as the detection function. In some cases, such as line transect surveys using towed hydrophone arrays, a PAM system itself is capable of localising detected vocalisations and animal locations are used to estimate a detection function directly (Barlow and Taylor 2005, Gordon et al. 2011). In other surveys the detection probability must be measured using auxiliary data. This can involve using an external method (e.g. visual tracking, tagging or acoustic localisation) to locate animals around a recording PAM sensor(s) ; the acoustic data and animal locations can then be used to generate a detection function (Marques et al. 2009, Kyhn et al. 2012). When no suitable location data is available to directly estimate a detection function, then physical simulations based on knowledge of the acoustic propagation conditions and animals' source levels, beam profiles and diving behaviour can be utilised to estimate detection probability (Küsel et al. 2011, Frasier et al. 2016, Hildebrand et al. 2019). In

these simulation studies, or any methods which require auxiliary information, it must be assumed that the simulation inputs/auxiliary information adequately represent the spatial or temporal scale of the survey. Another assumption in distance sampling-based surveys is that the track lines or distribution of sensors are placed at random with respect to animals. Tidal rapid habitats are atypical and highly dynamic environments in which animal behaviour, bathymetry and noise change substantially at fine spatial and temporal scales (Wilson et al. 2013, Benjamins et al. 2017). Thus, any auxiliary information not collected directly in the habitat likely does not adequately represent animal behaviour and designing a survey in which PAM recorders are randomly distributed with respect to animals in such a heterogenous habitat is challenging.

Whilst many studies focus on density estimation, specific types of PAM systems can also be used to accurately localise the position of animals. The time delays between a vocalisation arriving at different hydrophones within a multi-hydrophone array can be used to determine the position of an animal (see Chapter 3). Generally such PAM systems are compact rigid linear/planar or volumetric arrays (e.g. Villadsgaard et al. 2007; Ladegaard et al. 2017; Wiggins et al. 2012), much larger flexible free floating vertical hydrophone arrays (e.g. Heerfordt et al. 2007; Hastie et al. 2006; Macaulay et al. 2017) or seabed mounted systems (e.g. White et al. 2006; Gassmann et al. 2015). The localised positions of animals can allow for the calculation of apparent source levels of received vocalisations (Møhl et al. 2000) and the tracking of fine scale movements (e.g. Miller & Dawson 2009). These tracks can then be cross referenced with characteristic acoustic behaviour, such as foraging buzzes (high repetition rate clicks which occur before prey capture) and changing inter click intervals (e.g. Wahlberg 2002), which potentially allows for detailed information on foraging ecology to be collected (Hastie et al. 2006).

Three types of (PAM) configuration have so far been used to survey porpoises acoustically in tidal rapids; towed hydrophone arrays, static seabed mounted devices, and drifting units. Traditional acoustic and visual line transect surveys using towed arrays have been carried out in tidal rapid habitats (Gordon et al. 2011, Wilson et al. 2013) . However, due to noise from the research vessel, these surveys have the potential to disturb animals (Palka & Hammond 2001; Wisniewska et al. 2018) and are therefore not particularly suited to this study, which is attempting to measure both fine scale sub surface behaviour and density. Diving behaviour is also usually not possible to calculate from

towed arrays because the target motion methods generally used for acoustic localisation are too inaccurate to measure fine scale movements. Another potential option is to use localisation capable static devices on the seabed (Malinka et al. 2018), however, achieving acceptable spatial coverage in any area in which porpoise habitat usage can change at small spatio-temporal scales requires many devices (Benjamins et al. 2017). Further, in tidal rapid habitats, high currents often result in flow noise over static hydrophones resulting in a strong tidal influence on the detection probability (Malinka et al. 2018) and large (therefore expensive) moorings are required to maintain station in strong currents. The final option is drifting PAM units. These have the advantage of low flow noise, likely cause significantly less disturbance than an active vessel and are cost effective to deploy and recover (Wilson et al. 2013). However, the spatial coverage achieved is unpredictable and will therefore need to be considered in relation to density estimation.

Here we describe a PAM methodology to study harbour porpoises, but applicable to all toothed whales, which can be used to describe fine scale sub surface behaviour and density at small spatial scales within tidal rapid areas. A combination of drifting single channel PAM systems and vertical hydrophone arrays capable of tracking the movement of porpoises underwater were deployed in a tidal rapid habitat in Scotland. Behavioural data from the hydrophone arrays were used to inform a simulation of the probability of acoustically detecting animals in different parts of the tidal habitat. This was then applied to both vertical hydrophones arrays and single hydrophone drifting units to estimate porpoise densities across a range of depths and foraging rates within a tidal stream habitat.

5.2 DATA COLLECTION

5.2.1 Study Site

The study took place in the narrow tidal channel of Kylerhea and the Sound of Sleat (see Figure 1), which separate the Isle of Skye from the west coast of mainland Scotland (~57.2° N, 5.65° W), between August 20-27, 2014 and August 16-27,2015. Maximum water depths are~ 30 m and ~150m, in Kylerhea and the Sound of Sleat respectively (Digimap bathymetry, 2014). The flood tide runs from south to north, and the ebb tide in the opposite direction. During both ebb and flood, the Kylerhea narrows have substantial current speeds up to 3-4ms^{-1}. During the ebb tide a water mass from the narrows moves into the Sound of Sleat, creating a jet of faster moving water which gradually spreads out to much slower current speeds of less than 0.5 ms^{-1}

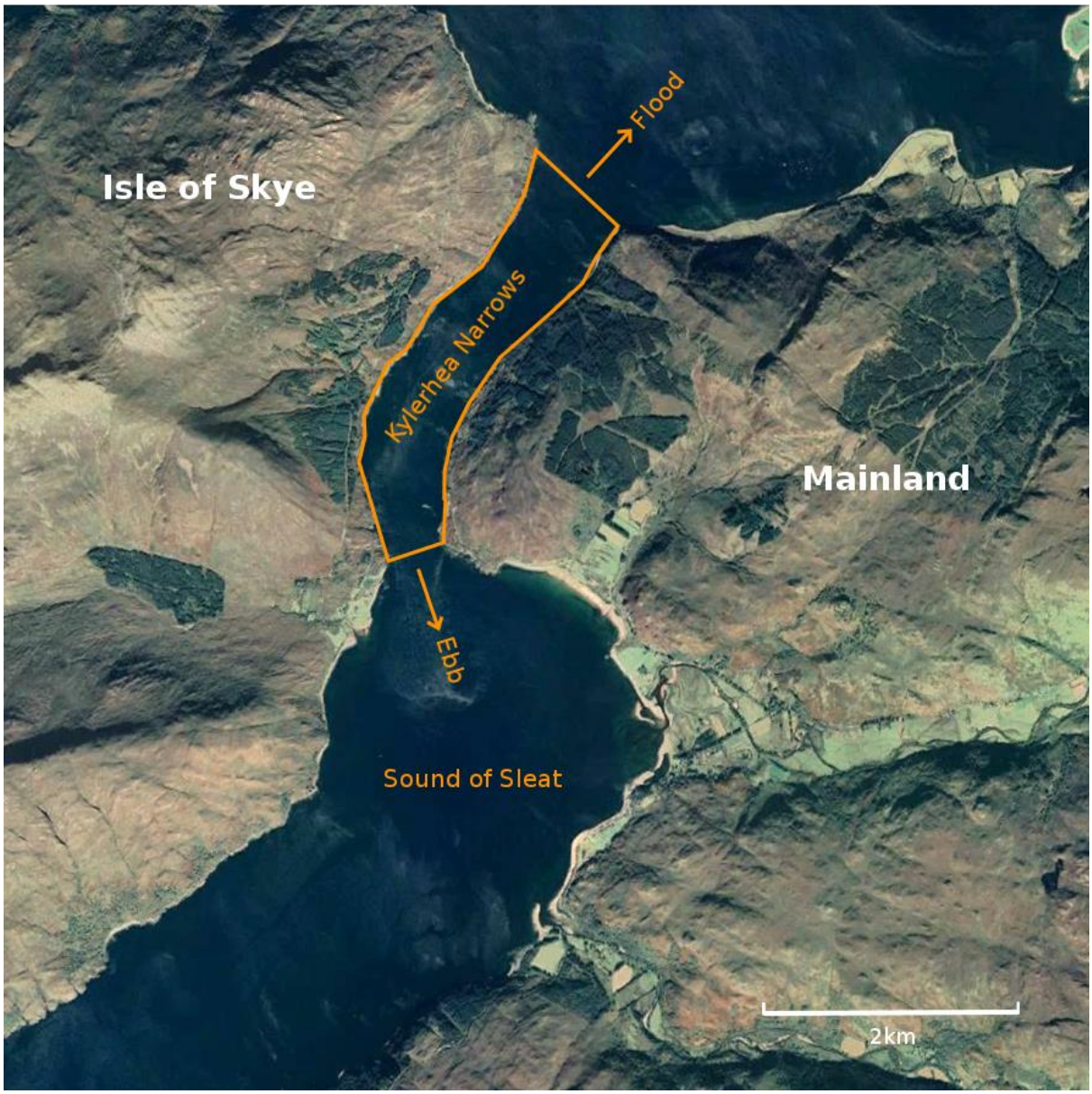

Figure 1. Satellite image of Kylerhea narrows and the Sound of Sleat. Kylerhea narrows are shallow (~ 12 -30m) which creates current speeds up to 4ms^{-}1. A jet of water moves into the much deeper (~150m) Sound of Sleat immediately south of the narrows. The flood tide moves south to north and the ebb tide moves north to south. ©Google 2020.

5.2.2 PAM Drifters

A combination of single or dual-channel recorders and multi-channel hydrophone arrays in a drifting configuration were deployed from a research-vessels and used to map the 3D spatial distributions of porpoises in the study area (Figure 2).

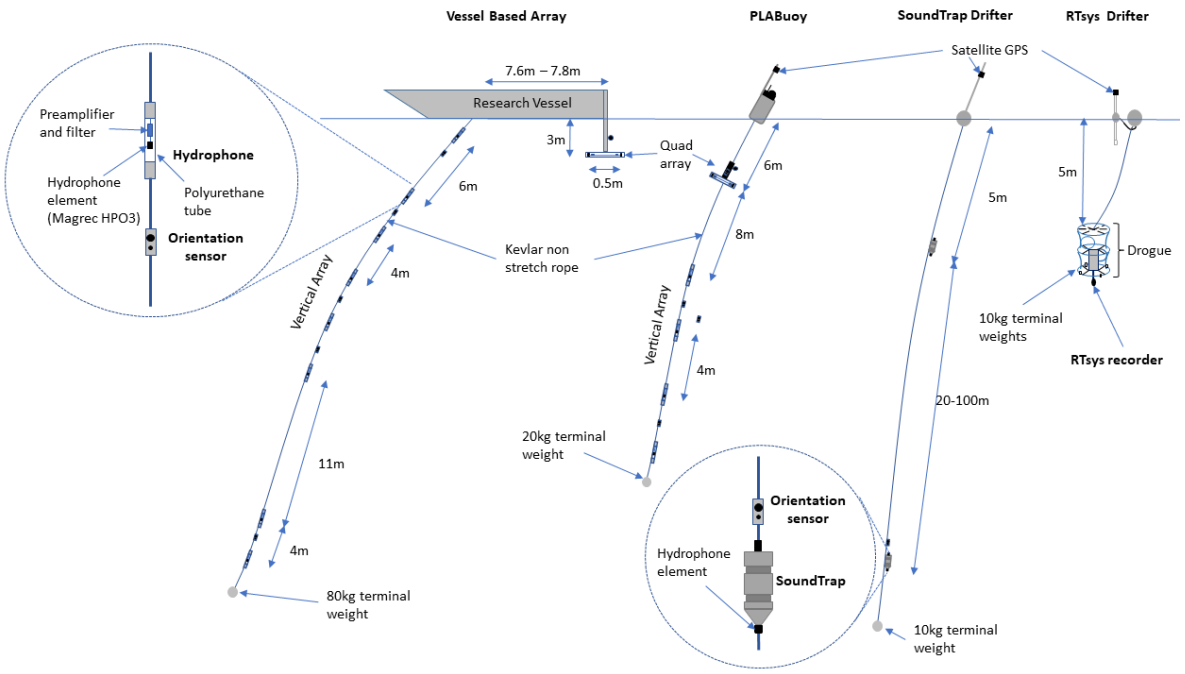

Figure 2. Diagram of the various drifting devices used in the 2014 and 2015 survey of Kylerhea (not to scale). The vessel based array and PLABuoy are capable of localising 3D position of animals underwater. The SoundTrap and RTsys drifters had no localisation capabilities but were more numerous (6 devices in total) and easier to deploy.

The majority of survey effort was undertaken by single or dual channel drifters in two configurations. The first configuration comprised of one or two SoundTrap HF-202 digital acoustic recorders (Ocean Instruments Ltd., NZ) attached to a nylon rope at interchangeable depths of 5 m, 20 m and 100 m; these recorded sound at a sample rate of 576 kHz. A 10 kg terminal weight was used to keep the rope taught and near vertical in the tidal stream, and the top end of the rope was attached to a danbuoy at the water surface. An OpenTag 3-axis orientation and depth sensor (Loggerhead Instruments, USA) was used to measure the angle of the rope and depth of each device at a sample rate of 100 Hz. RoyalTek GPS loggers (Quanta Inc., USA) and Spot Satellite transmitters (SPOT LLC, USA) were used to record GPS position and assist in recovering the buoy if it moved out of visual range. The second type of drifter was based on an RTsys multi-channel recorder (Swale technologies, France) recording stereo data at a sample rate of 384 kHz from two Reson TC4032 (-164 dB re 1V/µPa at 120 kHz) or TC4014 (-180 dB re 1V/µPa at 120kHz) hydrophones (Teledyne RESON, Denmark). Hydrophones were attached to a nylon rope at a depth of 5 m and separated vertically by 10 cm. The rope was kept taught by a 5 kg terminal weight. These drifters also had an attached GPS logger which recorded position every second and utilised a drogue to minimise the effects of windage on the buoy.

Two drifting vertical multichannel hydrophone arrays were also deployed to measure the three-dimensional dive behaviour of harbour porpoises in the study area. The first array was deployed from a drifting research vessel (16 m yacht) and consisted of either 8 or 10 hydrophones. Acoustic data were digitised using 3x SAIL (SAIL, UK) data acquisition cards at 500KHz. A vector GPS and inclinometers were used to determine the orientation of the drifting vessel and hydrophone array. All acoustic and orientation data were saved to hard drives by a laptop computer onboard the vessel running PAMGuard software ((Gillespie et al. 2008) www.pamguard.org: methods described in detail in Chapter 3).

The second drifting vertical multichannel array had a similar hydrophone configuration using the same hydrophones (-201 dB re 1V/µPa at 120kHz and 28dB pre-amplifier) but was designed to function autonomously. The porpoise locating array buoy (PLABuoy) comprised of four hydrophones distributed vertically at 4m intervals on non-stretch Kevlar rope and a further four hydrophones arranged in a rigid tetrahedral configuration with 30 cm between hydrophones. Hydrophones were individually housed within small polyurethane tubes for mechanical protection and to reduce self-noise from water flow. Two OpenTag orientation and depth sensors were attached to the vertical section of the array and a single OpenTag attached to the tetrahedral section of the array. These provided measurements of the 3D orientation of the tetrahedral array and the orientation of the vertical cable. Together, the hydrophone array and orientation sensors allowed for the depth, range, and 3D bearings to a vocalising animal to be calculated, providing a full set of 3D co-ordinates relative to the array. When combined with location data from a GPS logger all localisations could be geo-referenced (see Chapter 3).

The PLABuoy recording system was based on a National Instruments (National Instruments, USA) cRio 9068 computer and two synchronised NI9222 DAQ cards recordings at 500 kHz with a custom ETEC amplifier (ETEC, Denmark) providing gain and anti-aliasing filters. A RaspberryPi 2 computer (Raspberry Pi Foundation, Cambridge) interfaced via ethernet to the cRio was used to send status information wirelessly to the research vessel. The cRio computer was mounted inside a 30 x 30 x 10 cm Peli case with an attached 60 A·h lead acid battery. These were packaged within a waterproof barrel which had external connectors for the hydrophones, wireless antennae, and mount for the GPS antennae. The system was designed to run autonomously and continuously for ~ 2 days. Custom built

open source software (https://sourceforge.net/projects/plabuoy) running on the cRio was used to save audio recordings as WAV files and GPS data to a hard drive. In 2014 the cRio was damaged and a Microsoft (Microsoft, USA) Surface tablet running PAMGUARD (version 1.15.00) and a National Instruments 6256 USB DAQ card (same 20V range 16-bit) were used as the recording device

The PLABuoy and autonomous drifters were deployed and recovered from a rigid hull inflatable boat and visually monitored from the research vessel until out of visual range after which they were tracked using satellite transceivers. The depth of the PLABuoy array and SoundTrap drifters was adjusted depending on whether a drift was likely to enter the Kylerhea narrows which have shallow areas ~ 12 m deep depending on the tide height. The "shallow configuration" for the PLABuoy involved reducing the length of the vertical array from 30 m to 12 m (with even spacing between hydrophones) and for the SoundTrap drifter meant removing one device so that there was only one SoundTrap at 5 m depth. The SoundTrap/RTsys drifters were both more numerous and less complex to deploy, thus they covered a higher proportion of the survey effort. Table 1 shows a summary of the PAM hardware used and survey effort.

Table 1. Summary of technical specifications of drifters and survey effort.

Device Type	**Number drifters**	**Number hydrophones (Used in analysis)**	**Sample Rate per channel (kHz)**	**Clip level (dB re 1µPa pp)**	**Bit rate**	**Year**	**Survey Effort Ebb (hours)**	**Survey Effort Flood (hours)**
SoundTrap drifter	2	1-2 (1)	576	184	16	2014/ 2015	45.9	53.3
RTsys drifter	4	2 (1)	385	171/169	16	2015	34.3	37.0
Boat based vertical array	1	10-12 (10-12)	500	160	16	2014/ 2015	25.3	26.4
PLABuoy vertical array	1	8 (8)	500	160	16	2014/ 2015	19.6	17.4

5.3 ANALYSIS

Four primary data analysis tasks were required to determine the density of porpoises and their dive and foraging behaviour. First, data was assembled on relevant environmental variables such as bathymetry, tide speed and the general soundscape (section 5.3.1). Porpoise echolocation clicks, foraging buzzes and communication calls were then extracted from acoustic recordings using automated detection algorithms (section 5.3.2). Clicks detected on the vertical hydrophone arrays

were localised and georeferenced which provided 3D locations that were used to generate dive tracks (section 5.3.3 and see Chapter 3). Finally, the probability of detecting clicks and buzzes was estimated allowing animal density, foraging buzz rates and communication call rates to be calculated (section 5.3.4).

5.3.1 Tide speed and soundscape

All drifter tracks recorded from GPS loggers (once or twice per second) were interpolated (linear) to provide a value for position and speed every 0.5 seconds.

The tidal area was divided into 50 m by 50 m squares and the median speed and direction of all combined drifters within each square calculated using a boxplot algorithm (McGill et al. 1978) to remove outliers. The averaged data was then interpolated using a biharmonic spline interpolation (Sandwell 1987) to create an average map of the tide speed and direction. The drifting research vessel was not included in tide speed calculations due to much higher windage.

Background noise was highly variable within the study area. The drifting hydrophones resulted in very low flow noise, however, bottom sediments moving in strong currents introduced significant levels of broadband noise which could render porpoise clicks almost undetectable (see Figure 3). In the context of detecting porpoise echolocation clicks it is the noise that the automatic detection algorithm considers which is relevant to whether a click is detected or not. The PAMGuard click detector module (version 2.00.14) was used to automatically extract transients within the porpoise frequency band from raw recordings. This utilised a basic energy sum algorithm which first filtered raw acoustic recordings using a 80-150kHz band pass (Chebyshev 4^{th} order) and registered a click if a transient reached a threshold above an internal measure of noise (Gillespie and Leaper 1996) . Internal noise measurements from the click detector module were used to construct a noise map using the same boxplot and biharmonic spline interpolation methods that generated tide speed surface. The system sensitivity values in Table 1 were used to ensure cross calibrations between devices.

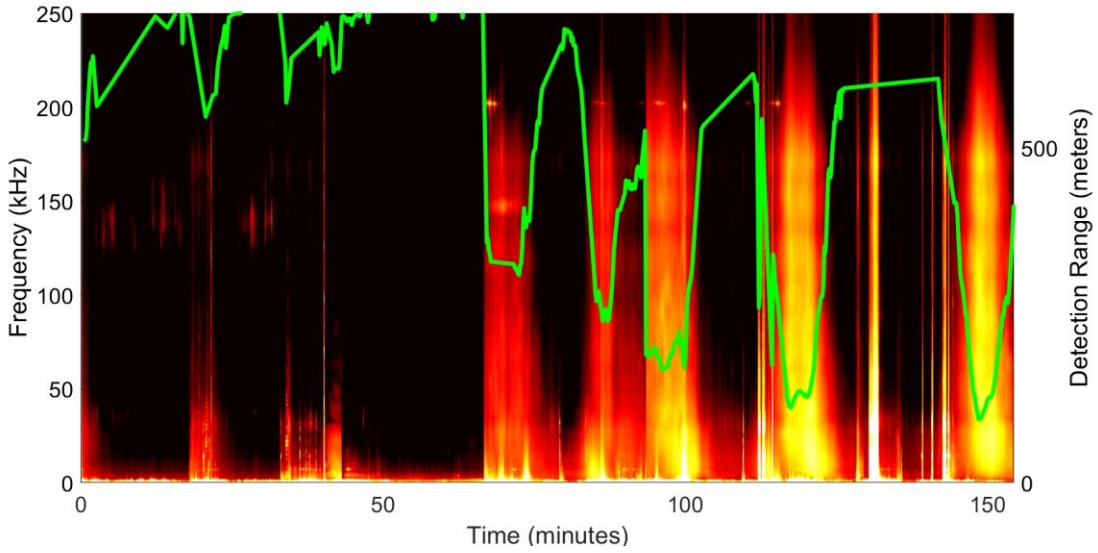

Figure 3. An example of a long-term spectral average collected in Kylerhea with an overlay of the maximum detection range versus time for 191 dB re 1µPa pp at 1m on-axis harbour porpoise click. The broadband noise in tidal rapid areas can causes large variations in the detection range of harbour porpoises. Note that the porpoise frequency band is 100 to 160kHz (from Chapter 3).

5.3.2 Detection of porpoise clicks and foraging buzzes

5.3.2.1 Detecting clicks

The PAMGuard click detector (threshold set to 10dB) (version 2.00.14) saved small snippets of associated waveforms of each transient detection. These waveforms were then classified as either 'porpoise' or 'unknown' based on spectral content and other acoustic parameters using a PAMGuard click classifier. Detailed configuration for the click detector and click classifier can be found in supplementary information section 5.9.1.

The performance of the click classifier was validated by sub sampling 3x5 minute sections of acoustic data from each type of drifter and manually classifying click detections within each sub sample. The three sections were selected to have high, medium and very low/no porpoise numbers of porpoise clicks. Manually classified clicks were then compared to the automated algorithm and the false positive rate and detection efficiency with respect to signal to noise ratio (SNR) calculated. Further details can be found in supplementary section 5.9.2.

High levels of background noise in some areas of the Kylerhea narrows led to many thousands of false porpoise detections being registered within short periods of time <2 minutes. These sections of data were identified, manually verified for porpoises clicks and any false click detections were excluded from further analysis.

5.3.2.2 Detecting buzzes

Clicks within buzzes are less directional but acoustically similar to regular echolocation clicks (Wisniewska et al. 2015). The distinguishing feature for buzz clicks is that they occur in short (<2 s) sequences (click trains) with relatively low and slowly varying inter-click-intervals (<16 ms) (Deruiter et al. 2009). The PAMGuard multi hypothesis tracking (MHT) click train detector was used to track repeating sequences of clicks, which included both buzzes and slower repetition standard echolocation click trains (see Chapter 2). MHT algorithms are well suited to identifying click trains in acoustically cluttered environments where two or more animals may be echolocating at the same time and/or there are high levels of transient noise, making it particularly useful for analysing data from relatively noisy tidal environments with high animal densities. Detected click trains were classified as buzzes or standard echolocation clicks trains based on inter click interval (ICI) (see supplementary section 5.9.4).

To validate the click-train algorithm buzz classifier, a representative 24 hours of acoustic data from a SoundTrap, the PLABuoy, and the Vertical Hydrophone array were annotated manually for buzzes. The manually detected buzzes were then compared to results from the MHT algorithm and precision recall curves (Roch et al. 2011) were calculated based on differing thresholds for χ^2 values produced by the MHT method. These provided an optimal maximum value for χ^2 to balance click train false negatives which was used across all devices and deployments (see supplementary section 5.9.4.1).

5.3.2.3 Discrimination between communication and foraging buzzes

Buzzes were divided into foraging and communication buzzes based on their median ICI. Sørensen et al. (2018) plotted ICI distributions of both foraging and communication buzzes for tagged animals and noted that communication buzzes occupy a range of ICI values which are rarely used for foraging. Thus, for each buzz, the relative likelihoods of being a communication or foraging buzz was calculated using the relevant ICI power density functions in (Sørensen et al. 2018). A binary classification as either foraging attempt or communication call was then applied depending on which likelihood was highest.

5.3.3 Localisation and tracking of individual porpoises

Analysis of data from the multi-hydrophone arrays provided geo-referenced 3D localisations of individual clicks. It was rare for an entire dive to be recorded because animals could move out of

localisable range or turn away from the array, in which case their narrow beam profile made them undetectable unless at close range (see Chapter 4). Thus, dive data consisted of many dive fragments. These were interpolated to produce dive track fragments (interpolated sections of 3D dive tracks) using methods described in Chapter 3 section 3.3.3.

The orientation of animals with respect to the tide was calculated from the geo-referenced track fragments and the mean interpolated current speed (see section 5.3.1) at the track location.

5.3.4 Modelling detection probability and calculating density of clicks and buzzes

To calculate the distribution of porpoises and foraging behaviour in the study area, an absolute density of both buzzes and standard echolocation clicks, after allowing for detection probability, was required.

The standard density equation based on counting clicks on a fixed PAM recorder is:

$$\widehat{D} = \frac{n(1-\widehat{f_p})}{a_c \hat{P} T \hat{c}} \qquad \text{Eq. 5.1}$$

where n is the number of detected cues (clicks or buzzes in this case), $\widehat{f_p}$ is the estimated proportion of false positives (see section 5.3.2 and supplementary section 5.9.2), a_c is the maximum area covered by the instrument (taken to be a circle with a radius of the maximum detection range), $\hat{P}$ is the average probability of detecting a cue in the area a_c, T is the total time spent monitoring, and $\hat{c}$ is the cue rate per animal in clicks/buzzes per unit time of T (Marques et al. 2013) .

The average cue rate ($\hat{c}$) is unknown and cannot be calculated accurately using PAM because non vocalising animals are undetectable; $\hat{c}$ was therefore estimated to be a range of values between the minimum click rate of a wild animal reported by (Linnenschmidt et al. 2013) (under 1 click per second on average) and a maximum calculated from the average inter click interval of detected click trains within the tidal rapid site (see section 5.3.2.2) i.e. the maximum cue rate assumes that animals do not have any silent periods. Density was then estimated for values between the minimum and maximum value of $\hat{c}$.

a_c is the area of a circle, the radius of which is the maximum possible detection range for a harbour porpoise. The maximum detection range can be estimated as the range at which:

$$SL - TL = NL + SNR_{min} \quad \text{Eq. 5.2}$$

where SL is the source level (dB re 1µPa pp at 1m) calculated from clicks detected on the vertical arrays, NL is the noise level (dB) in the 100 to 160 kHz frequency band and SNR_{min} is the minimum signal to noise ratio (dB) at which clicks can be detected (in this case 10dB). TL is the transmission loss (dB) which was calculated using a simple spherical propagation model (DeRuiter et al. 2010):

$$TL = 20\log_{10}(R) + \alpha R \quad \text{Eq. 5.3}$$

where R is the range (m), and α is the absorption coefficient. Here, α was assumed to be 0.041 at 130 kHz (peak porpoise click frequency) (Ainslie and Mccolm 1998). Eq. 5.2 was solved for R assuming a minimum peak to peak equivalent NL of 90dB re 1µPa pp using the upper 95% SL calculated from the vertical hydrophone arrays (see results in section 5.4.6)

The final term required to estimate density is $\hat{P}$, the probability of detecting a porpoise click or buzz within area a_c; this is derived using the following approach:

5.3.4.1 Modelling detection probability $\hat{P}$

Tidal rapid habitats are highly heterogeneous areas; current flows, and therefore background noise, can change markedly over fine spatio-temporal scales (Benjamins et al. 2017). Although a drifter and animals may be in the same reference frame, i.e. both are within the same body of moving water, rapid changes in bathymetry, noise, and current as the device drifts through the tidal stream are likely to impact porpoise behaviour. Therefore, the probability of detecting a porpoise click or buzz in a tidal area may be highly dependent upon the location of a drifter and the tidal cycle (time). This spatially and temporally dependent $\hat{P}$ must be quantified to effectively estimate changes in density within the tidal habitat.

Here, the detection probability of clicks and buzzes for all drifting devices could not be determined empirically from distances to localised porpoises because the probability of detecting a click or buzz exceeded the operational localisation range of the hydrophone arrays (~200 m). Therefore, a Monte Carlo simulation-based approach (Küsel et al. 2011, Frasier et al. 2016) was integrated with behavioural data collected from the vertical hydrophone arrays. The simulation placed an animal at a random x,y location with a total range from the hydrophone (array) between 0 and the radius used to calculate a_c at a depth drawn from a known depth distribution calculated using dive track data

from the vertical arrays. The simulated porpoises' source level and orientation at each location were drawn randomly from pre-defined distributions obtained from behavioural data also from the vertical hydrophone arrays. With a value for simulated position, the location of a hydrophone, animal source level and orientation known, the apparent source level (source level minus the attenuation due to beam profile) could be calculated from the full 4π beam profile of a harbour porpoise (see Chapter 4). Transmission loss was then estimated using (Eq. 5.3) and a received level calculated. The simulated received click was deemed detected (or not) according to the following criteria; if the simulated received level was above a defined noise level (dB) + detector threshold a Bernoulli trial was conducted based on the $\hat{p}_d(SNR)$, the detection efficiency of the automated click and buzz detectors for each PAM device, to determine if a detection occurred. If detected, then the simulated click/buzz at that location was assigned a value of 1 to denote a successful detection otherwise, the location was recorded as being unsuccessful (assigned a value of 0). This process was repeated 50,000 times and the resulting probability of detection for a specific noise level and porpoise behaviour state was calculated as the total number of successful detections divided by the total number of attempts. The process was then repeated 50 times and results averaged to give a final value for $\hat{P}$.

Where possible, the input distributions for the simulation were calculated from data collected directly in the tidal habitat. The data sources for each input are as follows.

5.3.4.1.1 Noise

The output from the click detection algorithm's internal noise calculations as described in section 5.3.1 and supplementary 5.9.3 is relevant noise metric for modelling detection probability. However, the Monte Carlo simulation model was based on peak to peak measurements and the click detector's noise metric is essentially a filtered zero to peak noise measurement. This can be converted to an equivalent peak to peak noise by adding 6dB, however, the click detection algorithm as described in 5.9.3 also performs some averaging on the click amplitude and thus the threshold value used in the simulation is not exactly equivalent to the threshold value used by the click detection algorithm. Therefore, a 5 dB compensation factor was required such that, in the Monte Carlo simulation, a click is detected if the click amplitude was greater than the click detector noise measurement + 6 dB (convert to peak to peak) + 10 dB (click detector threshold) +5 dB (compensation factor) (see supplementary material 5.9.3 for a detailed explanation).

5.3.4.1.2 Relative Heading angle

For the purposes of the simulations, the horizontal orientation angle of harbour porpoises was assumed to be uniformly random between -180 and 180°.

5.3.4.1.3 Vertical angle

The vertical orientation angle for porpoises in the simulations were provided from porpoise tracks localised by the vertical arrays. To compensate for potential differences in vertical orientation during surfacing behaviour and diving (Westgate et al. 1995), two vertical angle distributions were used, one distribution for porpoises between 0-10m depth, and a second for all deeper depths. The deeper vertical angle distribution was calculated using localised tracks between 10 to 30/45 m (see supplementary section 5.9.5). It was assumed the distribution of vertical angles remained the same for animals below this depth.

5.3.4.1.4 Beam profile

The full 4π (all horizontal and vertical angles) beam profile was measured from a captive animal in Fjord and Bælt, Denmark in Chapter 4. A wider beam profile was assumed for buzzes (60% increase in -3dB beam width) to account for porpoises broadening of their bio sonar beam in the terminal phase of prey capture (Wisniewska et al. 2015).

5.3.4.1.5 Source levels and propagation

Source levels were calculated from the drifting vertical array recordings using methods similar to (Villadsgaard et al. 2007). Sequences of detected clicks were identified manually. As porpoises scanned their biosonar across the array, sequences of clicks typically rose in amplitude, reached a peak when they were closest to being on-axis, and subsequently decreased in amplitude as the beam moved off the array. When the highest amplitude click within these sequences was detected on a minimum of 4 hydrophones, it was localised, and a source level back calculated using the sonar equation:

$$SL = RL + TL \qquad \text{Eq. 5.4}$$

where SL is the source level, RL is the received level, and TL spherical spreading and absorption loss using Eq. 5.3.

All hydrophones within the vertical arrays were calibrated and an associated mean and standard deviation calculated for hydrophone sensitivity. The standard deviation in hydrophone sensitivity was on average ~2-6 dB (likely due shadowing from the protective housings) which can produce substantial error in calculated source levels. Therefore, to estimate source level uncertainty, source level calculations were bootstrapped (n=100) with each iteration resampling the sensitivity of each hydrophone in the vertical array. These were then used to inform the sensitivity analysis in section 5.3.4.6. The mean and standard deviation of source level measurements (without bootstrapping) were used in the Monte Carlo detection probability simulation as input for the source level distribution.

Given that buzzes are relatively short and rare events, determining whether a buzz is on axis is difficult and so using the above method to calculate source levels was not possible. Buzzes were therefore assumed to be 30 dB lower than regular echolocation clicks as has been observed in studies of wild harbour porpoises tagged with acoustic sensors (Wisniewska et al. 2016)

Sound speed profiles were calculated using CTD profiles from the British Oceanographic Data Centre (BODC) database for the study area and potential refraction modelled using AcTUP software (Duncan and Maggi 2006). Refraction was insignificant and variation in speed of sound at different depths was no greater than 5.7 ms^{-1} and thus straight-line spherical spreading was deemed an appropriate propagation model for the simulation and source level calculations.

5.3.4.1.6 Depth Distribution

Once all input distributions were quantified, the Monte Carlo simulation described above was run to calculate $\widehat{P}$ for both buzzes and echolocation clicks over a range of specified background noise levels. This was a two-stage process for each survey region; the depth distribution for a porpoise in that region were calculated using data from the vertical hydrophones and this was then applied to all drifter data to calculate detection probability as a function of noise.

Depth distributions are highly dependent on both behaviour and bathymetry and so are likely to vary significantly in heterogeneous tidal rapid habitats. Depth distributions in different areas of tidal rapids were estimated empirically using localised depths of porpoises from the drifting vertical arrays. Detections on at least 4 hydrophones were required before a localisation attempt was made; importantly, this means that the probability of localising ($\widehat{Pl}$) is lower than detection probability and

may vary depending on the depth of the animal (e.g. a porpoise significantly deeper than the array is less likely to ensonify four hydrophones than a porpoise at similar depth to the array). $\widehat{Pl}$ was therefore estimated using a modified version of the Monte Carlo simulation which placed animals evenly in x,y and z and only registered a successful localisation if at least 4 hydrophones (the minimum set to attempt a localisation) were ensonifed (instead of just one). The number of successful localisations in each depth bin were then divided by the total number of simulation attempts (i.e. total number of simulated animals) and normalised to give $\widehat{Pl}$ for a specified depth bin. The value of $\widehat{Pl}$ is a function of depth and noise and was applied individually to each localisation point depending on its depth and the noise conditions at the time of the localisation. The relative depth distribution $d(z)$ of clicks is then given by:

$$d(z) = \frac{l(z)}{\left(\sum_{i=1}^{n} \widehat{Pl}(z_i, N_i)\right)/n} \qquad \text{Eq 5.5}$$

where $l(z)$ is the relative number of localised clicks within depth bin z, $Pl(z,N)$ is the localisation probability for each localised click i at depth bin z and noise N. Note that this is the depth distribution of clicks, not of porpoises**.** The calculation of the depth distribution of porpoises would require Eq. 5.5 to be further divided by $\hat{c}(z)$, the cue rate, at the specified depth bin which is unknown.

The detection probability (as opposed to the probability of localisation) was then calculated by running a new Monte Carlo simulation for all drifters (not just the vertical arrays) with $d(z)$ incorporated as the depth distribution. $\widehat{P}(R)$ (R is horizontal range) was calculated by summing $\widehat{P}(R, z)$ across all depths (Figure 4). $\widehat{P}(R)$ was then multiplied by a triangular step function to weight probability correctly by range; i.e. account for the fact there are more porpoises as surveyed area increases with increasing range bins (Marques et al. 2013) .

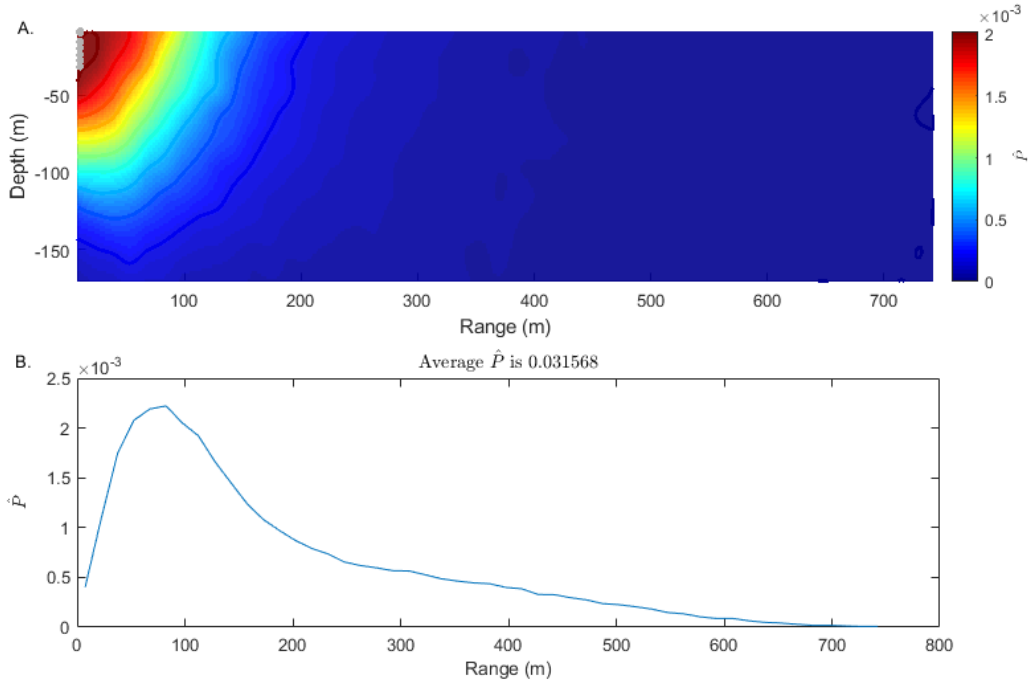

Figure 4. Plot A shows the 2D probability of localisation *for the boat based vertical hydrophone array. The grey dots indicate the boat-based vertical hydrophone array for scale. Plot B is the probability of* detection *over all depths which accounts for animal depth distribution and has been weighted by range to account for the fact that more animals are present at larger range bins (because the covered area is greater). The total probability of detecting a harbour porpoise in a circular area around the array is ~ 3%.*

5.3.4.2 Foraging Rate

If the density of both clicks and buzzes is known, then the number of buzzes per animal per second can be calculated by

$$F = \frac{\hat{c}_c \hat{D}_b}{\hat{D}_c} \qquad \text{Eq. 5.6}$$

were F is the number of buzzes per second, $\hat{D}_b$ is the density of buzzes, $\hat{D}_c$ is the density of standard echolocation clicks and $\hat{c}_c$ is the cue rate standard echolocation clicks.

5.3.4.3 Temporal and Spatial Subdivision of Effort

To quantify the density of porpoises by habitat, the study area was divided into ten regions based on current speed and bathymetry contours (Figure 5). Regions 1 and 2 contain the fast-flowing jet immediately south of the Kylerhea narrows with a water speed which was, on average, greater than 1ms^{-1} whilst regions 3 to 6 are regions which surround the jet with lower current speeds. Regions 1-2, 3-4 and 5-6 are also divided based on the 100m depth contour i.e. Regions 1,3 and 5 have water

depths of less than 100m while 2,4 and 6 have depths greater than 100m. Regions 7 and 9 were characterised by fast-flowing water in the Kyle Rhea narrows with Region 7 a particularly shallow (~12m) area. Region 8 is everything else in the south side of Kyle Rhea and region 10 is the fast-moving jet of water which leaves the north side of Kyle Rhea in the flood tide. Region 10 was only surveyed in 2015 and there was not sufficient survey effort to analyse surrounding areas.

The survey effort was also divided into two tidal states: ebb and flood. Ebb included times between one hour after high tide to one hour before low tide, and flood included times between one hour after low tide to one hour before high tide. There was little effort outside these times and these data have not been analysed here. Thus, for each year, there was a total of 20 analysis areas for click and buzz density: 10 regions during flood tide, and 10 regions during the ebb tide.

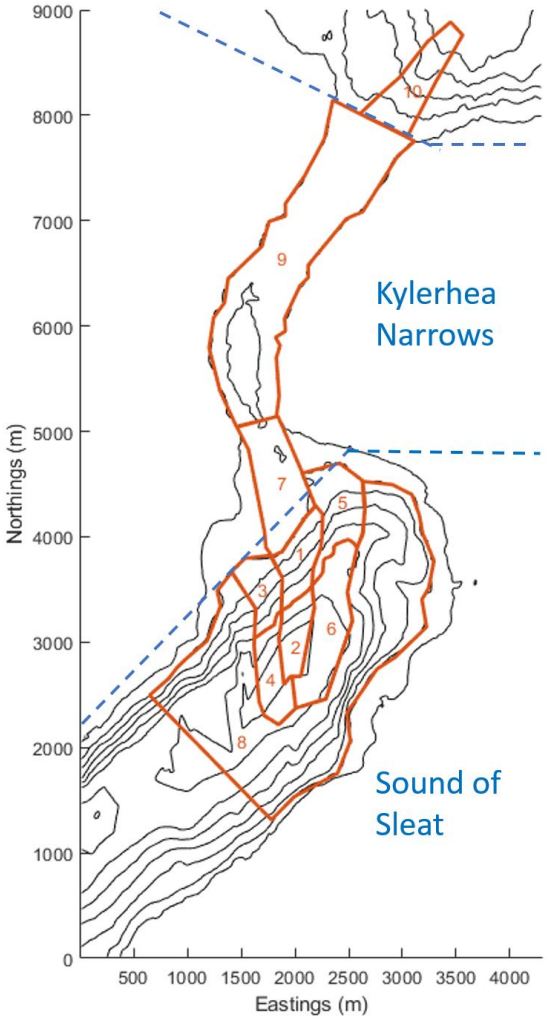

Figure 5. Division of Kylerhea and the Sound of Sleat into discrete survey regions. The regions are based on both tidal speed and bathymetry. Regions 1 and 2 contains a rapid spit of water which then exits immediately south of the Kylerhea narrows into the deeper Sound of Sleat. Regions 3-6 surround the high current area and region 8 is everything remaining. Regions 7 and 9 are the tidal rapids in the Kylerhea narrows. Region 10 is a spit of water similar to region 1 which enters deeper water north of the narrows during the flood tide (This was only surveyed in 2015).

5.3.4.4 Summary of Distribution Values

A summary of the input distributions to the simulation discussed above along with information sources is shown is Table 2. Some input distributions were measured using the vertical hydrophone arrays in each region and others were acquired from previous chapters and literature. Supplementary section 5.9.7 has a full table with measured distribution values for all region.

Table 2. Summary of the inputs into the probability of detection Monte Carlo simulation. Two simulations were performed. One using source level distribution and beam profile for echolocation clicks and the other using lower source levels and a wider beam profile for buzzes.

Data input	***Data source***	***Value or Distribution.***	***Varies by Region***	***Reference***
Horizontal orientation	-	Uniform	No	-
Vertical orientation	Tracks from vertical arrays	Example for region 1: Normal: mean 4.86°, SD 10.2° between 0 and 10 meters and 9.29° SD 16.74° for the rest for the water column	Yes	Section 5.3.4.1.3
Click source level	Vertical array data	Normal: mean 191 SD 4.7 dB re 1µPa pp at 1m	No	Section 5.4.6
Click beam profile	External captive porpoise study	Data from Chapter 4	No	Chapter 4 (see Figure 4)
Depth distribution of clicks	Localisation data from vertical array data	Custom depth distribution for different areas	Yes	Section 5.4.4
Buzz source level	Vertical array data	Normal: mean 161 SD 4.7 dB re 1µPa pp at 1m (Click source level -30dB)	No	(Wisniewska et al. 2016)
Buzz beam profile	External captive porpoise studies.	Data from Chapter 4 and Wisniewska *et al.*, (2015)	No	Chapter 4 (see Figure 4) and Wisniewska *et al.*, (2015)
Depth distribution of buzzes	Localisation data from vertical array data	Same depth distribution as clicks	Yes	Section 5.4.4
Threshold	PAMGuard click detector settings	10 dB + 5 dB compensation value	No	Supplementary 5.9.3
Noise	PAMGuard click detector noise output	Variable	Yes	Section 5.3.4.1.1

5.3.4.5 Summary of Density Estimation

For *each region* the density of standard echolocation clicks and buzzes was calculated. Buzzes were then sub divided into foraging buzzes and communication calls. A foraging buzz rate per animal, a proxy for foraging rate, could then be determined for a given standard echolocation click production rate (see Eq 5.6)

A summary of the density process based on the Monte Carlo simulation described in section 5.3.4.1 was as follows;

For each survey region

1. *For each localising array*
    - Vertical orientation angle distributions were calculated from dive track data collected on the vertical arrays in the current region.
    - The *localisation* probability for both vertical arrays was simulated using a modified Monte Carlo simulation using the input values from Table 2 for noise values between 95 and 140 dB re 1µPa in 1 dB bins.
    - A localisation probability was assigned to each localised click based on its depth and instantaneous noise measurement.
2. A depth distribution was calculated for the region from localised clicks of both arrays and assigned localisation probabilities using Eq 5.5.
3. *For all PAM drifters*
    - The probability of *detection,* $\hat{P}$, was calculated using a Monte Carlo simulation for noise values between 95 and 140 dB re 1µPa in 1dB bins using input data from Table 2. Each simulation applied the depth distribution and vertical dive angles calculated in the previous step.
    - A time series of the probability of detection $\hat{P}\ (noise)$ was constructed based on the received noise level on the instrument. This was then averaged to give a single value for $\hat{P}$.
    - $\hat{P}$ was input in the density estimation equation (Eq 5.1), along with the number of clicks detected, the false positive rate, and the expected detection area. Cue rate was removed so that $\hat{D}$ is the *density of clicks/buzzes*.
4. The mean density of clicks over all instruments, weighted by effort in the survey region, was calculated.
5. Absolute porpoise density for the survey region was calculated for a range of values between the minimum and maximum cue rate limits.
6. Steps 3-5 were repeated for buzzes, changing the source level distribution and beam profile in the Monte Carlo simulation and false positive rate in Eq 5.1.
7. Buzz density divided by clicks density gave the number of buzzes per click and thus the number of buzzes per animal for a given click rate (Eq 5.6).

5.3.4.6 Sensitivity Analysis and Variance Estimation

To understand how potential uncertainties in the input parameters of the Monte Carlo simulation propagated through to precision in the final density estimation, a sensitivity analysis was carried out. Five core sources of uncertainty were considered: the vertical and horizontal orientation angles of the porpoise, the biosonar beam profile, the source levels, and the ambient noise/system sensitivity (the error in hydrophone sensitivity and propagation combine within the model via the same mechanism; the detection threshold i.e. system sensitivity).

Uncertainties were calculated for each input into the simulation as shown in Table 3. 200 full simulations of $\hat{P}$ were conducted and for each simulation uncertainties were drawn randomly from the pre-defined distributions in Table 3 and added to the relevant input parameters for simulation model e.g. if the input was a normal distribution then a random offset was added to the mean and standard deviation. The simulation was run exactly as in section 5.3.4.5 (including re calculation of depth distribution) and a probability of detection ($\hat{P}$) recorded.

The uncertainty in $\hat{P}$ was calculated from the distribution of all simulation results and the six input errors (predictor variables) were input into a least squares boosting linear regression model to determine which had the most significant effect on the estimation of $\hat{P}$ (response variable).

Table 3. Description of uncertainty estimates for input parameters to estimate the likely precision in density. The sensitivity simulation adds a random value from each uncertainty distribution to the relevant input distributions for the detection probability simulation.

Input	**Uncertainty Distribution**	**Source**
Vertical Dive Angle Mean	Normal: Mean: 0, Std 3.142°	From vertical angle simulations in supplementary section 5.9.5
Vertical Dive Angle Std	Normal: Mean: 0, Std 3.078°	From vertical angle simulations in supplementary section 5.9.5
Beam profile	Uniform: 5.5 to 7.4 cm aperture diameter.	Variation in forward beam measurements adapted from (Koblitz et al. 2012)
Source Level Mean	Normal: Mean: 0, Std 4.5 dB	Propagation of system sensitivity and localisation range errors in source level measurements (see section 5.3.4.1.5)
Source Level Std	Normal: Mean: 0, Std 2.3 dB	Propagation of system sensitivity and localisation range errors in source level measurements (see section 5.3.4.1.5)
Noise/System Sensitivity	Uniform: -3 to 3 dB	Variation in hydrophone sensitivity/experienced guess

5.4 RESULTS

5.4.1 Survey Effort, Tide and Soundscape

Two surveys were carried out in August 2014 and 2015 using drifting vertical arrays and SoundTraps/RTsys recorders. Figure 6 shows the survey effort for the flood and ebb tide periods. In total, 125.1 hours of high frequency acoustic recordings were collected on the ebb tide, and 134.1 hours on the flood tide. In 2014 the majority of survey effort was in the Sound of Sleat whilst in 2015 a significant portion of survey effort was concentrated in the Kylerhea narrows. Figure 7 shows the mean current speeds and direction and background noise levels during the ebb and flood tides from combined 2014 and 2015 GPS logger and acoustic data.

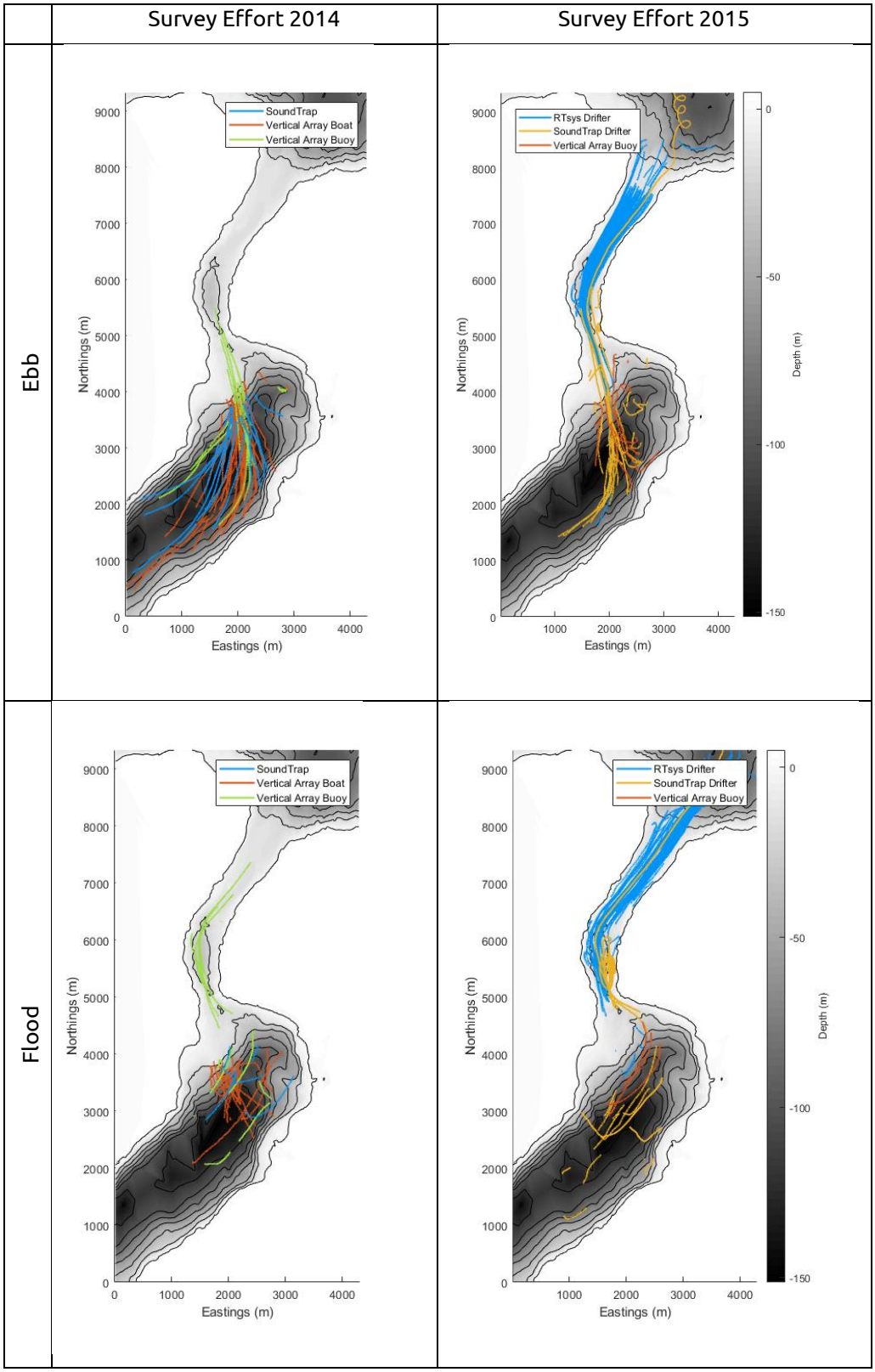

Figure 6. Survey effort in 2014 and 2015. In 2014 localisation arrays (Vertical Array Buoy/Boat) were used to localise the 3D locations of harbour porpoises. The SoundTrap and RTsys drifters in 2014/2015 were used to increase survey effort. Note that the length of tracks does not necessarily correspond to time surveyed; drifters in the narrows move much faster than drifters in the Sound of Sleat, especially during the flood tide. The colours of the line indicate that the type of device used.

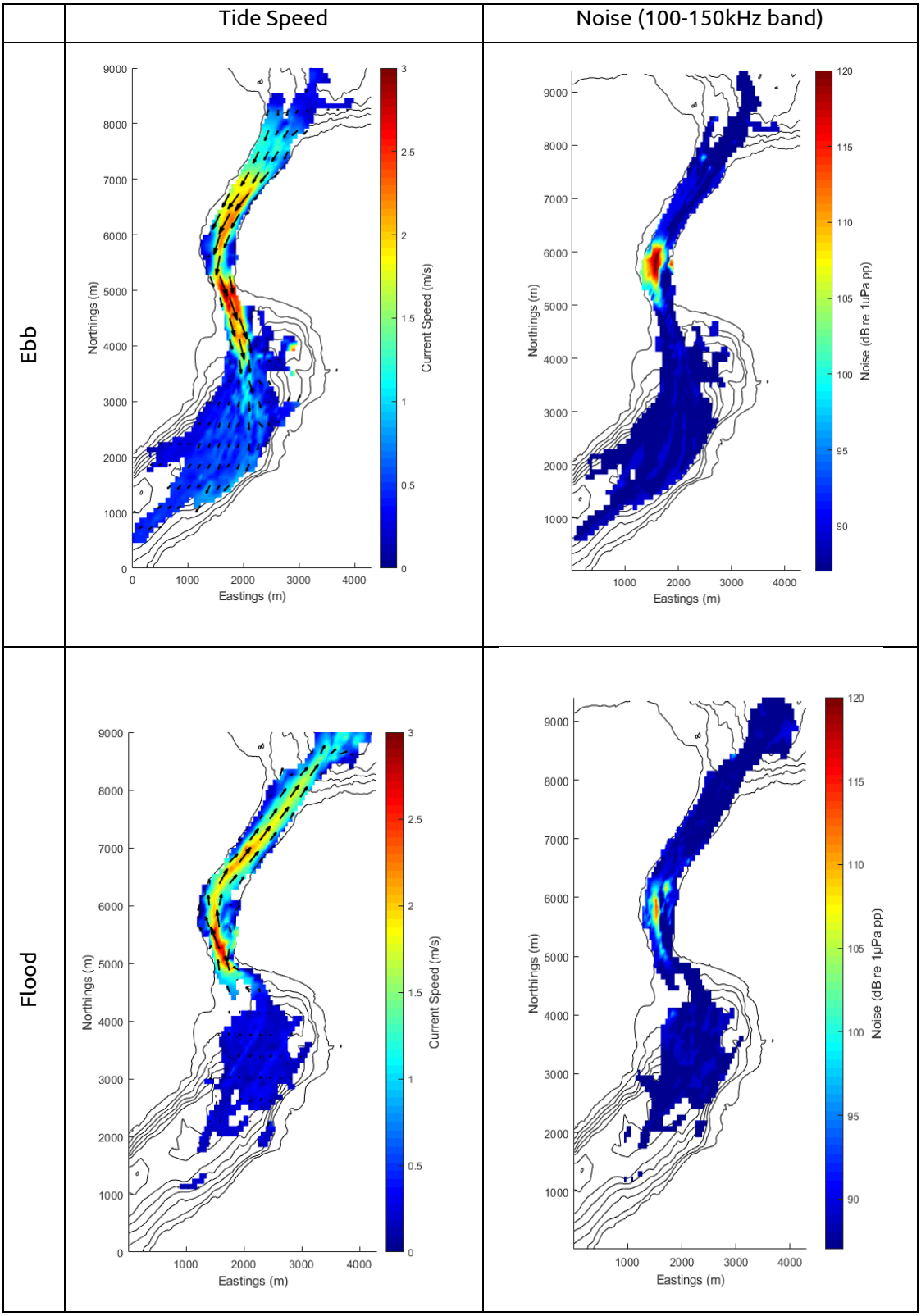

Figure 7. Average current speed and noise surface in Kylerhea and the Sound of Sleat for both the flood and ebb tides. Drifter speeds were used as a proxy for tide speed. Tide speeds are indicated by colour and the direction of the tide shown with arrows. Noise is the equivalent peak to peak noise between 80 and 150kHz from the click detector algorithm (see section 5.9.3) i.e. this is the noise relevant for the detection of clicks scaled so it can be compared easily to peak to peak source/received level. Note that noise can vary by ~6dB in most areas, however, noise in the tidal channel can be >120 dB re 1uPa pp.

5.4.2 Buzz and Click detections.

663,000/408,000 (5845/2845 h^{-1}) ebb/flood confirmed porpoise clicks and 3687/1512 (13/6 h^{-1}) ebb/flood buzz click sequences were detected during the study once false positives and duplicates between hydrophones in the same array had been removed.

5.4.3 Tracks and Horizontal distribution

A total of 56, 058/60,811 (ebb/flood) clicks were localised using the vertical hydrophone arrays. This resulted in a total of 1541/1034 (ebb/flood) 3D dive track fragments. Figure 8A shows a 3D plot of all the dive tracks in the Sound of Sleat and an example of dive tracks is shown in Figure 8B. Note that in Figure 8A the dive tracks are concentrated on the slope immediately south of the Kylerhea narrows and in both figures animals are sometimes diving close to the seabed.

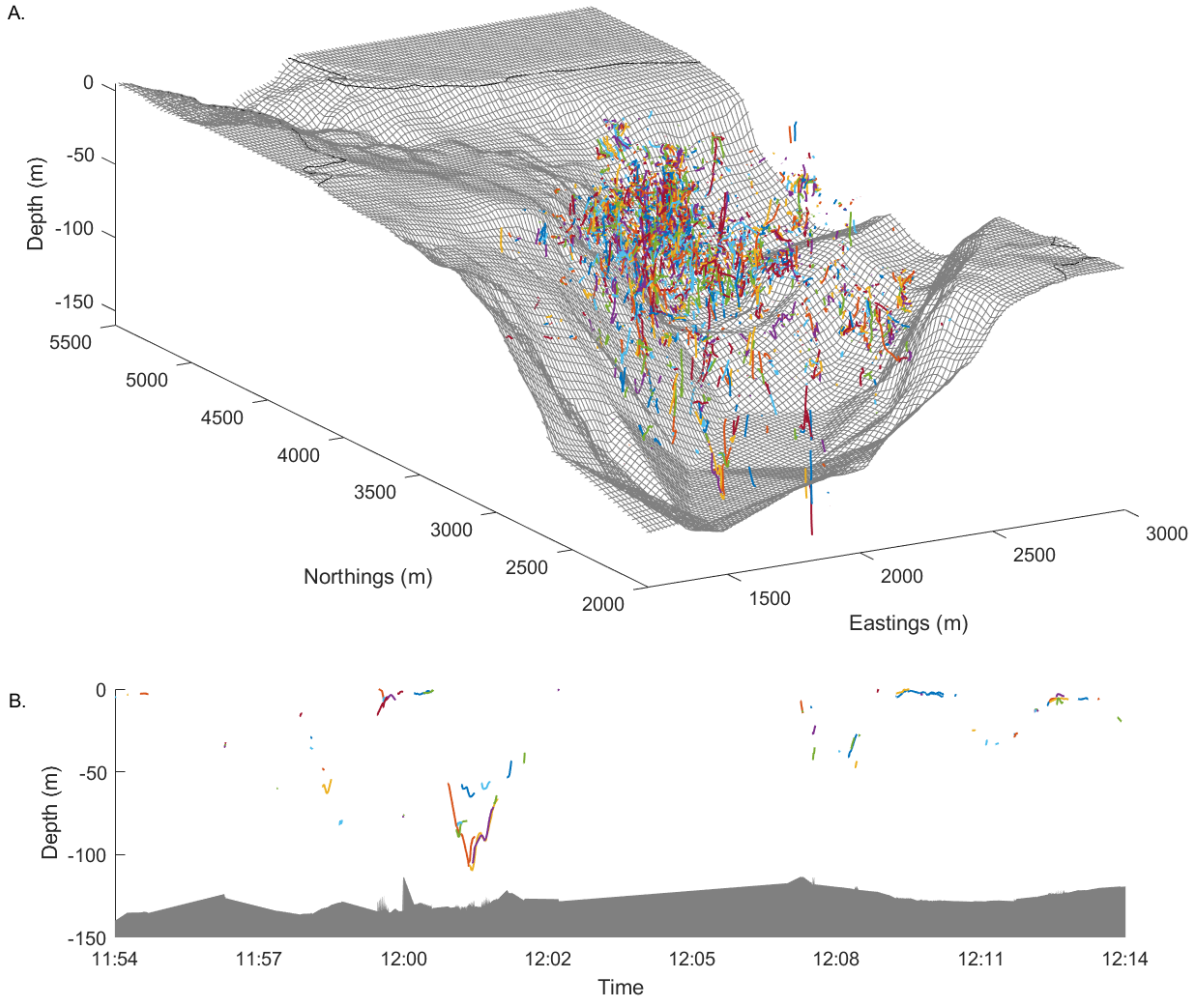

Figure 8. Plot of 3D porpoise tracks collected in the Sound of Sleat using the boat based and autonomous vertical array. Plot A. shows all collected 3D tracks in the study area (no porpoises were detected on vertical arrays in the tidal narrows). The southern entrance to the Kylerhea narrows is in the top left corner ((x,y)=(1600, 5000)). Note the apparent concentration of tracks on the slope, where the fast-moving current moves into the deeper water of the Sound of Sleat. For illustrative purposes, the z axis has been exaggerated. Plot B. Shows an example of a time and depth of tracks over a 20-minute period. Multiple harbour porpoises are tracked diving close together to over 100m. Grey indicates the depth at the location of the track.

5.4.4 Depth distribution

The depth distributions during the ebb and flood tides were calculated for all regions of the tidal stream using the distribution of localised depths and simulations of $\widehat{Pl}$ as described in section 5.3.4. Figure 9 shows depth profile for different regions during the ebb and flood tides. Depth profiles are only shown for regions where more than 500 successfully localised clicks were detected.

Depth distributions in the same regions differed between ebb and flood tides. During the ebb tide, in most regions, the depths were distributed in a log-normal-like profile with peaks towards the water surface. However, during the flood tide (dashed lines) there is an additional peak in the depth distributions at around 30-40m in most regions.

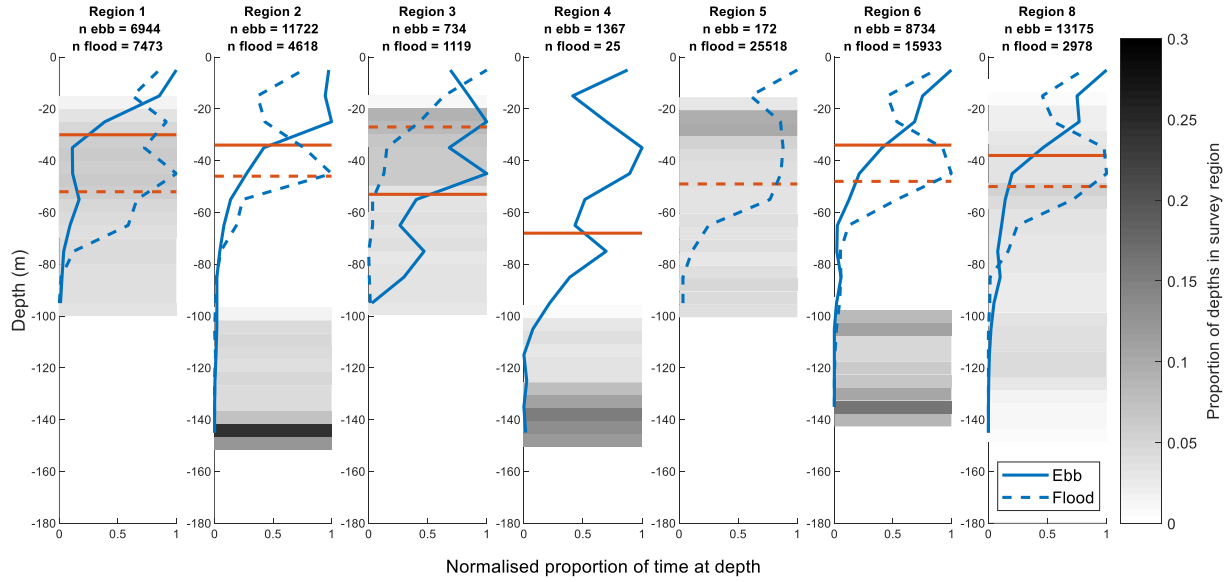

Figure 9. Depth distribution of clicks for different regions of the tidal stream. Blue lines show the depth distributions during the ebb (solid line) and flood (dashed line). The horizontal solid and dashed line shows the depth above which animals spend 75% of their time for ebb and flood respectively. The depth of the seabed is shown in greyscale, with different colours indicating the distribution of bathymetric depths within the region. Assuming production rate of standard echolocation clicks (cue rate) does not vary substantially with depth, this represents the depth distribution of animals.

5.4.5 Orientation Distribution

Dive tracks were used to calculate the orientation of porpoises with respect to the tide. Orientation was based on the current speed and the 3D dive tracks calculated form the vertical hydrophone array. The orientation is in the frame of reference of the moving body of water; e.g. an orientation of 180° indicates that an animal is swimming directly against the current, however, not necessarily faster than the current speed i.e. it's movement across land may be in a different direction. An orientation of 0° indicates a harbour porpoise swimming with the current. Only tracks within 75m of the array were used as these are the most accurate localised positions (see Chapter 3 Figure 3). The regions in these plots have been merged to increase sample size. There are three combined regions which correspond to regions 1-2, 2-3 and 5-6 (see Figure 5).

The orientation plots in Figure 10 show that, during the ebb tide, in regions 1-2 porpoises predominately swim against the tide, which would be consistent with maintaining position, and in regions 3-4, appear to swimming laterally with respect to the tide, however, this has low sample size. Regions 5-6 show near random orientation. During the flood tide, orientations appear more random or have very low sample size with porpoises perhaps moving with the current in regions 1-2.

Ebb

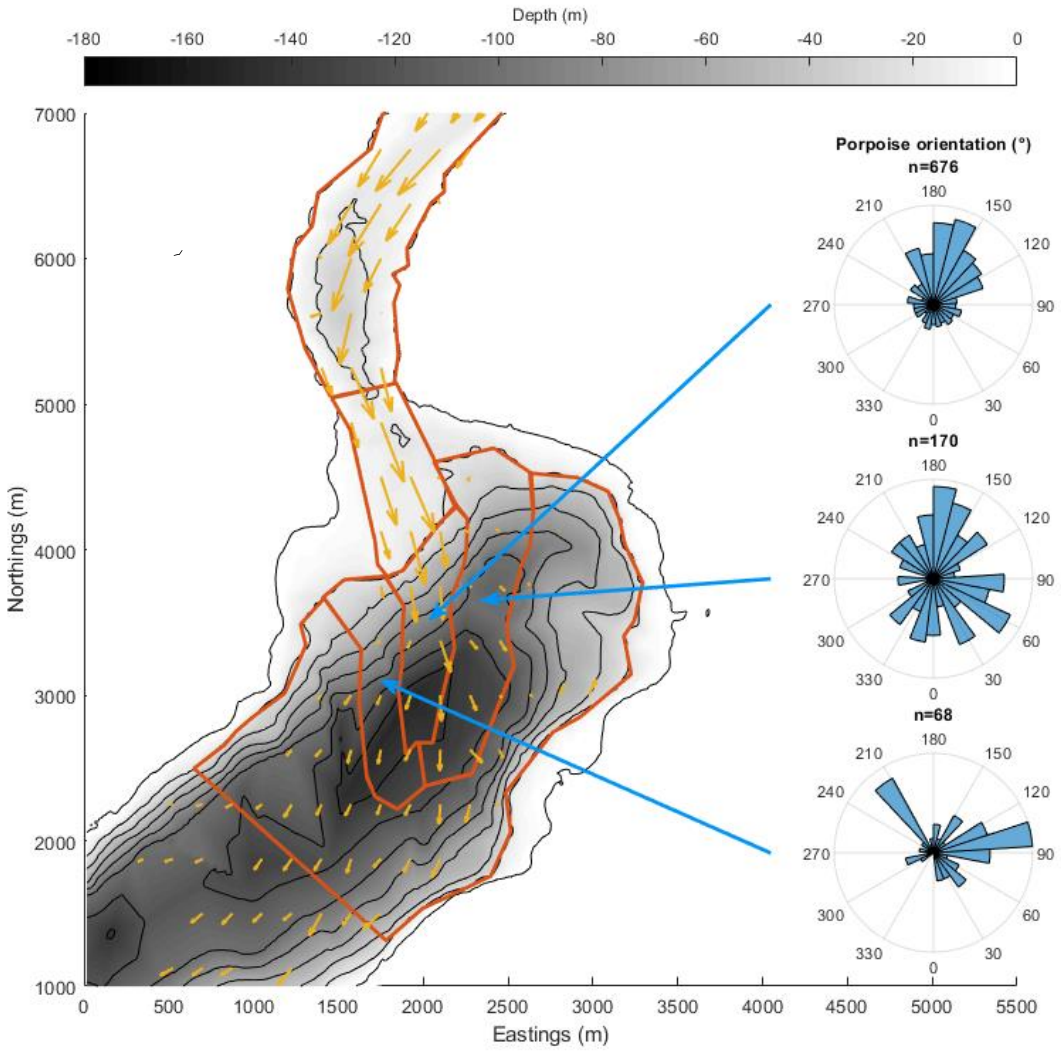

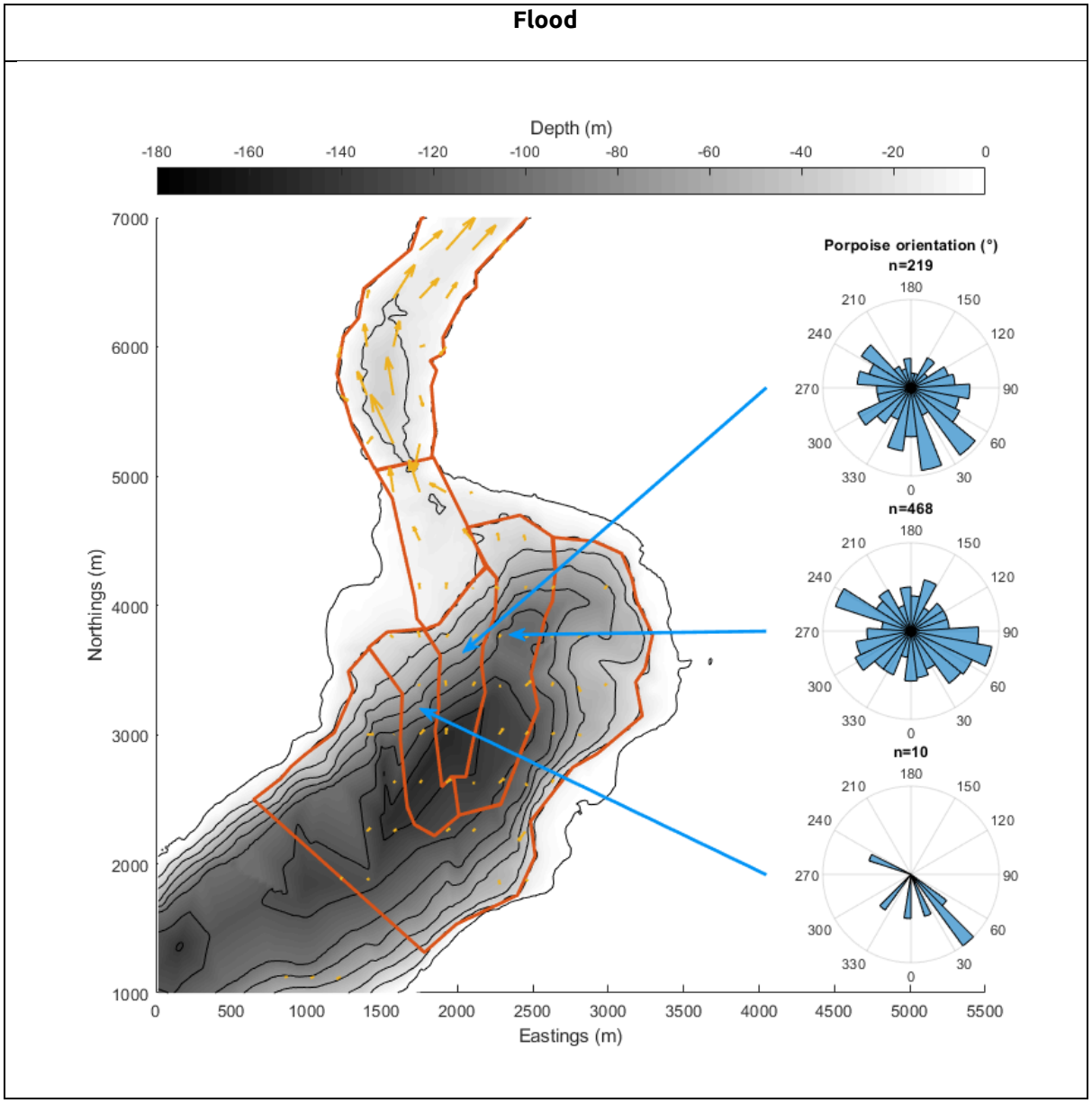

Figure 10. Orientation plots of porpoise tracks during the ebb and flood tides for different regions of the tidal stream. The orientation plots show the direction of the porpoise with respect to the direction of the tidal flow in a specified region. 180° indicates that a porpoise is swimming directly against the current and 0° indicate the porpoise is swimming in the direction of and with the current. In the ebb tide porpoises are almost always swimming against the tide in combined region 1-2.

5.4.6 Source Levels

A total of 35 click trains with obvious scanning behaviour and manually validated on axis clicks were used to calculate source levels. The mean source level was 191 (SD= 4.7) dB re 1µPa pp at 1m.

Using Eq 2, the maximum detection range using the upper 95% source level (200 dB re 1 µPa pp at 1m) was calculated to be ~750 m (for an assumed noise level of 95 dB + detector threshold of 10 dB +5dB compensation factor (see section 5.3.4.1.1)). This equates to a value of 0.56 km^2 for a_c in Eq. 5.1

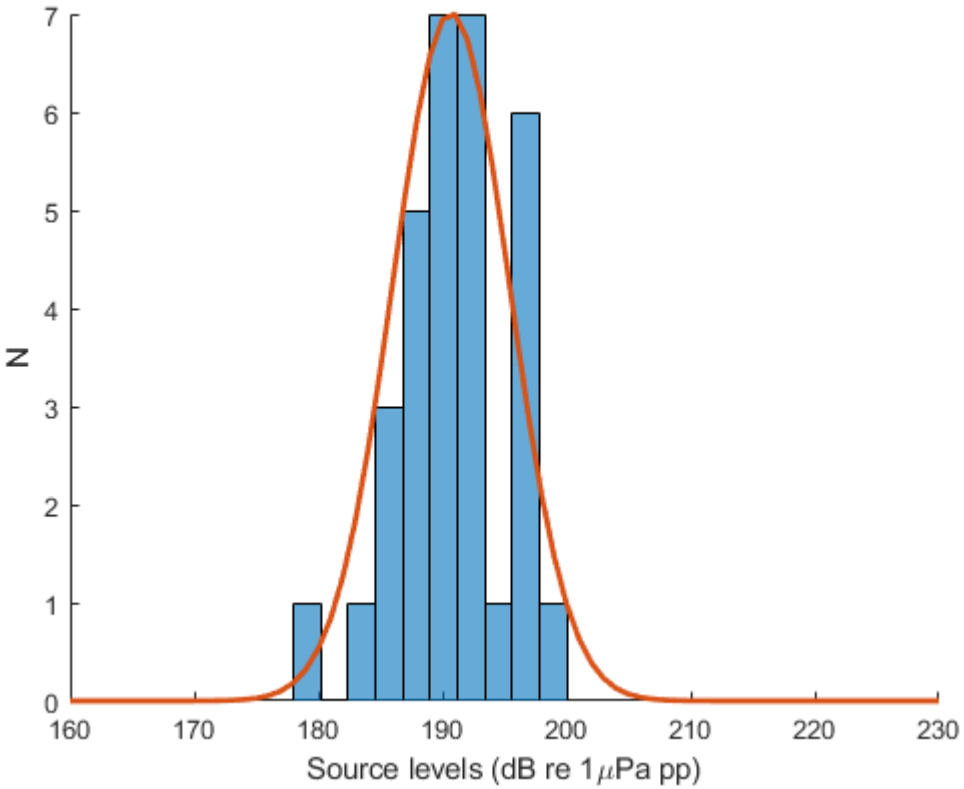

Figure 11. Source levels of echolocation clicks (not buzzes) with fitted normal distribution 191 (SD= 4.7) dB re 1µPa pp. There were a total of 35 measurements of the apparent on-axis source levels. Buzz clicks used the same distribution but with -30 dB mean source level i.e. 161 (SD= 4.7) dB re 1µPa pp at 1m.

5.4.7 Density and Foraging Rate Estimation

Figure 12 shows an example of estimated porpoise density and foraging rate for all regions on the ebb/flood tide in 2014/2015. A click production rate ($\hat{c}$ in Eq. 5.1) of 3 clicks per second was assumed to generate an animal density. The number of foraging and communication buzzes per animal was then calculated using Eq. 5.6. The SoundTrap drifter with a deep hydrophone at ~100 m (see Figure 2) had a detection probability for buzzes an order of magnitude lower compared to other drifters because animals were primarily located at much shallower depths and the detection range of a buzz is low. This meant that very small uncertainties in $\hat{P}$ could propagate to very large errors in density and thus this data from this drifter were not included in foraging rate calculations. PLABuoy data was also not included in buzz detection in 2015 due to electrical noise triggering false positive buzz

detections. A minimum of at least two hours of survey effort was required for density to be plotted in a region. This condition was never met for region 7 because it was one of the fastest moving areas of the tidal stream; however, very few clicks were ever detected in this region (see supplementary 5.9.7).

The highest density of porpoises was observed during the ebb tide, 2014, in region 1 and 4 (11.3 and 13.5 porpoises $\cdot km^{-2}$ respectively). The proportion of buzzes in each region determined to be communication calls rather than foraging attempts was on average 34/32% (ebb/flood).

The total number of harbour porpoises in all regions was (36.9/30.4) ± (12.9/ 10.6) (ebb/flood) in 2014 and (15.2/9.3) ± (5.32/3.3) (ebb/flood) in 2015. There is therefore a 59/70% (ebb/flood) drop in harbour porpoise density between 2014 and 2015.

Uncertainty in density is due to the simulated uncertainty in $\widehat{P}$ of around ~±35% detailed in section 5.4.8. It should be noted that density also scales with cue rate (see Figure 14) which was assumed to be 3 clicks per second but is impossible to accurately calculated from PAM data (see section 5.3.4).

A summary of all calculated metrics and densities for each survey region, tide state and year is provided in supplementary material 5.9.7.

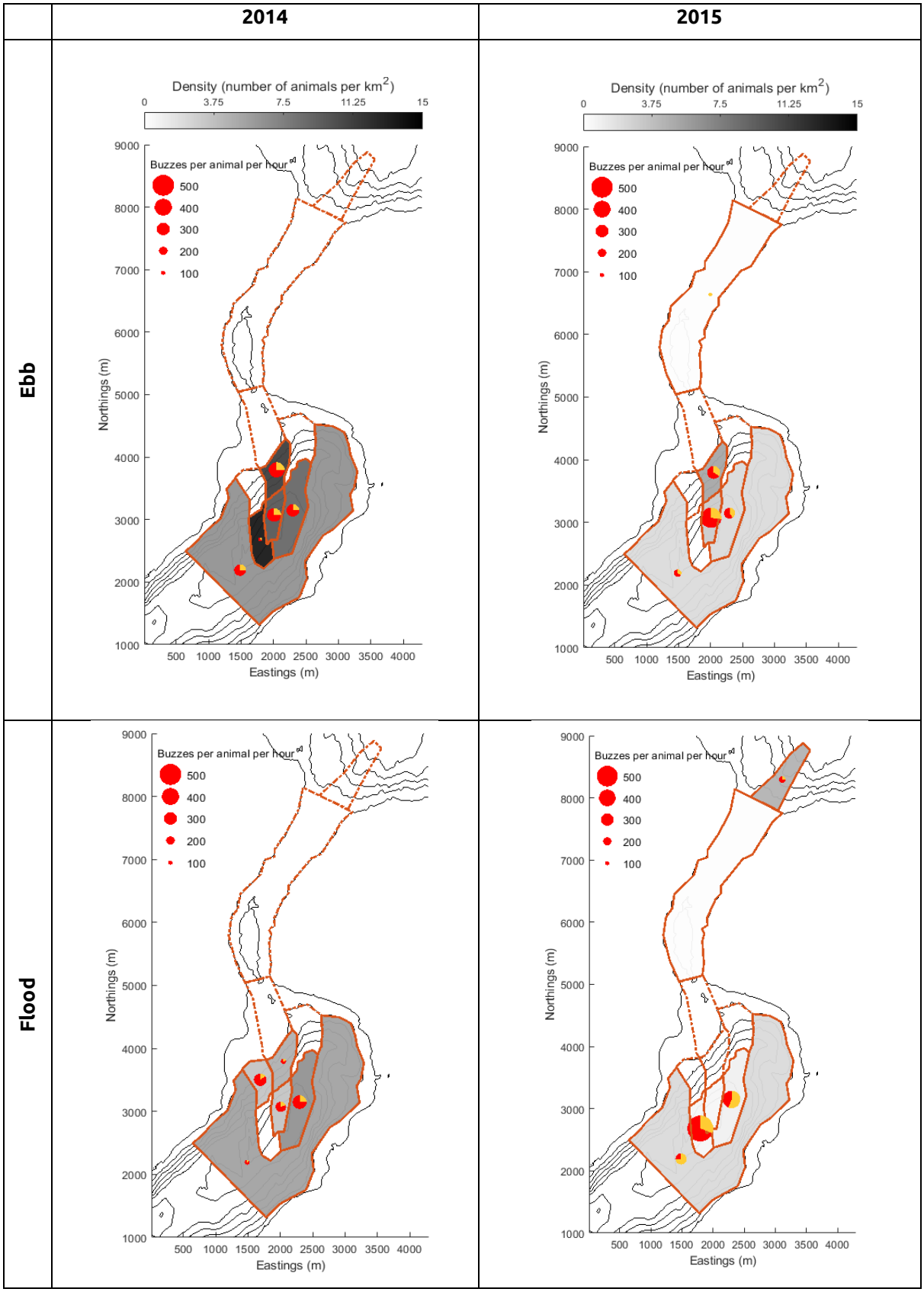

Figure 12. Density and foraging rate/communication rate estimates for ebb and flood tides during 2014 and 2015 surveys. Each region is shaded by the density of animals assuming an average click production rate (cue rate) of 3 clicks per second. The size of red/yellow circles within each region indicate the number of buzzes per animal per hour. These are further sub divided into likely foraging buzzes (red) and communication calls (yellow). Regions which

have a dashed line and no fill did not have the minimum 2 hours of drifting survey effort. Note the Kylerhea narrows was only adequately surveyed in 2015 but there were almost no porpoise detections and as such density is almost zero.

5.4.8 Sensitivity analysis

Figure 13 shows results from the regression analysis of detection probability, $\hat{P}$ (region 1, ebb tide) bootstrapped (n=200) with estimated uncertainties for the simulation input parameters (see Table 3). Figure 13A plots the relative importance of each input in calculating $\hat{P}$ and indicates that mean source levels are by far the primary drivers of uncertainty in $\hat{P}$, explaining 72% of variation. Thus, alongside cue rate, source level is one of the largest contributors to uncertainty in the density of animals. Figure 13A shows a boxplot of all simulated detection probabilities with outliers removed. Mean/median $\hat{P}$ was 0.089/0.085 (SD = 0.388) and 25th and 75th percentiles were 0.0580 and 0.1161 respectively. This indicates that the uncertainty in $\hat{P}$ is around ~±35% (using the average of 25th and 75th percentiles).

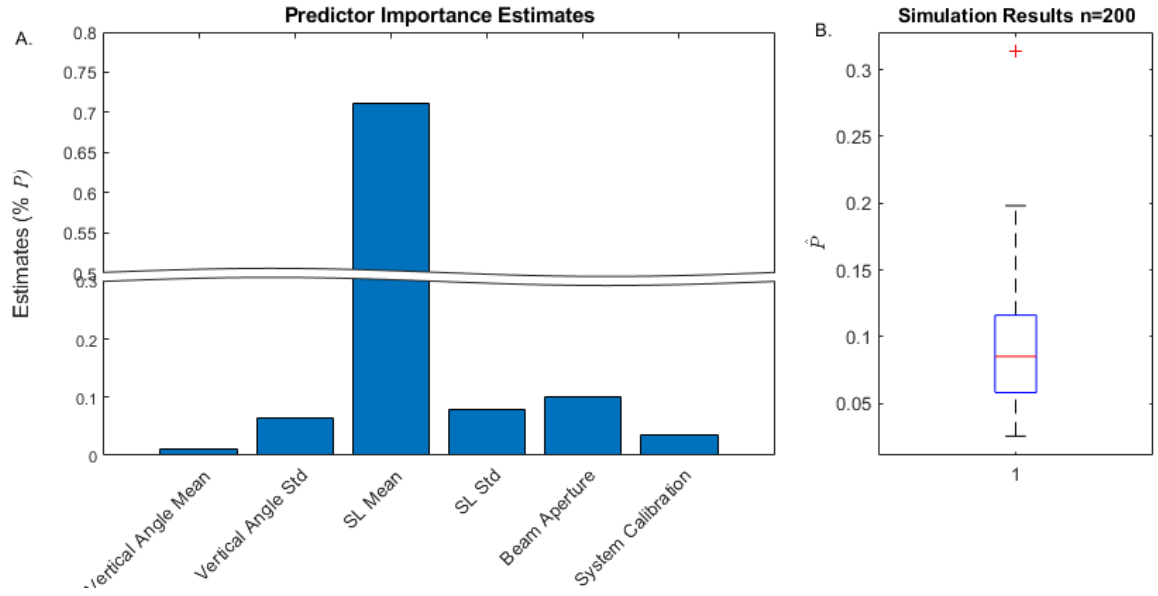

Figure 13. Results from the sensitivity analysis for simulating the probability of detection $\hat{P}$. Graph A. shows the relative importance each input to the simulation has on overall $\hat{P}$. Note that there is a break on the y-axis. Mean source level (SL) has by far the greatest effect on $\hat{P}$. Graph B. shows a boxplot of all values of $\hat{P}$ calculated from the 200 sensitivity simulations. The central red line indicates the median, and the bottom and top edges of the blue box indicate the 25th and 75th percentiles, respectively. The whiskers (black dashed) extend to the most extreme data points not considered outliers (red + symbol(s)).

Figure 14 shows the density of harbour porpoises and buzz (foraging and communication) rate for a single region (region 1) with respect to cue rate (see Eq . 5.1 and Eq 6.) during the ebb tide in

2014/2015. The filled areas show the 25th and 75th percentiles in density and foraging rates propagated from the sensitivity analysis of $\widehat{P}$ using Eq 1. i.e. they are the uncertainty estimates from Figure 13B. The vertical dashed line shows the mean click production rate calculated directly from the ICI of click train detections. This represents the maximum likely mean click rate as it assumes there were no periods in which animals were silent. Figure 14 shows how density and foraging rates scale with estimated cue production rate and the uncertainty that propagates from $\widehat{P}$. This demonstrates that cue rate is an important parameter to establish for accurate density estimation and that minimising uncertainty in input parameters, primarily source level, can significantly improve the precision of results. The porpoise density in region 1 is lower in 2015 compared to 2014, however, the buzz rates remain broadly consistent between both years.

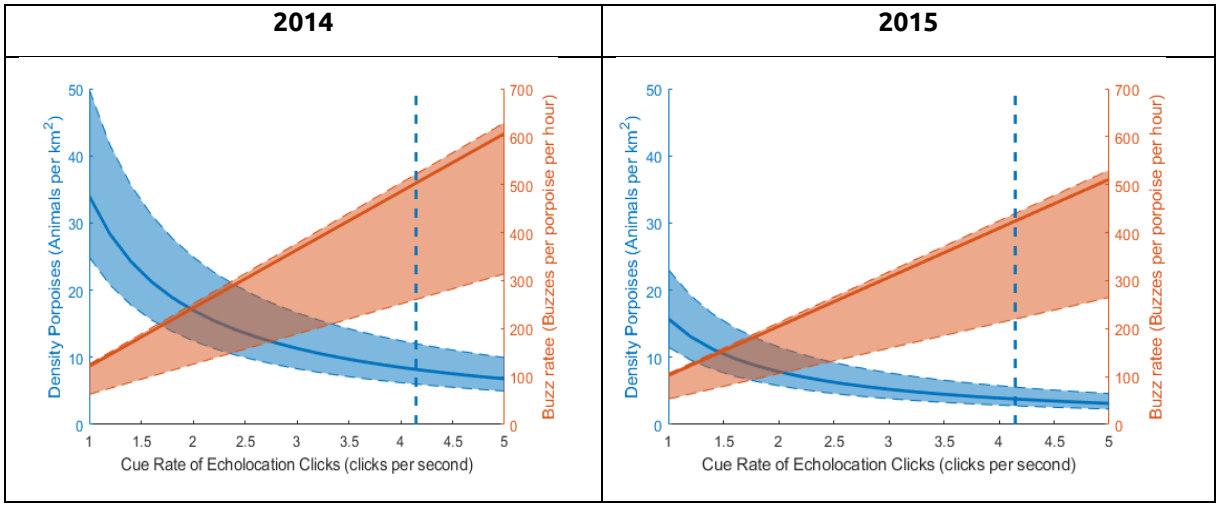

Figure 14. Example plots of density and buzz rate versus the estimated cue rate with uncertainty estimates for region 1 (directly south of the main tidal rapids) during the ebb tide in 2014 and 2015. Blue shows the number of animals per square kilometre and orange indicates the number of buzzes per animal per hour. Dashed lines are the 25th and 75th percentile interval error estimates from the sensitivity analysis of $\widehat{P}$. The dashed vertical line is the cue rate measured from click train detections. This represents the likely maximum cue rate. Note that region 2014 had the highest density of animals but foraging rates remain broadly consistent for both years.

5.5 DISCUSSION

This study describes the development and application of PAM methods to calculate the density, distribution and fine scale diving and foraging behaviour of harbour porpoises in a complex tidally energetic habitat. The density estimation methods were based on using a Monte Carlo approach to model detection probability of clicks and buzzes, a method which has been used in a variety of other studies (Küsel et al. 2011, Frasier et al. 2016, Hildebrand et al. 2019). The key innovation in this study is that almost all the input information for the model (noise, on-axis source levels, vertical dive angles

and depth distribution) was collected at the study site and during the survey using vertical 3D hydrophone arrays. This meant that the only external information required for the Monte Carlo simulation of $\widehat{P}$ was the beam profile which has been measured from a captive animal (see Chapter 4) (and is unlikely to change with location) and buzz source levels which were acquired from a previous study of tagged wild animals (Wisniewska et al. 2016). Hence this method provides a framework for estimating behaviour and density of toothed whales in tidal rapid habitats using data from drifting PAM devices. Both the simple PAM recorders and more complex arrays can be fully autonomous and easily deployed, meaning that large research vessels are not necessarily required. Further this methodology can likely be generalised to other environments and other echolocating taxa, including bats.

5.5.1 Uncertainty in density estimation and foraging rates

However, whilst this approach shows promise, the core of the method is a Monte Carlo model which can give inaccurate results if there is biased input data (which I have tried to minimise here via direct measurement), erroneous assumptions, and unknown unknowns. In this application several critical assumptions were made. Firstly, it was assumed that harbour porpoises were randomly distributed with respect to drifter tracks, a key requirement of any distance sampling methodology. This a weakness of drifting PAM systems in tidal rapids because it is likely that the distribution of animal's is related to current speed and direction which also determines the track of a drifter. However, the track a drifter takes through a tidal stream is very sensitive to starting location and tide state, thus tracks would pass through smaller regions randomly because drifters were deployed at semi-random upstream locations and times. In region 8, which is relatively large, tracks were not close to being distributed randomly and so it is highly likely that the realised survey effort, and resulting density estimates, are not representative across the entirety of region 8. Another key assumption was that the horizontal angle of porpoises was uniformly distributed between -180° and 180°. Although the horizontal tracks of porpoises were measured in Figure 10 these will be biased by detectability and so, although they can be used to infer general behaviour, they cannot be used to calculate accurate horizontal distributions. However, it is likely that horizontal angles will not affect density estimates regardless of the animal's true orientation distribution. For example, if porpoises were consistently oriented against the tidal current, then a drifter approaching the porpoise from upstream will detect proportionally more clicks as it approaches an animal than if that porpoise were randomly orientated.

Once the drifter passes the porpoise, it will detect proportionally fewer clicks. If porpoises are indeed distributed evenly within the study area with respect to the drifters, then the net effect over many drifts is to detect the same number of clicks regardless of whether the animal is orientated randomly, against or with the tide. The same cannot be assumed for vertical angles because porpoises are definitely not distributed evenly in depth. Vertical dive angles were calculated using the vertical hydrophone array which means there is a potential for a circular argument in these data because harbour porpoise clicks are highly directional and so the number of clicks detected and localised will depend on the vertical angle of the porpoise and position and depth of the hydrophones. This was explored with simulations (see supplementary section 5.9.5) which demonstrated that, based on recorded source levels and the assumed beam profile, vertical dive angles were robust if calculated from tracks within 50 m horizontal range of the hydrophone array and no deeper than the deepest hydrophones, in this case 30 and 45 m. This is because, at close ranges, the beam profile is detectible regardless of an animal's orientation, thus negating the circular argument. Thus, the assumption here is that vertical angles below the bottom of the array are the same as those above. This is unlikely to be true, however, sensitivity analysis in Figure 13 showed that any uncertainty in this assumption is unlikely to make a large difference to the final results. Finally, buzzes were relatively rare and so calculating an accurate depth distribution was not possible for each region. Thus, it was assumed that the depth distribution of buzzes followed that of echolocation clicks.

Sensitivity analyses showed that the simulation was most sensitive to the assumed on-axis source level of animals and that errors in mean source level can lead to order of magnitude changes in detection probability and thus density, as shown in Figure 13. However, the mean source levels directly measured at the site were within 1dB of source level measurements of wild harbour porpoises measured in Denmark (Villadsgaard et al. 2007). This provides some degree of confidence that the source levels of clicks measured here (and thus density) are not at the extreme end of uncertainty distributions. However, a key requirement in this type of survey in the future is the ability to measure source level with a high degree of certainty. This would likely require a hydrophone array designed primarily for source level measurement such as that used by Ladegaard et al. (2017).

One of the issues with density estimation for marine mammals using PAM is that it is very difficult to perform a control experiment i.e. there are very few situations in which density can be measured in

an area where the number of animals' is precisely known. One way to increase confidence in estimates is to calculate density using two different datasets, e.g. a visual and acoustic dataset, and compare results. Here there were no suitable additional datasets to use to calculate density, however, Figure 14 shows that the buzz rate in region 1 during the ebb tide (one of the areas with most effort) was very similar (within 17%) between 2014 and 2015, despite an over 50% drop in density; this is what would be expected for animals which employed a specific foraging strategy in tidal streams. Different instruments with different noise floors, depths, hydrophones etc. were used in 2004 and 2015 and so, if the underlying Monte Carlo simulation model were wrong, then it would be unlikely that buzz rates would be similar.

5.5.2 Harbour Porpoise Behaviour and Distribution

From a biological perspective, the results appear to show two modes of behaviour which are influenced by tidal state.

5.5.2.1 Ebb Tide

The most distinct tidally coupled behaviour occurred during the ebb tide in fast moving currents in the Sound of Sleat. During the ebb tide in 2014 and 2015 harbour porpoises were found throughout the Sound of Sleat and in particularly high numbers in region 1, where a strong spit enters the deeper waters of the Sound of Sleat. There were almost no animals detected in the Kylerhea narrows. Animals located within the Sound of Sleat tidal rip (regions 1 and 2) were often orientated against the current flow (Figure 10) and there was also higher rates of foraging in this region (Figure 12). In 2014 (data deficient region in 2015) animals were also found in high numbers in region 4, just outside the faster moving spit of water. However, despite the high density of animals, the foraging rates were very low compared to regions 1 and 2. The distribution of orientation in this area suggested animals were moving laterally which could indicate them moving into and out of the faster moving waters of regions 1 and 2.

There are several theories as to why top predators, including harbour porpoises might be attracted to tidal rapids areas. It has been suggested that tidal narrows, may provide a "conveyor belt" increasing the animal's prey encounter rate without incurring high costs of movement (Hall 2011). However, to benefit from this, a predator must be able to balance the energetics of swimming in a high flow environment with the advantages of increased foraging success. The conveyor belt

hypothesis suggests that this is achieved if animals can "observe" the conveyor belt from a water body which is moving at a different speed. Harbour porpoises can detect prey using echolocation at ranges of 24 - 64m (Villadsgaard et al. 2007). At these scales, tidal currents can change significantly. A harbour porpoise could therefore hold position in a lower current area echolocating into a higher current area to locate prey. This could provide two energetic advantages. The first is that a higher number of prey animals per unit time would pass through the porpoise echolocation beam. Secondly, if the porpoise were echolocating upstream, then prey items can be intercepted efficiently as they are carried in the current towards the porpoise. Therefore, there is likely only an energetic advantage in a tidal stream if an area has a high current *gradient.* In Kylerhea there are two such areas; a large eddy in the middle of narrows (within region 9) and the fast spit of water (within regions 1 and 2) from the narrows into the deeper Sound of Sleat. If the hypothesis on high tidal gradients conferring an energetic advantage were correct, then it would be expected that most animals would be orientated against the tide and high levels of foraging activity would be evident. This is indeed the case, with region 1 and 2 the only areas in which animals are mostly orientated against the tidal stream and the locations with amongst the highest animal density and foraging buzzes per individual. Several studies have also suggested that schools of fish may be disorientated or broken up by eddies in tidal stream, leading to increased vulnerability to predators (Enstipp et al. 2007, Crook and Davoren 2014) and prey can be forced to the surface by strong currents which could help reduce the energetic cost in foraging dives for predators. This study did not analyse prey distribution, so it is difficult to draw concrete conclusions on this, however, the shift to shallower depth distributions during the ebb tide suggests harbour porpoise are foraging closer to the sea surface and likely indicates some shift in prey distribution, loosely supporting these hypotheses. Therefore, this type of tidal rapid habitat possibly confers an advantage for all the above reasons i.e. during the *ebb* tide there is a greater abundance of prey items passing through a harbour porpoises acoustic field of view, the time to intercept prey is reduced (in both range and depth) and foraging success might be increased if prey are disorientated.

5.5.2.2 Flood Tide

During the flood tide, harbour porpoises are more evenly distributed in the Sound of Sleat, change their diving behaviour significantly but maintain foraging buzz rates similar to that of the ebb tide (Figure 9 and Figure 12). This suggests a switch in foraging strategy from the ebb tide. During the

flood tide there are very few distinct tidal features in the Sound of Sleat and thus prey may be less concentrated in any single region. This would explain the more even distribution of harbour porpoises. Whilst harbour porpoises may not gain the same energetic advantages compared to the ebb tide it has been shown in other studies that prey concentrations are higher in the immediate vicinity of a tidal rips during both states of the tide (Benjamins et al. 2015). Thus, harbour porpoises may continue foraging in the area simply due to higher concentrations of prey. The maxima in depth distribution at ~40m during the flood tide could be a preference for a certain prey type; further studies using active sonar are needed to verify this.

It is interesting that in both tidal states, harbour porpoise do not take advantage of the eddy in region 9. This area contains high densities of common seals (Hastie et al. 2016) and high levels of high frequency noise. Thus, there may be a degree of very fine scale niche partitioning occurring and/or high levels of noise in this eddy (Figure 7) may degrade the effectiveness of harbour porpoise echolocation.

5.5.3 Energetic implications of high foraging rates

Previous studies of wild harbour porpoises using acoustic tags have shown that animals can produce foraging buzzes at rates of up to 500 buzz·hr^{-1}, with average rates of ~100 buzz·hr^{-1} and capture success per buzz around >90% (Wisniewska et al. 2016). Here the average number of foraging buzzes per animal over all regions, years and tides was 151 buzz·hr^{-1} with 306 buzz·hr^{-1} in the tidal rapids (region 1 and 2) during the ebb tide which is towards the upper scale of what has been recorded on wild tagged animals. Rojano-Doñate et al. (2018) measured the field metabolic rate of wild harbour porpoises and suggested individuals need to consume between 500 to 10000 fish or 21,600 kJ of fish (~4.32kg) per day, which is consistent with the high foraging rates buzz rates recorded by Wisniewska et al. (2016). If the buzz rates measured here reflect foraging rates, harbour porpoises could be consuming ~1836 fish per tidal cycle (6 hours). If prey in these tidal rapids are at the higher or medium end of the typical energetic content, it is possible a harbour porpoise could fulfil its energetic requirements in one or two tidal cycles (ebb and flood) (Booth 2020). It should be noted, however, that the absolute number of foraging attempts is highly dependent on capture success, prey type and the assumed buzz source level which was one of the few parameters that could not be measured directly at the site. However, the -30dB drop in source levels recorded on wild animals (Wisniewska et al. 2012) is higher than that recorded in captive animals (Deruiter et al. 2009, Wisniewska et al.

2012) and did not account for beam widening in apparent source levels (Wisniewska et al. 2015). Thus, it is more likely that foraging rates have been underestimated rather than overestimated (because source level has been over estimated). Thus, the type and energetic content of prey and the distribution of source levels of buzzes are two key information gaps that will help us better understand harbour porpoise foraging ecology in tidal rapids.

5.5.4 Absolute Density

Even at the higher end of possible cue rates and thus lower end of density estimates, as shown in Figure 14, the density of porpoises in the Kyle Rhea stream in 2014 is amongst the highest density of harbour porpoises ever quantified (Gordon et al. 2011). However, although the density is high, the area studied is small and so the total number of animals is likely between 15 to 60 at a given time. 2015 saw a ~50% decrease in the density of animals; it is unknown as to why this might be.

5.5.5 Future application of the methodology

It should be noted that this study described harbour porpoise density at a single tidal rapid site over a single month. Although the survey took place twice in consecutive years, the density and distribution of porpoises may change with the seasons. Thus, long-term monitoring efforts to investigate temporal trends in density over seasonal time scales are recommended for future studies. The continued miniaturisation and simplification of PAM hardware, that can record at the high sample rates required for porpoise click detection, mean that it should be relatively straightforward and inexpensive to implement the methods for density estimation presented here at other sites. Because all such habitats are unique, it is likely that the acoustic behaviour of porpoises observed in Kyle Rhea are not indicative of their behaviour at all tidal rapid sites, and therefore bespoke surveys are required before any inferences about harbour porpoise distribution and behaviour can be made about other tidal rapid sites.

5.6 CONCLUSION

Using a combination of complex PAM arrays and much simpler single channel systems it has been possible to obtain high resolution behavioural, population and distribution data on harbour porpoises in a tidal stream. Although significant uncertainty in density and foraging rates exists, these results indicate that Kylerhea/Sound of Sleat is an important habitat for harbour porpoises with high foraging rates and densities. The most likely explanation for this is that the tidal rapids

provide an energetic advantage during foraging. The west coast of Scotland contains many similar broadly un-studied tidal rapid areas which may be equally important habitats for harbour porpoises and other marine mammals.

5.7 ACKNOWLEDGEMENTS

Thanks to the Scottish Association of Marine Science, Oban and Denise Risch, Steven Benjamins and Ben Wilson for supplying their RTsys PAM data in 2015. The RTsys PAM data were collected during the NERC/Defra RESPONSE project NE/J004251/1 EU FP7-REGPOT program for the MERIKA project (2014–2017) awarded to the University of the Highlands and Islands (UHI) under Grant Agreement No. 315925.

Thanks to Carol Sparling and Gordon Hastie for managing the overall project and Danielle Harris, Tiago Marques and Len Thomas for helpful discussions.

5.8 REFERENCES

Ainslie, M. A., and J. G. Mccolm. 1998. A simplified formula for viscous and chemical absorption in sea water. The Journal of the Acoustical Society of America 103:1671.

Akamatsu, T., K. Nakamura, R. Kawabe, S. Furukawa, H. Murata, A. Kawakubo, and M. Komaba. 2010. Seasonal and diurnal presence of finless porpoises at a corridor to the ocean from their habitat. Marine Biology 157:1879–1887.

Barlow, J., and B. L. Taylor. 2005. Estimates of sperm whale abundance in the northeastern temperate pacific from a combined acoustic and visual survey. Marine Mammal Science 21:429–445.

Benjamins, S., A. Dale, N. van Geel, and B. Wilson. 2016. Riding the tide: use of a moving tidal-stream habitat by harbour porpoises. Marine Ecology Progress Series 549:275–288.

Benjamins, S., A. Dale, G. Hastie, J. Waggitt, M.-A. Lea, B. Scott, and B. Wilson. 2015. Confusion Reigns? A Review of Marine Megafauna Interactions with Tidal-Stream Environments. Pages 1–54 Oceanography and Marine Biology: An Annual Review.

Benjamins, S., N. van Geel, G. Hastie, J. Elliott, and B. Wilson. 2017. Harbour porpoise distribution can vary at small spatiotemporal scales in energetic habitats. Deep Sea Research Part II: Topical Studies in Oceanography 141:191–202.

Booth, C., C. Embling, J. Gordon, S. Calderan, and P. Hammond. 2013. Habitat preferences and distribution of the harbour porpoise Phocoena phocoena west of Scotland. Marine Ecology Progress Series 478:273–285.

Booth, C. G. 2020. Food for thought: Harbor porpoise foraging behavior and diet inform vulnerability to disturbance. Marine Mammal Science 36:195–208.

Carlén, I., L. Thomas, J. Carlström, M. Amundin, J. Teilmann, N. Tregenza, J. Tougaard, J. C. Koblitz, S. Sveegaard, D. Wennerberg, O. Loisa, M. Dähne, K. Brundiers, M. Kosecka, L. A. Kyhn, C. T. Ljungqvist, I. Pawliczka, R. Koza, B. Arciszewski, A. Galatius, M. Jabbusch, J. Laaksonlaita, J. Niemi, S. Lyytinen, A. Gallus, H. Benke, P. Blankett, K. E. Skóra, and A. Acevedo-Gutiérrez. 2018. Basin-scale distribution of harbour porpoises in the Baltic Sea provides basis for effective conservation actions. Biological Conservation 226:42–53.

Crook, K., and G. Davoren. 2014. Underwater behaviour of common murres foraging on capelin: influences of prey density and antipredator behaviour. Marine Ecology Progress Series 501:279–290.

Deruiter, S. L., A. Bahr, M.-A. Blanchet, S. F. Hansen, J. H. Kristensen, P. T. Madsen, P. L. Tyack, and M. Wahlberg. 2009. Acoustic behaviour of echolocating porpoises during prey capture. The Journal of experimental biology 212:3100–3107.

Davies IM, Gubbins M, Watret R (2012) Scoping study for tidal-stream energy development in Scottish waters. Scottish Marine and Freshwater Science Report 3(1). Available at www. scotland. gov. uk/ Publications/ 2012/ 04/ 2639 (accessed 23 October 2014)

DeRuiter, S. L., M. Hansen, H. N. Koopman, A. J. Westgate, P. L. Tyack, and P. T. Madsen. 2010. Propagation of narrow-band-high-frequency clicks: measured and modeled transmission loss of porpoise-like clicks in porpoise habitats. The Journal of the Acoustical Society of America 127:560–567.

Duncan, A. J., and A. L. Maggi. 2006. A Consistent, User Friendly Interface for Running a Variety of Underwater Acoustic Propagation Codes. Pages 471–477 Proceedings of the First Australasian Acoustical Societies' Conference. Christchurch, New Zealand.

Embling, C. B., P. a. Gillibrand, J. Gordon, J. Shrimpton, P. T. Stevick, and P. S. Hammond. 2010. Using habitat models to identify suitable sites for marine protected areas for harbour porpoises (Phocoena phocoena). Biological Conservation 143:267–279.

Enstipp, M. R., D. Grémillet, and D. R. Jones. 2007. Investigating the functional link between prey abundance and seabird predatory performance. Marine Ecology Progress Series 331:267–279.

Frasier, K. E., S. M. Wiggins, D. Harris, T. A. Marques, L. Thomas, and J. A. Hildebrand. 2016. Delphinid echolocation click detection probability on near-seafloor sensors. The Journal of the Acoustical Society of America 140:1918–1930.

Gassmann, M., S. M. Wiggins, and J. A. Hildebrand. 2015. Three-dimensional tracking of Cuvier ' s beaked whales ' echolocation sounds using nested hydrophone arrays. Journal of the Acoustical Society of America 138:2483–2494.

Gillespie, D., J. Gordon, R. Mchugh, D. Mclaren, D. Mellinger, P. Redmond, A. Thode, P. Trinder, and X. Y. Deng. 2008. PAMGUARD: Semiautomated, open source software for real-time acoustic detection and localisation of cetaceans. Proceedings of the Institute of Acoustics 30:2547.

Gillespie, D., and R. Leaper. 1996. Detection of sperm whale (Physeter macrocephalus) clicks and discrimination of individual vocalisations. Eur. Res. Cetaceans:87–91.

Gordon, J., D. Thompson, R. Leaper, D. Gillespie, C. Pierpoint, S. Calderan, J. Macaulay, T. Gordon, and N. Simpson. 2011. Assessment of risk to marine mammals from underwater marine renewable devices in Welsh waters - Phase 2 - Studies of marine mammals in Welsh high tidal waters. Page Welsh Government Assembly Report.

Hall, A. 2011. Foraging behaviour and reproductive season habitat selection of Northeast Pacific porpoises. University of British Columbia.

Hammond, P. S., K. Macleod, P. Berggren, D. L. Borchers, L. Burt, A. Cañadas, G. Desportes, G. P. Donovan, A. Gilles, D. Gillespie, J. Gordon, L. Hiby, I. Kuklik, R. Leaper, K. Lehnert, M. Leopold, P. Lovell, N. Øien, C. G. M. Paxton, V. Ridoux, E. Rogan, F. Samarra, M. Scheidat, M. Sequeira, U. Siebert, H. Skov, R. Swift, M. L. Tasker, J. Teilmann, O. Van Canneyt, and J. A. Vázquez. 2013. Cetacean abundance and distribution in European Atlantic shelf waters to inform conservation and management. Biological Conservation 164:107–122.

Hastie, G. D., D. M. Gillespie, J. C. D. Gordon, J. D. J. Macaulay, B. J. McConnell, and C. E. Sparling. 2014. Tracking Technologies for Quantifying Marine Mammal Interactions with Tidal Turbines: Pitfalls and Possibilities. Pages 127–139.

Hastie, G. D., D. J. F. Russell, S. Benjamins, S. Moss, B. Wilson, and D. Thompson. 2016. Dynamic habitat corridors for marine predators; intensive use of a coastal channel by harbour seals is modulated by tidal currents. Behavioral Ecology and Sociobiology 70:2161–2174.

Hastie, G. D., B. Wilson, and P. M. Thompson. 2006. Diving deep in a foraging hotspot: acoustic insights into bottlenose dolphin dive depths and feeding behaviour. Marine Biology 148:1181–1188.

Hastie, G. D., G. Wu, S. Moss, P. Jepp, J. MacAulay, A. Lee, C. E. Sparling, C. Evers, and D. Gillespie. 2019. Automated detection and tracking of marine mammals: A novel sonar tool for monitoring effects of marine industry. Aquatic Conservation: Marine and Freshwater Ecosystems 29:119–130.

Heerfordt, A., B. Møhl, and M. Wahlberg. 2007. A wideband connection to sperm whales: A fiber-optic, deep-sea hydrophone array. Deep Sea Research Part I: Oceanographic Research Papers 54:428–436.

Hildebrand, J. A., K. E. Frasier, S. Baumann-Pickering, S. M. Wiggins, K. P. Merkens, L. P. Garrison, M. S. Soldevilla, and M. A. McDonald. 2019. Assessing Seasonality and Density From Passive

Acoustic Monitoring of Signals Presumed to be From Pygmy and Dwarf Sperm Whales in the Gulf of Mexico. Frontiers in Marine Science 6:1–17.

IJsseldijk, L. L., K. C. J. Camphuysen, J. J. Nauw, and G. Aarts. 2015. Going with the flow: Tidal influence on the occurrence of the harbour porpoise (Phocoena phocoena) in the Marsdiep area, The Netherlands. Journal of Sea Research 103:129–137.

Koblitz, J. C., M. Wahlberg, P. Stilz, P. T. Madsen, K. Beedholm, and H.-U. Schnitzler. 2012. Asymmetry and dynamics of a narrow sonar beam in an echolocating harbor porpoise. The Journal of the Acoustical Society of America 131:2315.

Küsel, E. T., D. K. Mellinger, L. Thomas, T. A. Marques, D. Moretti, and J. Ward. 2011. Cetacean population density estimation from single fixed sensors using passive acoustics. The Journal of the Acoustical Society of America 129:3610–3622.

Kyhn, L. a., J. Tougaard, L. Thomas, L. R. Duve, J. Stenback, M. Amundin, G. Desportes, and J. Teilmann. 2012. From echolocation clicks to animal density—Acoustic sampling of harbor porpoises with static dataloggers. The Journal of the Acoustical Society of America 131:550.

Ladegaard, M., F. H. Jensen, K. Beedholm, V. M. F. Da Silva, and P. T. Madsen. 2017. Amazon river dolphins (Inia geoffrensis) modify biosonar output level and directivity during prey interception in the wild. Journal of Experimental Biology 220:2654–2665.

Linnenschmidt, M., J. Teilmann, T. Akamatsu, R. Dietz, and L. A. Miller. 2013. Biosonar, dive, and foraging activity of satellite tracked harbor porpoises (*Phocoena phocoena*). Marine Mammal Science 29:E77–E97.

Macaulay, J., J. Gordon, D. Gillespie, C. Malinka, and S. Northridge. 2017. Passive acoustic methods for fine-scale tracking of harbour porpoises in tidal rapids. The Journal of the Acoustical Society of America 141:1120–1132.

Malinka, C., D. Gillespie, J. Macaulay, R. Joy, and C. Sparling. 2018. First in situ passive acoustic monitoring for marine mammals during operation of a tidal turbine in Ramsey Sound, Wales. Marine Ecology Progress Series 590:247–266.

Marques, T. A., L. Thomas, S. W. Martin, D. K. Mellinger, J. A. Ward, D. J. Moretti, D. Harris, and P. L. Tyack. 2013. Estimating animal population density using passive acoustics. Biological reviews of the Cambridge Philosophical Society 88:287–309.

Miller, B., and S. Dawson. 2009. A large-aperture low-cost hydrophone array for tracking whales from small boats. The Journal of the Acoustical Society of America 126:2248–2256.

Møhl, B., M. Wahlberg, P. T. Madsen, L. a Miller, and a Surlykke. 2000. Sperm whale clicks: directionality and source level revisited. The Journal of the Acoustical Society of America 107:638–648.

Palka, D. L., and P. S. Hammond. 2001. Accounting for responsive movement in line transect estimates of abundance. Canadian Journal of Fisheries and Aquatic Sciences 58:777–787.

Pierpoint, C. 2008. Harbour porpoise (Phocoena phocoena) foraging strategy at a high energy, near-shore site in south-west Wales, UK. Journal of the Marine Biological Association of the United Kingdom 88:1167–1173.

Roch, M. A., T. Scott Brandes, B. Patel, Y. Barkley, S. Baumann-Pickering, and M. S. Soldevilla. 2011. Automated extraction of odontocete whistle contours. The Journal of the Acoustical Society of America 130:2212–2223.

Rojano-Doñate, L., B. I. McDonald, D. M. Wisniewska, M. Johnson, J. Teilmann, M. Wahlberg, J. Højer-Kristensen, and P. T. Madsen. 2018. High field metabolic rates of wild harbour porpoises. The Journal of Experimental Biology 221:jeb185827.

Sandwell, D. T. 1987. Biharmonic spline interpolation of GEOS-3 and SEASAT altimeter data. Geophysical Research Letters 14:139–142.

Sørensen, P. M., D. M. Wisniewska, F. H. Jensen, M. Johnson, J. Teilmann, and P. T. Madsen. 2018. Click communication in wild harbour porpoises (Phocoena phocoena). Scientific Reports 8:9702.

Thomas, L., A. Jaramillo-Legorreta, G. Cardenas-Hinojosa, E. Nieto-Garcia, L. Rojas-Bracho, J. M. Ver Hoef, J. Moore, B. Taylor, J. Barlow, and N. Tregenza. 2017. Last call: Passive acoustic monitoring shows continued rapid decline of critically endangered vaquita. The Journal of the Acoustical Society of America 142:EL512–EL517.

Tollit, D., R. Joy, J. Wood, A. M. Redden, C. Booth, T. Boucher, P. Porskamp, and M. Oldreive. 2019. Baseline presence of and effects of tidal turbine installation and operations on harbour porpoise in minas passage, Bay of Fundy, Canada. The Journal of Ocean Technology 14:24–48.

Villadsgaard, A., M. Wahlberg, and J. Tougaard. 2007. Echolocation signals of wild harbour porpoises, Phocoena phocoena. Journal of Experimental Biology 210:56–64.

Waggitt, J. J., H. K. Dunn, P. G. H. Evans, J. G. Hiddink, L. J. Holmes, E. Keen, B. D. Murcott, M. Piano, P. E. Robins, B. E. Scott, J. Whitmore, and G. Veneruso. 2018. Regional-scale patterns in harbour porpoise occupancy of tidal stream environments. ICES Journal of Marine Science 75:701–710.

Wahlberg, M. 2002. The acoustic behaviour of diving sperm whales observed with a hydrophone array. Journal of Experimental Marine Biology and Ecology 281:53–62.

Waring, G. T., E. Josephson, and K. Maze-foley. 2015. NOAA Technical Memorandum NMFS-US Atlantic and Gulf of Mexico Marine Mammal Stock Assessments -- 2014. NOAA Tech Memo NMFS NE 231; 361 p.

Westgate, A. J., A. J. Head, P. Berggren, H. N. Koopman, and D. E. Gaskin. 1995. Diving behaviour of harbour porpoises, Phocoena phocoena. Canadian Journal of Fisheries and Aquatic Sciences 52:1064–1073.

White, P. R., T. G. Leighton, D. C. Finfer, C. Powles, and O. N. Baumann. 2006. Localisation of sperm whales using bottom-mounted sensors. Applied Acoustics 67:1074–1090.

Wiggins, S. M., M. a. McDonald, and J. a. Hildebrand. 2012. Beaked whale and dolphin tracking using a multichannel autonomous acoustic recorder. The Journal of the Acoustical Society of America 131:156.

Wilson, B., S. Benjamins, and J. Elliott. 2013. Using drifting passive echolocation loggers to study harbour porpoises in tidal-stream habitats. Endangered Species Research 22:125–143.

Wisniewska, D. M., M. Johnson, K. Beedholm, M. Wahlberg, and P. T. Madsen. 2012. Acoustic gaze adjustments during active target selection in echolocating porpoises. The Journal of experimental biology 215:4358–73.

Wisniewska, D. M., M. Johnson, J. Teilmann, U. Siebert, A. Galatius, R. Dietz, and P. T. Madsen. 2018. High rates of vessel noise disrupt foraging in wild harbour porpoises (Phocoena phocoena). Proceedings of the Royal Society B: Biological Sciences 285:20172314.

Wisniewska, D. M. M., M. Johnson, J. Teilmann, L. Rojano-Doñate, J. Shearer, S. Sveegaard, L. A. A. Miller, U. Siebert, and P. T. T. Madsen. 2016. Ultra-High Foraging Rates of Harbor Porpoises Make Them Vulnerable to Anthropogenic Disturbance. Current Biology 26:1441–1446.

Wisniewska, D. M., J. M. Ratcliffe, K. Beedholm, C. B. Christensen, M. Johnson, J. C. Koblitz, M. Wahlberg, and P. T. Madsen. 2015. Range-dependent flexibility in the acoustic field of view of echolocating porpoises (Phocoena phocoena). eLife 4:1–16.

Zamon, J. E. 2003. Mixed species aggregations feeding upon herring and sandlance schools in a nearshore archipelago depend on flooding tidal currents. Marine Ecology Progress Series 261:243–255.

5.9 SUPPLEMENTARY MATERIALS

5.9.1 Click detection and Classification Settings

The PAMGuard click detector used a signal to noise threshold ($SNR_{\min}$) set to 10 dB. Acoustic data was pre-filtered using a 4th order digital Chebyshev band pass filter between 80 and 160 kHz.

Porpoise clicks were classified based the length of the click, the energy distribution in different frequency bands and peak frequency using the PAMGuard click classifier. The exact parameters were as follows:

A detection was classified if all the following criteria were met.

1) The energy between 40 – 90 kHz and 160 – 190 kHz was 6 dB less than the energy between 100 kHz and 150 kHz.
2) There was a peak in frequency between 100 and 180 kHz in the frequency band between 40-240 kHz
3) The length of the click, measured as 6 dB down either side of the maximum amplitude, was greater than 0.02 ms and less than 0.22 ms.

5.9.2 Click Detection Efficiency

The number of detected clicks in the density estimation equation ($n(1-\hat{f}_p$) (see Eq 5.1) is the number of automatically detected transients which have been classified as porpoise clicks with false positives removed. The click detection algorithm in PAMGuard is simple and so it's behaviour is predictable. Thus, it was assumed that if there were a porpoise click above noise threshold it would be *detected.* However, the detector records all transient sounds including echolocation clicks from other species, cavitation from propellers and tidal noise. A further classification process is therefore required. PAMGuard's click classifier was used to determine whether a detected transient was a porpoise click or not. The PAMGuard click classifier is binary (i.e. either yes or no) and based on both the waveform and spectral properties of a received click. Like any classifier there is a trade-off between successfully classifying as many detected porpoises clicks as possible and minimising false positives. In general porpoise clicks are quite stereotyped signals, however, high levels of tidal noise, especially in the narrows, could create significant numbers of false positives. In addition, reflections from both the seabed and sea surface resulted in large number of echoes. Whilst false positives were relatively common, false negatives, i.e. porpoise clicks that were detected but not classified, tended to occur either when recordings were clipped resulting in distorted waveforms or when received clicks had a low signal to noise level. Different instruments had different clip levels and noise floors (see Table 1) and therefore for each type of instrument (both vertical arrays, SoundTraps and RTsys recorders), 3 x 5 minute sections of data were manually annotated to test effectiveness of the automated classifier. The false positive rate and false negative (detection efficiency) were then calculated with respect to the SNR of clicks. Figure 15S shows the results.

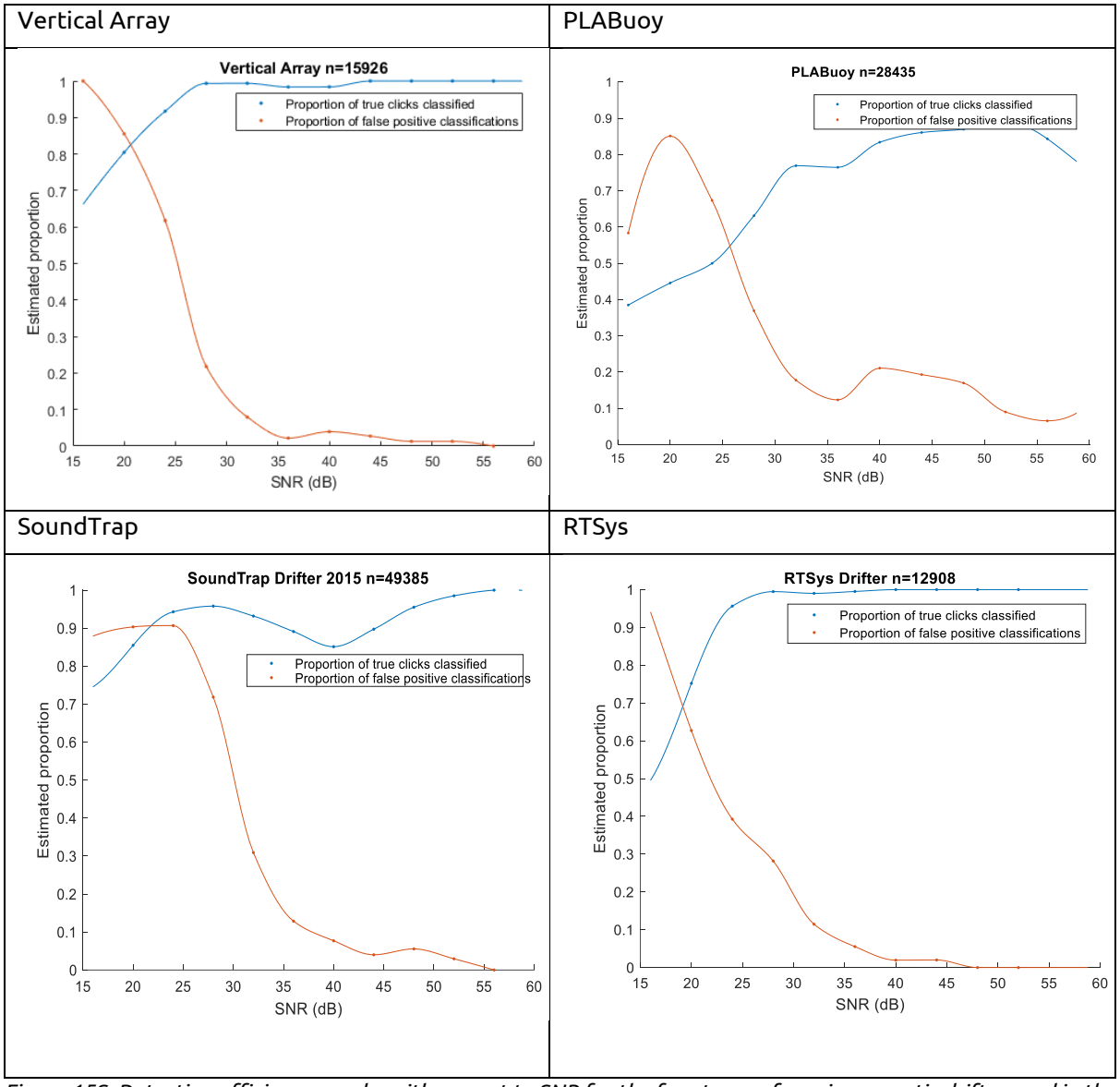

Figure 15S. Detection efficiency graphs with respect to SNR for the four types of passive acoustic drifter used in the survey. Blue lines are the detection efficiency, i.e. the proportion of true porpoise clicks (manually annotated) which were classified. The orange line is the false positive rate (1-precision), i.e. the proportion of total classified clicks which were false positives. Note the drop in detection efficiency in the PLABuoy at higher SNR is due to clipping distorting the waveform. The larger number of false positives in both the PLABuoy and SoundTrap is due to low level electrical noise triggering the classifier.

The graphs clearly show that at low SNR levels the proportion of false positives is high and thus there is likely a large effect on click counts. Note the PLABuoy has lower detection efficiency, this is due to clipping and the fact there was some transient electrical noise.

The detection efficiency (proportion of true clicks detected and then classified) was integrated directly into the Monte Carlo simulation i.e. when a simulated click was above the threshold it was

detected and classified with a probability corresponding to the $\hat{p}_d(SNR)$ where $\hat{p}_d$ is the detection efficiency curve for the relevant PAM drifter in Figure 15S.

The false positive rate was included in the $n\left(1-\widehat{f_p}\right)$ term of the density estimation equation Eq 5.1. Each classified click was assigned a probability of being a false positive based on it's SNR value. These were then summed so that

$$n\left(1-\widehat{f_p}\right)=\sum_{i=1}^{n}\left(1-\hat{p}_f(SNR_i)\right) \qquad \text{Eq 5.7}$$

where $\hat{p}_f(SNR_i)$ is the probability of click i being a false positive based on the false positive graph for the relevant PAM drifter in Figure 15S.

5.9.3 Calculating the click detection threshold

Inputs for the simulation, e.g. source levels, are in units of dB re 1µPa peak to peak (pp) at 1m. Calculating the correct type of noise for the simulation is important as noise is one of the primary factors driving the final density estimation. In this study, automated click detectors are used to detect and classify porpoise clicks and so the relevant noise is whatever is measured by the detection algorithm. The detection of clicks in PAMGuard is based on two moving averaging windows, the noise level

$$N_i=\alpha_N|x|_i+(1-\alpha_N)N_{i-1} \qquad \text{Eq. 5.8}$$

and the signal level

$$S_i=\alpha_s|x|_i+(1-\alpha_s)S_{i-1} \qquad \text{Eq. 5.9}$$

were α_N is the long filter parameter specified in the click detector module and α_s is the short filter parameter. If the ratio between $S_i$and $N_i$reaches over a specified threshold then a click raw data snippet is recorded until the ratio either moves below threshold or a maximum click length is reached. The relevant noise input for the Monte Carlo simulation is therefore N_i. N_i is essentially a 0 to peak noise measurement. It can be converted to peak to peak by multiplying by 2 and converting to received dB re 1µPa pp by adding the correct calibration factors for the recording system via

$$N_{pps} = 20\log_{10}(2N_i V_{pp}) - (H_{sens} + G) \qquad \text{Eq. 5.10}$$

where N_{pps} is the peak to peak equivalent noise in dB re 1µPa pp, V_{pp} is the peak to peak voltage of the ADC card, H_{sens} is the hydrophone sensitivity in dB re 1V/µPa and G is the total gain in dB. The Monte Carlo simulation compares the received peak to peak amplitude of a simulated click to N_{pp} and then registered a successful detection if the click amplitude is above N_{pp}+ threshold. If $\alpha_s < 1$ then S_i essentially acts a damping factor and so does not actually truly represent the click amplitude. i.e. a received click peak to peak amplitude has to be some value higher than threshold + N_{pps} to trigger a detection when using the click detector module, thus the Monte Carlo simulation is over estimating detectability.

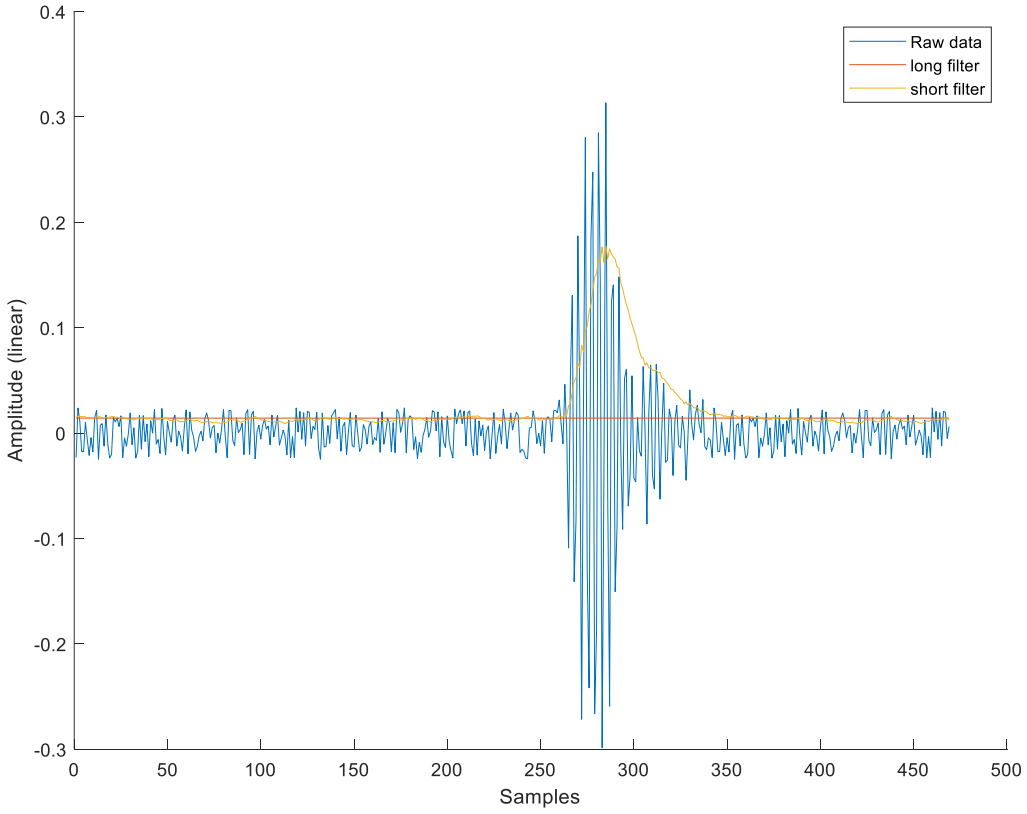

Figure 16S. A typical porpoise clicks with corresponding N_i (long filter) and S_i (short filter) measurements from the PAMGuard click detector. Note that the short filter does not reach the peak of the click. Thus the click has to be some dB greater than threshold to trigger the detector.

To compensate for this, it is necessary to add an additional compensation factor to the threshold or noise. The value of this additional factor is entirely dependent on the received waveform, however, can be estimated as the difference between the peak of S_i and the 0 to peak maximum amplitude for a typical click. In the case of a porpoise this is 5dB (see Figure 16S). Thus, the peak to peak equivalent noise becomes

$$N_{pp} = N_{pps} + \ D_{sens} \qquad \text{Eq 5.11}$$

Where N_{pp} is the compensated peak to peak noise and D_{sens} is the compensation factor.

The click detector settings in PAMGuard were

$\alpha_N = \ 0.000001$

$\alpha_s = 0.1$

$Threshold$ = 10dB

5.9.4 Click Train Detection

The detection of click trains was based on a multi hypothesis click train detector which extracts sequences of click detections which have repeating patterns in ICI and amplitude (see Chapter 2). Each click train was assigned a χ^2 value by the click train detection algorithm. χ^2 measures how consistently a click train changes in ICI and amplitude over time with higher values indicating more random ICI and amplitude changes and thus a click train which is less likely to be biological in origin (see Figure 17S) .

Detected clicks trains were then classified as a buzz if the following conditions were met.

1) The median ICI of the click train was greater than 1 ms and below 16 ms (Deruiter et al. 2009) and the ratio between the mean and median ICI was no greater than 2.
2) The click train contained at least 8 clicks
3) The χ^2 value of the click train was below a threshold of 1200 (see section 5.9.4.1).
4) The minimum length of the buzz was greater than 5 ms.

5) More than 30% of the clicks were classified by the click-by-click classifier as porpoise

Click train were classified as standard echolocation click trains using same criteria as buzzes except that ICI had to be >16 ms

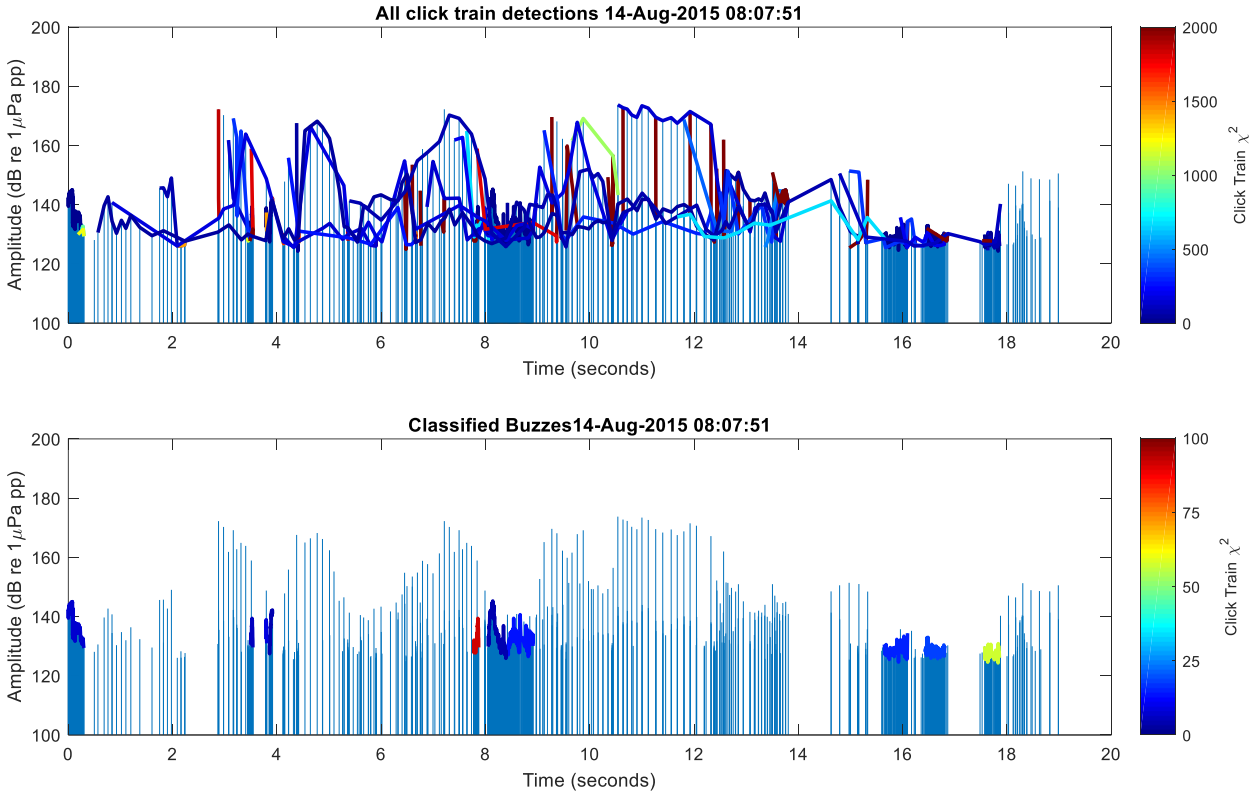

Figure 17S. An example of click train detection using the click train detector. Each vertical line represents a detected transient (not necessarily a porpoise click). The thicker coloured lines are click trains coloured by their respective χ^2 values. The click train detector first associates almost all detected clicks into click trains as shown in the top plot. Some of these click trains are spurious associations of transients and some belong to harbour porpoise. These are then classified based on a maximum χ^2 threshold and ICI to extract only harbour porpoise buzzes as shown in the bottom plot.

5.9.4.1 Detection efficiency

For each type of recording device (boat based vertical array, PLABuoy, SoundTrap, RTsys), buzzes were marked out by a manual analyst in PAMGuard viewer mode. Marked out buzzes were then imported in MATLAB using the PAMGuard MATLAB library (www.pamguard.org) and compared to automated buzz detections. Precision recall curves were constructed for using the classification settings above but with varying minimum buzz χ^2 values. These were then used to select an optimal χ^2 threshold (1200) and estimate the false positive rate ($\widehat{f_p}$) (1 - precision) for Eq 5.1 and detection efficiency (recall) of buzzes for the Monte Carlo simulation. Note that because the RTsys drifters

were primarily focused on the Kylerhea narrows (see Figure 6) very few buzzes were detected because the density of porpoises in this area was almost zero. Thus, the sample size was too low to generate a meaningful precision recall curve. The RTSys buzz detection efficiency was therefore considered to be the same as the average of the precision recall curves of the other devices.

Figure 18 shows the precision and recall curves were

$$Precision = \frac{Number\ of\ manually\ annoted\ buzzes\ detected\ by\ the\ automated\ algorithm}{Number\ of\ manaully\ annotated\ buzzes}$$

and

$$Recall = \frac{Number\ of\ true\ positive\ automated\ buzz\ detections}{Number\ of\ automated\ buzz\ detections}$$

Each point on the precision/recall curve represents automated buzzes with a χ^2 below a specified threshold (labelled).

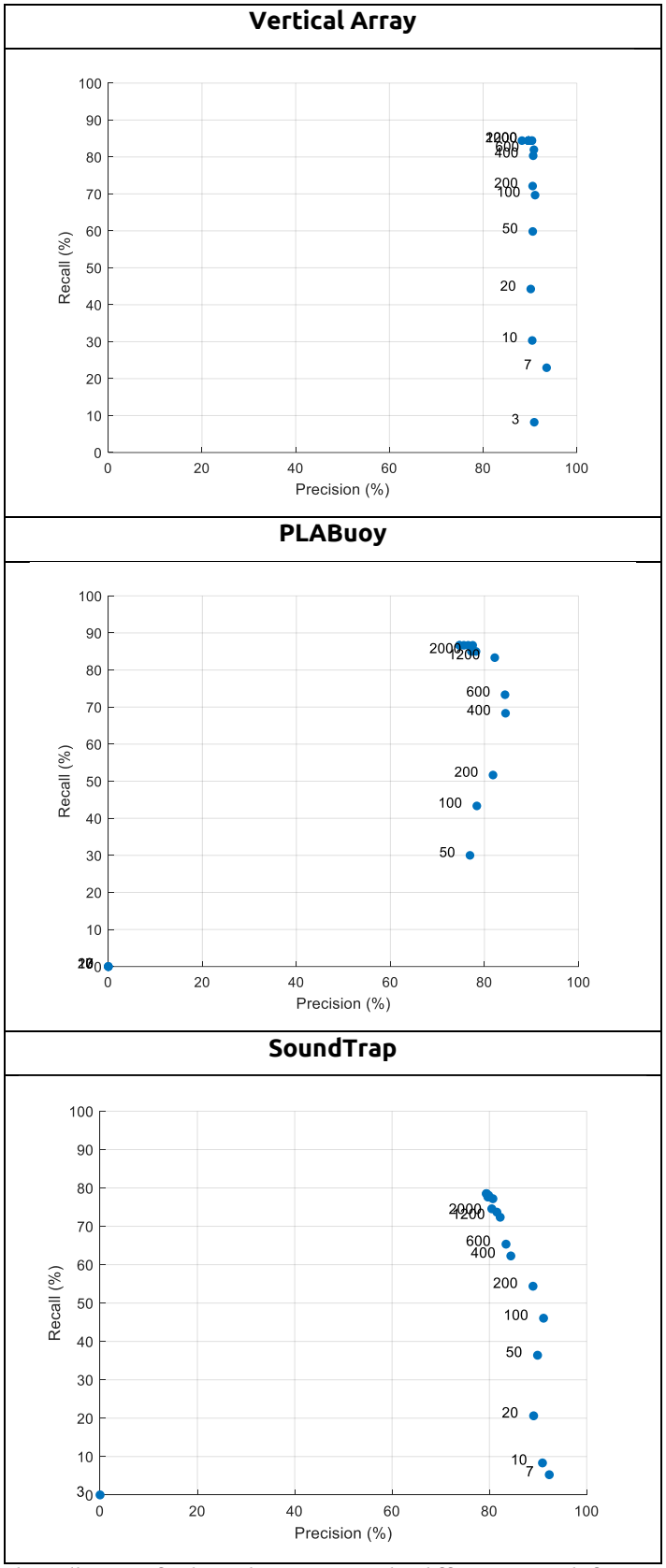

Figure 18S. Precision and recall curves for buzz detections on the different PAM drifters. Each point represents the precision and recall for the automated click train detector and classifier for a specified χ^2 threshold.

Note that the reason the SoundTrap has worse performance than the boat based vertical array and PLABuoy is because there were low levels of electrical noise which generated regular transients in the porpoise frequency band that confounded the click train detection algorithm. This is also evident in Figure 15S were the SoundTrap has a very high false positive rate generated by this low level electrical noise up to an SNR of ~25dB which then decreases rapidly to a rate equivalent to the other PAM recorders. This was a common problem with the first generation of SoundTraps related to a faulty capacitor and has been rectified in later models.

5.9.5 Vertical Angles from Tracks

The vertical angle distribution of animals is an important parameter used in both the probability of localisation and probability of detection Monte Carlo simulations. Calculating vertical tracks from animals which have a narrow beam profile is potentially circular because the probability of localising an animal will depend on its vertical angle distribution. For example, a harbour porpoise which is vertical in the water column is less likely to be detected than an animal which is a horizontal because most of the acoustic energy is restricted to a few tens of degrees in front of the animal. For any animal which has a uniform beam profile (i.e. no beam profile) this is not a problem because it is equally detectible no matter what it's vertical angle is. A porpoise echolocating at 191 dB re 1uPa pp at 1m creates a large detectible volume. When an animal is closer to a recording system, it is detectible over a larger set of vertical angles and may be equally detectible in all directions within some ranges from the array. Hence using tracks which are close to the hydrophone arrays may produce little or bias in determining vertical angles so negating the circular argument.

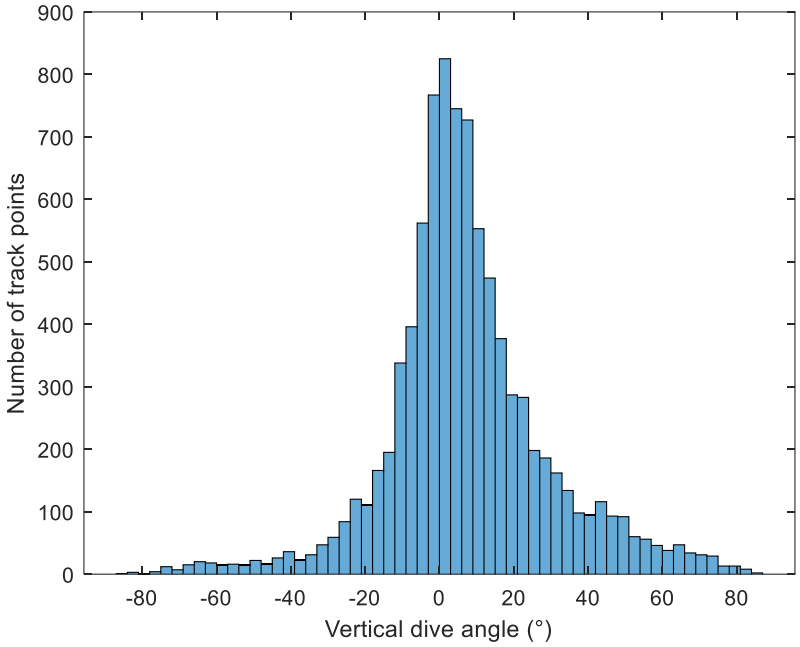

Figure 19S. The distribution of vertical angles of all animal tracks in all regions in Kylerhea and the Sound of Sleat. The vertical angles fit a normal distribution (mean 7.33° SD 22.0°)

To test whether vertical angles could be accurately calculated from dive tracks near a hydrophone array, a modified probability of *localisation* Monte Carlo simulation was run and compared to localised tracks from the 10 channel vertical array (maximum hydrophone depth 30 m). The simulation assumed a set of normally distributed vertical angle distributions, each with different mean and standard deviation. The mean values were between -45° and 45° in 5° bins and standard deviation of 5° to 60° in 5° bins. When combined, these created 228 possible normal distributions. For each distribution, 1 million animals were simulated, evenly scattered between maximum range and depth limits with each simulated animal drawing a vertical angle from the current distribution and all other parameters the same as in section 5.3.4.4. The distribution of vertical angles of *detected* simulated animals at different range bins was then compared to the original input vertical angle distribution and errors calculated as the difference between the mean and standard deviation between the two distributions. An example of a simulation for a mean vertical angle of 15° and standard deviation values between 6° and 55° with overlaid vertical angle distribution of tracks in Figure 19 is shown in Figure 20S.

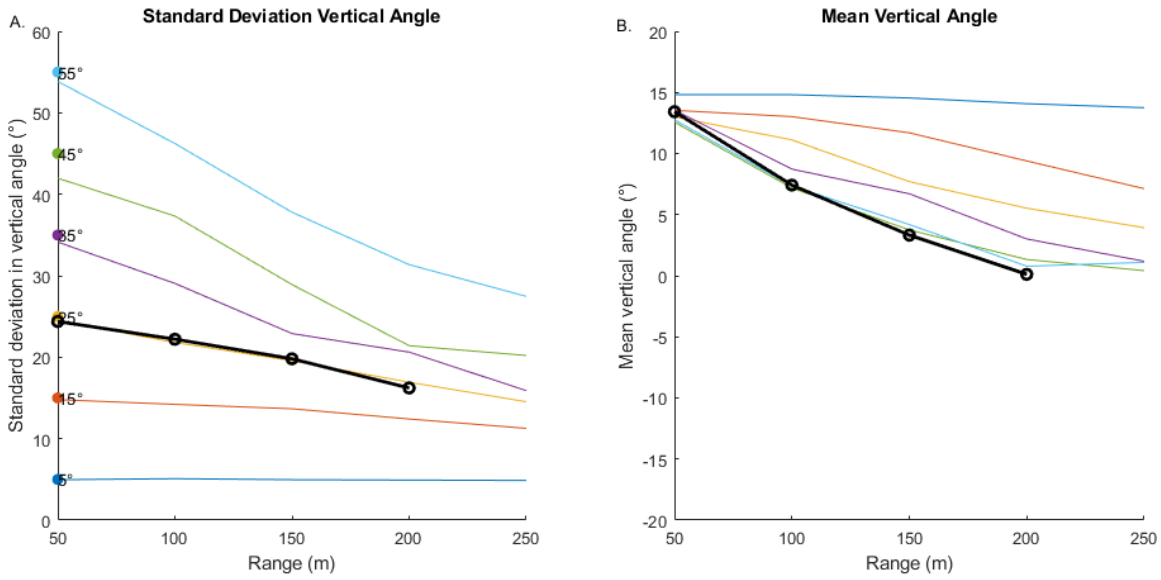

Figure 20S. An example of a simulation of six vertical angle distributions with a mean of 0° and 6° -55° for 0-30m depth and 50m range bins (on the x axis 100 = ranges between 50m and 100m etc). The points on plot A represent the input distribution standard deviation. The black line is the standard deviation and mean of vertical angles from real tracks combined for all regions. Results show that the standard deviation is accurately calculated for the 0-50m range bin but errors gradually increase as range increases. The true vertical angles calculated by the track follow the same pattern, showing the assumptions of the simulation are broadly sensible.

The simulation shows that both the mean and standard deviation in vertical angles can become biased at larger ranges but is robust in the first range bin (0-50m). The real animal tracks roughly follow the same pattern suggesting that the model is realistic.

Simulations were run in different depth and range bins and the upper 95% mean and standard deviation error in vertical angles for all distributions plotted as an error surface in Figure 21S.

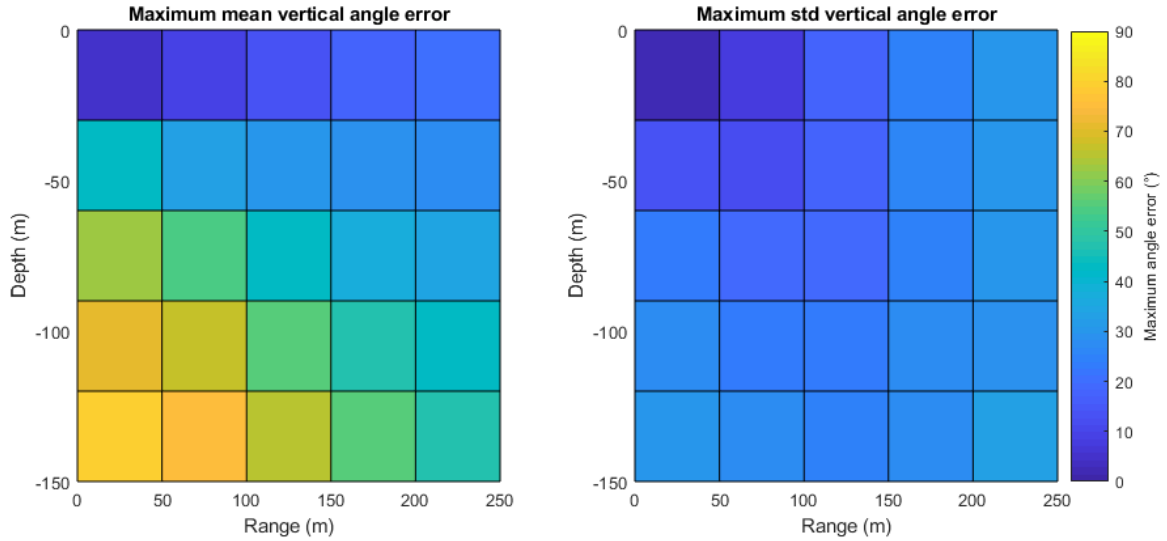

Figure 21S. Error estimations for calculating the mean and standard deviation in vertical angle from simulated animals. The error in the mean and std vertical angle (assuming a normal distirbution) increase at larger distances and depth from the array.

Results showed that the vertical angle measurements made within 50m of the array and for animals which were within the maximum depth of the array (30m) produced an average error of 3.14° in mean vertical angle and 3.08° in the standard deviation of vertical angles. However, directly below the array, errors are much larger, which would be expected as animals orientated towards the seabed will be undetectable. Thus, vertical angles for probability of localisation and detection Monte Carlo simulations were calculated from tracks within 50m of the hydrophone array and no deeper than the depth of the deepest hydrophone. It was assumed that tracks below 30m followed the same vertical angle distribution.

5.9.6 Software

All acoustic data was analysed using PAMGuard (2.00.14) to detect clicks as detailed in section 5.3.2.1. Detected clicks were imported into MATLAB (2017b) using the PAMGuard MATLAB library. Custom MATLAB scripts calling the PAMGuard click train API were then used to run the MHT click train detection on the data and extract buzzes.

The Monte Carlo simulation was programmed in Java which decreased typical simulation time by a factor of 30 compared to MATLAB. The Java code was packaged into an open source library CetSim

(https://github.com/macster110/cetacean_sim). Detection, GPS and environmental data was organised using MATLAB and density simulations run by directly accessing the compiled java code of CetSim from a custom MATLAB library.

Multiple linear regression on the sensitivity analysis results was performed using

```
ens =fitrensemble(X,p,'Method','LSBoost','Learners',t);
```

and

```
imp = predictorImportance(ens);
```

functions in MATLAB.

5.9.7 Summary of Results

Table 4 shows a summary of region-specific calculated inputs into the detection probability simulation (e.g. vertical angles, depth distribution) and the density estimation results (density of clicks and buzzes (foraging/call) assuming a cue rate of 3 clicks·s^{-1}) during ebb/flood in 2014/2015. The table is divided by region for 2014/2015 and by ebb/flood tide state so that there are 40 results in total. Totals or mean values (weighted by effort) were calculated over all regions for each year/tidestate.

Table 4. Summary for all regions and years. Note that totals are the average values weighted by region area. Italics in the Total/Weighted Mean column indicates a weighted mean whilst no italic indicates a sum. The blue areas in 2015 indicate inputs that were used from 2014.

2014 Ebb											
	Region 1	**Region 2**	**Region 3**	**Region 4**	**Region 5**	**Region 6**	**Region 7**	**Region 8**	**Region 9**	**Region 10**	**Total/*Weighted Mean***
P^(echolocation clicks)	0.078679	0.058338	0.06921	0.048479	0.069595	0.068769	0.04868	0.080081	0.009513	NaN	*0.0708*
P^(buzzes)	0.004832	0.003891	0.004328	0.004119	0.004046	0.00409	0.002716	0.004378	0.000362	NaN	*0.0042*
Mean vertical dive angle (0-10m) (°)	4.859155	-3.24207	2.654228	20.50315	2.654228	5.707559	2.654228	11.99754	2.654228	4.859155	*8.23*
Std vertical dive angle (0-10m) (°)	10.12172	22.68651	20.07231	12.33521	20.07231	11.21382	20.07231	15.61691	20.07231	10.12172	*15.25*
Mean vertical dive angle (10m-seabed) (°)	9.28723	29.54539	16.49855	38.09947	16.49855	16.49855	16.49855	0.893539	16.49855	9.28723	*13.02*
Std vertical dive angle (10m-seabed) (°)	16.74478	18.3117	27.02128	10.87866	27.02128	27.02128	27.02128	22.04104	27.02128	16.74478	*21.46*
75% depth (m)	-30	-34	-54	-69	-26	-34	-31	-38	NaN	NaN	*-39.53*
No. clicks detected	122042	110881	62214	107494	19877	182900	11739	354989	218	0	972354
No. buzzes detected	177	170	25	51	4	225	3	318	0	0	973
No. Localised Clicks	6.94E+03	1.17E+04	7.34E+02	1.37E+03	1.72E+02	8.73E+03	3.40E+01	1.32E+04	1.00E+00	0.00E+00	56058
Effort (seconds)	14567	19432	9734	14927	2780	30117	2017	65741	318	0	159633
Density Clicks (clicks·km^{-2})	3.40E-05	2.96E-05	2.84E-05	4.06E-05	2.39E-05	2.68E-05	2.11E-06	1.93E-05	NaN	NaN	*0.00002568*
Density (porpoises·km^{-2})	11.33709	9.854652	9.453046	13.52705	7.97063	8.927158	0.701817	6.443282	NaN	NaN	*8.56*

Foraging buzz rate (buzz·hr^{-1})	344.7569	330.1575	116.5938	78.36359	47.48193	318.6078	1613.439	267.8678	0	0	*278*
Communication rate (calls·h^{-1})	121.0597	115.2931	22.20835	39.1818	47.48193	100.613	0	100.8853	0	0	*91.46*
Number of porpoises in region	2.740674	1.880808	2.02652	3.21635	2.787217	4.362199	0.351736	18.9459	0.608312	NaN	36.92
	2014 Flood										
	Region 1	**Region 2**	**Region 3**	**Region 4**	**Region 5**	**Region 6**	**Region 7**	**Region 8**	**Region 9**	**Region 10**	**Total**
Pˆ(echolocation clicks)	0.072414	0.093234	0.068156	0.072859	0.074321	0.073692	0.07361	0.060117	0.033797	NaN	*0.0708*
Pˆ(buzzes)	0.005256	0.006335	0.004169	0.004817	0.00492	0.004141	0.004316	0.004404	0.00187	NaN	*0.0047*
Mean vertical dive angle (0-10m) (°)	14.2581	14.2581	14.2581	14.2581	13.94308	-5.65966	14.2581	21.63366	14.2581	14.2581	*12.7169*
Std vertical dive angle (0-10m) (°)	23.00308	23.00308	23.00308	23.00308	18.67292	22.63179	23.00308	27.75521	23.00308	23.00308	*23.9338*
Mean vertical dive angle (10m-seabed) (°)	18.90076	7.31835	19.84168	19.84168	19.24919	6.116538	19.84168	32.12105	19.84168	18.90076	*18.6062*
Std vertical dive angle (10m-seabed) (°)	9.496352	5.933862	18.26107	18.26107	14.80534	22.03797	18.26107	21.95284	18.26107	9.496352	*15.8899*
75% depth (m)	-52	-46	-27	NaN	-50	-48	NaN	-50	-26	NaN	*-42.56*
No. clicks detected	154427	72582	32224	13249	93508	122333	46301	148483	0	0	683107
No. buzzes detected	70	72	46	5	182	151	2	65	0	0	593
No. Localised Clicks	7.47E+03	4.62E+03	1.12E+03	2.50E+01	2.55E+04	1.59E+04	2.10E+01	2.98E+03	148	0	60811
Effort (seconds)	38362	21208	13698	3418	5777	26402	5808	38397	5567	0	158637.00
Density Clicks (clicks·km^{-2})	1.41E-05	1.05E-05	1.06E-05	1.23E-05	6.08E-05	1.94E-05	2.68E-06	1.65E-05	NaN	NaN	*0.00001554*
Density (porpoises·km^{-2})	4.691139	3.513482	3.54263	4.090031	20.2647	6.468111	0.894392	5.511768	NaN	NaN	*5.18*
Foraging buzz rate (buzz·hr^{-1})	118.1952	250.0246	394.8227	150.7497	485.9313	324.936	85.65393	120.1557	0	0	*203*
Communication rate (calls·hr^{-1})	35.0208	60.35076	70.86562	0	150.3241	109.2705	85.65393	21.84649	0	0	*54.74*
Number of porpoises in region	1.134055	0.670565	0.75946	0.972494	7.086281	3.160602	0.448252	16.20686	0	NaN	30.44
	2015 Ebb										
	Region 1	**Region 2**	**Region 3**	**Region 4**	**Region 5**	**Region 6**	**Region 7**	**Region 8**	**Region 9**	**Region 10**	**Total/*Weighted Mean***
Pˆ(echolocation clicks)	0.064814686	0.095935524	0.057547899	0.068109333	0.074696358	0.077063761	0.056396056	0.060766574	0.052579452	0.064259694	0.0621
Pˆ(buzzes)	0.004198293	0.006907927	NaN	0.004810621	0.004102814	0.004111874	0.003338573	0.004524396	0.00298621	0.004527755	0.0037

Mean vertical dive angle (0-10m) (°)	14.26	14.26	14.26	14.26	13.94	-5.66	14.26	21.63	14.26	14.26	12.53
Std vertical dive angle (0-10m) (°)	23.00	23.00	23.00	23.00	18.67	22.63	23.00	27.76	23.00	23.00	23.64
Mean vertical dive angle (10m-seabed) (°)	18.90	7.32	19.84	19.84	19.25	6.12	19.84	32.12	19.84	18.90	18.99
Std vertical dive angle (10m-seabed) (°)	9.50	5.93	18.26	18.26	14.81	22.04	18.26	21.95	18.26	9.50	18.13
75% depth (m)	-52	-46	-27	NaN	-50	-48	NaN	-50	-26	NaN	-35.22
No. clicks detected	2888.054877	3008.787776	2068.578251	3250.727577	7971.126134	8716.091126	85.34404076	16614.4848	3884.619214	39268.43329	87756
No. buzzes detected	5	4	7	16	41	16	0	96	0	45	230
No. Localised Clicks	7473	4618	1119	25	25518	15933	21	2978	148	0	60811.00
Effort (seconds)	4218	11941	8057	13928	10270	22399	1328	22715	76231	25187	196274
Density Clicks (clicks·km^{-2})	6.88E-06	1.53E-06	2.54E-06	1.93E-06	6.45E-06	2.89E-06	NaN	6.73E-06	NaN	1.36E-05	0.00000226
Density (porpoises·km^{-2})	2.294164419	0.508778354	0.846405435	0.643092814	2.149913943	0.961701615	NaN	2.244822932	NaN	4.539443 67	0.752
Foraging buzz rate (buzz·hr^{-1})	0	0	NaN	427.7828315	0	183.7500319	0	67.02167816	0	115.3771331	48
Communication rate (calls·hr^{-1})	0	0	NaN	194.4467416	0	236.250041	0	201.0650345	0	41.95532114	73.00
Number of porpoises in region	0.55	0.10	0.18	0.15	0.75	0.47	0.11	6.60	0.35	1.64	9.27
	2015 Flood										
	Region 1	**Region 2**	**Region 3**	**Region 4**	**Region 5**	**Region 6**	**Region 7**	**Region 8**	**Region 9**	**Region 10**	**Total**
P^(echolocation clicks)	0.082130845	0.06332559	0.074938031	0.052189	0.07429	0.068132	0.053958	0.076304	0.039321389	0.083559	*0.0559*
P^(buzzes)	0.004553741	0.003610892	0.004358769	0.004154	0.004087	0.004118	0.003027	0.004169	0.002011497	0.004997	*0.0031*
Mean vertical dive angle (0-10m) (°)	4.86	-3.24	2.65	20.50	2.65	5.71	2.65	12.00	2.65	4.86	*4.80*
Std vertical dive angle (0-10m) (°)	10.12	22.69	20.07	12.34	20.07	11.21	20.07	15.62	20.07	10.12	*17.51*
Mean vertical dive angle (10m-seabed) (°)	9.29	29.55	16.50	38.10	16.50	16.50	16.50	0.89	16.50	9.29	*14.85*
Std vertical dive angle (10m-seabed) (°)	16.74	18.31	27.02	10.88	27.02	27.02	27.02	22.04	27.02	16.74	*24.76*
75% depth (m)	-30	-34	-54	-69	-26	-34	-31	-38	NaN	NaN	*-19.41*
No. clicks detected	27948.77525	15562.99696	12783.01562	3198.418	20496.72	29938.56	2935.337	37778.79	3151.109335	10028.29	163822

No. buzzes detected	90	76	1	3	57	159	0	130	2	0	518
No. Localised Clicks	6944	11722	734	1367	172	8734	34	13175	1	0	56058.00
Effort (seconds)	11970	15502	6193	5368	5738	35677	6090	40260	113855	8230	248883
Density Clicks (clicks·km^{-2})	1.57E-05	9.26E-06	1.58E-05	6.24E-06	2.73E-05	6.74E-06	NaN	6.56E-06	4.67E-07	NaN	*0.00000489*
Density (porpoises·km^{-2})	5.245201268	3.085029624	5.265961679	2.079554	9.084814	2.245712	NaN	2.187597	0.155805788	NaN	*1.631*
Foraging buzz rate (buzz·hr^{-1})	201.098518	350.3076906	0	0	80.07322	151.5656	0	113.3467	0	0	*76*
Communication rate (calls·hr^{-1})	39.95735	84.82531	0	293.4747	220.3517	216.7672	0	201.065	0	41.08472	*99.10*
Number of porpoises in region	0.554601	0.097103	0.18145	0.152909	0.751795	0.469929	0.111983	6.600701	0.345025	1.636744	9.27

Chapter 6: General Discussion

An autonomous vertical array with 8 hydrophones between 3 and 30m depth

CHAPTER 6: GENERAL DISCUSSION

6.1 SYNTHESIS

This thesis focused on the development of PAM methods to provide information on the 3D behaviour, distribution and density of harbour porpoises in tidal stream habitats. The emphasis here was to enhance existing density estimation methods with the inclusion of detailed auxiliary information on harbour porpoise diving behaviour, bioacoustics and aspects of their biosonar. PAM methods were developed to measure behavioural parameters, such as dive tracks and source levels, directly in tidal rapid habitats and a study on a captive animal provided high resolution 4π beam profile measurements. These were then input into a simulation to estimate spatially and temporally varying detection probability and thus the density of harbour porpoises in Kylerhea, a tidal rapid habitat in Scotland. The ability to efficiently measure detailed behavioural parameters in-situ during a PAM survey is particularly important in atypical environments, such as tidal rapids, where the habitat (e.g. currents, noise, bathymetry) is highly dynamic, animals are likely to use distinctive foraging strategies and their distributions change at fine spatial and temporal scales.

6.2 CHAPTER 2

Chapter 2 introduced a method of detecting click trains based on a multi hypothesis tracking (MHT) pattern recognition algorithm. Click train detection requires a contextual based approach to classification i.e. the likelihood of detecting a received sound (in this case an echolocation click) is based on spatial (bearing), temporal (ICI) and frequency (correlation) information of preceding and subsequently detected clicks. These algorithms are potentially advantageous because they can minimise classification errors due to variability between received sounds. They are therefore especially suited to the detection of echolocating animals (primarily toothed whales and bats) which produce clicks in consistent temporal patterns but have narrow beam profiles that can introduce significant variance between successive click waveforms and spectra received on PAM devices (Beedholm and Møhl 2006, Au et al. 2012, Finneran et al. 2014). For example, chapter 4 showed that the beam profile of a harbour porpoise introduces considerable distortion to the waveforms and spectra of NBHF clicks and these can constitute a significant portion of received click detections on PAM instruments, especially at higher source levels (see Chapter 4: Figure 5 and Figure 10).

The open source MHT click train algorithm developed in Chapter 2 generally outperformed a click-by-click classifier for all three different click types tested: the low frequency clicks of sperm whales, broadband delphinid clicks and highly stereotyped NBHF harbour porpoise clicks. In particular, the click train detector had a consistently lower false positive rate compared to a click-by-click classifier. This is because the click-by-click classifier had a low but relatively constant background rate of false positive detections which falsely identified a small proportion of the millions of detected transient sounds, especially those at a lower SNR. The click train detector was generally more robust to this because it additionally required a sequence of clicks to register a detection, and such sequences are usually rare within transients generated by noise. However, when high levels of transients were present, the click train detector began to identify spurious sequences of clicks because the large number of transients meant there was, by chance, some combination of clicks which could be associated that had a consistent ICI, bearing, and amplitude, etc. A relatively simple binary classification process which correlated the average spectra of click trains to a spectral template meant that some of these spurious trains were incorrectly classified.

To improve click train detection performance, more complex machine learning methods should be applied to classify the click trains detected by the MHT algorithm. These methods could be based on the average spectra, concatenated spectrogram, and/or other metrics (such as times series of ICI, STD ICI, χ^2 values of the different descriptors, etc.). This may be particularly advantageous in detecting click trains produced by delphinids, as many species from this family have less stereotyped clicks which are easily confused with transient noise sources (e.g. propeller cavitation) by automated algorithms. Even using a very simple spectral correlation method to classify click trains, the click train detector presented here showed significant performance increases in detecting delphinid clicks compared to click-by-click detection approaches. Delphinid clicks are also one of the most difficult to classify to species (see Soldevilla et al. 2008), however, recent machine learning based methods which have grouped large numbers of delphinid clicks (Frasier et al. 2017, Rankin et al. 2017) have shown promise in identifying individual delphinid species, even when mixed groups are present. MHT click train algorithms could be integrated as an alternative or additional data stream for these classifiers, particularly because it provides cleaner data inputs than grouping all detected clicks within a specified time period.

Click train detection therefore provides a promising PAM detection and classification methodology in that it minimises false positive detections and may aid in species classification by grouping multiple clicks together, especially for species with less stereotyped clicks. However, whilst minimising the false positive rate can be important for density estimation of rare species (Caillat et al. 2013), click trains are difficult to incorporate into the Monte Carlo simulations of detection probability discussed in Chapters 4 and 5. This is because detectability is predicated on behaviour of an animal over a period of time whilst detectability using click by click classifiers requires only the instantaneous behavioural state of a porpoise e.g. orientation, source level, beam profile. Thus, click train detection should only be used with current density estimation methods where detection probability is independently calculated, such as in towed array surveys, or where group size estimates are used rather than cue counting.

6.3 CHAPTER 3

Tidal rapid habitats are usually small and uniquely atypical areas within the much larger harbour porpoise range. However, very little is known about harbour porpoise behaviour, distribution or density in these habitats despite there being interest in utilising the strong currents in tidal rapid areas to generate renewable energy (Wilson et al. 2007, Benjamins et al. 2015). Because the physical conditions in tidal rapid habitats are so unusual it is not possible to extrapolate knowledge of porpoise behaviour and distribution patterns from other areas. Thus it was essential to be able to measure fine scale animal behaviour and distributions in situ to examine behavioural ecology at these sites, obtain essential parameters for the density estimation methods (e.g. diving behaviour and depth distribution) in Chapter 5 and thus assess the impact the potential industrialisation of such habitats might have on animals.

Chapter 3 focused on the development of a drifting vertical array suitable for deployment in fast-moving tidal streams, which would provide the 3D geo-referenced locations of porpoise clicks and therefore the first detailed information on the underwater behaviour of harbour porpoises in tidal rapids. Working with drifting PAM arrays in tidal areas brought three key challenges, 1) a significant quantity of data was collected which required automated localisation, 2) a high density of animals resulted in a significant click aliasing problem, and 3) widely spaced hydrophones, required for accurate localisation at range, meant that a non-rigid vertical array was required, which could be deformed by strong currents in the tidal stream. To manage the challenge of disentangling and

identifying multiple vocalising animals, a fully automated click matching algorithm was developed in conjunction with a tracking algorithm which grouped localised clicks into animal tracks (see Chapter 5 Figure 8 for multiple simultaneously tracked animals). Movement of the array was addressed by the addition of movement sensors that provided data to inform models of array movement which could then be incorporated into localisation calculations during analysis

The ability to efficiently analyse large quantities of acoustic data to obtain tens of thousands of individual porpoise dive track fragments in tidal rapids (see section 5.4.3) was crucial for both behavioural inference (e.g. orientation in the tide, depth distributions) and porpoise density estimations presented in Chapter 5. Thus, whilst chapter 3 focused on iterative improvements to a relatively commonly used methodology (localising animals using vertical hydrophone arrays), these developments were a central aspect of this thesis.

6.4 CHAPTER 4

In addition to dive behaviour an important input into simulation-based approaches to density estimation is the animal's beam profile. An initial data exploration of the localised dive tracks detected on the vertical array in Chapter 3 showed that the number of detected dive tracks was greatest when a harbour porpoise was approaching the array, exactly as would be expected for an animal with directional clicks. There was also a clear increase in the number of detected clicks as animals moved away from the array (see Chapter 4 Figure 1 and Malinka et al. (2015)). This suggested that the harbour porpoise may have a previously unreported peak in energy output directed behind it. This curiosity prompted the measurement of the full beam 4π beam profile of a harbour porpoise presented in Chapter 4 and measured beam profile of a captive porpoise indeed showed +10 dB (compared to the lowest energy) diffuse back-ended energy.

6.4.1 NBHF beam profiles and communication

Chapter 4 also showed that the harbour porpoise has a narrower beam and contains none of the side lobes predicted by a piston model. The piston model assumes a hard aperture for sound production which generates side lobes for narrowband signals. However, there is no known biological analogue to a hard edge of a piston model in the anatomy of a harbour porpoise's click production mechanism and so it is perhaps not surprising that there are no side lobes present. The beam profile shows a roughly stable -40dB drop from on axis source levels between 90-150° (and -

30dB towards 180°). Thus, near the porpoise there is diffuse acoustic energy (see Chapter 4 Figure 6) which, at high source levels, means a harbour porpoise should be detectible to other animals and PAM systems regardless of orientation at closer ranges. This more omnidirectional and diffuse portion of the beam is almost certainly due to some acoustic energy escaping the head of the animal during sound production i.e. the air sacs, skull and melon which allow harbour porpoises and other toothed whales to generate highly directional sounds (Madsen et al. 2010) are not perfect. Whilst this diffuse section of the beam may be incidental to click production, could it still confer some biological or behavioural advantage?

Aguilar de Soto et al. (2020) introduce the idea that beaked whales have evolved in a "soundscape of fear" due to predation from killer whales which has driven remarkable behaviour such as not vocalising at the sea surface, only communicating at depths greater than 170m (Aguilar de Soto et al. 2012) and foraging with extreme synchronicity in groups. Rather than develop extreme behavioural adaptions, it is theorised that harbour porpoises and other NBHF species have evolved an alternate strategy, by losing their ability to produce tonal vocalisations and adopting a high frequency low source level click which cannot be detected by killer whales (Madsen et al. 2005, Morisaka and Connor 2007, Kyhn et al. 2009, 2010) or indeed other predators such as the extinct macroraptorial sperm whales *Acrophyster deinodon* (Galatius et al. 2019). There are significant disadvantages in using a high frequency click which has limited range due to relatively high absorption (Villadsgaard et al. 2007), contains less information in the returning echo compared to broadband clicks (Simmons et al. 2014) and then also losing all lower frequency tonal vocalisations which perform important social functions in other toothed whale species (e.g. Janik et al. 2006). Little is known about harbour porpoise social structures, however, they are thought to communicate by encoding information in the inter-click-interval of some rapid bursts of clicks (Clausen et al. 2010) and DTAG data has suggested they make hundreds of such calls per day (840-1320 per day for adults) (Sørensen et al. 2018). Drone footage has also shown them hunting cooperatively (Stedt et al. 2019) and large aggregations of animals that must necessitate social interactions have been reported in some areas ((e.g. Hoek 1992) and see Chapter 5). This limited evidence suggests that harbour porpoise invest significant time in communication and interaction with conspecifics and thus, ssince social calls are thought to be produced using the same sound production mechanism as echolocation clicks, they and likely other obligate NBHF species must

somehow balance their ability to communicate for social interaction with their echolocation capabilities and acoustic crypsis.

How they achieve this is uncertain. All species of toothed whales studied so far have a highly directional beam with directionality indices which are remarkably similar between species; thus it appears that beam directionality is highly selected for, probably because it functions in reducing acoustic clutter and allows longer range prey detection for the same acoustic energy expenditure (Jensen et al. 2018). As has been shown in Chapter 4 and previous literature (Au et al. 1999, Koblitz et al. 2012), porpoises are no exception to this rule. They must therefore optimise their active space for communication whilst maintaining the ability to produce highly directional clicks. Heaveside's dolphins (*Cephalorhynchus heavisidii*) may have achieved this by using a low frequency click type for communication that propagates further and thus increases the animal's active acoustic space. Martin et al. (2018) theorise that this is a compromise between a whistle which would propagate much further and the restricted active space which can be achieved using only NBHF clicks. However, Galatius et al. (2019) note that these delphinids evolved NBHF clicks later than other NBHF species and thus may simply be in the evolutionary process of losing the ability to produce lower frequency clicks. Sperm whales, like obligate NBHF species, produce no tonal vocalisations and instead utilise click packets called codas (Watkins 1977, Rendell and Whitehead 2003) and slow clicks (clangs) (Oliveira et al. 2013) for communication. Madsen et al. (2002) proposed that codas are produced in a different way to echolocation clicks, whereby, instead of most energy being directed in single pulse, the production of coda clicks involves using reflected energy in the nasal complex to generate much less directional clicks. Thus, the click production mechanism in sperm whales likely has a bimodal function for both communication and echolocation, however, the sound production mechanism in sperm whales is very different to that of the much smaller NBHF species (Møhl 2001) and thus it does not necessarily follow that harbour porpoises or other obligate NBHF species should be able to change their directionality in a similar way. Bats are clearly not subject to evolutionary pressure from killer whale predation; however, they only have one sound production mechanism which they use for echolocation and so must similarly balance echolocation capabilities and social communication. Social calls produced by many species are often lower frequency then echolocation calls which results in a wider beam profile and so optimises their active space for communication (e.g. Pfalzer and Kusch, 2003). However, social information, including identification

of individuals, may also be conveyed in search-phase echolocation calls, probably as a way to facilitate contact between individuals during foraging (Kohles et al. 2020). Thus, although the acoustic parameters of bat echolocation calls are driven primarily by ecological factors leaving little acoustic space to encode social information, it seems that within these constraints a number of species have evolved sufficient intraspecies variation to encode some social information (Jones and Siemers 2011, Knörnschild et al. 2012). However, bats usually have significantly wider beam profiles than toothed whales (e.g. Brinkløv et al., 2011; Jakobsen et al., 2013b, 2012; Surlykke et al., 2013) and can actively adapt their beam volume by changing echolocation parameters (e.g. frequency, duration) (Jakobsen et al. 2013a). Thus, they generally have a less directional and possibly a more adaptive active space than toothed whales which may mean that encoding extra social information in echolocation calls is a more effective strategy for communication than it would be for toothed whales.

Harbour porpoises have a very weak 1-2 kHz component in their clicks but with a very limited active space (Hansen et al. 2008), they do not significantly change frequency to widen their beam, and there is no evidence of additional information encoded within standard echolocation clicks (although there have been no comprehensive experiments testing this to date). It is perhaps then tempting to think that the diffuse energy described in Chapter 4 might indeed be useful and perhaps even an adaptation for short ranged communication. However, between -150° and -90°, the off axis energy of bottlenose dolphins (*Tursiops truncatus*) (Finneran et al. 2014) and sperm whales (Zimmer et al. 2005) falls to around -45dB from on-axis source levels, and so both species have only a slightly narrower off-axis beam than harbour porpoises with off-axis measurements in all studies well within the error bounds of each other. Thus, harbour porpoises may still use this diffuse energy but it does not appear to be a specific NBHF adaptation, probably because any such increase in this diffuse energy might introduce additional clutter into their echoic scene.

However, harbour porpoise may be able to optimise their active space for communication by actively widening their acoustic beam. Wisniewska et al. (2015) showed that harbour porpoises widen their beam during foraging buzzes, to increase their field of view and facilitate the final stage of prey capture. This is achieved by conformational changes to their melon, air sacs and phonic lips and is likely under active cognitive control, providing porpoises with a mechanism for flexible control over their beam during buzzing without needing to module the frequency content

of their clicks. They are thought, therefore, to have substantially more dynamic control of their field of view *during buzzing* than documented bat species which widen their beams by reducing the frequency of their echolocation clicks (Jakobsen and Surlykke 2010, Wisniewska et al. 2015). There have been no such beam widening studies on porpoise communication calls, however, they are very similar to buzzes but apparently produced at higher output levels off-axis and, since widening the beam is thought to be actively controlled, it is reasonable to assume that a harbour porpoise could also widen its beam during communication. This could triple the ensonified area of a porpoise beam increasing the active space for the same on-axis source level. However, even at the maximum widening shown by Wisniewska et al. (2015) (directivity index of 21 dB) this is still nowhere near as omni directional as dolphin whistles (directivity index of 6 dB at lower harmonics (Branstetter et al. 2012)).

Active widening of the beam pattern of echolocation clicks (buzzes were not studied) has also been observed in Atlantic spotted dolphins (*Stenella frontalis*) (Jensen et al. 2015) and both Jensen et al. (2015) and Wisniewska et al. (2015) theorise that the advantages a dynamic field of view provides in facilitating prey capture, means it is likely most or all toothed whales have the ability to actively adjust their beam width without substantially altering frequency. If beam widening is the primary method to increase the active space of communication calls for obligate NBHF species, then it might be expected that they have evolved additional strategies or capabilities in how they actively utilise their dynamic beam compared to other toothed whales. For example Sørensen et al. (2018) theorise that the wider, albeit still restricted, beam may be used in conjunction with multiple calls in different directions to increase active space, which may explain the high number of calls observed in DTAG data. Thus, comparative beam dynamics in relation to behaviour is an area in which further research could yield insights into the evolution and adaptions required for obligate NBHF species, especially social interaction with conspecifics. Thus, the hypothesis for a future set of experiments is that obligate NBHF species actively widen their beam profile to provide the most optimal active space for communication calls. The extreme off axis components of the beam (e.g. the diffuse back beam) should also be investigated to determine whether there is any evidence they are more pronounced in NBHF species (especially the back beam which has not yet been measured in broadband clicking dolphins) and if they are utilised in communication, perhaps by behavioural changes such as swimming closer to other animals during periods of communication. This could be

achieved by the study of tagged wild animals using drones, and/or multiple captive animals using a similar experiment setup to Chapter 4.

6.4.2 Implication for PAM

An exploration of detection probability using Monte Carlo simulations indicated that side and back energy of a biosonar beam is crucial to generate accurate detection probabilities and thus density estimates (see Chapter 4 Figure 8). There was also significant distortion in click spectra and waveforms beyond 20° off-axis from the forward beam, which forms a large portion of the beam that would be detectable by a PAM device (5-65%) depending on source level (see Chapter 4 Figure 5). Automated detection and classification of harbour porpoise clicks is often considered one of the simpler analysis challenges in PAM. Chapter 2 demonstrated that a large portion of the clicks received on a PAM device will have distorted waveforms and spectra; thus simple analysis methodologies which assume detections will be on-axis clicks (e.g. matched filters) and thus do not take account of this distortion, are unlikely to be particularly effective. This could also partially explain the high false positive rate of porpoise clicks by the matched click classifier in Chapter 2 Figure 6 and Chapter 5 Figure 15S. Using more sophisticated automated algorithms, for example the click train detector in Chapter 2 or machine learning based approaches, should provide more reliable detectors. This is also a good example of why the automatic detection of even the most stereotyped clicks is not a simple signal processing problem and perhaps explains why, after decades of research, automated PAM analysis still has very few standardised methodologies and is an active (an interesting) area of research.

Two key requirements of a simulation based approach to estimating detection probability and thus animal density are accurate knowledge of the beam profile of animals and quantification of the false positive rates of automated click detectors (Küsel et al. 2011, Frasier et al. 2016). Chapter 4 provided the full 4π beam profile of a harbour porpoise and information on potential sources of error in click detection algorithms. Thus, it is perhaps the best example in this thesis of why the synergy between detailed studies of the biosonar of toothed whales is important for PAM applications and provides a link between what is often considered blue skies research with applied conservation and management methodologies.

6.5 CHAPTER 5

6.5.1 Density Estimation in Tidal Rapids

Chapter 5 brought together information and methods from the detection and classification algorithms in Chapter 2, localisation methods in Chapter 3, and beam-profile measurements in Chapter 4 to estimate the fine-scale patterns in distribution, density and behaviour of harbour porpoises in a tidal stream.

In general, the use of Monte Carlo simulation for calculating detection probability and thus animal density is considered a method of last resort (Marques et al. 2013), and calculating detection probability directly during surveys, e.g. when using localising towed arrays (Lewis et al. 2007, Gordon et al. 2011) are preferred. This is because the accuracy of estimated detection probabilities is dependent both on assumptions made in the modelling process and on the accuracy of the input data, e.g. source levels, beam profiles, etc. (Küsel et al. 2011). However, in many situations, it can be difficult to measure the detection probability directly, especially in circumstances where simple long term recording devices are used, and/or conducting auxiliary experiments to determine the detection probability directly are not feasible, e.g. in deep-sea environments (Hildebrand et al. 2019).

Tidal rapids are one such habitat where environmental conditions and animal behaviour, and thus detection probability, can change rapidly. Towed PAM arrays could not be used to measure fine-scale animal behaviour and density because there was concern that boat could disturb animals, and that the position of an array streaming 100-200 m behind a research vessel would be difficult to calculate in such a fast moving currents. Other monitoring modalities, such as visual studies were not a feasible option because they could not assess behaviour other than at the sea surface. Biotelemetry was also considered, but there is no tagging program for porpoises in tidal waters. Moored PAM devices were a possibility, but bottom-mounted devices are expensive to deploy and may suffer from the masking effects of flow noise. Thus, a simulation-based approach to density estimation using a drifting hydrophone array was indeed the “last resort”. The primary emphasis in this study was therefore to try and minimise the potential for errors in density estimation by measuring relevant aspects of harbour porpoise behaviour directly at the study site. The click train detector (Chapter 2) was used to extract buzzes and maximum click production (cue rate) estimates, localising vertical arrays (Chapter 3) determined the depth distribution and diving behaviour of harbour porpoises in different

regions, and the full 4π measurements of a harbour porpoise beam profile (Chapter 4) provided a more accurate beam profile input for the detection probability simulations. The main missing parameter was the source level of buzzes, which could not be accurately calculated on the vertical array, however, studies have measured source level of buzzes from captive and tagged wild animals (Deruiter et al. 2009, Wisniewska et al. 2012, 2016). There is little reason to believe harbour porpoises would substantially change their buzz source levels in a tidal rapid habitat unless there were high levels of noise – however, porpoises appear stay out of these area in Kylerhea (see Chapter 5 Figure 12).

Thus, the Monte Carlo detection probability simulation for density estimation should provide accurate values for the probability of detection. Calculating density was then based on the distance sampling equation for a fixed acoustic sensor (drifting units are considered fixed because they are in the same reference frame as the water). A key assumption of distance sampling is that the distribution of animals is random with respect to the acoustic sensor (Buckland et al. 2001). In a tidal stream, random animal distribution in relation to a drifter is not a valid assumption because animal distribution may be highly correlated with currents which also influence the track of a drifter. This was somewhat mitigated by breaking the tidal area into small sections where random starting positions of drifters meant that they passed through each area of the tidal stream with very different tracks. However, some of the larger areas could not be randomly sampled. For a larger tidal rapid area (e.g. the Great Race (Benjamins et al. 2016)) either many more drifters or switching survey methodology to something which offered more control over survey design may be required (e.g. towed arrays or bottom mounted recorders).

6.5.2 Tidal Rapid Use by Harbour Porpoise

Narrow habitat corridors can increase prey encounter rates or foraging success rates (Knowlton and Graham 2010, Hastie et al. 2016), e.g. bears prey on salmon in narrow and shallow portions of rivers rather than in deep low-flow areas (Gard 1971). However, in any hydrographically dynamic environment, a predator must find some mechanism by which balance their energetics of being in an high flow environments with increased foraging success. An obvious strategy is to find a mechanism to stay out of the high current flows. In riverine environments, this can simply involve anchoring or staying out of the flowing water, e.g. bears often wait for salmon on rocks or in shallow portions of the river. However, in marine habitat corridors, this is usually not possible with both predator and

prey fully immersed in a 3D environment which is in a constant state of flux. Many aquatic animals have developed strategies to minimise large energetic expenditure in high flow environments; for example coral reef fish utilise flow refuges (Johansen et al. 2008), trout take advantage of fine scale vortices in rivers (Liao 2004, Stewart et al. 2016) and fin whales and minke whales are often observed in the lee of islands (Johnston et al. 2005). Thus, it is likely that any marine predator in a tidal rapid environment is using some strategy to both increase foraging rates and/or success and at the same time minimise energy expenditure in fast currents. Kylerhea, the tidal rapid where data for Chapters 3 and 5 were collected, has flow speeds that can be up to 4 ms^{-1} (Wilson et al. 2013) which would incur significant energy expenditure for harbour porpoises to directly swim against (Otani et al. 2001). The density of harbour porpoises in the fast-flowing tidal narrows was almost zero suggesting they mostly stay out of the highest flow environment. Instead animals were concentrated in large numbers in the slower-moving spit of water at the entrance and exit of the narrows. Acoustically reconstructed animal movement tracks showed that animals were orientated against the tide within the spit (Chapter 5 Figure 10), and the large number of buzzes in these regions suggested high foraging rates (Chapter 5 Figure 12). The water speeds in these areas still likely incur significant energy expenditure to swim against, and despite the detailed behavioural information collected by the vertical hydrophone arrays, the exact mechanism by which harbour porpoises are utilising this spit of water remains unclear.

As such, the question remains: how do harbour porpoises minimise their energy expenditure and/or maximise their prey intake in these fast currents? The orientation of porpoises suggests that they are echolocating upstream. It is possible that they are exploiting fine scale tidal features such as boils and upwelling areas that were not recorded in the survey, and/or utilising steep current velocity gradients to increase the number of prey passing through their echolocation beam (see section 5.5.2.1). To test these hypotheses, data on both fine scale spatial and temporal hydrographic properties within the tidal stream environment and the comprehensive behaviour of individual animals is required. The hydrophone arrays were capable of collecting track fragments from any animal within range; these could be used for broad behavioural inference, however, a single animal was very rarely tracked over an extended period due to narrow beam profile, meaning that animals which turned away from the array or moved out of range became undetectable. To investigate fine scale foraging strategies employed in these environments, a methodology which links fine scale

animal behaviour with detailed hydrographic features within a tidal stream (e.g. upwelling, eddies, boils, etc. , (see Benjamins et al. 2015) is required. One potential way to do this is a combined acoustic doppler current profiler (ADCP) and a drone survey to obtain hydrophobic features alongside a tagging study using acoustic tags that can record foraging attempts (e.g. Wisniewska et al. 2016). However, this would be a highly complex and difficult study to perform, there is no porpoise tagging program in the UK, and even if there was, there would be no guarantee that the tagged porpoises would enter the tidal rapid in which we wished to observe them in. A more cost-effective approach might be to use active acoustic monitoring. Drifting high frequency multibeam sonar systems have been used to record the 3D movements of seals (Hastie et al. 2019) and can also image some fine scale hydrographic features including turbulence in tidal streams. Although they suffer from the same disadvantage of vertical PAM arrays, in that drifting systems cannot track an individual animal over an extended period, drifting active acoustic devices could be used to relate fine scale movements of porpoises to detailed hydrographic features. This could be used in tandem with passive acoustics to record acoustic behaviour and verify species ID.

6.5.3 Conservation Implications

Information on porpoise behaviour, foraging rates and densities is important for assessing the possible impacts of anthropogenic activities in tidal rapids. This has become especially relevant in recent years with plans to deploy tidal turbines in large numbers in some tidal habitats tidal to generate renewable energy (Sangiuliano 2017). The industrialisation of tidal habitats in this way introduces concerns that animals may suffer collisions with turbine blades causing injury or death (Wilson et al. 2007, Onoufriou et al. 2019) and/or that increased anthropogenic activity may result in habitat exclusion. The fine scale diving behaviour of porpoises collected here can be used to parametrise collision risk models (Scottish Natural Heritage 2016) - a current information gap - whilst the more general abundance and foraging behaviour can be used to estimate the impact of habitat exclusion.

Harbour porpoises in Kylerhea were present in high densities and there were high levels of foraging buzzes (mean of 278 buzz·hr^{-1} ebb 2014 (assuming a click production rate of 3 clicks·s^{-1})). Wisniewska et al. (2016) used acoustic tags to show that harbour porpoises in Danish waters have very high foraging rates, likely due to having high field metabolic rates which are almost double that of equivalently sized terrestrial animals (Rojano-Doñate et al. 2018). Wisniewska et al. (2016) and

Rojano-Doñate et al. (2018) suggest that this means harbour porpoises are particularly vulnerable to impacts from any disturbance that disrupts foraging. If the foraging success rates are similar to that of tagged wild animals (>90%), then foraging rates measured at Kylerhea suggest that the daily energetic requirements for a harbour porpoise could almost be fulfilled in one or two tidal cycles if fish with an energetic content similar to a harbour porpoises average seasonal diet were consumed (Booth 2020). Thus, results here indicate that exclusion from a tidal rapid habitat could potentially have a significant impact on harbour porpoises that forage there, although the magnitude of this impact will depend on whether individual animals are specialist tidal rapid feeders. In addition, because Kylrhea comprises a relatively small area, the overall number of animals feeding in these sites is relatively low (~35 animals in the area on average in 2014). The methods used here can only estimate how many harbour porpoise there were on average in the study area at any one time. It cannot be determined how many individuals were using the area i.e. whether there is a specialised group of tidal rapid feeders or many different animals visiting the area. Thus, further work on identification and behavioural ecology of individual harbour in tidal rapids would be beneficial to assess the potential impact of disturbance.

This study is the first example of combined fine scale behaviour and animal abundance estimates being measured for cetaceans in a tidal stream habitat. However, the behaviour and distribution of harbour porpoises measured in Kylerhea should not necessarily be generalised to other tidal habitats. Other studies have shown that porpoises likely behave differently in other tidal habits e.g. a study by Benjamins et al. (2016) used PAM drifters to show that harbour porpoises move with the tide stream rather than against; thus behaviour in tidal rapids is likely be highly habitat and context dependent. This study should therefore be considered as an exemplar demonstrating how PAM methods can be used to cost effectively obtain behaviour, distribution and density of toothed whales in a tidal stream.

6.6 FUTURE DEVELOPMENT OF PAM

The focus in this thesis has been on developing methods to classify, localise and estimate the density of echolocating toothed whales, in particular the harbour porpoise. Whilst many of the methods developed in this thesis can be generalised to other taxa (e.g. other toothed whale species and perhaps bats), the case study of harbour porpoise in tidal rapid habitats, presented here, is only a

small subset of the potential species, vocalisation types, and environments which can be monitored using PAM.

Biodiversity loss and climate breakdown mean there is an increasing requirement for ecological monitoring to track shifts in the abundance, distribution and vulnerability of a range of species (Cardinale et al. 2012). PAM has the potential to provide a taxonomically broad, scalable and long-term means of delivering monitoring and, in many cases, has significant advantages complimenting or replacing other survey methodologies. For example, PAM can reduce observer bias, increase sample size (Barlow and Taylor 2005), can be used day and night and is often highly cost-effective. PAM methods can be applied to a wide range of ecological and conservation focused questions. Towed hydrophone arrays or deployments of long term autonomous devices can be used to monitor the absolute abundance of animals, e.g. a network of underwater PAM devices have recorded the precipitous decline, and likely extinction, of vaquita (Thomas et al. 2017). PAM has direct conservation applications, such as real time monitoring of poachers in tropical forest (Wrege et al. 2017), identifying the extent of illegal dynamite fishing (Braulik et al. 2017), performing rapid assessments of species diversity (Braulik et al. 2018) and is used extensively in mitigating the risk to cetaceans of anthropogenic activity such as high levels of underwater noise produced by sonar (Barlow and Gisiner 2006), seismic exploration (Weir and Dolman 2007, Castellote 2007) and ship strikes (Van Parijs et al. 2009). PAM is also used in behavioural monitoring (see Chapter 3) and extensively in bioacoustics and biosonar studies (e.g. Jensen et al. 2015; Ladegaard et al. 2017)

There have been relatively few dedicated large scale multi sensor network deployments for long term density estimation (e.g. Thomas et al. 2017; Carlén et al. 2018). Within the marine environment, this can be somewhat attributed to the expense of putting many devices out at sea, however, such sensor networks are also not particularly common in terrestrial PAM but have been implemented in other aspects of marine science, e.g. for the collection of oceanographic data (Roemmich et al. 2009). Thus, despite its potential in conservation, ecological and behavioural applications, large scale multi sensor PAM methods appear to be currently under-utilised (Gibb et al. 2019). There are several potential bottlenecks in PAM methodologies which may explain this.

6.6.1 Data Collection

In the marine environment, deploying long term monitoring devices from vessels is expensive and time consuming and thus large-scale PAM studies require hardware which can record for an extended period to maximise cost efficiency. In large scale studies of high frequency species, hardware used so far has generally sacrificed data quality for simplicity and longevity. For example, large scale deployments of CPODs were used for monitoring of the vaquita (Thomas et al. 2017) and Baltic harbour porpoise (Carlén et al. 2018) populations. These devices worked by saving a list of the time and peak frequency of detected high frequency transients but saved no information on either noise or the broader soundscape. Long term studies of lower frequency species have been able to collate raw acoustic data at much lower sampling rates (e.g. Davis et al. 2017) and in some cases have also taken advantage of other types of instruments which record low frequency data, for example seismometers (e.g. Harris et al. 2013) and/or hydrophones used to enforce the nuclear test ban treaty (e.g. Sousa & Harris 2015).

However, as microprocessor and storage capabilities continue to improve, this bottleneck is fast disappearing; there is a new generation of devices which are both open source and can record higher frequency data or run detectors with far less data degradation for significant periods of time (e.g. the SoundTrap (Ocean Instruments, NZ)). In terrestrial PAM applications, easy to use open source hardware has recently dropped the price of autonomous high-quality recording devices by an order of magnitude, making large scale deployments far more feasible (Hill et al. 2018)

6.6.2 Analysis Algorithms

Large scale deployments of PAM devices generate large volumes of acoustic data. A decade ago, it could have been argued that a fundamental problem for PAM was the ability to analyse large datasets, especially as the complex nature of terrestrial and marine soundscapes makes extracting variable sounds received at different SNR levels a complex pattern recognition problem (Von Ahn et al. 2008). However, the introduction of easily accessible deep learning algorithms API's (e.g. TensorFlow (Google)) is rapidly removing this bottleneck from acoustics. For example, right whale upsweeps (~1 second long 100-200Hz) are a notoriously difficult call to classify due to variability in the call, high levels of background noise at low frequency and the more numerous and vocal humpback whales producing confounding calls. In almost two decades (e.g. Gillespie 2004) there was very little progress on increasing the efficiency of acoustic classifiers for right whale upsweeps,

however, recently Shiu et al. (2020) applied deep learning methods which dropped the false positive rate by an order of magnitude compared to the next best classifiers, and was able to recognize calls in contexts which were not present in the training data (i.e. the classifier was not over trained). This was a particularly interesting study because a standardised set of performance metrics and testing datasets have been used to test classifiers on right whale upsweeps in much of the previous literature- thus direct comparisons of the algorithm's substantially improved performance were possible. Other machine learning based approaches are also showing great promise; a generalised classifier, BANTER (BioAcoustic EveNT ClassifiER) with extensive open source and public API has shown marked improvements in identifying similar dolphin species, even in mixed groups (Rankin et al. 2017), convolutional neural networks have been useful in automatically extracting sperm whale codas (Bermant et al. 2019) and, in terrestrial acoustics, the application of deep learning methods has also shown considerable potential in identifying bat and bird species (e.g. Stowell et al. 2019; Mac Aodha et al. 2018).

Thus, bottlenecks in automated analysis are less likely to be due to the fundamental ability of a computer to recognize target sounds within complex acoustic environments. The issue is, instead, providing suitable training data sources and developing easy to use implementations of these algorithms for the wider acoustics community.

Any classification algorithm needs some degree of training; this could be simply setting bespoke parameters, or, in the case of more complex machine learning algorithms, inputting large manually annotated training datasets which reflect the acoustic repertoire of the target species, any confounding sounds and the surrounding environment e.g. ensuring sounds at different distances are recorded (Ainslie 2013). If training data is not adequate, then an algorithm can be over trained, i.e. it becomes very specific to context within the training data and thus not useful as a general classifier. In much of the literature is it difficult to tell whether a new algorithm performs well because it has been over trained or because it is a genuinely good algorithm (e.g. Luo et al. 2017; Cosentino et al. 2019) and it should be noted that Chapter 2 is not an exception to this problem (however, by making the algorithm accessible and open source so other researchers can train and test, it is hoped this is somewhat mitigated). Thus, the field would significantly benefit from a set of large, multi-species, multi-environment training datasets and standardised performance metrics so that analysis methodologies can be compared. The reason large technology companies (such as

Google, Microsoft, Amazon etc.) can produce such good classifiers is partly because they have large datasets to train on, for example tagged images on the internet. Such datasets are rare for PAM studies and thus an important aspect of PAM in the future will be to use a unified metadata system so that training data can be effectively shared and accessed between research groups (Roch et al. 2016).

Once a classifier has been proven to be effective it needs to be made accessible to the wider community, as has been done with the click train detector in Chapter 2 (and many mother algorithms) via implementation in PAMGuard. This may be in the form of a programming library or into a widely used software package (e.g. Raven, PAMGuard, Ishmael). Even if a classifier is adequately trained, in complex marine environments it is likely that some situation will arise where a manual analyst is required to verify certain aspect of the dataset. Machine learning tools may be good at dealing with highly complex data, but they can still suffer from unexpected inconsistencies i.e. unknown unknowns (Yuan et al. 2019). Thus, powerful visualisation tools which allow manual analysts to rapidly navigate large datasets and assess results from automated analysis will be vitally important for the foreseeable future and should not be overlooked. In addition, intuitive user tools to modify existing classifiers, i.e. by adding new training data without requiring specialist researchers, could be implemented in tandem this software, further lowering analysis barriers.

6.6.3 Density Estimation

Automated analysis data from large multi sensor networks could be used for a variety of ecological and conservation applications (Sugai et al. 2019, Gibb et al. 2019). Chapter 5 of this thesis demonstrated one such application, calculating the animal density and distribution in a tidal stream environment. Other habitats will require different types of PAM hardware and present different data collection and analysis challenges (e.g. Marques et al. 2011; Küsel et al. 2011; Harris et al. 2013; Hildebrand et al. 2015). However, for almost all density estimation studies, it is essential to understand the fine scale behaviour of the study species both to obtain any required auxiliary information required and appreciate the potential caveats that may arise in the PAM density estimation methods. For example, understanding that beaked whales do not click at the sea surface has had significant implications for estimating population size from PAM (Johnson et al. 2004, Marques et al. 2009). For many echolocating species, detailed information on aspects of their biosonar and acoustic behaviour, such as beam profiles and click rates, is a key information gap

required for density estimation. Much of this information is difficult to collect directly with visual studies or PAM and thus additional and complementary studies, such as those using sound and movement tags (Johnson and Tyack 2003), are vital for component for continued progress in density estimation.

6.7 CONCLUSION

This study has demonstrated the highly detailed information that PAM can provide on behaviour and abundance. Results from the application of these methods in Kylerhea showed that there were almost no harbour porpoises in the narrow fast moving channel, instead they were concentrated in a spit of water immediately south, appeared to be producing high rates of foraging buzzes in both the ebb and flood tide and were consistently diving throughout the water column. The behaviour and high density of harbour porpoises in Kylerhea suggests that tidal rapids and surrounding areas may be important foraging habitats and as such, there should be careful consideration of the conservation implications of deploying tidal turbines in these areas.

The continued development and deployment of PAM methods have significant potential in the future for large-scale long-term monitoring of multiple taxa. However, PAM is hindered by the accessibility of advanced automated analysis algorithms, intuitive software for the visualisation of large datasets and the lack of unified training data. Density estimation requires continued close interdisciplinary work on the biosonar (if echolocators) and acoustic and behavioural ecology of the target species.

6.8 REFERENCES

Aguilar de Soto, N., P. T. Madsen, P. Tyack, P. Arranz, J. Marrero, A. Fais, E. Revelli, and M. Johnson. 2012. No shallow talk: Cryptic strategy in the vocal communication of Blainville's beaked whales. Marine Mammal Science 28:E75–E92.

Aguilar de Soto, N., F. Visser, P. L. Tyack, J. Alcazar, G. Ruxton, P. Arranz, P. T. Madsen, and M. Johnson. 2020. Fear of Killer Whales Drives Extreme Synchrony in Deep Diving Beaked Whales. Scientific Reports 10:13.

Von Ahn, L., B. Maurer, C. McMillen, D. Abraham, and M. Blum. 2008. recaptcha: Human-based character recognition via web security measures. Science 321:1465–1468.

Ainslie, M. A. 2013. Neglect of bandwidth of Odontocetes echo location clicks biases propagation loss and single hydrophone population estimates. The Journal of the Acoustical Society of America 134:3506–3512.

Mac Aodha, O., R. Gibb, K. E. Barlow, E. Browning, M. Firman, R. Freeman, B. Harder, L. Kinsey, G. R. Mead, S. E. Newson, I. Pandourski, S. Parsons, J. Russ, A. Szodoray-Paradi, F. Szodoray-Paradi, E. Tilova, M. Girolami, G. Brostow, and K. E. Jones. 2018. Bat detective—Deep learning tools for bat acoustic signal detection. PLOS Computational Biology 14:e1005995.

Au, W. W. L., B. Branstetter, P. W. Moore, and J. J. Finneran. 2012. The biosonar field around an Atlantic bottlenose dolphin (Tursiops truncatus). The Journal of the Acoustical Society of America 131:569–576.

Au, W. W. L., R. A. Kastelein, T. Rippe, and N. M. Schooneman. 1999. Transmission beam pattern and echolocation signals of a harbor porpoise (Phocoena phocoena). The Journal of the Acoustical Society of America 106:3699–3705.

Barlow, J., and R. Gisiner. 2006. Mitigating, monitoring and assessing the effects of anthropogenic sound on beaked whales. Journal of Cetacean Research and Management 7:239–249.

Barlow, J., and B. L. Taylor. 2005. Estimates of sperm whale abundance in the northeastern temperate pacific from a combined acoustic and visual survey. Marine Mammal Science 21:429–445.

Beedholm, K., and B. Møhl. 2006. Directionality of sperm whale sonar clicks and its relation to piston radiation theory. The Journal of the Acoustical Society of America 119:EL14.

Benjamins, S., A. Dale, N. van Geel, and B. Wilson. 2016. Riding the tide: use of a moving tidal-stream habitat by harbour porpoises. Marine Ecology Progress Series 549:275–288.

Benjamins, S., A. Dale, G. Hastie, J. Waggitt, M.-A. Lea, B. Scott, and B. Wilson. 2015. Confusion Reigns? A Review of Marine Megafauna Interactions with Tidal-Stream Environments. Pages 1–54 Oceanography and Marine Biology: An Annual Review.

Bermant, P. C., M. M. Bronstein, R. J. Wood, S. Gero, and D. F. Gruber. 2019. Deep Machine Learning Techniques for the Detection and Classification of Sperm Whale Bioacoustics. Scientific Reports 9:12588.

Booth, C. G. 2020. Food for thought: Harbor porpoise foraging behavior and diet inform vulnerability to disturbance. Marine Mammal Science 36:195–208.

Branstetter, B. K., P. W. Moore, J. J. Finneran, M. N. Tormey, and H. Aihara. 2012. Directional properties of bottlenose dolphin (Tursiops truncatus) clicks, burst-pulse, and whistle sounds. The Journal of the Acoustical Society of America 131:1613–1621.

Braulik, G. T., M. Kasuga, A. Wittich, J. J. Kiszka, J. MacCaulay, D. Gillespie, J. Gordon, S. S. Said, and P. S. Hammond. 2018. Cetacean rapid assessment: An approach to fill knowledge gaps and target conservation across large data deficient areas. Aquatic Conservation: Marine and Freshwater Ecosystems 28:216–230.

Braulik, G., A. Wittich, J. Macaulay, M. Kasuga, J. Gordon, T. R. B. Davenport, and D. Gillespie. 2017.

Acoustic monitoring to document the spatial distribution and hotspots of blast fishing in Tanzania. Marine Pollution Bulletin 125:360–366.

Brinkløv, S., L. Jakobsen, J. M. Ratcliffe, E. K. V. Kalko, and A. Surlykke. 2011. Echolocation call intensity and directionality in flying short-tailed fruit bats, Carollia perspicillata (Phyllostomidae) . The Journal of the Acoustical Society of America 129:427–435.

Buckland, S. T., D. R. Anderson, K. P. Burnham, J. L. Laake, D. L. Borchers, and L. Thomas. 2001. Introduction to Distance sampling: estimating abundance of biological populations. Page New York USA. New York.

Caillat, M., L. Thomas, and D. Gillespie. 2013. The effects of acoustic misclassification on cetacean species abundance estimation. The Journal of the Acoustical Society of America 134:2469–2476.

Cardinale, B. J., J. E. Duffy, A. Gonzalez, D. U. Hooper, C. Perrings, P. Venail, A. Narwani, G. M. Mace, D. Tilman, D. A. Wardle, A. P. Kinzig, G. C. Daily, M. Loreau, J. B. Grace, A. Larigauderie, D. S. Srivastava, and S. Naeem. 2012. Biodiversity loss and its impact on humanity. Nature 486:59–67.

Carlén, I., L. Thomas, J. Carlström, M. Amundin, J. Teilmann, N. Tregenza, J. Tougaard, J. C. Koblitz, S. Sveegaard, D. Wennerberg, O. Loisa, M. Dähne, K. Brundiers, M. Kosecka, L. A. Kyhn, C. T. Ljungqvist, I. Pawliczka, R. Koza, B. Arciszewski, A. Galatius, M. Jabbusch, J. Laaksonlaita, J. Niemi, S. Lyytinen, A. Gallus, H. Benke, P. Blankett, K. E. Skóra, and A. Acevedo-Gutiérrez. 2018. Basin-scale distribution of harbour porpoises in the Baltic Sea provides basis for effective conservation actions. Biological Conservation 226:42–53.

Castellote, M. 2007. General Review of Protocols and Guidelines for Minimizing Acoustic Disturbance to Marine Mammals from Seismic Surveys. Journal of International Wildlife Law & Policy 10:273–288.

Clausen, K. T., M. Wahlberg, K. Beedholm, S. Deruiter, and P. T. Madsen. 2010. Click communication in harbour porpoises Phocoena phocoena. Bioacoustics 20:1–28.

Cosentino, M., F. Guarato, J. Tougaard, D. Nairn, J. C. Jackson, and J. F. C. Windmill. 2019. Porpoise click classifier (PorCC): A high-accuracy classifier to study harbour porpoises (Phocoena phocoena) in the wild. The Journal of the Acoustical Society of America 145:3427–3434.

Davis, G. E., M. F. Baumgartner, J. M. Bonnell, J. Bell, C. Berchok, J. Bort Thornton, S. Brault, G. Buchanan, R. A. Charif, D. Cholewiak, C. W. Clark, P. Corkeron, J. Delarue, K. Dudzinski, L. Hatch, J. Hildebrand, L. Hodge, H. Klinck, S. Kraus, B. Martin, D. K. Mellinger, H. Moors-Murphy, S. Nieukirk, D. P. Nowacek, S. Parks, A. J. Read, A. N. Rice, D. Risch, A. Širović, M. Soldevilla, K. Stafford, J. E. Stanistreet, E. Summers, S. Todd, A. Warde, and S. M. Van Parijs. 2017. Long-term passive acoustic recordings track the changing distribution of North Atlantic right whales (Eubalaena glacialis) from 2004 to 2014. Scientific Reports.

Deruiter, S. L., A. Bahr, M.-A. Blanchet, S. F. Hansen, J. H. Kristensen, P. T. Madsen, P. L. Tyack, and M. Wahlberg. 2009. Acoustic behaviour of echolocating porpoises during prey capture. The Journal of experimental biology 212:3100–3107.

Finneran, J. J., B. K. Branstetter, D. S. Houser, P. W. Moore, J. Mulsow, C. Martin, and S. Perisho. 2014. High-resolution measurement of a bottlenose dolphin's (Tursiops truncatus) biosonar transmission beam pattern in the horizontal plane. The Journal of the Acoustical Society of America 136:2025–38.

Frasier, K. E., M. A. Roch, M. S. Soldevilla, S. M. Wiggins, L. P. Garrison, and J. A. Hildebrand. 2017. Automated classification of dolphin echolocation click types from the Gulf of Mexico. PLoS Computational Biology 13:1–23.

Frasier, K. E., S. M. Wiggins, D. Harris, T. A. Marques, L. Thomas, and J. A. Hildebrand. 2016. Delphinid echolocation click detection probability on near-seafloor sensors. The Journal of the Acoustical Society of America 140:1918–1930.

Galatius, A., M. T. Olsen, M. E. Steeman, R. A. Racicot, C. D. Bradshaw, L. A. Kyhn, and L. A. Miller. 2019. Raising your voice: evolution of narrow-band high-frequency signals in toothed whales (Odontoceti). Biological Journal of the Linnean Society 126:213–224.

Gard, R. 1971. Brown Bear Predation on Sockeye Salmon at Karluk Lake, Alaska. The Journal of Wildlife Management 35:193.

Gibb, R., E. Browning, P. Glover-Kapfer, and K. E. Jones. 2019. Emerging opportunities and challenges for passive acoustics in ecological assessment and monitoring. Methods in Ecology and Evolution 10:169–185.

Gillespie, D. 2004. Detection and classification of right whale calls using an edge detector operating on a smoothed spectrogram. Canadian Acoustics 32:39–47.

Gordon, J., D. Thompson, R. Leaper, D. Gillespie, C. Pierpoint, S. Calderan, J. Macaulay, T. Gordon, and N. Simpson. 2011. Assessment of risk to marine mammals from underwater marine renewable devices in Welsh waters - Phase 2 - Studies of marine mammals in Welsh high tidal waters. Page Welsh Government Assembly Report.

Hansen, M., M. Wahlberg, and P. T. Madsen. 2008. Low-frequency components in harbor porpoise (Phocoena phocoena) clicks: communication signal, by-products, or artifacts? The Journal of the Acoustical Society of America 124:4059–4068.

Harris, D., L. Matias, L. Thomas, J. Harwood, and W. H. Geissler. 2013. Applying distance sampling to fin whale calls recorded by single seismic instruments in the northeast Atlantic. The Journal of the Acoustical Society of America 134:3522–35.

Hastie, G. D., M. Bivins, A. Coram, J. Gordon, P. Jepp, J. MacAulay, C. Sparling, and D. Gillespie. 2019. Three-dimensional movements of harbour seals in a tidally energetic channel: Application of a

novel sonar tracking system. Aquatic Conservation: Marine and Freshwater Ecosystems 29:564–575.

Hastie, G. D., D. J. F. Russell, S. Benjamins, S. Moss, B. Wilson, and D. Thompson. 2016. Dynamic habitat corridors for marine predators; intensive use of a coastal channel by harbour seals is modulated by tidal currents. Behavioral Ecology and Sociobiology 70:2161–2174.

Hildebrand, J. A., S. Baumann-Pickering, K. E. Frasier, J. S. Trickey, K. P. Merkens, S. M. Wiggins, M. a McDonald, L. P. Garrison, D. Harris, T. a Marques, and L. Thomas. 2015. Passive acoustic monitoring of beaked whale densities in the Gulf of Mexico. Scientific reports 5:16343.

Hildebrand, J. A., K. E. Frasier, S. Baumann-Pickering, S. M. Wiggins, K. P. Merkens, L. P. Garrison, M. S. Soldevilla, and M. A. McDonald. 2019. Assessing Seasonality and Density From Passive Acoustic Monitoring of Signals Presumed to be From Pygmy and Dwarf Sperm Whales in the Gulf of Mexico. Frontiers in Marine Science 6:1–17.

Hill, A. P., P. Prince, E. Piña Covarrubias, C. P. Doncaster, J. L. Snaddon, and A. Rogers. 2018. AudioMoth: Evaluation of a smart open acoustic device for monitoring biodiversity and the environment. Methods in Ecology and Evolution 9:1199–1211.

Hoek, W. 1992. An unusual aggregation of harbor porpoises (Phocoena phocoena). Marine Mammal Science 8:152–155.

Jakobsen, L., S. Brinkløv, and A. Surlykke. 2013a. Intensity and directionality of bat echolocation signals. Frontiers in Physiology 4 APR:1–9.

Jakobsen, L., E. K. V. Kalko, and A. Surlykke. 2012. Echolocation beam shape in emballonurid bats, Saccopteryx bilineata and Cormura brevirostris. Behavioral Ecology and Sociobiology 66:1493–1502.

Jakobsen, L., J. M. Ratcliffe, and A. Surlykke. 2013b. Convergent acoustic field of view in echolocating bats. Nature 493:93–96.

Jakobsen, L., and A. Surlykke. 2010. Vespertilionid bats control the width of their biosonar sound beam dynamically during prey pursuit. Proceedings of the National Academy of Sciences of the United States of America 107:13930–13935.

Janik, V. M., L. S. Sayigh, and R. S. Wells. 2006. Signature whistle shape conveys identity information to bottlenose dolphins. Proceedings of the National Academy of Sciences 103:8293–8297.

Jensen, F. H., M. Johnson, M. Ladegaard, D. M. Wisniewska, and P. T. Madsen. 2018. Narrow Acoustic Field of View Drives Frequency Scaling in Toothed Whale Biosonar. Current Biology 28:3878-3885.e3.

Jensen, F. H., M. Wahlberg, K. Beedholm, M. Johnson, N. A. de Soto, and P. T. Madsen. 2015. Single-click beam patterns suggest dynamic changes to the field of view of echolocating Atlantic spotted dolphins (Stenella frontalis) in the wild. Journal of Experimental Biology 218:1314–

1324.

Johansen, J., D. Bellwood, and C. Fulton. 2008. Coral reef fishes exploit flow refuges in high-flow habitats. Marine Ecology Progress Series 360:219–226.

Johnson, M., P. T. Madsen, W. M. X. X. Zimmer, N. Aguilar de Soto, and P. L. Tyack. 2004. Beaked whales echolocate on prey. Proceedings of the Royal Society of London. Series B: Biological Sciences 271:S383–S386.

Johnson, M. P., and P. L. Tyack. 2003. A digital acoustic recording tag for measuring the response of wild marine mammals to sound. IEEE Journal of Oceanic Engineering 28:3–12.

Johnston, D., L. Thorne, and A. Read. 2005. Fin whales Balaenoptera physalus and minke whales Balaenoptera acutorostrata exploit a tidally driven island wake ecosystem in the Bay of Fundy. Marine Ecology Progress Series 305:287–295.

Jones, G., and B. M. Siemers. 2011. The communicative potential of bat echolocation pulses. Journal of Comparative Physiology A 197:447–457.

Knörnschild, M., K. Jung, M. Nagy, M. Metz, and E. Kalko. 2012. Bat echolocation calls facilitate social communication. Proceedings of the Royal Society B: Biological Sciences 279:4827–4835.

Knowlton, J. L., and C. H. Graham. 2010. Using behavioral landscape ecology to predict species' responses to land-use and climate change. Biological Conservation 143:1342–1354.

Koblitz, J. C., M. Wahlberg, P. Stilz, P. T. Madsen, K. Beedholm, and H.-U. Schnitzler. 2012. Asymmetry and dynamics of a narrow sonar beam in an echolocating harbor porpoise. The Journal of the Acoustical Society of America 131:2315.

Kohles, J. E., G. G. Carter, R. A. Page, and D. K. N. Dechmann. 2020. Socially foraging bats discriminate between group members based on search-phase echolocation calls. Behavioral Ecology:1–10.

Küsel, E. T., D. K. Mellinger, L. Thomas, T. A. Marques, D. Moretti, and J. Ward. 2011. Cetacean population density estimation from single fixed sensors using passive acoustics. The Journal of the Acoustical Society of America 129:3610–3622.

Kyhn, L. A., F. H. Jensen, K. Beedholm, J. Tougaard, M. Hansen, and P. T. Madsen. 2010. Echolocation in sympatric Peale's dolphins (Lagenorhynchus australis) and Commerson's dolphins (Cephalorhynchus commersonii) producing narrow-band high-frequency clicks. Journal of Experimental Biology 213:1940–1949.

Kyhn, L. A., J. Tougaard, F. Jensen, M. Wahlberg, G. Stone, A. Yoshinaga, K. Beedholm, and P. T. Madsen. 2009. Feeding at a high pitch: source parameters of narrow band, high-frequency clicks from echolocating off-shore hourglass dolphins and coastal Hector's dolphins. The Journal of the Acoustical Society of America 125:1783–1791.

Ladegaard, M., F. H. Jensen, K. Beedholm, V. M. F. Da Silva, and P. T. Madsen. 2017. Amazon river dolphins (Inia geoffrensis) modify biosonar output level and directivity during prey interception in the wild. Journal of Experimental Biology 220:2654–2665.

Lewis, T., D. Gillespie, C. Lacey, J. Matthews, M. Danbolt, R. Leaper, R. McLanaghan, and A. Moscrop. 2007. Sperm whale abundance estimates from acoustic surveys of the Ionian Sea and Straits of Sicily in 2003. Journal of the Marine Biological Association of the United Kingdom 87:353–357.

Liao, J. C. 2004. Neuromuscular control of trout swimming in a vortex street: implications for energy economy during the Karman gait. Journal of Experimental Biology 207:3495–3506.

Luo, W., W. Yang, Z. Song, and Y. Zhang. 2017. Automatic species recognition using echolocation clicks from odontocetes. Pages 1–5 2017 IEEE International Conference on Signal Processing, Communications and Computing (ICSPCC). IEEE.

Madsen, P. T., D. A. Carder, K. Bedholm, and S. H. Ridgway. 2005. Porpoise Clicks From a Sperm Whale Nose—Convergent Evolution of 130 Khz Pulses in Toothed Whale Sonars? Bioacoustics 15:195–206.

Madsen, P. T., R. Payne, N. U. Kristiansen, M. Wahlberg, I. Kerr, and B. Møhl. 2002. Sperm whale sound production studied with ultrasound time/depth-recording tags. The Journal of experimental biology 205:1899–906.

Madsen, P. T., D. Wisniewska, and K. Beedholm. 2010. Single source sound production and dynamic beam formation in echolocating harbour porpoises (Phocoena phocoena). Journal of Experimental Biology 213:3105–3110.

Malinka, C. E., J. D. J. Macaulay, J. Gordon, D. Gillespie, and S. Northridge. 2015. Fine-scale acoustic tracking of harbour porpoises in tidal rapids. Page Conference: 21st Bienniel Society of Marine Mammalogy Conference. San Francisco.

Marques, T. A., L. Thomas, S. W. Martin, D. K. Mellinger, J. A. Ward, D. J. Moretti, D. Harris, and P. L. Tyack. 2013. Estimating animal population density using passive acoustics. Biological reviews of the Cambridge Philosophical Society 88:287–309.

Marques, T. A., L. Thomas, J. Ward, N. DiMarzio, and P. L. Tyack. 2009. Estimating cetacean population density using fixed passive acoustic sensors: An example with Blainville's beaked whales. The Journal of the Acoustical Society of America 125:1982–1994.

Marques, T., L. Munger, L. Thomas, S. Wiggins, and J. Hildebrand. 2011. Estimating North Pacific right whale Eubalaena japonica density using passive acoustic cue counting. Endangered Species Research 13:163–172.

Martin, M. J., T. Gridley, S. H. Elwen, and F. H. Jensen. 2018. Heaviside's dolphins (Cephalorhynchus heavisidii) relax acoustic crypsis to increase communication range. Proceedings of the Royal Society B: Biological Sciences 285:20181178.

Møhl, B. 2001. Sound transmission in the nose of the sperm whale Physeter catodon . A post mortem study. Journal of Comparative Physiology A: Sensory, Neural, and Behavioral Physiology 187:335–340.

Morisaka, T., and R. C. Connor. 2007. Predation by killer whales (Orcinus orca) and the evolution of whistle loss and narrow-band high frequency clicks in odontocetes. Journal of Evolutionary Biology 20:1439–1458.

Oliveira, C., M. Wahlberg, M. Johnson, P. J. O. Miller, and P. T. Madsen. 2013. The function of male sperm whale slow clicks in a high latitude habitat: Communication, echolocation, or prey debilitation? The Journal of the Acoustical Society of America 133:3135–3144.

Onoufriou, J., A. Brownlow, S. Moss, G. Hastie, and D. Thompson. 2019. Empirical determination of severe trauma in seals from collisions with tidal turbine blades. Journal of Applied Ecology 56:1712–1724.

Otani, S., Y. Naito, A. Kato, and A. Kawamura. 2001. Oxygen consumption and swim speed of the harbor porpoise Phocoena phocoena. Fisheries Science 67:894–898.

Van Parijs, S., C. Clark, R. Sousa-Lima, S. Parks, S. Rankin, D. Risch, and I. Van Opzeeland. 2009. Management and research applications of real-time and archival passive acoustic sensors over varying temporal and spatial scales. Marine Ecology Progress Series 395:21–36.

Pfalzer, G., and J. Kusch. 2003. Structure and variability of bat social calls: implications for specificity and individual recognition. Journal of Zoology 261:S0952836903003935.

Rankin, S., F. Archer, J. L. Keating, J. N. Oswald, M. Oswald, A. Curtis, and J. Barlow. 2017. Acoustic classification of dolphins in the California Current using whistles, echolocation clicks, and burst pulses. Marine Mammal Science 33:520–540.

Rendell, L. E., and H. Whitehead. 2003. Vocal clans in sperm whales (Physeter macrocephalus). Proceedings of the Royal Society of London. Series B: Biological Sciences 270:225–231.

Roch, M. A., H. Batchelor, S. Baumann-Pickering, C. L. Berchok, D. Cholewiak, E. Fujioka, E. C. Garland, S. Herbert, J. A. Hildebrand, E. M. Oleson, S. Van Parijs, D. Risch, A. Širović, and M. S. Soldevilla. 2016. Management of acoustic metadata for bioacoustics. Ecological Informatics 31:122–136.

Roemmich, D., G. Johnson, S. Riser, R. Davis, J. Gilson, W. B. Owens, S. Garzoli, C. Schmid, and M. Ignaszewski. 2009. The Argo Program: Observing the Global Oceans with Profiling Floats. Oceanography 22:34–43.

Rojano-Doñate, L., B. I. McDonald, D. M. Wisniewska, M. Johnson, J. Teilmann, M. Wahlberg, J. Højer-Kristensen, and P. T. Madsen. 2018. High field metabolic rates of wild harbour porpoises. The Journal of Experimental Biology 221:jeb185827.

Sangiuliano, S. J. 2017. Turning of the tides: Assessing the international implementation of tidal

current turbines. Pages 971–989 Renewable and Sustainable Energy Reviews. Elsevier Ltd.

Scottish Natural Heritage. 2016. Assessing collision risk between underwater turbines and marine wildlife. SNH guidance note.

Shiu, Y., K. J. Palmer, M. A. Roch, E. Fleishman, X. Liu, E.-M. Nosal, T. Helble, D. Cholewiak, D. Gillespie, and H. Klinck. 2020. Deep neural networks for automated detection of marine mammal species. Scientific Reports 10:607.

Simmons, J. A., D. Houser, and L. Kloepper. 2014. Localization and Classification of Targets by Echolocating Bats and Dolphins. Pages 169–193 *in* A. Surlykke, P. E. Nachtigall, R. R. Fay, and A. N. Popper, editors. Biosonar.

Soldevilla, M. S., E. E. Henderson, G. S. Campbell, S. M. Wiggins, J. a Hildebrand, and M. a Roch. 2008. Classification of Risso's and Pacific white-sided dolphins using spectral properties of echolocation clicks. The Journal of the Acoustical Society of America 124:609–24.

Sørensen, P. M., D. M. Wisniewska, F. H. Jensen, M. Johnson, J. Teilmann, and P. T. Madsen. 2018. Click communication in wild harbour porpoises (Phocoena phocoena). Scientific Reports 8:9702.

Sousa, A. G., and D. Harris. 2015. Description and seasonal detection of two potential whale calls recorded in the Indian Ocean. The Journal of the Acoustical Society of America 138:1379–1388.

Stedt, J., T. Ortiz, Sara, and M. Wahlberg. 2019. Harbour porpoise hunting from a bird's eye view. Page 2nd World Marine Mammal Conference. Barcelona.

Stewart, W. J., F. Tian, O. Akanyeti, C. J. Walker, and J. C. Liao. 2016. Refuging rainbow trout selectively exploit flows behind tandem cylinders. The Journal of Experimental Biology 219:2182–2191.

Stowell, D., M. D. Wood, H. Pamuła, Y. Stylianou, and H. Glotin. 2019. Automatic acoustic detection of birds through deep learning: The first Bird Audio Detection challenge. Methods in Ecology and Evolution 10:368–380.

Sugai, L. S. M., T. S. F. Silva, J. W. Ribeiro, and D. Llusia. 2019. Terrestrial Passive Acoustic Monitoring: Review and Perspectives. BioScience 69:15–25.

Surlykke, A., L. Jakobsen, E. K. V. Kalko, and R. A. Page. 2013. Echolocation intensity and directionality of perching and flying fringe-lipped bats, Trachops cirrhosus (Phyllostomidae). Frontiers in Physiology 4:1–9.

Thomas, L., A. Jaramillo-Legorreta, G. Cardenas-Hinojosa, E. Nieto-Garcia, L. Rojas-Bracho, J. M. Ver Hoef, J. Moore, B. Taylor, J. Barlow, and N. Tregenza. 2017. Last call: Passive acoustic monitoring shows continued rapid decline of critically endangered vaquita. The Journal of the Acoustical Society of America 142:EL512–EL517.

Villadsgaard, A., M. Wahlberg, and J. Tougaard. 2007. Echolocation signals of wild harbour porpoises, Phocoena phocoena. Journal of Experimental Biology 210:56–64.

Watkins, W. A. 1977. Sperm whale codas. The Journal of the Acoustical Society of America 62:1485.

Weir, C. R., and S. J. Dolman. 2007. Comparative Review of the Regional Marine Mammal Mitigation Guidelines Implemented During Industrial Seismic Surveys, and Guidance Towards a Worldwide Standard. Journal of International Wildlife Law & Policy 10:1–27.

Wilson, B., R. S. Batty, F. Daunt, and C. Carter. 2007. Collision risks between marine renewable energy devices and mammals, fish and diving birds. Page Report to the Scottish Executive.

Wilson, B., S. Benjamins, and J. Elliott. 2013. Using drifting passive echolocation loggers to study harbour porpoises in tidal-stream habitats. Endangered Species Research 22:125–143.

Wisniewska, D. M., M. Johnson, K. Beedholm, M. Wahlberg, and P. T. Madsen. 2012. Acoustic gaze adjustments during active target selection in echolocating porpoises. The Journal of experimental biology 215:4358–73.

Wisniewska, D. M. M., M. Johnson, J. Teilmann, L. Rojano-Doñate, J. Shearer, S. Sveegaard, L. A. A. Miller, U. Siebert, and P. T. T. Madsen. 2016. Ultra-High Foraging Rates of Harbor Porpoises Make Them Vulnerable to Anthropogenic Disturbance. Current Biology 26:1441–1446.

Wisniewska, D. M., J. M. Ratcliffe, K. Beedholm, C. B. Christensen, M. Johnson, J. C. Koblitz, M. Wahlberg, and P. T. Madsen. 2015. Range-dependent flexibility in the acoustic field of view of echolocating porpoises (Phocoena phocoena). eLife 4:1–16.

Wrege, P. H., E. D. Rowland, S. Keen, and Y. Shiu. 2017. Acoustic monitoring for conservation in tropical forests: examples from forest elephants. Methods in Ecology and Evolution 8:1292–1301.

Yuan, X., P. He, Q. Zhu, and X. Li. 2019. Adversarial Examples: Attacks and Defenses for Deep Learning. IEEE Transactions on Neural Networks and Learning Systems 30:2805–2824.

Zimmer, W. M. X., P. L. Tyack, M. P. Johnson, and P. T. Madsen. 2005. Three-dimensional beam pattern of regular sperm whale clicks confirms bent-horn hypothesis. The Journal of the Acoustical Society of America 117:1473–1485.